Photosynthetic and Hydraulic Responses in Mulberry to Water Stress: Patterns, Architecture and Acclimation

Thesis Submitted to the University of Hyderabad for the Degree of

Doctor of Philosophy in Plant Sciences

By

ANIRBAN GUHA

(Registration No. 09LPPH07)

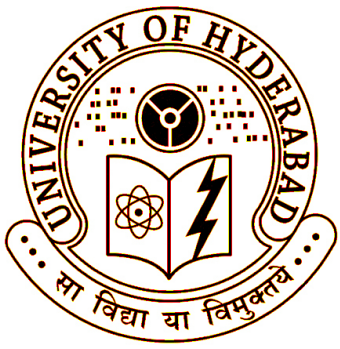

DEPARTMENT OF PLANT SCIENCES

SCHOOL OF LIFE SCIENCES

UNIVERSITY OF HYDERABAD

HYDERABAD 500 046

April 2013

University of Hyderabad
School of Life Sciences
Department of Plant Sciences
Hyderabad 500 046

DECLARATION

I, Anirban Guha, hereby declare that this thesis entitled "**Photosynthetic and hydraulic responses in mulberry to water stress: Patterns, architecture and acclimation** " submitted by me, was carried out in the Department of Plant Sciences, School of Life Sciences, University of Hyderabad, Hyderabad, under the guidance and supervision of Professor Attipalli R. Reddy is an original and independent research work. I also declare that no part of the work has been submitted for the award of any other degree or diploma to any University or institution till this date.

Date: **Name : Anirban Guha**

Signature :

Registration No.: 09LPPH07

University of Hyderabad
School of Life Sciences
Department of Plant Sciences
Hyderabad 500046

CERTIFICATE

This is to certify that this thesis entitled "**Photosynthetic and hydraulic responses in mulberry to water stress: Patterns, architecture and acclimation**" is a record of bonafide work done by Mr. Anirban Guha, a research scholar for Ph.D. programme in Plant Sciences (Registration No. 09LPPH07), Department of Plant Sciences, School of Life Sciences, University of Hyderabad under my guidance and supervision. The thesis has not been submitted previously in part or in full to this or any other University or Institution for the award of any degree or diploma.

Professor Attipalli R. Reddy
(Supervisor)

(Head of the Department) **(Dean of the School)**

Dedicated to the smallholder mulberry farmers of India

Acknowledgements

My deepest gratitude and greatest thanks go to my supervisor Prof. Attipalli Ramachandra Reddy who, for the duration of my research, encouraged me to seize any opportunity that arose and turned it into reality. He appreciated my achievements, endured my failures, offered advice, tutelage and so much more. His guidance and support are greatly appreciated and I feel fortunate to have had him as my supervisor.

My most sincere thanks go to Prof. A. S. Raghavendra and Dr. K. P. M. S. V. Padmasree for periodically evaluating my progress in research and also for their interest, advice and support.

I would like to express my gratitude towards Dr. S. Masilamani for his support, guidance and help in several aspects during my PhD. I am also greatly indebted to Dr. Jhansi Lakshmi, Dr. Jalaja S. Kumar and Dr. J. Kodandaramaiah, for their vast wealth of information on physiology and agronomy of mulberry and their willingness to share it.

The support from Prof. Appa Rao Podile, Prof. Aparna Dutta Gupta, Prof. M. N. V. Prasad, Prof. R. P. Sharma, Prof. G. Padmaja and Dr. S. Rajagopal provided encouragement to me throughout my studies.

I also thank the administrative, communication, support and technical staffs from the office of Dean School of Life Sciences, Department of Plant Sciences, Central facilities, Indira Gandhi Memorial Library, Chief warden's office and hostels, Registrar's office, Finance officer's office, Development and Projects Section, Controller of examination's office, Student welfare section, Fellowship section and other administrative units at University of Hyderabad for their assistance in logistics.

I thank DBT, DST, CSIR and DST-Nanotechnology for funding in the lab and DST-FIST, UGC-SAP and DBT-CREEB for funding to the department and school. I acknowledge the senior research fellowship award from CSIR, New Delhi, DAAD

fellowship award for educational visit to Germany under 'New Passage to India' program and junior research fellowship from DST, Govt. of India. I also thank DST-SERB, New Delhi and CICS, Chennai for providing me travel grants towards attending Ecophysiology Technique Workshop held in Lisbon, Portugal.

I acknowledge Central Sericultural Germplasm Resources Center, Hosur and Regional Sericultural Research Stations, Anantapur and Salem for providing mulberry germplasm. I am thankful to Dr. M. Sujatha for facilitating leaf nitrogen analyses.

My colleagues and friends at University of Hyderabad, Chalapathi anna, Girish bhaiya, Prabhakar, Debashree, Chaitanya, Shalini, Sumit, Madhan, Harsha, Rajiv, Vamsi, Anirudh, Shuklaji, Dilipji, Abhay, Kiran, Abin, Subhasji, Mujahid, Sunil bhaiya, Sreedhar, Mahesh, Deepankar, Suresh, Ahanda, Swapna and Kapil have been very supportive, as well as a source of motivation. I am greatly indebted to Debashree who assisted me in many experiments, as well as extended her help with data collection. My experience in Münster has been enlightened by Prof. M. Hippler, Dimitris, Kerstin, Leonardo, Dema, Bernadeta and Ana. I would especially like to thank Jyotirmoy and Sanjit, without whom the last few months of my PhD life would not have been so enjoyable. I owe much to my friends Siddhartha, Subarna, Debasis, Tanmoy, Khasru, Prakash, Parnashree, Rameshwar and Nazir for their unfailing support over many years, and for always being there whenever I needed them.

I also wish to express my gratitude to Panduji, Vinod, Lakshman and Ashok for their valuable help during fieldwork.

My periodic visit to my family, who dwell in Kolkata, has helped me to rejuvenate and maintain a high spirit in all perspective throughout my PhD tenure. Together with my parents, my sister Ankita, my cousins, uncles, aunts, nephews and nieces, we all share a mutual love, enthusiasm and affection for our family, its culture and tradition. This bond and enthusiasm have always been a source of inspiration in my life. Most of all, this sense of belonging, I owe it to my mum and dad for their commitment to my family. I deeply thank them for their patience, understanding, and for giving me the love and motivation needed to pursue higher studies.

Table of Contents

Chapter 5 - Characterizing anisohydric behavior among mulberry genotypes in response to water deficit

Chapter 6 - Genotypic variation in stem wood hydraulic architecture in relation to anisohydric behavior

Abbreviations and symbols

$_1O^2$	Singlet oxygen
a. u	Arbitrary unit
AA	Ascorbic acid
ABA	Abscisic acid
ABS/Csm	Absorption flux per excited cross-section
ACN	Acetonitrile
ACT	Actin
AG_{dw}	Total above ground dry biomass
AG_{fw}	Total above ground fresh biomass
AG_W	Above ground woody biomass
ANOVA	Analysis of variance
ANOVAR	Repeated measures analysis of variance
APG	Average performance group
APX	Ascorbate peroxidase
BMD	Biomass duration
CE	Crown exposure
CGR	Crop growth rate
CHCA	α-cyano-4-hydroxycinnamic acid
Chl	Chlorophyll
C_i	Sub stomatal (internal) CO_2 concentration
C_i/C_a	Internal to ambient CO_2 ratio
CLSM	Confocal laser scanning microscope
CR	Congo red
CRBD	Completely randomized block design
D_{100}	Stem diameter at 100 cm height from the stem base
DF	Driving force
DI_O/CSm	Dissipated energy flux per excited cross section
D_L	Diameter of fibre cell lumen
DMSO	Dimethyl sulfoxide
DNTB	5'- dithio-bis(2-nitrobenzoic acid)
DNTPH	2,4-Dinitrophenyl hydrazine
D_W	Wood density
dw	Dry weight
E	Transpiration rate
E_{crit}	Upper limit of transpiration
E_{max}	Peak transpiration rate
EST	Expressed sequence tag
ET	Evapotranspiration
ET_O/CS_m	Electron transport flux per excited cross-section
ETC	Electron transport chain
exp	Experimental
FAA	Formalin acetic acid
FC_d	Fibre cell diameter
FCL_A	Cross sectional area of fibre cell lumen
FC_n	Number of fibre cells
FC_{wt}	fibre cell wall thickness
F_m	Maximum fluorescence induction
F_o	Minimum fluorescence yield

F_t	Fluorescence intensity
F_v	Variable fluorescence
F_v/F_m	Maximum quantum yield
fw	Fresh weight
FYM	Farm yard manure
GLM	General linear model
GR	Glutathione reductase
G_s	Stomatal conductance
GSH	Glutathione
G_{smax}	Maximum stomatal conductance
G × E	Genotype × environment interaction
H_2DCFDA/DCF	(2',7'- dichlorofluroescin diacetate)
H_2O_2	Hydrogen peroxide
ha	Hectare
HGR	Height growth rate
H_{max}	Maximum adult height of plant
HPG	High Performance group
HRM	Heat ratio method
H_t	Plant height
I_{comp}	Photosynthetic light compensation point
IF	Induction factor
IRGA	Infra-red gas analyzer
I_{sat}	Light saturation point of photosynthesis
kDa	Kilodalton
K_h	In-situ leaf specific hydraulic conductance
K_{leaf}	Hydraulic conductance of leaf
K_{plant}	Hydraulic conductance of plant
K_{root}	Hydraulic conductance of root
KSL	In-situ root- to- leaf specific hydraulic conductance
K_{soil}	Hydraulic conductance of soil
K_{stem}	Hydraulic conductance of stem
LAI	Leaf area index
L_d	Leaf dry biomass
L_f	Leaf fresh biomass
LHCII	Light harvesting complex II
LMC	Leaf moisture content
LMR	Leaf mass ratio
LSD	Leaf significant difference
LY	Leaf yield
MDA	Malondialdehyde
MIPIP1.3	*Morus indica* PIP1.3 aquaporin
MPa	Mega pascal
Mr	Molecular weight
Ms	Dry mass
MSL	Mean sea level
MTP	Multiple turn over phases
NAR	Net assimilation rate
NBT	Nitroblue tetrazolium
NH_4HCO_3	Ammonium bicarbonate
NIPs	NOD26-like intrinsic proteins
N_L	Leaf nitrogen

NPK	Nitrogen phosphorous potassium
NPQ	Non-photochemical quenching
$O_2^{\cdot}$	Superoxide anion radical
OEC	Oxygen evolving complex
OEE	Oxygen evolving enhancer
$OH^{\cdot}$	Hydroxyl radical
OPH	Open pollinated hybrid
P_A	Pith area
PAR	Photosynthetically active radiation
PC	Pot water holding capacity
PCA	Principal component analysis
Pd_H	Horizontal diameter of pit
Pd_V	Vertical diameter of pit
PEA	Plant efficiency analyzer
PET	Photosynthetic electron transfer
PG	Performance group
PI	Performance index
PIPs	Plasma membrane intrinsic proteins
P_n	Net CO_2 fixation rate
P_{ncap}	Photosynthetic capacity
P_{nmax}	Light saturated rate of photosynthesis
POD	Peroxidase
PP	Precipitation
PPFD	Photosynthetic photon flux density
PPG	Poor performance group
PQ	Plastoquinone
PQH_2	Reduced plastoquinone
PSI	Photosystem-I
PSII	Photosystem-II
PSII-S	Photosystem-II minor subunit
QA	Quinone A
QA^-	Reduced quinone A
qPCR	Quantitative PCR
RBD	Randomized block design
RCs	Reaction centres
Rd	Dark respiration rate
RH	Relative humidity
RHGR	Relative plant height growth rate
ROS	Reactive oxygen species
RSV	Relative spot volume
RWC	Relative water content
SEM	Scanning electron microscope
S_f	Stem fresh biomass
SFI	Structure-function index
SIPs	Small basic intrinsic proteins
SLA	Specific leaf area
SMC	Soil moisture content
SMR	Stem mass ratio
SOD	Superoxide dismutase
SPAC	Soil-plant-atmosphere-continuum
SRC	Short rotation coppice

STP	Single turn over phases
SV	Solitary vessel
SWC	Soil water content
T_a	Air temperature
T_B	Total number of axillary shoots
TBA	Thiobarbituric acid
TCA	Trichloroacetic acid
TFA	Trifluoroacetic acid
TI	Tolerance index
TIPs	Tonoplasts intrinsic proteins
T_L	Leaf temperature
T_m	Time intervals
T_{max}	Maximum air temperature
T_{min}	Minimum air temperature
TR_O/CS_m	Trapped energy flux per excited cross section
TSL	Total shoot length
TSTM	Total number of stems
tw	Turgid weight
V_A	Stem cross sectional area occupied by xylem
V_D	Density of xylem vessels
V_d	Diameter of xylem vessels
VGI	Vessel grouping index
VPD	Vapour pressure deficit
V_W	Green wood volume
W_A	Total cross-sectional area of wood
WS	Water-stressed
WUE_i	Instantaneous water use efficiency
WW	Well-watered
Y × G	Year × genotype interaction
$\Delta\Pi$	Difference of osmotic potential
Π	Osmotic potential
φ	Apparent quantum yield
Ψ	Water potential
Ψ_{crit}	Water potential value causing 100% cavitation
Ψ_L	Leaf water potential
Ψ_{Lmax}	Maximum leaf water potential
Ψ_{Lmin}	Minimum leaf water potential
Ψ_{md}	Midday water potential
Ψ_{pd}	Predawn leaf water potential
Ψ_{soil}	Water potential of soil
$\Psi_{stem\ xylem}$	Water potential of stem xylem

List of Figures

List of Tables

List of Boxes

Chapter 1

Drought stress impacts a broad rage of climates and ecosystems, on a regional to sub- continental scale. The geographic area affected by drought globally has increased strongly in the last four decades (Dai et al. 2004). Drought events are predicted to be more frequent in future with a potential for adverse impacts on numerous sectors, such as agriculture, water supply, energy production, and health (Trenberth et al. 2007). Occurrences of intense drought and elevated temperature have been associated with increased tree mortality in many regions of the world (Allen 2009; Allen et al. 2010). Physiological responses of trees to soil water deficit vary, but have been fairly well-characterized (McDowell et al. 2008). They vary from draw-down in leaf water potential (Ψ_L) to maintenance of Ψ_L above a threshold with various strategies in between. Many tree species shed leaves during severe drought, reducing transpiration and photosynthesis, and adjust partitioning into storage tissues (McDowell et al. 2008). Tree growth can be reduced through impairment of cell division and cell expansion, which occurs at a lower water stress threshold than does photosynthetic inhibition. A variety of physiological processes respond at different plant water potentials (Ditmarová et al. 2010). With the increase in stress severity, trees adapt multiple defensive mechanisms, many of which involve coordination within the whole tree. While we have many clues and puzzle pieces in plant drought responses, our understanding of photosynthetic carbon fixation, carbon balance,

carbon storage, water relations and whole tree coordination is not robust enough for predicting tree responses to a changing climate (McDowell 2011).

Trees adjust to drought in several ways and simply looking at one of them is not likely to be effective. Metcalfe et al. (2010) provided an excellent example of insights into the complex ways in which trees respond to drought through coordinated water and carbon measurements. As tree response to drought is likely to be complex and involve the entire tree, we need to broaden our measurements to the entire tree and coordinate measurements of water and carbon to make better inferences. The first component of a whole tree approach while studying drought response is measurements of CO_2 fixation capacity. Carbon fixation is a complex function of photosynthetic capacity, leaf area, light environment, temperature and stomatal conductance (itself a complex function of light, hydraulic feedbacks and vapor pressure deficit). The second component of a whole tree approach is to integrate measurements of water and carbon fixation while characterizing drought response (Larcheveque et al. 2011; Galvez et al. 2011). Often, studies making inferences about the effects of water on carbon measure only water (Ryan et al. 2000). Potential coupling of carbon starvation and hydraulic failure have been demonstrated in the case studies of piñon pine (*Pinus edulis*) and one-seed juniper (*Juniperus monosperma*) (McDowell et al. 2008), seedlings of four Australian species (Brodribb and Cochard 2009) and other woody species (Vilagrosa et al. 2003; Rice et. al. 2004; Adams et al. 2009). Based on these analyses, it appears that carbon limitation and hydraulic failure are coupled rather than independent and teasing apart the role of each process cannot be done because the processes co-occur with each other.

Hydraulic conductance in trees

Water transport in plants is a physical process that requires no energy input from the plant and has been described as a soil–plant–atmosphere continuum where a continuous water column links soil water through the plant vascular system (xylem) with atmospheric humidity (Sperry et al. 2002). Water evaporates from leaves and diffuses out into the atmosphere and the evaporative demand is transmitted to mesophyll and bundle sheath cells and to the vascular system where adhesive and capillary forces of water molecules maintain the flow of water (Pickard and Melcher 2005). To understand water transport in

trees, it is essential to visualize how trees are structured and where water can flow. All the water crossing the tree comes from the soil which is a porous media constituting small aggregates and particles retaining water between them. From soil, water enters the root xylem by reverse osmosis and flows across stem and leaves (Cochard 2006). Trees, like any plants, are made of cells with rigid and hygrophilous walls formed of cellulose and hemicellulose microfribrils. Most cells are surrounded by a lipid bilayer plasmalemma membrane in contact with the wall which delimits the cytoplasm, a solution with a high solute concentration with osmotic potential (Π) typically ranging from −1 to −2 MPa. Cytoplasm can communicate between cells in contact through plasmodesmata without crossing plasmalemma membranes. Therefore, the interconnected cytoplasm determines a specific water compartment, the symplasm. Water located outside of the symplasm, e.g. in the wall matrix, forms a second compartment, the apoplasm (Cochard 2006). Trees, like other vascular plants, have developed xylem, a very specific tissue devoted to long-distance water transport. In broadleaves trees, xylem cell end-walls are partly or completely dissolved, thus forming very long conduits known as vessels. Water in the xylem conduits belongs to the apoplasm as water moves from one conduit to another across cell walls without crossing any membrane (**Fig. 1.1**). To account for the water movements across a plasmalemma membrane (i.e. from the symplasm to the apoplasm between two cytoplasts not connected by plasmodesmata), the difference of osmotic potential ($\Delta\Pi$) between the two compartments and the reflection coefficient of the membrane are considered to be the most important factors (Cochard 2006).

How hydraulic conductance and photosynthesis are linked?

Water transport and photosynthesis are highly distinct processes that become tightly linked the moment photosynthetic structures emerge into the atmospheric air (Sack and Holbrook 2006). Photosynthesis has the unavoidable consequence that in exchange for CO_2, leaves release vast quantities of water as transpiration. Failure to replace this transpired vapour with water transported from the soil would lead to desiccation and destruction of the photosynthetic apparatus. Water flows passively along the water potential gradient from the soil to the leaves. Water potentials (Ψ) are analogous to electrical potentials (Cowan

1972) in the sense that Ψ gradients determine water flow through the resistive hydraulic system in the same way that electrical resistors affect current flow produced by electrical potential gradients: $ET = (\Psi_{soil} - \Psi_L) K_{plant}$, where ET is the leaf evapotranspiration rate, $(\Psi_{soil} - \Psi_L)$ is the water potential gradient from the soil to leaf and K_{plant} is the hydraulic conductance of the whole plant (**Fig. 1.2**) (Brodribb 2009).

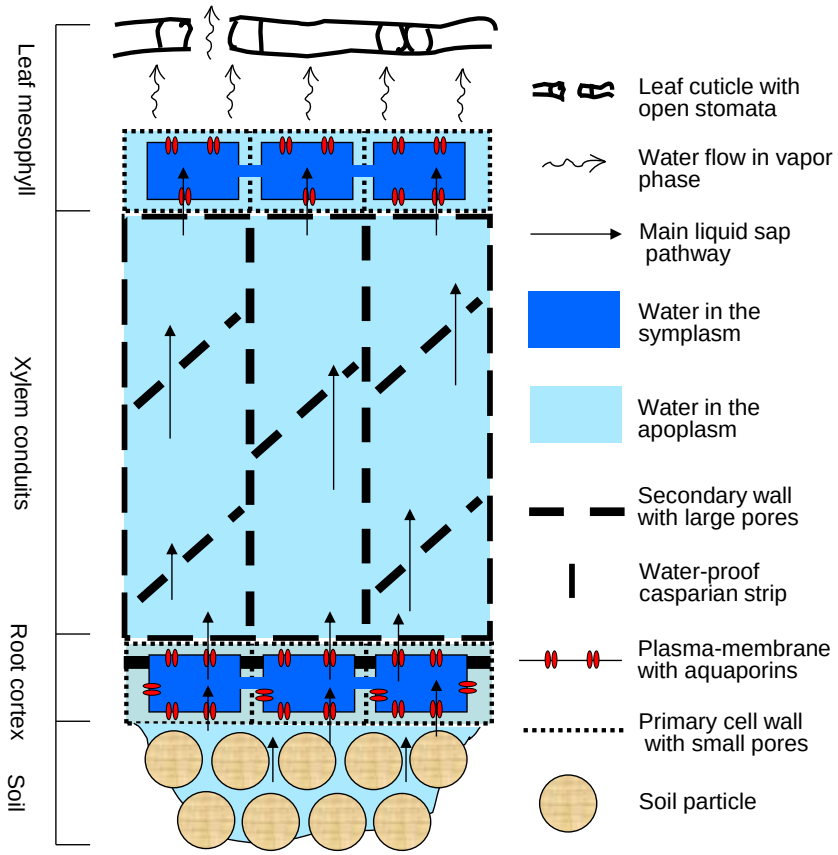

Fig. 1. 1 Water transport in trees (modified from Cochard 2006). Tree roots are in direct contact with soil water. When water enters the roots, the flow is mostly directed to the symplasm for two reasons. First, in the root cortex the apoplasmic pathway is usually interrupted by the casparian strip, a deposit of hydrophobic suberin. Hence, the water flow is here forced to enter the symplasm. Second, aquaporins in the plasmalemma membrane greatly increase its permeability and water will flow in this least resistive pathway. Water enters the root xylem by reverse-osmosis and flows to the leaves in the xylem conduits. This xylem pathway represents about 99% of the total water path length in the tree. The water flow from the xylem conduits to the leaf mesophyll is virtually symmetrical to flow from the root cortex to the xylem, with the difference that leaves lack casparian trip. While water evaporates in the leaves, the capillary force due to the surface tension of water pull upwards the water molecules, but because the cohesive forces between water molecules are much larger, it is the entire water column which is pulled upwards. This mechanism is known as the Cohesion–Tension Theory and was first proposed in the late 19th century.

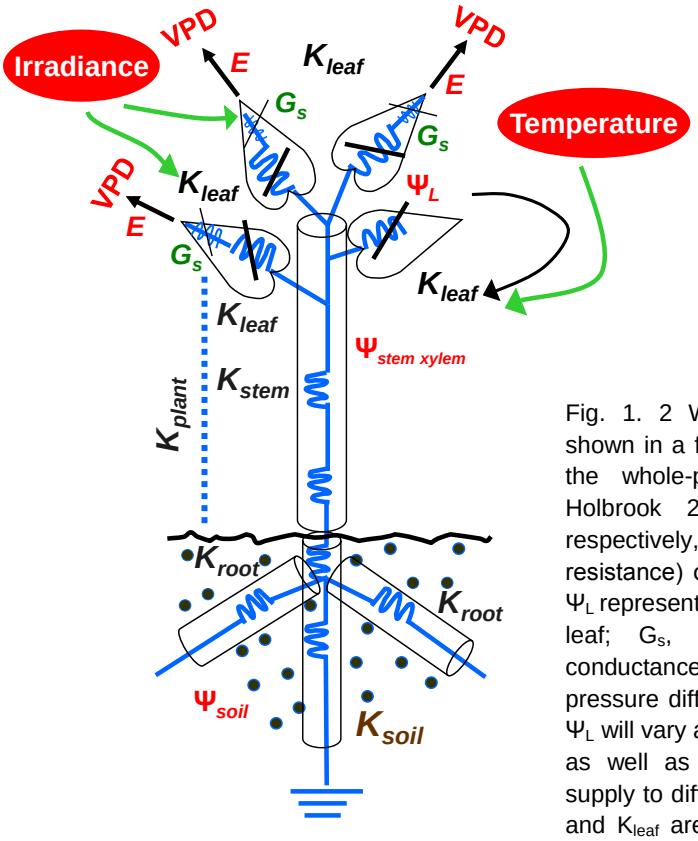

Fig. 1. 2 Whole plant hydraulic conductance (K_{plant}) shown in a form of simplified electronic circuit analog of the whole-plant system (modified from Sack and Holbrook 2006). K_{soil}, K_{root}, and K_{stem} represent, respectively, the hydraulic conductance (inverse of resistance) of soil, root and stem; Ψ_{soil}, $\Psi_{stem\ xylem}$, and Ψ_L represent the water potentials of soil, stem xylem, and leaf; G_s, E, and VPD represent the stomatal conductance, transpiration rate, and leaf to air vapour pressure difference. This scheme is much simplified, as Ψ_L will vary across a crown because of height differences as well as differences in transpiration and hydraulic supply to different leaves. Impacts of microclimate on G_s and K_{leaf} are shown with arrows; thus, K_{leaf}, like G_s, is represented as a variable conductance; decreases in Ψ_L, an internal variable, "drive" declines in K_{leaf} via its linkage with increasing xylem tensions.

According to the equation mentioned above (which does not consider water stored inside the plant as a water source), high transpirational fluxes from leaves can only be sustained by producing a large soil–leaf Ψ gradient, or a highly conductive hydraulic system (K_{plant}). In practice, it is mostly K_{plant} that constrains evaporation from leaves under well-watered soil conditions. The stomata of plants grown under natural conditions begin to limit ET (and assimilation) as Ψ_L falls below -1.5 MPa with 60% closure typically occurring close to -2 MPa (Brodribb 2009). An explanation for this conservative range is elusive, with suggestions ranging from osmotic control (Meinzer et al. 2008), to photosynthetic biochemistry (Lawlor and Cornic 2002) and xylem function (Domec et al. 2008) as potential limiters. Conservative stomatal response to turgor ensures that a maximum sustainable plant transpiration rate (E_{max}) is proportional to K_{plant}. This is the first of two conditions that connect hydraulic and photosynthetic capacities in well-watered plants. The

other key link is that leaves exchange gaseous CO_2 and H_2O through a common pore, and therefore the same diffusive limitation applies to both E and photosynthesis (**Fig. 1.3**). Furthermore, stomatal aperture in most species is regulated in such that water loss is optimized relative to photosynthetic gain (Brodribb 2009). Combined, the effects of uniform stomatal control and gas exchange optimization can lead us to a close theoretical relationship between K_{plant} and photosynthetic capacity (P_{ncap}) that is mediated by hydraulic limitation of E_{max}. Under most circumstances, this view is well-supported by experimental evidence (Buckley 2005) indicating that guard cells are like "hydromechanical valves" which respond to changes in Ψ_L either directly or via a signal generated very close to the guard cells. ''Hydraulic signalling'' of this type contrasts with the type of signalling associated with stomatal closure in response to the hormone, abscisic acid (ABA) (Brodribb 2009). The substantial investment in research on the biochemistry and genetics of ABA synthesis and guard cell ABA transduction is disproportionate to the apparent significance of ABA-mediated versus hydraulic-mediated models. Indeed, hydraulic models have far better empirical support from a broad range of species growing under both stressed and non-stressed natural conditions.

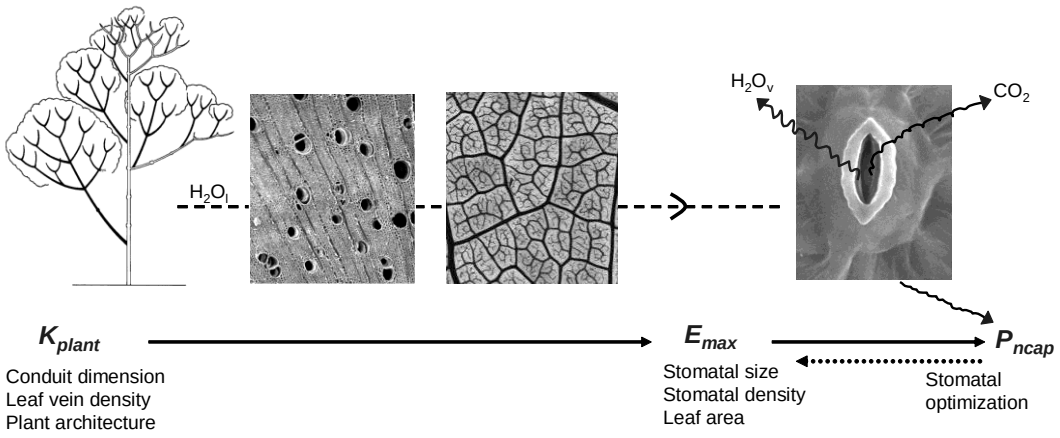

Fig. 1.3 Schematic diagram showing how the hydraulic capacity (K_{plant}) of plants is linked through the stomatal pore to photosynthetic capacity (P_{ncap}). The same water that leaves the stomata as vapour (H_2O_v) must be replaced by liquid water (H_2O_l) flowing through the vascular system. Under non-stressed conditions, the traits that determine K_{plant} should be coordinated through plant development with photosynthetic traits. Such hydraulic/photosynthetic coordination has been demonstrated at the level of whole-plant as well as within branches and also at leaf-level (modified from Brodribb 2009).

Hydraulic-photosynthetic coordination

The theoretical linkage between hydraulic capacity and CO_2 assimilation rate has enormous implications for understanding how hydraulic structure limits photosynthetic performance. The hydraulic system of vascular plants constitutes a large proportion of the total dry mass of an individual (Mencuccini 2003), and increasing K_{plant} requires substantial investment in the xylem tissue of the roots, stems and leaves (Zimmermann 1983). As such, it would be expected that developmental control of photosynthetic and hydraulic systems would ensure that resource allocation is balanced between these linked processes. Observations of plants growing under natural and experimental conditions provide strong evidence of such a linkage indicating that coordination between hydraulics and photosynthesis is a universal feature amongst vascular plants. Given that the development of hydraulic and photosynthetic systems are tightly interlinked in vascular plants, it is also crucial to understand how these developmentally distinct tissues are coordinated in a growing tree. Anatomical studies have demonstrated positive correlations between hydraulic, stomatal and photosynthetic traits in a range of woody plants (Aasamaa et al. 2001; Sack and Frole 2006). Also at the functional level, the rate of photosynthesis has been tied to whole plant (Hubbard et al. 2001; Aranda et al. 2005), branch (Brodribb and Field 2000; Salleo et al. 2000; Campanello et al. 2008) and leaf (Brodribb et al. 2005) hydraulic conductances (K_{plant}, K_{stem}, K_{leaf}, respectively) both within and between species. These data come from a range of techniques including whole-plant sap flow, and different measures using excised plant tissues including the traditional pressure-flow method (Sperry and Tyree 1988) as well as transient pressure (Franks 2006) and steady state evaporative methods (Sack et al. 2002).

At the whole-plant scale, allometry appears to be closely regulated such that the demand and supply of water are matched (Meinzer 2002). However, at a smaller scale, leaves provide an excellent opportunity to study coordinated development because they can be considered as somewhat self-contained units (Sack and Holbrook 2006). Furthermore, leaf hydraulic and photosynthetic capacities are genetically correlated (Maherali et al. 2008) suggesting that in leaves, the same developmental genes might be involved in the expression of hydraulic and photosynthetic traits. The significance of K_{leaf} as a potentially limiting component of the vascular system is highlighted by the strong

hydraulic–photosynthetic coordination observed across a large sample of diverse species (**Fig. 1.4**) (Brodribb et al. 2007). Importantly, K_{leaf} is closely related to the anatomy of the leaf, specifically to the architecture of veins and their location in the lamina (Sack and Frole 2006; Brodribb et al. 2007; Noblin et al. 2008). Other leaf traits such as palisade thickness, stomatal size and density, and leaf size vary in concert with vein density again supporting a unified control of hydraulic and photosynthetic traits (Aasamaa et al. 2001).

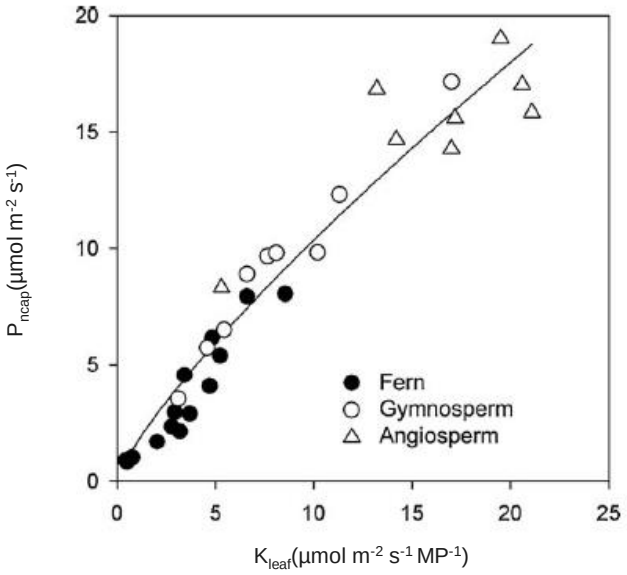

Fig. 1.4 A strong curvilinear correlation between leaf hydraulic (K_{leaf}) and photosynthetic capacity (P_{ncap}) in a diverse sample of ferns, conifers and angiosperms. (Brodribb 2009).

Drought-carbon starvation-hydraulic failure

In a broad scale, the two major recently proposed mechanisms of drought-induced tree mortality include hydraulic failure and carbon starvation (McDowell et al. 2008). The carbon-starvation hypothesis predicts that to prevent hydraulic failure, stomatal closure causes photosynthetic CO_2 assimilation to diminish and the plant starves as a result of continued metabolic demand for carbohydrates. The primary means of reduced photosynthesis during drought is the constraint on CO_2 diffusion into leaf intercellular spaces as a result of stomatal closure. However, respiratory consumption of stored carbohydrates continues during drought to maintain plant metabolism, even if growth is zero leading to carbon starvation (**Fig. 1.5**) (Amthor 2000). Drought may also reduce

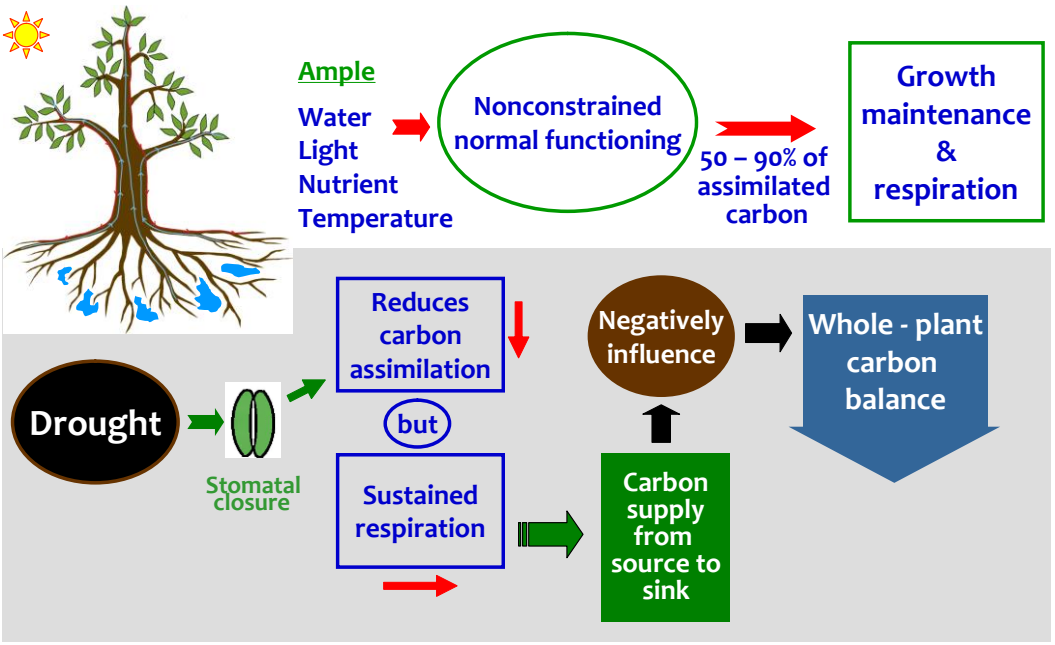

Fig. 1.5 Carbon depletion is one of the underlying mechanisms of drought-induced plant mortality due to a negative carbon balance where respiration > carbon assimilation. During normal functioning with ample water, light and nutrient supply and under normal temperature, plants can spend more than 50% (and maybe even up to 90%) of their assimilated carbon for maintenance/growth respiration. In autotrophic tissues, water stress reduces carbon assimilation through stomatal closure but has little effect on respiration and this leads to negative net carbon assimilation rates. The sustained maintenance of respiration in heterotrophic tissues during drought requires that carbon is supplied from sources (storage) to the sinks and this will further and negatively influence the whole-plant carbon balance (McDowell et al. 2008).

photosynthesis by other mechanisms including loss of leaf turgor, leaf shedding and increased leaf temperature (Brodribb 2009). When elevated temperature accompany drought, reduced photosynthesis may result from the impact of temperature on photosynthetic optima, both on electron transport and Rubisco activity (Breshears et al. 2005; Sage and Kubien 2007). Mesophyll conductance to CO_2 also shows temperature optima, and therefore may also be a constraint on photosynthesis under temperature extremes (Diaz-Espejo et al. 2007).

Recent reports on drought-induced tree mortality suggest that carbon starvation under drought stress is to a large extent hydraulically driven (**Fig. 1.6**) (McDowell et al. 2008). To maintain tissue hydration and photosynthesis, plants must replace water lost through transpiration (E). As described by the cohesion tension theory, E generates tension that pulls water from the soil through the plant to the crown, where it diffuses to the

atmosphere. Thus, E can be explicitly described via the steady-state formulation of the soil–plant–atmosphere hydraulic continuum (modified from Whitehead 1998): $E = K_{leaf}(\Psi_{soil} - \Psi_L - hp_wg)$. In this corollary to Darcy's law, K_{leaf} is leaf-specific hydraulic conductance of the soil-plant continuum, Ψ_{soil} and Ψ_L are soil and leaf water potentials, respectively, and hp_wg is the gravitational pull on a water column of height h and density p_w. However, E has an upper limit (E_{crit}) because increasing tension causes decreased K_{leaf} as a result of air entry through pit pores into conduits, thereby initiating cavitation (nucleation of vaporization) and producing an embolized, or air-filled conduit (McDowell et al. 2008).

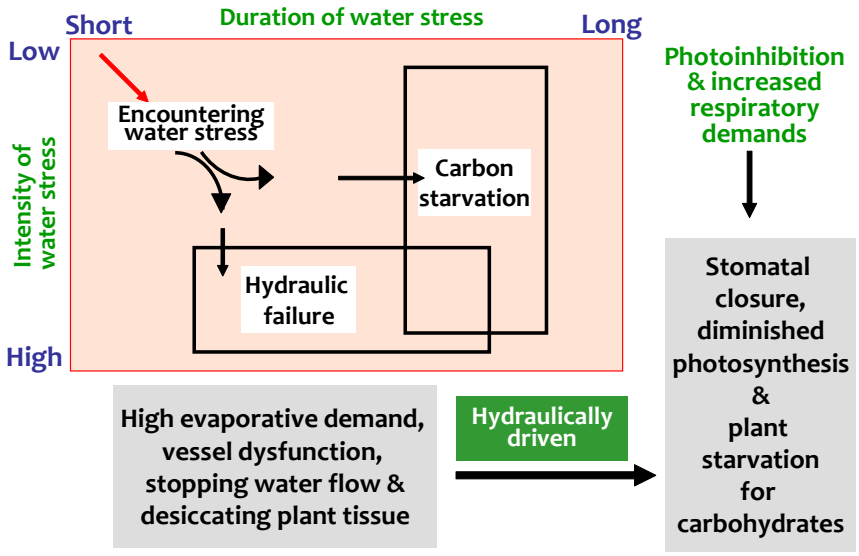

Fig. 1. 6 Theoretical relationship, based on the hydraulic framework, between the temporal length of drought (duration), the relative decrease in water availability (intensity), and the mechanisms underlying mortality. Carbon starvation is hypothesized to occur when drought duration is long enough to curtail photosynthesis longer than the equivalent storage of carbon reserves for maintenance of metabolism. Hydraulic failure is hypothesized to occur if drought intensity is sufficient to push a plant to cross its threshold for irreversible desiccation before carbon starvation occurs (modified from MacDowell et al. 2008).

In other words, hydraulic failure occurs when E exceeds the critical Ψ, K_{leaf} approaches zero, and the plant can no longer move water. The Ψ_{crit} value causing 100% cavitation

varies widely among species (Pockman and Sperry 2000; Maherali et al. 2004) and is thought to be a function of interconduit pit structure (Pittermann et al. 2005). The concept underlying the hydraulic-failure hypothesis is that drought causes the species- and site-specific E_{crit} to be surpassed so that the plant irreversibly desiccates. The prediction that hydraulic failure and not carbon starvation is a key driver of mortality in woody tree species was examined by Breshears et al. (2009). During the 2000-2002 drought, when piñon and juniper experienced region-scale mortality, Breshears et al. (2009) observed that predawn water potential in those trees was below –2.0 MPa for 11 months before the observed mortality, effectively precluding carbon gain for a year. Further support to this prediction on mortality of tree species has come from some of the recent studies examining a broader set of plant species (van der Molen et al. 2011).

Mechanisms to maintain homeostasis in hydraulic and leaf gas exchange functions under drought

The morpho-physiological adjustments that maintain homeostasis between water supply, water demand, and plant metabolism may all play a role in the survival or mortality of plants during drought (Cinnirella et al. 2002; Katul et al. 2003; Bréda et al. 2006). These adjustments are influenced over time scales in response to climate, plant size, edaphic properties such as soil texture and depth, and stand density (Maherali and DeLucia 2001; McDowell et al. 2002, 2006; Sperry et al. 2002; Mencuccini 2003). The homeostatic factors that have been empirically documented include: (i) vulnerability of xylem conductance to low water potentials (Pockman and Sperry 2000; Ogle and Reynolds 2002; Maherali et al. 2004); (ii) xylem permeability (McElrone et al. 2004); (iii) refilling of cavitated elements (Holbrook and Zwieniecki 1999; Tyree et al. 1999; Salleo et al. 2004; West et al. 2007a); (iv) the soil-to-leaf water potential gradient (Hacke et al. 2000; McDowell et al. 2002; Barnard and Ryan 2003); (v) vertical distribution of root density as a function of soil water availability (Ewers et al. 2000; Hacke et al. 2000; Lloret et al. 2004; West et al. 2007b); (vi) ratio of root absorbing area to leaf area (Ewers et al. 2000; Hacke et al. 2000; Magnani et al. 2000); (vii) ratio of sapwood area to leaf area (Mencuccini and Bonosi 2001; McDowell et al. 2002, 2006; Barnard and Ryan 2003);

(viii) leaf shedding (Suarez et al. 2004; Hultine et al. 2006); (ix) optimizing height (McDowell et al. 2005; Addington et al. 2006); and (x) capacitance (water storage, Phillips et al. 2003). Others, such as osmotic regulation of leaf turgor (Kozlowski and Pallardy 2002), foliar water absorption (Breshears et al. 2008), aquaporin mediated hydraulic conductance (McElrone et al. 2007) and cellular desiccation tolerance (Sherwin et al. 1998), may also play important roles in drought tolerance or avoidance. Each of these factors may strongly impact the likelihood of plants to survive or succumb to drought. Over diurnal timescales, plants maintain E below E_{crit} through stomatal closure. Plants reduce stomatal conductance (G_s) in response to increasing E, with the degree of closure linked to Ψ_{crit} that causes embolism (Sperry et al. 2002). Stomatal conductance is regulated not only by water supply and demand, and their impact on E, but also by plant structural adaptations that impact the supply or demand for water, for example rooting volume or leaf area, respectively (McDowell et al. 2008). While reducing G_s serves the benefit of reducing water loss, it has the cost of reducing CO_2 diffusion from the atmosphere to the site of carboxylation, and thereby constraining photosynthetic CO_2 uptake. This balance between water loss and CO_2 uptake may partition plants between survival, hydraulic failure or carbon starvation during drought.

Mulberry – An ideal tree model to study drought-induced photosynthetic and hydraulic responses

Mulberry (*Morus* spp L. Moraceae), a pioneer tree of secondary succession, is one of the first commercialized foliage crops in the world and has been cultivated transcontinentally covering 50 countries across the globe. There are about 68 species of the genus *Morus*, the majority of them occur in Asia, especially in China (24 species) and Japan (19 species). Mulberry is also widely represented in Europe, North and South America, Africa and Latin America (Biasiolo et al. 2004). In the past, mulberry trees were predominantly cultivated for sericulture industry to rear the silkworm *Bombyx mori* L. However, research studies for the last two decades have revealed several other potential uses of mulberry. In China, India and many other Asian countries mulberry leaves are now used as medicinal herb and leafy vegetable. But the newest and most modern use of the mulberry is for animal feeding. Recently, mulberry is gaining popularity in many countries (Mediterranean areas of

Europe, India, Cambodia, Tanzania, Turkey, China, etc.) as forage for livestock feeding as the leaves are highly rich in protein, antioxidants and minerals without any toxic elements (Machii et al. 2000; Papanastasis et al. 2008). Several reports have emphasized the prospect of mulberry foliage as a feed for both ruminants and non-ruminant animals. In India, leaves are fed to cattle and stated to improve milk yield when fed to dairy animals (Papanastasis et al. 2008). The 'SILK-N-MILK' scheme is gaining wide popularity in India in which sericulture farmers are exploiting mulberry foliage for both silkworm rearing as well as for dairy milk production. Mulberry is maintained as low to high bush plantation and it produces very large amounts of renewable biomass in the form of branches, shoots, leaves and fruits (Dandin et al. 2003). As the tree is mainly propagated by cuttings in tropics and sub-tropics, certain quantity of pruned branches are used for preparation of cuttings and the remaining as fuel-wood. One hectare of mulberry garden can yield about 12.1 MT of mulberry sticks from which the energy generated/ha (50% moisture loss) will be almost 27830 Kcal (@ 4600 calories/kg of mulberry wood) (Machii et al. 2000). Accordingly, mulberry can be exploited by raising the trees as "energy plantation" in cultivable/wasteland/low lying areas/canal bund/road side/fringe areas of the forest under various afforestation, watershed development and soil conservation programmes. Thus, mulberry is considered as an extremely versatile tree crop which can fulfill a number of roles in small-holder agricultural production. Its value is multifaceted and the potential for increasing and diversifying its use is enormous.

In India, there are four species of *Morus* of including *M. alba*, *M. indica*. *M. serrata* and *M. laevigata* of which most of the Indian cultivars of mulberry belong to *M. indica* and some belong to *M. alba*. Several cultivars have also been introduced to India belonging to *M. multicaulis*, *M. nigra*, *M. sinensis* and *M. phillippinensis*. Though mulberry cultivation is practiced in various agroclimates, the major area (90% of the cultivated area) is in tropical zone covering Karnataka, Andhra Pradesh and Tamil Nadu states. In the subtropical zone, West Bengal, Himachal Pradesh and north-eastern states have major areas under mulberry cultivation. The total acreage of mulberry in India is around 282,244 ha (Dandin et al. 2003). Mulberry growth and productivity are remarkably influenced by the climatic variations. Water availability is one of the most important determinants of leaf yield in mulberry (Chaitanya et al. 2003). Mulberry requires 500 to

700 litres of water to produce one kilogram of fresh leaf (Karaba et al. 2008). High yielding mulberry cultivars are prodigal water consumers due to their faster growth rate, large cumulative leaf area and canopy size. Hence water deprivation can arrest the growth and leaf yield performance of elite mulberry cultivars as a consequence of down-regulated photosynthesis and carbon assimilation (Karba et al. 2008).

The relationship between yield loss and water stress severity can differ largely among mulberry genotypes. From agro-economical viewpoint, the functional definition of drought tolerance in mulberry crop should be based on yield stability which precisely indicates less fluctuation in yield components in a drought tolerant genotype compared to the susceptible one when exposed to water deficit. Stabilizing yield performance requires optimization of the physiological processes involved in the critical stages of plant response to soil dehydration. Several morpho-physiological and biochemical mechanisms including water use efficiency, photosynthetic capacity, radiation use efficiency, rooting vigour, antioxidative protection, osmotic adjustment, stay green etc, are linked to enhanced performance and yield stability in agreement with stress-tolerance syndrome. A *priori* knowledge of these candidate crop traits contributing to drought tolerance is essential before designing crop improvement programmes for any crop model. Recent investigations on the functional linkage between hydraulic capacity and CO_2 assimilation rate have provided enormous implications for understanding how hydraulic capacity determines photosynthetic performance and whole plant productivity. Water transport physiology defines many aspects of the daily function of plants, and investigations on hydraulic capacity and resistance to cavitation will yield greater advances in our ability to manipulate plant function under drought.

Till date, we have only handful information on mulberry regarding its responses under different abiotic stress conditions including drought (**Table 1.1**). Only few reports provide preliminary information on photosynthetic characteristics in mulberry under water stress conditions (Ramanjulu et al. 1998; Chaitanya et al. 2003). Moreover, knowledge on hydraulic physiology and associated photosynthetic productivity in mulberry under soil moisture stress conditions is far from complete, particularly considering that the most limiting parts of the hydraulic pathway in stems and leaves remain poorly understood. In spite of being an age-old tree crop, such trait-based investigations for identifying

differential hydraulic capacity in mulberry genotypes and understanding the coordination, linking K_{plant} with photosynthetic capacity and biomass productivity as well as the shift of this coordination under water limitation have not been undertaken in mulberry crop. Thus, understanding the hydraulic-photosynthetic coordination, identifying physio-biochemical responses in relation to photoprotection, photostability and hydraulic capacity in dehydrated shoots and exploring genotypic diversity in hydraulic architecture in relation to hydraulic performance can provide important clues to manipulate photosynthetic and hydraulic traits for improving tree crop productivity in mulberry under drought. Moreover, the tree is amenable to short-term coppicing treatments and can grow in a wide range of agroclimatic conditions and possess several other unique attributes (see **Box 1.1**), it can also be a model tree species to study drought-induced photosynthetic and hydraulic responses.

Table 1.1 Summary of the important reports available on characterizing responses in mulberry under abiotic stress conditions.

Stressor	No. of cultivars	Parameters studied	References
PEPG	9	Morpho	Rao et al. (1997)
Coastal saline soil	12	Phy, Biochem	Agastian and Vivekanandan (1997)
Water stress	2	Phy, Biochem	Ramanjulu et al. (1998)
NaCl	2	Phy, Biochem	Giridara Kumar et al. (2000)
NaCl	5	Morpho	Tewary et al. (2000)
High temperature	1	Biochem	Chaitanya et al. (2001)
Water stress	1	Biochem	Barathi et al. (2001)
NaCl	63	Morpho	Vijayan et al. (2003)
Water stress	5	Phy, Biochem	Chaitanya et al. (2003)
Water stress	5	Phy, Biochem	Ramachandra Reddy et al. (2004)
NaCl	4	Phy, Biochem	Lal et al. (2006)
High temperature and drought	9	Biochem	Kotresha et al. (2007)
NaCl	5	Morpho, Anat, Biochem	Vijayan et al. (2008)
Water stress	2	Phy	Karatassiou et. al. (2008)
NaCl	5	Phy, Biochem	Lal and Khurana (2009)
Drought	4	Phy, Biochem	Ren (2009)
Drought	5	Biochem	Chaitanya et al. (2009)
NaCl	11	Morpho, Phy, Biochem	Vijayan et al. (2010)
$NaHCO_3$	2	Phy, Biochem	Ahmad and Sharma (2010)
Control	9	Phy, Mol	Mishra and Dandin (2010)
Aerial drying and NaCl	10	Phy, Biochem, Mol	Das et al. (2011)

Anat anatomical; *Biochem* biochemical; *Mol* molecular; *Morpho* morphological; *Phy* physiological

Box 1.1 Some of the important characteristic features of mulberry which make it a unique model tree species for conducting studies on drought-induced photosynthetic and hydraulic responses.

The sketch of mulberry is drawn by Gideon Kendall, a Brooklyn-based illustrator, artist, cartoonist and musician

- **Pioneer tree of secondary succession**
- **Well known perennial tree crop**
- **Potential biomass energy crop**
- **Wide biodiversity and genetic resources**
- **Evergreen, deciduous and semideciduous**
- **Distributed in temperate and tropical climates**
- **Deep root system**
- **Able to grow over a wide range of soil types**
- **Fast juvenile growth**
- **Profuse branching**
- **High foliage yielding capacity**
- **Amenable to sexual & vegetative propagation**
- **Respond well to coppicing treatments**

Framed objectives

In this PhD dissertation research, photosynthetic responses and hydraulic performances in mulberry under drought stress conditions were critically investigated. Particular emphasis was placed on examining how photosynthetic leaf gas exchange, photosystem-II efficiency and hydraulic conductance differ among the genotypes and determine plant functional responses in relation to drought which can in turn be related to crop growth and biomass productivity. The in-built hydraulic architecture of the mulberry genotypes in terms of safety and efficiency trade-offs was explored and the significance of hydraulic architectural traits in defining genotypic performance under water-limited conditions was also examined. The following research objectives are addressed in the thesis:

1. Investigating variation in growth and biomass yield among mulberry genotypes in relation to photosynthetic and hydraulic traits.

2. Screening of mulberry germplasm for drought stress tolerance and assessing photosynthetic and hydraulic performances of the tolerant and susceptible genotypes.

3. Dynamics of photosynthetic and hydraulic acclimation processes in mulberry during progressive drought stress.

4. Characterizing stomatal regulation and hydraulic behavior in mulberry under water deficit.

5. Exploring variation in stem wood hydraulic architecture among mulberry genotypes in relation to hydraulic behavior and drought stress tolerance.

Variation in Growth and Biomass Yield among Mulberry Genotypes in Relation to Photosynthetic and Hydraulic Traits

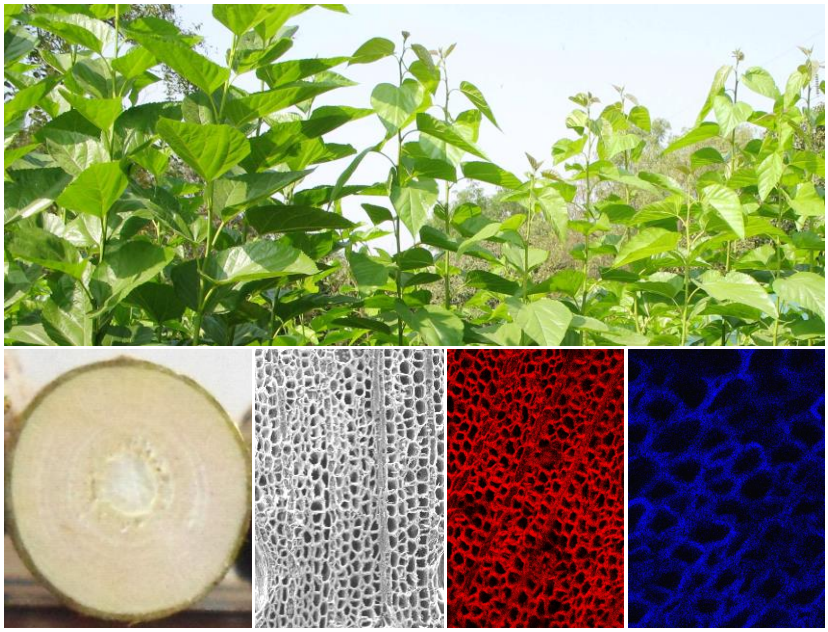

Chapter 2

Biomass energy is the most abundant and versatile renewable energy resource which is gaining popularity worldwide in bioenergy applications. In the past few decades, intensive research has been undertaken for the cultivation of fast-growing tree species to generate woody biomass energy. Several tree species including cottonwood, red alder, aspen, willow, poplar, *Acacia*, eucalyptus and Douglas fir, etc., have been evaluated in different countries for their bioenergy applications and many of them are still undergoing field reconnaissance surveys (Hinchee et al. 2009; Karp and Shield 2008). So far, only few tree species like *Salix*, poplar and eucalyptus have been predominantly cultivated as short rotation coppice (SRC); however, their cultivation is mostly restricted to developed countries dealing with specific energy requirements and commercial goals (Lu et al. 2009). No single woody species ranked highest for use in bioenergy system as the suitability of any species depends not only on its wood quality but also on several other factors including ease of propagation, ability to coppice, survivability, available silivicultural knowledge, ecosystem integrity and local acceptance for the species. A greater emphasis is now being laid on the identification and promotion of new candidate fast-growing woody trees which are easily propagatable, cultivable in varied agroclimatic regions, can undergo intensive coppicing treatments, produce quality fuel

wood and offer several other economic and social benefits (Christersson 2010). It will be a worthwhile exercise to identify new candidate trees which are easily propagatable, cultivable in varied agroclimatic regions, can undergo intensive coppicing treatments, exhibit resilience against stress conditions, produce quality fuel wood and offer several other economical and social benefits.

Earlier reports on biomass productivity of mulberry indicated that the trees grow very fast and can yield up to 45.2 tons $ha^{-1}year^{-1}$ dry biomass depending upon genotype, location, plantation density, fertilizer applications and harvesting techniques (Sánchez 2000). Depending on the end product needed, different cultural systems have been designed and followed in mulberry. The growth, branching, canopy size and shape of mulberry trees can be efficiently managed by periodical pruning and coppicing treatments. Coppicing has been a traditional practice in mulberry cultivation where the plantation is coppiced on very short rotation (3-4 months) as well as on longer ones (10-12 months), depending upon agroclimatic situations (irrigated/semi-irrigated/dryland) (Suzuki et al. 1988; Dandin et al. 2003). In irrigated farms, coppicing four to five times can be done annually without any loss in vitality, provided adequate fertilization and manuring are undertaken during each rotation (Dandin et al. 2003). Majority of mulberry species have rapid juvenile growth; the proleptic and sylleptic shoots show strong growth vigor and produce large amounts of woody biomass apart from their major economic commodities (foliage and berries) (Suzuki et al. 1988; Dandin et al. 2003). Such rapid growth and high biomass yielding capacity have bestowed upon mulberry the status of an excellent and potential energy crop. Moreover, recent findings showed that the stem wood in mulberry is dense with high cellulose content, low moisture and little ash content, possessing high calorific value and excellent combustion characteristics (Lu et al. 2009). Thus, the emerging prospect of mulberry as an energy crop seems to have crucial importance in future bioenergy applications.

A large genotypic variation in growth performance and biomass yield exists in mulberry (Dandin et al. 2003) which offers immense possibilities for breeding programmes capable of producing new improved genotypes with enhanced biomass productivity. For improved yield, appropriate ‘physiological traits’ need to be identified which are good indicators of better growth performances and high biomass productivity (Bunn et al. 2004).

Amongst various leaf-level photosynthetic traits, leaf growth physiology, leaf area, light interception, leaf gas exchange, biochemical efficiency of photosynthesis and intrinsic water-use efficiency are critical determinants of biomass productivity (Marron et al. 2007; Dillen et al. 2010). The importance of photosynthesis in crop yield arises from the role it plays in the productivity of both natural and agricultural ecosystems. Because plant biomass is largely derived from photosynthetically captured carbon (Flood et al. 2011), variation in the efficiency or capacity of photosynthesis can lead to variation in growth rate and productivity, which are important factors in species competition and crop yield. It is becoming apparent that photosynthesis will have a key role in any sustainable society. To this end there have been several recent reviews both on the importance of photosynthesis and putative ways in which it might be improved to benefit human society (Peterhansel et al. 2008; Murchie et al. 2009; Sun et al. 2009; Zhu et al. 2010). These reviews mostly have a largely biotechnological focus, considering the ways in which photosynthesis could be engineered to suit our needs. However, the potential of genetic diversity in photosynthesis has been largely ignored in recent years, with the last review on this topic published over 21 years ago (Austin 1989) and only a recent one by Flood et al. (2011).

The nature and significance of variation in photosynthesis are dependent on the unit of measurement chosen. The photosynthesis of a community of plants such as a crop can be quantified as the photosynthetic rate per unit ground area, the rate per individual or the rate per unit area of the leaf (Flood et al. 2011). Each of these has particular uses and applicabilities, and although it is relatively easy to translate rate per unit ground area to rate per plant and vice versa, the rate per unit leaf area is not easy to translate to either of the other two. Photosynthesis on a unit leaf area basis needs to be integrated to give the rate per plant or unit area of the crop, and this requires knowledge of factors such as leaf area index (LAI), the variation of photosynthetic properties on an area basis between leaves and the architecture of the canopy (Flood et al. 2011). The standard way of describing photosynthesis is as a rate of CO_2 fixation per unit leaf area with 'better' photosynthesis being that with the highest rate per unit area under specified circumstances. In the present study, while considering variation in the properties of photosynthesis, CO_2 fixation data will be expressed on a unit leaf area basis because this is how the activity of the photosynthetic process is best described and most easily understood in physiological terms.

In the other metrics of photosynthesis, such as the rate of carbon dioxide fixation per plant or per unit area of crop, the activity at the leaf-level is combined with other factors, such as plant morphology and architecture that are non-photosynthetic in character. Also, in the major crop plants, plant architecture and LAI have been brought close to optimal levels by breeders and thus show limited potential for future crop improvement (Long et al. 2006; Parry et al. 2011). This is in contrast to photosynthesis per unit leaf area, which has remained largely unexploited.

Net photosynthetic rate is intimately related to productivity across a wide array of plant species, although the relationship between photosynthetic capacity and biomass yield is not always positively correlated in trees, which might be due to the complexity of photosynthesis (polygenic control), complex allocation patterns of carbon as well as sampling error while measuring photosynthesis (Dillen et al. 2010; Flood et al. 2011). Often, for practical reasons, photosynthetic rates are measured on only one leaf and at only one time. Photosynthetic rate however, varies between leaves and with time in individual leaves. The tendency to use the photosynthetic rate per unit leaf area of a few leaves or even just a portion of one leaf, as a measure of the photosynthetic capacity of the plant as a whole has often led to a lack of correlation between photosynthetic capacity and plant yield. Measurement of the photosynthetic properties of leaves ideally requires a rigorous measuring regimen per plant. In the past, this has made it difficult to describe fully the photosynthetic properties of plants when large populations need to be investigated. To accurately estimate the photosynthetic capacity of a plant, care must be taken to sample a sufficient number of leaves; the necessary representative sample size will vary depending on factors such as canopy architecture and leaf age distribution. Because leaves are the basic unit of most photosynthetic measurements, particularly at the crop or ecophysiological level, the source of leaf level photosynthetic variation is of great interest.

Other leaf traits such as leaf longevity, leaf surface area per unit mass (specific leaf area; SLA) and leaf nitrogen content are sometimes correlated with biomass productivity depending on species, growth conditions and tree age (Monclus et al. 2005). Photosynthesis is intimately associated with leaf gas exchange which in turn is regulated by plant hydraulic conductance. Hydraulic conductance controls leaf osmotic potentials and plant morphology, such as the ratio of leaf area to fine-root area (Shimizu et al. 2005)

and twig hydraulic conductance regulates stomatal conductance and thus the rate of photosynthesis (Uemura et al. 2004). Wood density, in addition to being positively associated with mechanical strength of stems (Givnish 1995), is negatively associated with hydraulic conductivity in twigs (Santiago et al. 2004), percent loss of twig hydraulic conductivity under drought conditions (Hacke et al. 2001; Sperry 2003) and daily minimum water potentials in leaves (Ackerly 2004; Bucci et al. 2004a; Santiago et al. 2004). Leaf carbon economy and whole-plant hydraulic system are thus coordinated with each other and the coordination may be associated with life history features and biomass productivity potential of a tree species (Wright et al. 2006). The relevance of these productivity traits, both at whole-plant and leaf levels, is well documented in important bioenergy tree crops including poplar, willow and loblolly pine (Bunn et al. 2004; Marron et al. 2007; Dillen et al. 2010; Monclus et al. 2005; Jeżowski et al. 2011; Aspinwall et al. 2011). However, the implication of such productivity determinants still remains an open question in mulberry tree improvement programmes. As a major proportion of overall tree biomass constitutes of stem wood, it is also necessary to identify physical and structural traits of wood that are stable productivity determinants of high woody biomass. Wood density and fibre characteristics are the most important properties related to woody biomass production (Pliura et al. 2007). Further, important contributions of stem wood characteristics have been reported in trees, with implications for potential photosynthetic capacity and canopy productivity due to the inherent coordination of these traits (Brodribb and Feild 2000). In mulberry, the rationale and possibility of including stem wood characteristic features as important selection criteria for enhanced wood quantity and quality have not been tested till date and need to be explored.

With this background, the present study was undertaken to obtain insights into the productivity determinant traits of high biomass yielding mulberry genotypes as well as to assess the robustness of the relationships between yield and those productivity determinants. A field-based trial was undertaken using diverse mulberry genotypes of differential productivity potential. The genotypes were examined using suites of leaf-and stem wood-level productivity indices. The primary aim was to determine the extent to which variation in those productivity indices can explain genotypic variation in biomass productivity. Consequently, the three following questions were addressed in this chapter:

(1) To what extent do productivity traits including plant growth, shoot characteristics, foliage and woody biomass yields differed across the investigated mulberry genotypes? (2) Are leaf functional traits including photosynthetic gas exchange, light response traits, photosystem-II characteristics, hydraulic efficiency, SLA and nitrogen concentration correlated with biomass productivity? (3) Can quantitative yield of woody biomass be predicted from wood density, wood anatomical traits and stem wood fibre characteristics?

Materials and Methods

Study site

The present study was conducted in the mulberry plantation stand at University of Hyderabad (17.3°10´N and 78°23´E at an altitude of 542.6 m above mean sea level, MSL) located 20km north of Hyderabad metropolitan, Southern India. The regional climate is hot-steppe (Köppen climate classification) characterized by distinct hot dry summer lasting from Mar until Jun followed by south-west monsoonal rain during Jul-Sep. Our experiments were carried out for two consecutive years (2009 and 2010) during monsoon covering two experimental seasons: exp season-I (Jul 2009 to Oct 2009) and exp season-II (Jul 2010 to Oct 2010). Mean total precipitation during experimental time span was ~508.9 mm and 595.8 mm in exp season-I and II, respectively. Mean air temperature recorded during day time ranged from 22.6°C to 34.9°C (exp season-I) and from 22.2°C to 35.2°C (exp season-II), mean relative humidity (RH) varied between 34 to 82% (exp season-I) and from 43 to 86% (exp season-II), mean atmospheric CO_2 concentration was 390±5 µmol mol^{-1} and mean photosynthetically active radiation (PAR) (measured between 09.00 -11.00 h) ranged from 1500 to 2000 µmol m^{-2} s^{-1}(exp season-I) and from 1200 to 1800 µmol m^{-2} s^{-1}(exp season-II). The soil of the experimental plot was shallow alfisol with a pH of ~7.5 and soil organic carbon content of ~5.21%.

Plantation establishment, selection of genotypes and experimental design

Between Nov 2007 to Jun 2008 (establishment period), short rotation coppice (SRC) plantation of 22 mulberry genotypes (a mini-core collection: **Table 2.1**) was

established using four month old rooted saplings in a net plot size of 24.4 m x 24.4 m (12.6 m rows, 0.6 m apart with 224 plants in a plot) following randomized block design (RBD)

Table 2.1 Mini-core collection of 22 mulberry genotypes.

	Genotype (Code)	Species	Collection/Origin
1.	Alkaline Resistant-12 (AR12)	*M. indica* L.	Mysore, India
2.	Bogurai-4 (BOG4)	*M. indica* L.	Bogura, Bangladesh
3.	Dehradun (DD)	*M. indica* L.	Uttarakhand, India
4.	Dehradun -2 (DD2)	*M. indica* L.	Uttarakhand, India
5.	Dodda Sala (DS)	*M. indica* L.	Northern India
6.	Haridwar-4 (HD4)	*M. indica* L.	Uttarakhand, India
7.	Jhoropakari (JPK)	*M. indica* L.	North East India
8.	Kanva-2 (K2)	*M. indica* L.	Mysore, India
9.	Krishnaswami-2 (KS2)	*M. indica* L.	Karnataka, India
10.	Kollegal Local (KL)	*M. indica* L.	Kollegal, India
11.	Mildew Resistant-2 (MR2)	*M. indica* L.	Coonoor, India
12.	Mysore Local (ML)	*M. indica* L.	Mysore, India
13.	Mandalaya/Selection-1 (S1)	*M. alba* L.	Mandalay, Myanmar
14.	Papua New Guinea (PNG)	*M. alba* L.	Papua New Guinea
15.	Selection-13 (S13)	*M. indica* L.	Mysore, India
16.	Selection-20 (S20)	*M. indica* L	Mysore, India
17.	Selection-34 (S34)	*M. indica* L.	Mysore, India
18.	Selection-36 (S36)	*M. indica* L.	Mysore, India
19.	Selection-1635 (S1635)	*M. indica* L.	Berhampore, India
20.	Thai Beelad (TB)	*M. alba* L.	Thailand
21.	Triploid -10 (TR10)	*M. indica* L.	Berhampore, India
22.	Victory-1(V1)	*M. indica* L.	Mysore, India

Fig. 2.1 Short rotation coppice (SRC) stands of 22 mulberry genotypes raised in the experimental farm at University of Hyderabad, Hyderabad.

with four blocks per genotype (**Fig. 2.1**). After establishment period, all plants were manually cut (on 1st week of Jul 2008) at a stump height of 30 cm above soil surface to create a coppice culture system. Thereafter, the plantation is coppiced every time at an interval of four months (every 4-month constituted one short rotation cycle) following the schedule of 3 harvest cycles in a year. Once the plantation raised in the previous season was coppiced and harvesting was complete, the intercultural operations were undertaken (Dandin et al. 2003). Shoots, resprouted from the remaining stumps were grown for next 4 months for the subsequent harvest. Growth performance of the genotypes was assessed using two important indicators: plant height (H_t) and stem diameter (D_{100}, at 100 cm height from the stem base) as measured during initial two short-rotation cycles (cycle-1: Jul 2008 to Oct 2008; cycle-2: Nov 2008 to Feb 2009), just after the establishment period (**Fig. 2.2**). Based on the growth performance, mulberry genotypes were tagged and clustered into three different performance groups (PG) including high (HPG), average (APG) and poor (PPG) (**Table 2.2**). For the present study, we selected a representative sample of genotypes differing in growth strategies and biomass yield potential in order to represent the variability of functional types (**Table 2.3**). We included genotype Victory-1 (V1) as a reference because it is widely tested in Southern India and well-known for its fast growth, high leaf yield and huge biomass production capacity. Exp season-I and II were eventually the 4th (cycle-4) and 7th (cycle-7) short rotation cycles, respectively after the establishment season. Soil of the experimental site was analyzed at the rooting zone of the stands (30-40 cm soil depth) to determine gravimetric soil moisture content (SMC). Irrigations were applied whenever SMC dropped below 60%, so that the soil moisture remained constantly high and that the plants grew under optimal water conditions. It is also a commercial practice to maintain such optimum moisture level in irrigated mulberry farms of India in order to achieve higher crop yield (Dandin et al. 2003).

Leaf gas exchange and photosynthetic light response characteristics

Leaf gas exchange and microclimatic data were measured between 09.30 and 10.30 h on fifteen different sunny days during each experimental season. Six representative plants (tallest ones from the blocks) were tagged from each genotype for conducting gas-exchange studies and the same (plants originating from the same stumps) were used to

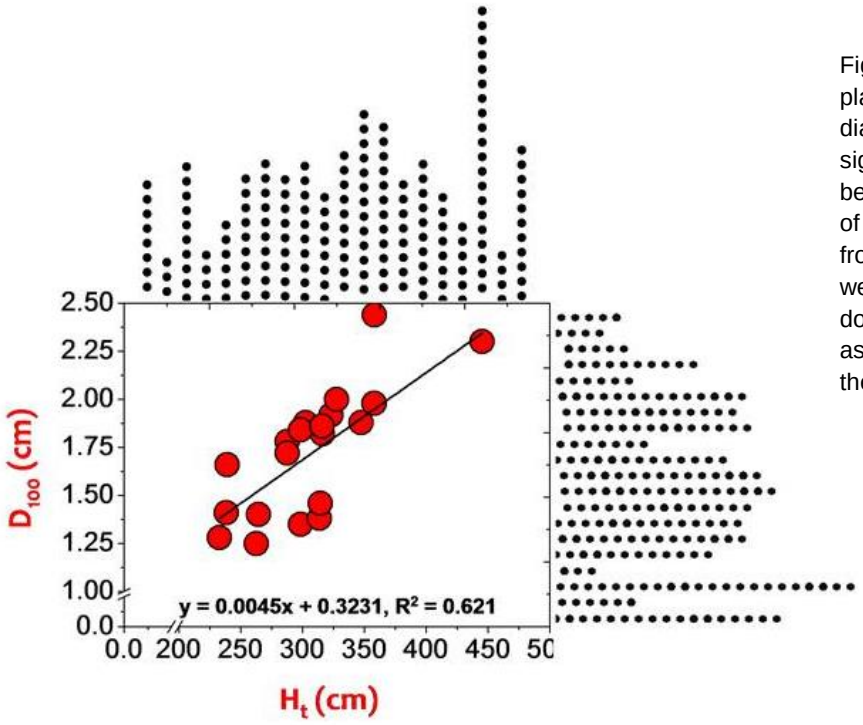

Fig. 2.2 Relationship between plant height (H_t) and stem diameter (D_{100}) showing significant positive correlation between these two yard sticks of biomass productivity. Data from 22 mulberry genotypes were used for analysis. The dotted histograms show the association of one trait with the other corresponding trait.

Table 2.2 Clustering of genotypes into three performance groups including high (HPG), average (APG) and poor performance group (PPG).

Performance group			
HPG	APG		PPG
TB	KL	KS2	JPK
S1	S34	S20	S1635
S13	ML	AR12	DS
V1	DD	MR2	TR10
PNG	K2	S36	BOG4

Table 2.3 List of mulberry genotypes including high, average and poor performance groups along with a reference high yielding genotype selected with respect to plant height (H_t) and stem diameter (D_{100}) measured during initial two SRC cycles (cycle-1: Jul 2008 to Oct 2008; cycle-2: Nov 2008 to Feb 2009). Presented H_t and D_{100} are the mean of data (±SE) obtained from the two SRC cycles. Values followed by the same letters within a single column are not statistically different.

Performance group	Genotypes	Collection/Origin	H_t (cm)	D_{100} (cm)
High	S1	Mandalay, Myanmar	357.8(7.0)b	1.98(0.01)c
High	TB	Thailand	445.2(6.2)a	2.30(0.02)a
Average	ML	Karnataka, India	314.1(8.6)c	1.46(0.03)d
Poor	TR10	West Bengal, India	238.4(5.1)d	1.41(0.01)e
Poor	JPK	North-east India	264.2(8.3)d	1.40(0.06)e
Poor	S1635	West Bengal, India	262.7(7.4)d	1.25(0.04)f
Reference	V1	Karnataka, India	327.5(5.8)bc	2.00(0.01)b

analyse photosystem-II (PSII) characteristics and leaf water relations. Net CO_2 fixation rate (P_n), leaf transpiration (E), stomatal conductance (G_s) and sub-stomatal CO_2 concentration (C_i) were measured simultaneously accessing fully-expanded and healthy sunlit leaves of the upper canopies using a portable infrared CO_2/H_2O gas analyzer (IRGA) (LCpro-32070, ADC Bioscientific Ltd. U.K.). The gas analyzer was equipped with a detachable broad leaf chamber (LCpro-32070, U.K.) with PAR sensor (silicon based sensor, LCpro-32070) and leaf thermistor probe (ADC, M.PLC-011, LICOR) attached to it. Microclimatic parameters such as irradiance (PAR: 1600-1800 µmol m^{-2} s^{-1}), relative humidity (RH: ~40%), air temperature (T_a: 28-32°C), CO_2 concentration (370-380 µmol mol^{-1}) and flow rate (~380 µmol s^{-1}) were recorded by the instrument. Each photosynthetic measurement was made after obtaining the steady state conditions (indicated by steady G_s and P_n readings), typically requiring a minimum of 2 min under standard conditions. Instant water use efficiency ($WUE_i = P_n/E$) was also determined for every genotype. Photosynthetic light response (0, 250, 500, 750, 1000 and 2000 µmol m^{-2} s^{-1} PPFD) studies were conducted using LCpro-32070 and the PPFD was provided by a LED light source attached to a broad light unit (LCpro Lamp 32070 - Broad, ADC Bioscientific Ltd. U.K.) of the leaf chamber. The microclimatic conditions inside the leaf chamber were kept the same as maintained during leaf gas exchange analysis. Photosynthetic rate was fitted as a function of incident light by using Mitscherlich model equation (Peek et al. 2002): $P_n = P_{nmax} [1- e^{- \phi (PPFD - Icomp)}]$ where P_{nmax} represents the asymptote of photosynthesis at high light, ϕ corresponds to the initial slope of the curve at low light levels, I_{comp} denotes the x-intercept, when net photosynthesis is equal to zero, PPFD refers to the incident photosynthetic photon flux density and P_n is net photosynthesis, the response variable. The P_{nmax}, ϕ and I_{comp} used in the model, identify the light-saturated rate of photosynthesis, apparent quantum yield and photosynthetic light compensation point, respectively. Dark respiration rate (R_d), and light saturation point of photosynthesis (I_{sat}) were also determined from the curves and the value of maximum stomatal conductance ($G_{s\ max}$) was recorded from the leaf gas exchange measurements.

Potential photosystem-II (PSII) efficiency and leaf nitrogen concentration

On the same day followed by leaf gas exchange analyses, during 10.00 to 11.00 h, when ambient PAR was saturating (≥1600 µmol m^{-2} s^{-1}), chlorophyll (chl) a fluorescence measurements were made on leaves (same leaves used for leaf gas-exchange analyses) using a portable Handy-PEA chlorophyll fluorometer (Handy-Plant Efficiency Analyser-2126, Hansatech Instruments, King's Lynn, UK). After dark-acclimation for 30 min, minimal fluorescence yield (F_O) and maximal fluorescence induction (F_M) were recorded by illuminating the leaves with a beam of saturating light (3000 µmol m^{-2} s^{-1}) of 650 nm peak wave length, obtained from three light-emitting diodes focused on the leaf surface through the clips of 5 mm diameter circle. Fast fluorescence kinetics (F_O to F_M) were recorded from 10 µs to 1s and the fluorescence intensity at 50 µs was considered as F_O. The variable fluorescence ($F_V = F_M - F_O$), maximum quantum yield of PSII (F_V/F_M) and PI (performance index, a multi-parametric expression) were then estimated from OJIP-test (Strasser et al. 2000) using Biolyzer software vl 31. For leaf nitrogen (N_L), six mature leaves from upper plant canopy were randomly collected and thereafter dried, ground to fine powder and analysed using macro-Kjeldhal technique. The N_L content was calculated on mass basis and was expressed as percentage of dry mass.

Leaf water relations

On six different sunny days during each experimental season, leaf water potential (Ψ_L) was measured diurnally in mature, fully expanded, upper canopy leaves from two to three apical twigs per stand using a portable pressure chamber (Plant Moisture System, SKPM 1400/40, Skye Instruments Ltd, England). All measurements were conducted within 3 min of leaf excision and minimum 6 leaves per genotype from the representative plants were sampled. In-situ leaf-specific hydraulic conductance (K_h) was calculated by analogy to Ohm's law (Tyree 2003) : $K_h = E_{max}/(\Psi_{soil} - \Psi_{md})$, where Ψ_{soil} and Ψ_{md} were predawn soil and midday leaf water potentials, respectively and E_{max} was the peak transpiration rate at the midday in a leaf area basis, measured with infrared gas-analyzer system (LCpro-32070). Instead of Ψ_{soil}, predawn leaf water potential (Ψ_{pd}) was used as a proxy under zero sap flow in the trees. Although stored water can uncouple the close relationship between transpiration and leaf water potential, the calculations of K_h in the present study were made

during peak transpiration (E_{max}) at midday when the effects of capacitance on transpiration were assumed to be minimal (Ryan et al. 2000). Ψ_{pd} and Ψ_{md} measurements were made between 04.00–05.00 solar hours and between 12.30-13.30 solar hours, respectively. Based on diurnal measurements of leaf water potential at the experimental site, Ψ_{pd} and Ψ_{md} corresponded to maximum (Ψ_{Lmax}) and minimum (Ψ_{Lmin}) leaf water potentials, respectively.

Measurements of plant growth and aboveground biomass yield

Eight representative plants per genotype (including the same six, used for studying leaf-level functional traits) were used to study plant morphology, growth characteristics and biomass yield in both the experimental seasons (exp season-I and II). Stem growth and branching patterns of the coppice stands were visually observed and photographed before biomass harvesting. At the end of each season (last weeks of Jun 2009 and Oct 2009 in exp season-I and II, respectively), when the stems were about 110±5 days old, the plants were coppiced for measuring growth characteristics and biomass yields. Stem diameter (excluding the rare thick 'champion' stems) was measured at a height of 100 cm above soil surface and the mean value was used to express the stem diameter (D_{100}). Plant height (H_t) from ground to the canopy top was measured using measuring tapes. Height (HGR) and diameter (DGR) growth rates were calculated by dividing H_t and D_{100} by stand age (Zhang and Cao 2009). The shoots of all the representative plants were coppiced using a sharp secature (a type of pruner) and the aboveground components (leaves, branches and stems) were separated, immediately weighed fresh in the field and the following measurements were undertaken per plant basis: total number of stems (T_{STM}), number of branches (axillary shoots) (T_B), total shoot length (T_{SL}), leaf fresh biomass (L_f), stem fresh biomass (S_f) and total aboveground fresh biomass (AG_{fw}). A sub-sample of leaves was used to determine specific leaf area (SLA), and the value was calculated from the data of leaf area and leaf dry biomass (L_d). After taking fresh weights of shoots, subsamples from stems and branches were chipped, mixed in order to evenly distribute wood of different densities and were oven-dried at 80ºC for several days until constant weight was achieved. Aboveground woody biomass (AG_w) was calculated as the sum of dry weights of all stems and branches and was expressed per plant basis. Dry weights of both wood and bark were included in the

woody biomass. Total above ground dry biomass (AG_{dw}) was determined by adding total L_d and AG_w of a plant.

Analyses of wood characteristics

Wood characteristics were studied at the end of exp season-II. After biomass harvest on the last week of Oct 2009, a subset of fresh stem samples from all the tested genotypes were separated and preserved for analyses of wood characteristics.

Wood density

Wood density (D_w) was calculated from 3-5 cm green (or 'fresh') stem segments cut out uniformly at a stem height of 100 cm from base of all the tested genotypes. To avoid any shrinkage in volume, the fresh stem segments were kept in shade and the green mass and volume were measured on the same day of stem cutting. After carefully removing the bark and pith, each stem segment was impaled on a thin needle. The green wood volume (V_w) was then measured by submerging the stem sample in a beaker of distilled water of known mass placed on a digital balance (Sartorius GD103, Germany) sensitive to 0.1 mg and the change in balance reading was recorded. The mass of the displaced water in grams was taken to correspond closely to sample volume in cm^3 (Hacke et al. 2000). Necessary precautions were undertaken to minimize movement of the wood sample while measuring on the balance. Measurements were quickly completed within 10s of immersion to minimize entry of water into the cut ends of the wood sample. Dry mass (M_s) of the sample was determined after the samples were dried in a vented electric oven at 103ºC (≥2 days) to obtain a constant weight. In our study, D_w is defined as 'basic density' which is calculated as the ratio between the oven dry mass and the fresh volume of the green wood ($D_w = M_s / V_w$) (Hacke et al. 2000).

Scanning electron microscopy (SEM) of wood anatomical traits and confocal laser scanning microscopy (CLSM) of fibre cell wall components

A subset of stem samples was preserved in 1:1 (v/v) ethanol:glycerol for long term storage (2 months) to undertake wood anatomical studies. Preserved samples were rinsed thoroughly with water and rehydrated in several changes of lukewarm water. The samples were then allowed to air dry in a dust free environment and were trimmed to small blocks

or sections. Thereafter, exposing transverse, radial or tangential surfaces, the samples were glued to specimen stubs using adhesive carbon tape and sputter coated with gold to a thickness of 15 mm at 1.5 keV for 10 min using a JEOL FC-1100 Fine Coat Ion Sputter Unit (JEOL, Tokyo, Japan). The samples were then examined using a Scanning Electron Microscope (FEI XL 30 ESEM, USA) and photographed. Total cross-sectional area of wood (W_A) and the area of pith (P_A) within the wood were calculated. The number of fibre cells (FC_n) along radial sections (from the pith to the cambium), fibre cell diameter (FC_d), fibre cell wall thickness (FCW_t), density of xylem vessels (V_D) and proportion of stem-cross sectional area occupied by xylem vessels (V_A) were determined. The diameter of fibre cell lumen (D_L) was calculated from the difference between FC_d and FCW_t. The cross-sectional areas of the fibre cell lumen (FCL_A) and of the fibre cell wall material (FCW_A) were calculated to determine FCL_A:FCW_A indicating the amount of voids within a fibre cell in relation to the amount of carbon deposited in fibre cell (Thomas et al. 2006).

For determination of cellulose, some of the additional stem sections (10 µm thickness) were incubated overnight in 0.2% aqueous solution of Congo red (CR) (HiMedia, India) in dark, then rinsed gently for 2-3 times in double distilled water and examined using confocal laser scanning microscopy (CLSM) (Leica Model DM 6000, Germany) using Argon laser (514 nm) according to (Bhattacharya et al. 2010). To determine lignin and lignin precursor molecules, some stem sections (10 µm thickness) without staining were directly examined for autoflourescence using CLSM using Argon laser (405 nm) according to (Bhattacharya et al. 2010). The exposures were strictly kept identical to ensure the comparability among samples. Bright-field and superimposed images were simultaneously taken for detailed comparisons.

Statistical analyses

To fit net CO_2 fixation rates with incident lights using Mitscherlich model equation, the *nonlinear curve fit* procedure in the OriginPro8 statistical package was used. For leaf-level traits and stem wood characteristics, analysis of variance (ANOVA) was carried out on data obtained from 6 representative trees (n=6), whereas for growth and biomass yield traits, ANOVA was performed on data obtained from 8 representative trees (n=8). The *compare many groups* statistical procedure of SigmaPlot11.0 was used to perform one way

ANOVA (significant threshold set at P<0.05) and whenever there was statistically significant difference, pair wise multiple mean comparison was conducted using Fisher's Least Significant Difference (LSD) method (alpha=0.050). To determine the influence of year, genotype and year × genotype (Y×G) interaction on the variance of growth and yield parameters measured across exp-season I and II, the ANOVA-general linear model (GLM) analysis was performed. The XLSTAT (ver 7.5.2) was used to determine correlations between different pairs of variables using Pearson correlation coefficient matrix and the threshold for significance was adjusted using Bonferroni correction, where 0.05 divided by the number of paired correlation assessed the adjusted significant level (Curtin and Schulz 1998; Perneger 1998).

Results

Genotypic variation in leaf gas exchange and light response characteristics

Mean P_n differed significantly amongst the genotypes ranging from 18.2 µmol m^{-2} s^{-1} for TB to 12.08 µmol m^{-2} s^{-1} for TR10 (**Fig. 2.3a**), which is in accordance with values recorded for certain pioneer trees of early successional stage (Nogueira et al. 2004). P_n of the HPG genotypes including V1 (reference), invariably maintained above 15.0 µmol m^{-2} s^{-1}, whereas amongst PPG, S1635 recorded relatively higher P_n (~13.7 µmol m^{-2} s^{-1}). G_s values were always higher in HPG including V1 when compared to other groups (APG and PPG) (**Fig. 2.3b**). G_s values in the HPG ranged from 0.35 to 0.26 mol m^{-2} s^{-1}, while those for PPG ranged from 0.22 to 0.16 mol m^{-2} s^{-1}. Leaf transpiration rates (E) also differed significantly amongst the genotypes exhibiting higher E in the HPG genotypes (>7.3 mmol m^{-2} s^{-1}), followed by APG and PPG genotypes (**Fig. 2.3c**). Mean C_i was above 200 µmol in all the genotypes except TR10 (193.5 µmol). The light-response curve equation provided close fit to the actual data and produced varying P_n-PPFD response curves for different performance group (**Fig. 2.3f-i**). The PPG genotypes showed light-saturation at a low light intensity, exhibiting P_{nmax} of ~15.7 µmol m^{-2} s^{-1} (**Table 2.4**). However, the P_{nmax} of HPG genotypes including V1 did not reach their I_{sat} until at least an intensity of 2000 µmol m^{-2} s^{-1} (**Table 2.4**). The HPG genotype S1 recorded the lowest ϕ followed by V1, whereas

S1635 and ML exhibited significantly higher ϕ values (**Table 2.4**). The genotypes also differed significantly in I_{comp} (**Table 2.4**).

Genotypic variation in PSII efficiency, leaf nitrogen (N_L) and water relations

In HPG genotypes, F_v/F_m values were always marginally, however, significantly higher than other performance groups (**Table 2.4**). The genotypes differed widely in PI and significantly lower values were recorded in PPG genotypes when compared to HPG and APG counterparts. Highest PI was recorded in V1, followed by S1 and TB. The present investigation shows that N_L was significantly higher in HPG genotypes when compared to PPG (**Table 2.4**).

In the present experiment, both Ψ_{Lmin} and K_h differed significantly among the performance groups (**Table 2.4**). HPG genotypes maintained relatively higher Ψ_{Lmin} (around -2.0 MPa) compared to PPG genotypes (around -2.7 MPa) and almost ~36.8% higher K_h was recorded in HPG when compared to PPG.

Genotypic diversity in growth characteristics of SRC stands

In exp season-I, the HPG genotype TB was tallest (~ 458 cm), followed by S1 and V1, whereas the PPG genotypes were far smaller in H_t (**Table 2.5**). In exp season-II, shifts in the ranking of some genotypes were recorded; nevertheless, TB maintained its top ranking in H_t and V1 reached almost equal height of S1 (**Table 2.6**). D_{100} also differed significantly among the genotypes with TB and S1 exhibiting highest value in exp season-I and II, respectively, whereas lowest D_{100} was recorded in S1635 in both the experimental seasons (**Table 2.5, 2.6**). In exp season-I, V1 and ML recorded maximum T_{STM} followed by S1 and TB, whereas minimum T_{STM} was recorded in JPK (**Table 2.5**). ML still scored maximum T_{STM} in exp season-II, whereas TB recorded second rank along with S1 and V1 (**Table 2.6**). The HPG genotypes had significantly higher T_B in both exp season-I and II when compared to PPG genotypes (**Table 2.5, 2.6**). T_{SL} was substantially more in HPG genotypes in exp season-II when compared to exp season-I, whereas in most of the PPG genotypes, except TR10, T_{SL} was less in exp season-II.

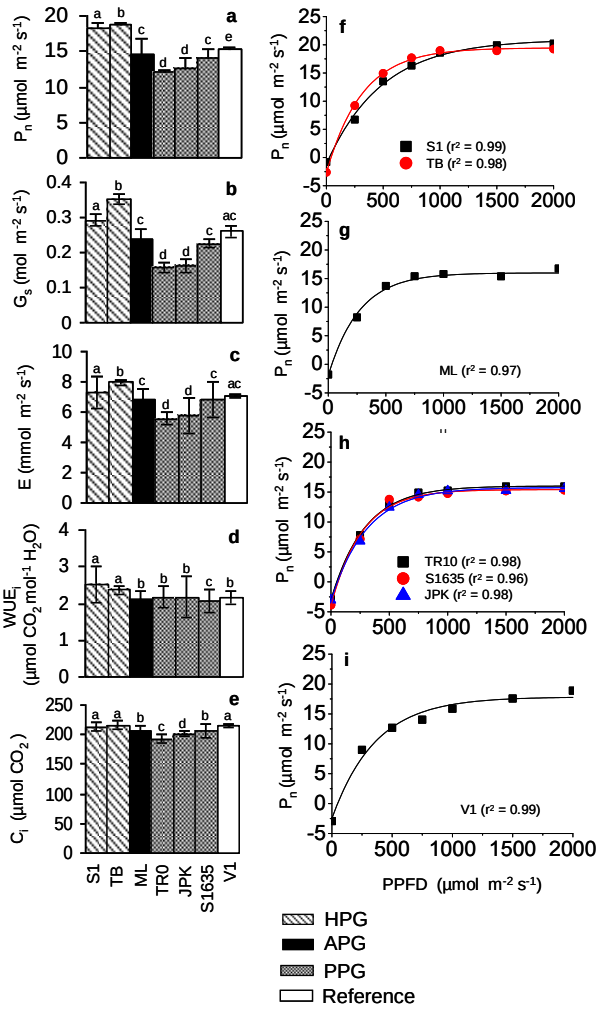

Fig. 2.3 Photosynthetic leaf gas exchange characteristics and light response curves of seven mulberry genotypes. The genotypes were analysed for (a) net CO_2 fixation rate (P_n), (b) stomatal conductance (G_s), (c) leaf transpiration (E), (d) instant water use efficiency (WUE_i) and (e) sub-stomatal CO_2 concentration (C_i). Photosynthetic light response curves fitted using Mitscherlich model equation and plotted for all the seven genotypes (f-i). Values are means ± SE of data (n=6) obtained from two experimental seasons (exp season-I and II). Differences between means were separated by Fisher's LSD test and same letters indicate that the means are not statistically different.

Table 2.4 Leaf functional traits in six different mulberry genotypes from three performance groups along with reference genotype V1. For trait abbreviations see Materials and Methods. Values are means of data (±SE) obtained (n=6) during two experimental seasons (exp season-I and II). Differences between means were separated by Fisher's LSD test. Values followed by the same letters within a single row are not statistically different.

	Performance group						
	High		Average		Poor		Reference
Leaf functional traits	S1	TB	ML	TR10	JPK	S1635	V1
$P_{n\,max}$ (µmol m^{-2} s^{-1})	20.9(0.12)a	19.3(0.08)b	15.9(0.02)de	16.2(0.12)d	15.7(0.12)de	15.4(0.18)e	17.8(0.20)c
$G_{s\,max}$(mol mol^{-1})	0.53(0.02)b	0.58(0.01)a	0.44(0.02)d	0.41(0.02)d	0.35(0.03)e	0.37(0.03)e	0.47 (0.01)c
I_{comp} (µmol m^{-2} s^{-1})	26.2(0.44)g	40.2(0.43)e	32.1(0.32)f	49.2(0.35)c	56.3 (0.29)b	60.4(0.27)a	41.6(0.52)d
R_d (µmol m^{-2} s^{-1})	-1.25(0.02)f	-2.91(0.07)d	-1.87(0.03)e	-3.30b(0.03)c	-3.51(0.02)b	-3.75(0.01)a	-2.90(0.02)d
ϕ (mol CO_2 mol quanta^{-1})	0.0021(0.002)d	0.0037(0.004)a	0.0037(0.004)a	0.0034(0.003)ab	0.0033(0.003)b	0.0038(0.004)a	0.0027(0.002)c
I_{sat} (µmol m^{-2} s^{-1})	not saturated	not saturated	1272.5(3.93)a	1276.3(1.25)a	1275.1(4.07)a	1274.6(2.28)a	not saturated
F_v/F_M (a.u.)	0.78(0.018)a	0.79(0.017)a	0.77(0.088)ab	0.74(0.006)b	0.76(0.020)b	0.75(0.017)b	0.80(0.012)a
PI (a.u.)	1.11(0.028)ab	0.96(0.017)bc	0.86(0.029)c	0.53(0.032)d	0.64(0.035)d	0.50(0.023)d	1.14(0.034)a
N_L (%)	4.21(0.07)a	3.87(0.09)b	3.62(0.06)c	1.91(0.08)g	3.10(0.10)e	2.49(0.04)f	3.27(0.05)d
Ψ_{Lmin} (-MPa)	0.22(0.020)abc	0.20(0.014)c	0.24(0.011)ab	0.26(0.017)a	0.28(0.011)a	0.26(0.017)a	0.20(0.008)bc
K_h (mmol MPa^{-1} m^{-2} s^{-1})	14.2(0.45)d	19.95(0.58)a	15.2(0.49)c	10.4(0.72)f	8.48(0.49)g	12.5(1.30)e	16.9(0.66)b

The HPG and APG genotypes exhibited open canopy and erect growth nature possessing completely straight/slightly curved stems and moderate-to-thick branches (**Fig. 2.4a,b,j**). In all the three genotypes of HPG including reference genotype V1, the leaf shape was interestingly the same (narrow ovate type) and they all had large intermodal distance (data not shown) and alternate phyllotaxy. PPG genotypes mostly had a closed canopy and bushy growth nature with slightly-to-highly curved stems and thin branches. Leaves in the PPG genotypes were wide ovate/cordate and had less intermodal distance (**Fig. 2.4 f, e, d**).

Aboveground biomass yield variation among the genotypes

Biomass yield differed significantly by year and genotype in both exp season-I and II (**Table 2.7**). At the end of exp season-I, mean AG_{fw} ranged from 2419.2 g for S1 to 1126.5 g for TR10. L_d of V1, JPK, TB and S1 were significantly higher than those of other genotypes. The HPG recorded significantly higher AG_w when compared to APG and PPG genotypes. S1 was the most productive stand to yield highest AG_{dw} followed by V1 and TB, while the PPG genotypes produced substantially less AG_{dw} (**Table 2.5**). In exp season-II, all genotypes produced substantially higher aboveground biomass when compared to exp season-I (**Table 2.6**). The HPG genotypes recorded significantly higher AG_w and S1 ranked first, followed by TB and V1 (**Table 2.6**). The AG_{dw} per plant was substantially more in HPG genotypes, whereas the APG and PPG recorded significantly less AG_{dw} (**Table 2.6**). Irrespective of genotypic differences, different yield attributing traits appeared to change across the year in all the mulberry genotypes exhibiting significant Y × G interaction in most of the parameters (**Table 2.7**). In exp season-I, genotype S1, TB and ML allocated more biomass to woody stem (72%, 65.6% and 63%, respectively); V1, S1635 and TR10 showed approximately equal biomass allocation to leaves and stem, while JPK allocated less biomass to woody stem (41.2%) and more to leaves (**Table 2.5**). However, in exp season-II, biomass allocation was found to shift heavily towards the woody stem in HPG genotype TB (75.4%) and S1 (72.3%) including reference V1 (65%) (**Table 2.6**). The SLA of the tested genotypes differed significantly among the genotypes (**Table 2.7**) in both the experimental seasons.

Fig. 2. 4 Short rotation coppice stands of seven mulberry genotypes grown in the experimental plot of University of Hyderabad (a–g). Photographs were taken at the end of exp season-II (last week of Oct 2010). Note the genotypic variations in canopy architecture including canopy height, openness, stem erectness, intermodal distance, leaf size, leaf shape and phyllotaxy. (h) Mulberry cuttings color coded by genotype used for vegetative propagation and (i) representative stem wood yield of mulberry. Photograph credit: A. Guha.

Variation in stem wood characteristics among the performance groups

The HPG genotypes including V1 maintained significantly higher D_w (>0.60 g cm^{-3}) when compared to others (**Fig. 2.5**). The HPG genotypes showed significantly greater FC_n and the cells were smaller in diameter and closely packed when compared to other performance groups (**Fig. 2.6b-h**). Mean FC_d was smallest in S1, followed by V1 and TB, whereas FC_d was highest in TR10 followed by JPK. The scanning electron micrographs of cells exhibited that within a genotype, the fibre cells were more or less uniform in size and also the cell wall of the fibre lumen was homogenously thick (**Fig. 2.6 i-o**). Significant difference in D_L was recorded amongst the mulberry genotypes with values ranging from 18.1 µm (for S1 and V1) to 25.2 µm (for S1635) (**Table 2.8**). FCW_t showed a mixed response among the performance groups and no proper trend could be drawn from our results, a finding that contrasts with previous studies of hardwood trees (Aguilar-Rodríguez et al. 2001). The HPG genotypes exhibited significantly low FCL_A: FCW_A when compared to PPG genotypes, whereas the ratio was intermediate in APG genotype ML (**Table 2.8**). V_D was significantly higher in APG and PPG genotypes when compared to HPG and the lowest V_D was recorded in V1 (~ 17.6 mm^{-2}), which also exhibited lowest V_A followed by S1 and TB. The HPG genotypes exhibited comparatively higher cellulose deposition in the cell wall when compared to other groups (**Fig. 2.6 p-s**). In contrast, the mean amplitude of the fluorescence intensities for lignin was significantly higher in PPG genotypes when compared to HPG (**Fig. 2.6 t-w**).

Discussion

Genotypic variation in leaf gas exchange and light response characteristics

In the present study, genotypic variation in leaf area-based gas exchange characteristics was investigated along with light response curve traits to determine the photosynthetic efficiency among the genotypes and to correlate such characteristics with growth performance of the coppice stands. Although photosynthetic CO_2 fixation rate and

Table 2.5 Growth and biomass yield characteristics of six mulberry genotypes from three performance groups along with reference genotype V1. For abbreviations see Materials and Methods. Values are means of data (±SE) obtained (n=8) at the end of exp season-I (Jul 2009 to Oct 2009). The differences between means were separated by Fisher's LSD test. Values followed by the same letters within a single row are not statistically different.

	Performance group						
	HPG		APG	PPG			Reference
Growth and biomass yield characteristics	S1	TB	ML	TR10	JPK	S1635	V1
H_I (cm)	373.4(6.9)b	458.1(4.2)a	346.7(8.5)c	252.5(6.7)d	277.6(7.2)d	274.7(7.3)d	347.2(5.5)c
D_{100} (cm)	2.12(0.03)b	2.32(0.05)a	1.48(0.008)d	1.40(0.05)e	1.36(0.005)f	1.26(0.008)g	2.05(0.005)c
HGR (cm day^{-1})	3.20(0.02)b	3.92(0.02)a	2.92(0.008)c	2.15(0.003)d	2.37(0.005)d	2.35(0.004)d	2.98(0.007)bc
DGR (cm day^{-1})	0.018(0.05)b	0.020(0.03)a	0.013(0.004)d	0.012(0.05)e	0.011(0.008)f	0.010(0.008)g	0.017(0.003)c
T_{STM} (plant^{-1})	8.33(2.3)a	7.66(2.6)ab	9.00(4.6)a	7.00(4.6)b	5.33(6.3)c	7.10(7.3)b	9.00(4.5)a
T_B (plant^{-1})	18.2(4.4)a	10.5(6.4)d	16.7(5.4)b	5.50(7.2)f	7.20(4.7)e	9.6(5.5)d	15.2(5.3)c
T_{SL} (cm plant^{-1})	3208.6(8.3)a	2689.8(7.8)bc	2576.9(10.5)c	1286.0(8.6)e	1369.3(9.4)e	1690.8(7.9)d	2740.3(8.5)b
L_T (g plant^{-1})	780.4(5.5)c	750.6(6.7)c	724.2(7.3)cd	680.4(6.9)d	846.3(9.3)b	684.7(12.4)d	1190.3(7.4)a
S_T (g plant^{-1})	1638.4(9.8)a	1454.7(8.7)b	784.6(8.5)d	446.2(6.8)f	530.5(7.4)ef	570.5(9.4)e	1066.4(6.9)c
AG_w (g plant^{-1})	2419.2(10.5)a	2205.7(9.8)b	1508.6(12.3)c	1126.5(14.4)f	1376.8(9.9)d	1255.2(12.7)e	2256.6(10.6)b
L_d (g plant^{-1})	313.3(7.7)b	328.2(6.8)b	247.4(6.9)c	185.3(7.2)d	331.3(8.6)b	196.9(9.6)d	482.4(8.6)a
SLA (cm^2 g^{-1})	298.2(0.003)d	255.7(0.005)g	332.5(0.004)b	324.3(0.006)a	289.1(0.003)e	270.9(0.004)f	306.6(0.003)c
AG_w (g plant^{-1})	807.6(10.2)a	626.3(9.6)b	421.4(12.4)c	203.5(8.8)e	232.9(10.5)de	250.6(7.9)d	597.4(8.8)b
AG_{dw} (g plant^{-1})	1120.9(9.5)a	954.5(8.9)b	668.8(11.3)c	388.8(12.6)f	564.2(10.5)d	447.5(10.8)e	1079.8(9.3)a

Table 2.6 Growth and biomass yield characteristics of six mulberry genotypes from three performance groups along with reference genotype V1. For abbreviations see Materials and Methods. Values are means of data (±SE) obtained (n=8) at the end of exp season-II (Jul 2010 to Oct 2010). The differences between means were separated by Fisher's LSD test. Values followed by the same letters within a single row are not statistically different.

	Performance group						
	HPG		APG	PPG			Reference
Growth and biomass yield characteristics	S1	TB	ML	TR10	JPK	S1635	V1
H_I (cm)	510.6(5.2)a	523.5(6.3)a	501.5(4.4)a	389.8(5.6)b	414.2(7.3)b	285.5(6.4)c	516.7(5.3)a
D_{100} (cm)	2.53(0.008)a	2.32(0.006)b	1.51(0.004)d	1.42(0.003)e	1.40(0.008)e	1.32(0.008)f	2.20(0.005)c
HGR (cm day^{-1})	3.92(0.04)a	4.03(0.08)a	3.86(0.003)a	2.95(0.05)b	3.16(0.08)b	2.15(0.006)c	3.96(0.004)a
DGR (cm day^{-1})	0.019(0.006)a	0.017(0.003)b	0.012(0.003)d	0.011(0.005)e	0.011(0.004)e	0.010(0.003)f	0.016(0.004)c
T_{STM} (plant^{-1})	7.2(3.6)a	7.5(4.5)a	8.3(4.4)a	6.3(5.3)ab	3.3(7.4)c	5.4(6.8)b	7.2(4.5)a
T_B (plant^{-1})	34.6(6.4)a	14.3(5.5)b	7.2(3.5)c	5.8(4.2)c	4.6(5.3)c	5.3(7.5)c	17.3(6.6)b
T_{SL} (cm plant^{-1})	5867.7(9.8)a	3878.6(12.3)b	2662.9(11.6)c	1709.2(8.6)d	1178.9(10.5)e	1102.8(12.4)e	4089.5(8.8)b
L_T (g plant^{-1})	2506.2(8.4)b	1718.3(9.6)c	1508.2(10.5)d	1032.6(8.9)e	1432.4(11.5)d	1222.3(9.5)e	2886.5(7.6)a
S_T (g plant^{-1})	5476.3(7.7)a	4151.2(8.6)c	1772.7(10.7)d	942.3(7.3)e	1016.2(9.7)e	818.4(10.4)e	4478.5(8.5)b
AG_w (g plant^{-1})	7982.5(10.3)a	5869.5(7.5)c	3280.9(8.4)d	1974.9(9.3)f	2448.6(8.8)e	2040.7(7.3)f	7365.7(8.6)b
L_d (g plant^{-1})	1006.7(6.5)b	755.2(7.8)c	525.3(8.6)d	291.2(7.7)f	570.4(10.6)d	371.4(7.3)e	1169.8(6.8)a
SLA (cm^2 g^{-1})	285.4(0.004)b	243.6(0.005)e	322.2(0.003)a	315.6(0.003)a	273.6(0.004)c	258.3(0.007)d	293.5(0.003)b
AG_w (g plant^{-1})	2632.8(9.4)a	2324.3(11.5)b	986.4(12.2)d	610.6(8.6)e	580.9(10.6)e	467.5(10.6)f	2095.7(8.7)c
AG_{dw} (g plant^{-1})	3639.5(8.7)a	3079.5(7.3)b	1511.7(8.4)c	901.8(9.5)e	1151.3(10.5)d	838.9(7.2)e	3265.5(8.3)b

Table 2.7 Significance of the influence of year, genotype and year × genotype interaction on the variance of 14 growth and yield parameters measured across exp season-I and II. For abbreviations see Materials and Methods.

Parameters	Year (Y)	Genotype (G)	Y × G
H_t	*	**	**
D_{100}	ns	*	ns
HGR	*	*	*
DGR	ns	*	ns
T_{STM}	**	**	**
T_B	**	**	**
T_{SL}	**	**	**
L_f	**	**	**
S_f	**	**	**
AG_{fw}	**	**	**
L_d	**	**	**
SLA	*	**	**
AG_w	**	**	**
AG_{dw}	**	**	**

* Significant at 0.05 probability level
** Significant at 0.01 probability level
ns Nonsignificant at the 0.05 probability level

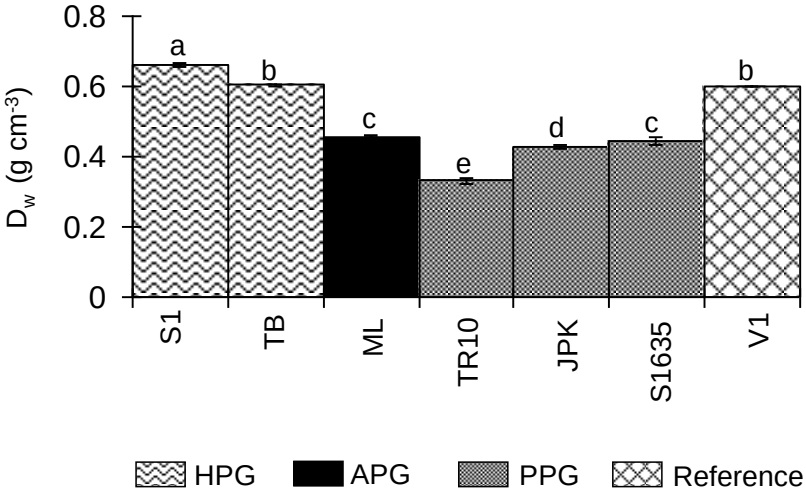

Fig. 2.5 Wood density (D_w) of seven mulberry genotypes determined at a stem height of 100 cm from base. Data are mean ± SE. Differences between means were separated by Fisher's LSD test and same letters indicate that the means are not statistically different.

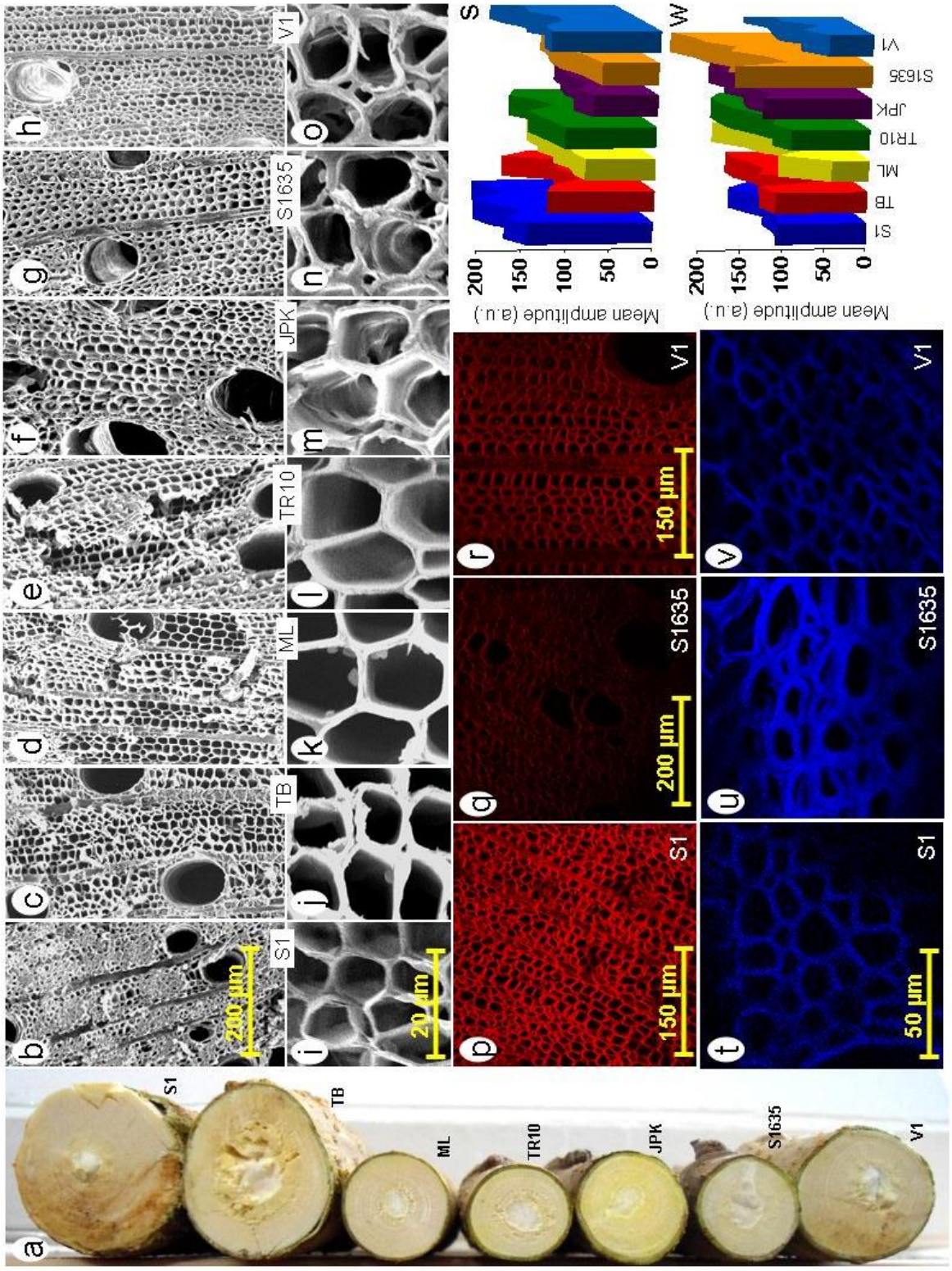

Fig. 2.6 Stem wood characteristics in seven mulberry genotypes. (a) Cross-sections of woody stem at a height of 100 cm from stem base. The scanning electron micrographs of woody stem transections showing genotypic variations in (b-c) fibre cell size, distribution and arrangement and (i-o) fibre cell wall thickness. CLSM images of woody stem transaction showing genotypic variations in (p-r) cellulose depositions in fibre cell wall determined by CR-labelled red fluorescence and (t-v) lignin deposition in fibre cell wall determined by blue autofluorescence. The mean amplitudes of fluorescence intensities showing comparative variations in (s) cellulose and (w) lignin depositions among the studied genotypes.

Table 2.8 Wood anatomical characteristics of six mulberry genotypes from three performance groups along with reference genotype V1. For abbreviations see Materials and Methods. Values are the means of data (±SE) obtained (n=6) during exp season-II. The differences between means were separated by Fisher 's LSD test. Values followed by the same letters within a single row are not statistically different.

	Performance group						
	High		Average		Poor		Reference
Wood characteristics	S1	TB	ML	TR10	JPK	S1635	V1
W_A (cm^2)	3.82(0.04)a	4.07(0.02)b	1.54(0.02)c	1.34(0.01)d	1.30(0.12)d	1.15(0.17)e	3.20(0.11)f
P_A (cm^2)	0.13(0.008)a	0.25(0.05)b	0.07(0.01)c	0.16(0.05)d	0.13(0.01)a	0.30(0.01)b	0.14(0.006)a
FC_n (no. mm^{-2})	5819.6(6.6)a	3510.0(6.4)b	3229.9(7.3)c	2996.3(8.3)d	2964.2(6.3)d	3208.2(4.4)c	4842.6(5.3)e
FC_d (µm)	16.8(0.18)a	22.0(0.57)b	23.1(0.44)b	31.0(0.43)c	30.2(0.38)c	22.6(0.42)b	19.1(0.20)ab
FCW_t (µm)	3.92(0.02)a	4.73(0.03)b	4.25(0.01)c	3.80(0.02)a	4.13(0.02)c	4.72(0.03)b	4.40(0.02)b
D_L (µm)	18.1(0.12)a	20.4(0.32)b	21.2(0.26)b	23.2(0.20)c	18.3(0.23)a	25.2(0.38)d	18.1(0.29)a
FCL_A:FCW_A	2.09(0.02)a	1.91(0.02)b	2.23(0.17)c	2.83(0.11)d	1.99(0.13)b	2.43(0.12)e	1.84(0.008)b
V_D (no. mm^{-2})	25.2(0.44)a	24.6(0.17)a	52.2(0.52)b	52.8(1.5)b	56.3(0.70)c	39.3(1.4)d	17.6(0.32)e
V_A (%)	22.0(0.46)a	32.9(1.3)b	39.4(1.1)c	40.5(0.40)c	72.2(0.95)d	33.7(0.87)b	13.8(1.2)e

Table 2.9 Pearson correlation coefficients between each pair of variable. For abbreviations see Materials and Methods. For each variable, the mean of data obtained from replicates (n=4) was used in correlation analysis. The Bonferroni correction-adjusted significance level for the correlations was P < 0.002. Significant values are indicated in bold. Negative correlations are indicated by '–' symbol.

P_{nmax}	R_d	F_v/F_m	PI	N_L	K_h	H_t	D_{100}	L_d	SLA	AG_w	AG_{dw}	D_w	W_A	P_A	FC_n	FC_d	FCW_t	V_D	V_A	D_L
-0.755																				
0.653	-0.437																			
0.785	-0.700	**0.932**																		
0.769	**-0.755**	**0.768**	**0.818**																	
0.779	-0.173	0.314	0.316	-0.032																
0.775	-0.695	**0.821**	**0.894**	**0.780**	0.132															
0.964	-0.606	**0.822**	**0.887**	**0.757**	0.028	**0.763**														
0.726	-0.492	**0.911**	**0.937**	0.695	0.288	0.733	**0.858**													
-0.259	-0.365	-0.225	0.005	-0.221	0.445	0.157	-0.258	-0.125												
0.951	-0.635	**0.848**	**0.919**	**0.786**	**0.772**	**0.796**	**0.997**	**0.860**	-0.232											
0.918	-0.615	**0.888**	**0.949**	**0.783**	**0.762**	**0.801**	**0.988**	**0.921**	-0.210	**0.991**										
0.868	-0.579	**0.878**	0.713	0.720	0.571	0.683	**0.936**	**0.890**	-0.382	**0.942**	**0.955**									
0.940	-0.516	**0.831**	**0.856**	0.744	-0.027	**0.756**	**0.984**	**0.803**	-0.361	**0.983**	**0.963**	**0.916**								
0.047	0.495	-0.062	-0.278	-0.116	-0.247	-0.433	0.023	-0.200	**-0.858**	0.003	-0.051	0.010	0.140							
0.817	-0.681	0.631	**0.811**	0.610	0.245	0.536	**0.835**	**0.849**	0.006	**0.823**	**0.853**	**0.830**	**0.757**	-0.206						
-0.688	0.617	-0.732	**-0.786**	-0.707	-0.464	-0.482	**-0.761**	-0.751	0.202	**-0.781**	**-0.795**	**-0.885**	-0.713	-0.115	**-0.815**					
-0.079	0.363	0.341	0.039	0.147	0.206	-0.104	0.053	0.066	-0.696	0.078	0.077	0.265	0.172	0.748	-0.193	-0.327				
-0.753	0.286	**-0.806**	**-0.760**	-0.515	-0.313	-0.486	**-0.862**	**-0.823**	0.407	**-0.858**	**-0.872**	**-0.879**	**-0.862**	-0.300	**-0.755**	**0.835**	-0.391			
-0.562	0.416	-0.551	-0.626	-0.273	-0.652	-0.360	-0.648	-0.588	-0.048	-0.660	-0.659	-0.620	-0.609	-0.095	-0.697	**0.806**	-0.192	**0.822**		
-0.555	0.466	-0.701	-0.754	-0.678	0.107	-0.723	-0.631	**-0.805**	-0.007	-0.628	-0.693	-0.627	-0.574	0.492	-0.597	0.323	0.257	0.371	0.038	
-0.455	0.243	**-0.871**	-0.731	**-0.766**	-0.040	-0.638	-0.608	**-0.788**	0.428	**-0.755**	**-0.786**	**-0.762**	-0.625	0.001	-0.436	0.532	-0.403	0.571	0.137	**0.777**

associated traits are key factors for biomass production, such parameterization not necessarily always show strong positive association with biomass productivity of trees as reported earlier (Gong et al. 2011). However, the results obtained in the present study advocate that better leaf gas exchange functioning can be considered as key indicator of higher carbon acquisition in HPG and in turn can be largely associated to high yield performance. As compared to P_n and G_s, less variation in C_i was recorded which was consistent with earlier reports indicating positive correlation of C_i with P_n and G_s (Marino et al. 2010). However, subsequent use of C_i in the interpretation of internal CO_2 diffusion might be misleading. Further studies on P_n/C_i response and mesophyll conductance can provide better insights to the variability in CO_2 diffusion among the genotypes. From ecophysiological perspective, the leaf gas exchange functionality of HPG can largely be termed as 'exploitative' which take advantage of available agroclimatic resources like high irradiance, soil moisture and additional inputs like fertilization/manuring and facilitate rapid juvenile growth to maximize biomass production under SRC system.

As the HPG genotypes including V1 did not reach their I_{sat} until at least an intensity of 2000 µmol m^{-2} s^{-1}, it indicates that the genotypes did not suffer from surplus irradiation or photoinhibition and consequently these genotypes are more likely to be able to protect their photosynthetic machinery against photo-degradation. The apparent quantum yield (ϕ) is an important index for understanding photosynthetic efficiency and the smaller the value of ϕ, plant converts light into photosynthesis more efficiently (Gong et al. 2011). The genotypes also differed significantly in I_{comp} and such variation might be primarily determined by the deviations in plants from the residuals of the P_{nmax}-R_d relationship. This is because I_{comp} is determined by the balance between R_d and ϕ, and an increasing R_d concomitantly increases I_{comp} (Marino et al. 2010). Due to lower R_d values, the HPG had lower I_{comp}, which might have favored higher photosynthetic accumulation. As the photosynthetic measurements were made during the peak growth stage, the measured R_d would largely correspond to growth respiration of foliage rather than maintenance respiration. During vegetative growth phase, with gradual increment in plant size, photosynthetic tissues are likely to decline as a function of biomass allocation trade-offs. Due to such changes, decrease in R_d with increasing size might be an essential strategy in plants to maintain whole-plant carbon balance (Tjoelker et al. 1999). In HPG genotypes, the observed increment in plant size

might have concomitantly caused decrease in R_d in order to maintain net carbon balance. The results denote that based on low R_d, selection of HPG genotypes can be a reliable strategy for enhanced biomass yield in mulberry.

Genotypic variation in PSII efficiency, leaf nitrogen (N_L) and water relations

The present study aimed to find whether PSII efficiency indices, N_L and leaf hydraulic traits can be used as useful indices for higher biomass yield in mulberry. Two important OJIP-test parameters were considered including F_v/F_m and overall performance index of PSII known as PI (describes the forces of redox reactions and fluxes of electrochemical Gibbs free energy in PSII light reactions) (Stirbet and Govindjee 2011). In HPG genotypes, higher F_v/F_m indicates relatively better photochemical efficiency of PSII which is largely attributed to higher electron transport capacity (Wu et al. 2009). Highest PI was recorded in V1, followed by S1 and TB depicting lower entropy in HPG when compared to PPG genotypes. Factors that may be responsible for decreased PI include increment in inactive reactive centres, low F_v/F_m and low electron transport rate beyond primary quinone (Q_A^-) (Hermans et al. 2003). As F_v/F_m did not differ substantially amongst the genotypes, it was the other two factors which might have profoundly varied amongst the performance groups. The results suggest that compared to F_v/F_m, PI can be considered as a much stronger predictor of photosynthetic efficiency in mulberry and thus can be used to screen high biomass yielding genotypes. Positive correlations between photosynthetic efficiency and N_L have been established in many plants (Kenzo et al. 2004) and this general finding was also confirmed in the present investigation. Such variation in N_L has major significance in understanding the photosynthetic efficiency as important photosynthetic traits e.g. P_{nmax}, electron transport capacity and PSII efficiency characteristics are well-correlated with N_L (Kenzo et al. 2004). A major proportion of N_L is allocated to the photosynthetic apparatus including enzymes that are important determinants of P_{nmax} (Kenzo et al. 2004).

In the present experiment, the obtained results indicate that P_n and hydraulic capacity are positively associated and highly interdependent in mulberry. Under optimal soil water supply, high K_h of HPG might have allowed quick water transport from stems to foliage to compensate leaf transpirational moisture loss and consequently high Ψ_{Lmin} was recorded in

the HPG when compared to remaining groups. Such high leaf water status might have facilitated increased carbon assimilation, higher cell turgor, plant cell expansion and higher tree growth of the HPG genotypes when compared to others (Santiago et al. 2004; Woodruff et al. 2004). The experimental findings corroborate the previous reports which also indicated functional dependency of leaf gas exchange on water transport capacity in woody trees (Zhang and Cao 2009; Santiago et al. 2004; Woodruff et al. 2004).

Genotypic diversity in growth characteristics of SRC stands

The present study was conducted to identify important canopy growth characteristics associated with high biomass productivity in mulberry under SRC system. Starting from establishment period until exp season-II, it was evident that the tallest H_t for every genotype was reached only during exp season-II (H_t data of intermediate seasons are not shown). The reason for such progressive increment in H_t might be due to the fact that the belowground parts need to grow for a required time period before attaining optimum height (Pontailler et al. 1999; Christersson 2010). T_{SL} was substantially more in HPG genotypes in exp season-II when compared to exp season-I, in compared to PPG genotypes, depicting poor responsiveness of PPG genotypes towards intensive coppice treatments. The experimental data indicate that quantitative growth features like T_{STM}, T_{SL} and T_B can be useful indices for high biomass yield in mulberry. As the superiority of HPG genotypes in terms of growth performance was largely stable in both the experimental seasons, it indicates their vitality, growth consistency and genotypic responsiveness towards intensive coppice treatments and in turn provides indication for sustainability of yield (Pearson et al. 2010).

The HPG and APG genotypes exhibited open canopy and erect growth nature and alternate phyllotaxy which altogether might have facilitated higher light interception and in turn maximized stand-level photosynthetic CO_2 assimilation and biomass gain (Zhu et al. 2010). PPG genotypes mostly had a closed canopy and bushy growth nature with slightly-to-highly curved stems and thin branches. Leaves in the PPG genotypes were wide ovate/cordate and had less internodal distance which resulted in fast canopy closure after a certain period of growth and thus might have significantly limited canopy light interception and overall growth of the stands.

Aboveground biomass yield variation among the genotypes

In the present study, the genotypic ability in foliar and woody biomass production was assessed and the Y × G interaction effects on biomass yield attributing parameters were also examined across the two experimental seasons. Such growth responses across the years can be attributed to the changes that are generally associated with stump age and rooting and not because of environment as the experimental seasons were same (monsoon) in both the years (2009 and 2010). The results obtained corroborate previous report of Madan and Sharma (1999) who also reported proportionate yield increment in mulberry stands in preceding years attributed to gradual increment in rooting vigour and increased accumulation of food reserves in the hardwood of stumps. The data suggest that S1 and TB which consistently allocated more biomass to woody stem in both the experimental seasons might be more suitable exclusively for woody biomass production, whereas V1 can be cultivated for both wood and foliage yields. Generally a high SLA is associated with rapid growth and better photosynthetic efficiency (Feng et al. 2008). However, in the present study, no such trend was evident and SLA varied independently. The study elucidates that all the HPG genotypes including V1 (reference) are highly promising for achieving high yields in a short time period and thus establishment of wider coppice plantations of those fast-growing genotypes on higher fertility sites could be economically justified where mulberry crops are used to produce alternate biomass energy resources besides regular sericultural purposes. However, the results from the present study should be considered suitable only under the same agroclimatic conditions in which the experiments were carried out, and should be used mainly as a reference elsewhere. ML, which is an indigenous land race of Southern Indian region, performed fairly well in yield attributes and exhibited relatively higher biomass yield than PPG. Thus, the genotype can also be utilized for biomass energy applications provided it is cultivated in the prevailing agroclimatic conditions of Southern India. In particular, since many biomass yield characteristics of SRC mulberry stands are strongly genotype specific, it is reasonable to predict that some outcomes may vary whenever the genotypes are grown in different agroclimatic zones due to genotype×environment (G × E) interaction effects (Tilman et al. 2002). Nevertheless, the present study may be useful to provide information to select

suitable mulberry genotypes and managing SRC plantation in order to achieve sustainable biomass yield for bioenergy applications.

Variation in stem wood characteristics among the performance groups

Wood density (D_w) describes the carbon storage per unit volume of stem and is essentially an emergent property for higher woody biomass (Chave et al. 2009). Thus, we attempted to identify dimensions of genotypic variation in D_w in relation to woody stem biomass yield of the studied mulberry genotypes. FCW_t showed a mixed response among the performance groups and no proper trend could be drawn from the results, a finding that contrasts with previous studies of hardwood trees (Aguilar-Rodríguez et al. 2001). A measure of the amount of voids within a fibre cell in relation to the amount of carbon deposited in the fibre cell walls, expressed as FCL_A: FCW_A is often a better predictor of higher D_w than FCW_t. The results elucidate that mulberry genotypes can achieve higher D_w by reducing fibre D_L and FCL_A: FCW_A ratio and by elevating the percentage of FC_n, an observation that agrees with earlier reports (Preston et al. 2006; Jacobsen et al. 2007; Jacobsen et al. 2005; Martínez-Cabrera et al. 2009). A direct spatial trade-off between vessel area and area occupied by fibre cells would predict that D_w should be inversely related to vessel area (Chave et al. 2009; Preston et al. 2006). However, as it is known that vessel traits and water transport efficiency are tightly linked, it was interesting to observe that in spite of less V_A%, the HPG genotypes still maintained higher K_h and Ψ_L. A high rooting capacity, greater water potential gradient (between leaf and root) as well as more number of embolism free conduits, as reported in other woody angiosperms, might be the possible driving factors for maintenance of such higher water transport efficiency (Chave et al. 2009). Under biochemical conversion perspective, as a high cellulose and low lignin content enhance the biomass-biochemical-conversion efficiency (Guidi et al. 2009), it can be predicted that the HPG mulberry genotypes identified from the present coppice rotation trials would potentially result in higher biochemical conversion yield.

Associations among investigated leaf/wood traits and biomass yield attributes

Aboveground biomass yield is shaped by multiple functional/structural leaf and stem wood characteristics that are interrelated, co-vary according to plant functional types and also

vary in the robustness of interrelationships with yield. To describe such interactions, correlations within investigated leaf/wood traits, growth characteristics and biomass yield attributes were examined and the strength of the relationships was determined from correlation matrix (**Table 2.9**). Leaf functional traits including P_{nmax}, F_v/F_m, PI, N_L and K_h were positively correlated with biomass yields (AG_w and AG_{dw}) and the strongest correlation was recorded with P_{nmax}. R_d was negatively correlated with P_{nmax} and the relationship between F_v/F_m and P_{nmax} was independent (due to lack of correlation), whereas PI, N_L and K_h showed strong positive correlations with P_{nmax}. The data obtained indicate that amongst different leaf functional traits related to photosynthesis, P_{nmax}, PI, N_L and K_h are the key factors in determining photosynthetic efficiency of mulberry genotypes. Among stand growth characteristics, H_t and D_{100} shared strong positive correlations with AG_w and AG_{dw}. Positive correlation was recorded between L_d and AG_{dw} as well as within L_d, F_v/F_m, PI and D_{100}.

Among the studied stem wood structural traits, W_A and FC_n were strongly correlated with AG_w and AG_{dw}, whereas negative correlationships were recorded with FC_d, V_D and FCL_A:FCW_A. The trade-off between V_D and AG_w supports the general idea that less conduit spaces lead to dense wood formation. One premise of this trade-off is that hydraulic efficiency should be reduced in woody plants having higher D_w (Baltzer et al. 2009; Slot and Poorter 2007). The experimental data from the present study, however, does not support this idea depicting that wood density and hydraulic efficiency may in fact be largely independent axes of the wood economics spectrum. Such experimental findings should be interpreted with following caveats. First, the results are based on well-irrigated field study, a condition where maintenance of a higher K_h can largely be independent of V_D and in turn D_w need not to be compromised. Second, many morphophysiological and anatomical traits change through ontogeny in trees; therefore extrapolating findings based on juvenile traits to adult tree performance should be exercised with caution (Baltzer et al. 2009). The correlation matrix further showed that W_A was positively correlated with P_{nmax}, F_v/F_m, PI, D_{100} and L_d. However, the relationships between W_A and other anatomical traits including FCW_t, V_A, D_L, and FCL_A:FCW_A were independent. D_w was strongly positively correlated with AG_w, AG_{dw} and D_{100} and also showed positive correlations with P_{nmax}, F_v/F_m, L_d and FC_n. The positive correlations among D_w, FC_n and AG_w strengthen the data

indicating that more fibre cells per unit area reinforce D_w and in turn AG_w (Martínez-Cabrera et al. 2009). The relationships between D_L and other stem wood anatomical traits remained independent; while a negative correlation was observed with L_d (**Table 2.9**). Overall, the general importance of functional and structural integration of variable traits as observed from the experimental data merits the importance of understanding trait functionality which is a prerequisite to improve biomass productivity in mulberry.

This work represents one of the first attempts to estimate leaf-level functional traits and stem wood characteristics of mulberry aiming to identify key traits that are linked to high biomass productivity. Although the trial accounted for few coppice rotations grown in small plots, the genotypic differences recorded in plant height, stem diameter, number of stems per stump and biomass yields were sufficiently confirmatory to indicate the coppicing ability and potential biomass production of the best performing genotypes when grown under the prevailing agroclimatic conditions. Genotype S13, TB and V1 seem highly promising for achieving high yields in a short time period and thus establishment of wider coppice plantations of those fast-growing genotypes on higher fertility sites could be economically justified where mulberry crops are used to produce alternate biomass energy resources besides regular sericultural purposes. Fifteen out of total 22 traits, used in computing correlation coefficient matrix were found to correlate with above ground biomass yield, whereas remaining traits showed negative, weak or no correlations with productivity. Based on the experimental data, it can be suggested that leaf functional traits including net CO_2 fixation, light-saturated rates of photosynthesis, performance index, leaf nitrogen content and leaf-specific hydraulic conductance could be most appropriate indicators to select mulberry genotypes with higher photosynthetic efficiency and biomass yield. Further, the positive correlations of woody biomass yield with wood density, stem wood cross-sectional area and fibre cell number indicate that integration of these stem wood traits could be useful to screen mulberry genotypes for high woody biomass productivity. Finally, the data from the present study suggest that the identified fifteen characteristics could be useful in the selection of suitable mulberry genotypes for higher biomass yield and a combination of these identified traits can be introduced in process-based mathematical models of tree crop productivity in mulberry in order to enhance biomass productivity under SRC cultivation system.

Screening of Mulberry Germplasm for Drought Stress Tolerance and Assessing Photosynthetic and Hydraulic Performances of Tolerant and Susceptible Genotypes

Chapter 3

To understand species' capacity to survive in stressful environments, it is important to understand their ability to tolerate resource limitation. A species is defined as tolerant when stress has a lower effect on its performance (e.g. growth and biomass productivity), to the point at which it may seem that it is not perceiving the stress. Such apparent lack of effect on fitness, however, could be explained by alterations in other traits, less visible and more distant to fitness (underlying traits sensu Alpert and Simms 2002, and functional traits sensu Violle et al. 2007). In other words, stress always has an effect at some level: sometimes at the 'macroscopic' level, affecting fitness, and sometimes at a more detailed level, modifying underlying traits that allow fitness stability. This distinction appears to answer Weiner's (2004) plea for a refinement of the plasticity concept and seems worthy of investigation. According to the trade-off model, there is a compromise between the ability to grow under benign environmental conditions and the ability to tolerate resource limitation (Lambers et al. 2008). Inherently fast-growing species are more strongly affected by stress than typical tolerant species. To such differential response between fast-growing species and tolerant species, statistical evidence was provided by the significance of the interaction between environment and species (Lambers and Poorter 2004). The alternative no-trade-off model is that both species respond

similarly to stress, with no significant interaction. In arid and semi-arid environments, the persistence and dominance of perennial species depend on their capacity to tolerate drought (Cuso and Fernández 2012). Tolerance could be defined on one extreme by fixed traits and, on the other, by plastic traits and this can even occur for the same trait. For example, allocation to the root system, would be expected to be inherently high (fixed) in drought-adapted species, and also to be increased (plastic) in response to stress. This is not the same as believed that plasticity is always adaptive; for example, a decrease in total plant biomass caused by stress is not adaptive. To understand drought tolerance of a species, it is necessary to know the degree of plasticity in physiological, growth and biomass productivity traits (i.e. position in the fixed–plastic continuum) (Cuso and Fernández 2012).

Mulberry is one of the major commercialized, perennially grown plantation tree crop which is worldwide cultivated mainly for its foliage. It is recently considered as a forage tree perfectly adapted to tropical conditions which has shown numerous possibilities for use in ruminant diets. Research work on mulberry in different countries (Gonzales and Milera 2002; Liu et al. 2002), was focused mostly on the utilization of the leaves, which like most forages, contain greater nutrient concentrations than the whole plant. Hence, the purpose of mulberry research is largely aimed to produce more foliage with palatable, succulent leaves of high nutritive value. Recently evolved high yielding mulberry genotypes and improved crop husbandry techniques have caused a massive hike in harvestable leaf yield in the moriculture sectors of India (Dandin et al. 2003). However, mulberry is also cultivated under resource-limited agroecosystems and many regions of the country are currently encountering the prospect of producing yields with low water availability. Nearly, 48% of the cultivated mulberry areas in India have been clustered under rainfed water-stress conditions. Water deprivation can severely arrest mulberry growth leading to yield loss and the relationship between yield loss and water stress severity can differ largely among crop genotypes. This has given rise to the concept of ‘drought tolerance’, with some genotypes performing better under a given severity of water stress than others. Even though, such variations have been recognized for many years, progress towards understanding and exploiting the mechanisms that confer tolerance has been slow in mulberry crop species due to lack of adequate knowledge on the

physiobiochemical and other mechanisms that are linked to drought tolerance of this perennial tree crop species.

Photosynthesis, one of the major metabolic processes determining crop growth and production, is both directly and indirectly affected by drought (Pieters and El Souki 2005; Praxedes et al. 2006). Upon mild and moderate water deficit conditions, photosynthesis decreases in plants mainly due to stomatal closure, whereas non-stomatal factors would limit carbon assimilation under severe drought (Angelopoulos et al. 1996). Even under adequate irrigation, stomatal conductance can substantially restrict CO_2 entry into the leaves as a result of the interaction of low vapor pressure deficits in the atmosphere with high temperature and irradiance (Osório et al. 2006). It has been demonstrated that the combination of these factors predispose plants to photoinhibition or down-regulation process. In particular, CO_2 deprivation at the chloroplast level by stomatal closure during the warmest period of the day could enhance the sensitivity of the photosynthetic apparatus to high irradiance (Faria et al. 1998; Flexas et al. 1998).

The limitation of CO_2 assimilation in water-stressed plants causes the over-reduction of photosynthetic electron transport chain. This excess of reducing power determines a redirection of photon energy into processes that favor the production of reactive oxygen species (ROS), mainly in the photosynthetic (Asada 1999) and mitochondrial electron transport chains (Møller 2001). An imbalance between photochemical activity at PSII and electron requirement for photosynthesis often leads to an over-excitation and subsequent photoinhibitory damage to PSII reaction centers (Riccardi et al. 2004). These changes in the photochemistry of chloroplasts, result in the dissipation of excess light energy in the PSII core and antenna, thus generating reactive oxygen species (ROS) ($O_2^{\bullet}$, $_1O^2$, H_2O_2 and $OH^{\bullet}$). Under drought stress, these may damage the plants by oxidizing photosynthetic pigments, membrane lipids, proteins and nucleic acids (Reddy et al. 2004). To eliminate ROS, all plants are endowed with detoxification mechanisms, including both enzymatic [superoxide dismuatase (SOD), ascorbate peroxidase (APX), peroxidase (POD), glutathione reductase (GR), etc.] and non-enzymatic (anthocyanins, carotenoids, ascorbic acid, etc.) antioxidants (Johnson et al. 2003). Moreover, an increase in dissipation of excess excitation energy or the production of photoprotective pigments (carotenoids and

anthocyanin) are known to play an important function in protecting against the damaging effect of ROS (Sherwin and Farrant 1998; Gould et al. 2002; Pietrini et al. 2002).

Plants also tend to cope with water deficit stress via a common response, known as osmotic adjustment. This includes the synthesis and accumulation of compatible (non-toxic) solutes, such as proline (Mahajan and Tuteja 2005; Molinari et al. 2007; Szira et al. 2008). In addition to being an osmoprotectant, proline acts as a free radical scavenger, a sub-cellular structure stabilizer, a redox potential buffer and as an important component of cell wall proteins (Matysik et al. 2002, Ashraf and Foolad 2007).

Looking at all these afore mentioned strategies opted by plants, it can be stated that maintaining photosynthesis is a crucial challenge for crop plants during drought and 'drought tolerance' can be largely associated with the capacity to maintain better photosynthesis even under water deficit conditions. There are broadly three approaches for the investigation of photosynthetic rates, photosynthetic capacity and photoprotection efficiency. The first one involves use of infrared gas exchange system for the measurement of the light-saturated rate of net photosynthetic carbon assimilation rate (P_n) per unit leaf area (**Box 3.1**).

Box 3.1 Applications, principle and different components of infrared gas exchange analyzer instrument.

Many different physical and chemical methods, ranging from conductimetric to opto-acoustic, could potentially be used to measure CO_2 mole fraction, but non-dispersive infrared gas analysis is the only method currently of widespread importance for measuring photosynthetic CO_2 uptake. Infrared gas analysis has also become the major method for simultaneous measurement of transpiration. The popularity of the method stems from the high resolution and simplicity of this technique compared to others, enhanced by the recent adoption of miniature solid-state infrared detectors and microprocessors. Hetero-atomic gas molecules absorb radiation at specific sub-millimetre infrared (IR) wave-bands, each gas having a characteristic absorption spectrum. Gas molecules consisting of two identical atoms (e.g. O_2, N_2) do not absorb IR radiation, and thus do not interfere with the determination of hetero-atomic molecules. The major absorption band of CO_2 is at 4.25 µm with secondary peaks at 2.66, 2.77 and 14.99 µm. The only hetero-atomic gas normally present in air with an absorption spectrum overlapping that of CO_2 is water vapour (both molecules absorb IR in the 2.7 µm region). Since water vapour is usually present in air at much higher concentrations than CO_2, this interference is significant, but may be overcome simply by drying the air. Absorption bands are in fact made up of a series of absorption lines corresponding to the rotational states of CO_2. Absorption of radiation by CO_2 at any one wavelength follows the Beer-Lambert Law, and thus depends on the radiation path length through the measuring cell and the molar concentration of CO_2. Most CO_2 IRGAs used broad-band radiation and total absorption will therefore be determined by integrating over all the absorption lines in the 4.25 µm band.

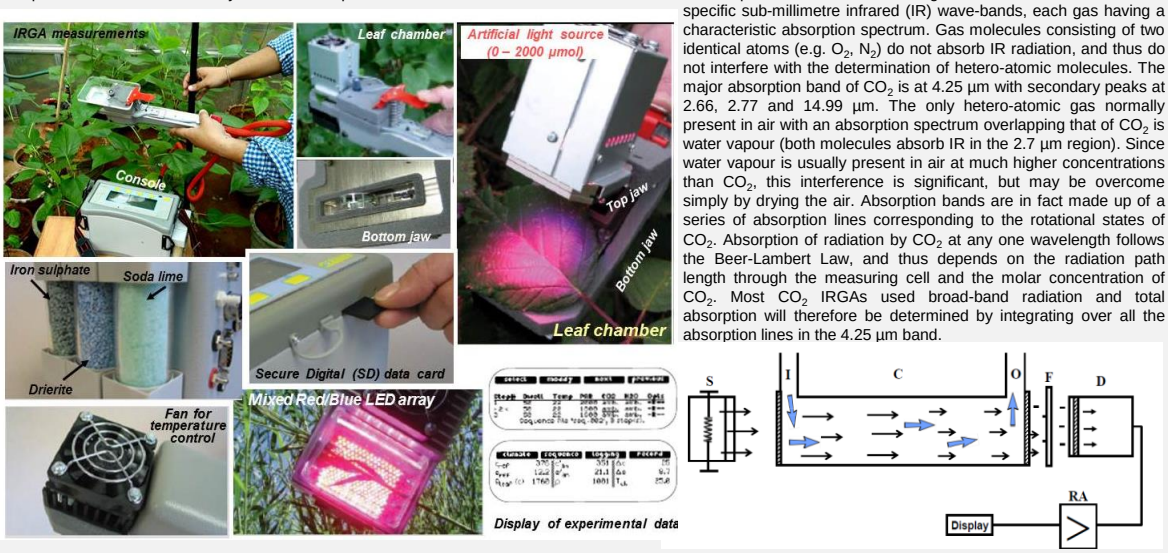

Generalised layout of a simple infrared CO_2 analyser. Infrared radiation from a source (S) is passed through a gas cell (C), with an inlet (I) and outlet (O), which allows a continuous flow of the gas being analysed. The infrared radiation leaving the cell may be filtered, typically with a 4.3 µm bandpass filter (F), before reaching the detector (D). The detector signal will be rectified and amplified (RA) before display.

The second approach involves use of chl fluorescence measurements to determine photosystem efficiency or photochemical capacity of photosystem. As mulberry has a great bio-diversity and exhibits extensive variation for stress tolerant traits, efficient and dependable screening tools are required to evaluate and screen the existing gene pool for identifying drought tolerant genotypes through non-invasive assessment of the plants at their growing phase. A chl fluorescence approach can complement to such screening tests for testing large germplasm and is reliable to discriminate among tolerant or sensitive genotypes (Sayar et al. 2008). In principle, chl fluorescence measurements are all sensitive to water stress and offer practical means for early detection of drought stress in higher plants (Maxwell and Johnson 2000) (**Box 3.2**). Although fluorescence measurements provide a useful measure of the photosynthetic performance of plants, its real strength lies in its ability to give information that is not readily available in other ways. In particular, fluorescence can give insights into the ability of a plant to tolerate environmental stresses and into the extent to which those stresses have damaged the photosynthetic apparatus.

Box 3.2 Principle and application of HANDY-PEA instrument used to determine chl a fluorescence.

If a healthy leaf is suddenly illuminated after a period of darkness, a time-dependent fluorescence induction (Kautsky Effect) is observed, the amplitude of which is proportional to the incident light level. Typically, illumination of a healthy leaf after 10 - 30 minutes dark adaptation results in an immediate rise to level (O or Fo) followed by a rapid polyphasic rise to a peak level (P or Fp). If sufficient light is used the primary electron acceptor from PSII (Qa) becomes fully reduced, transiently inhibiting photochemistry. In such circumstances the maximum fluorescence level is observed (Fm). The time to reach the fluorescence peak is very short (500 msec). Hence it is useful to plot the fluorescence rise on a logarithmic scale to view the polyphasic kinetic. The Handy PEA chlorophyll fluorimeter consists of a compact, light-weight control unit encapsulating sophisticated electronics providing the high time resolution essential in performing measurements of fast chlorophyll fluorescence induction kinetics. The chlorophyll fluorescence signal received by the sensor head during recording is digitised within the Handy PEA control unit using a fast Analogue/Digital converter. The chlorophyll fluorescence signal is digitised at different rates dependent upon the different phases of the induction kinetic. Initially, data is sampled at 10µs intervals for the first 300 µseconds. In addition to the standard fluorescence parameters, the Handy PEA offers the flexibility to analyse intermediate fluorescence data points at specific times within the fluorescence induction for further analysis. The analysis of these intermediate data points forms the basis of OJIP analysis more commonly now referred to as the JIP test. OJIP analysis and 'JIP Test' are terms adopted from the work of Prof. Reto Strasser and colleagues at the

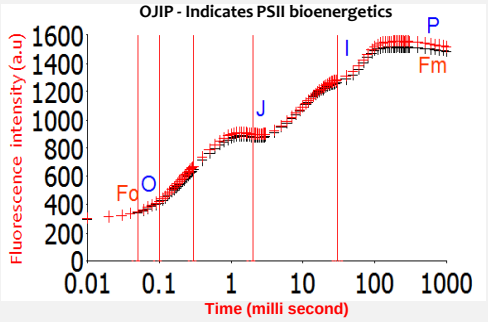

Laboratory of Bioenergetics, University of Geneva, Lullier-Jussy, Geneva, CH-1254 Switzerland. Historically, the literature reports fluorescence parameters which have been derived from the relative amplitudes of the extremes of the fluorescence signal e.g. Fo - the origin and Fm - the maximum under saturating light conditions. Whilst these parameters are still extremely valuable, thanks to the design of the Handy-PEA fluorometer we are now able to derive greater amounts of information from the fluorescence signal by monitoring the full kinetics of the rise from Fo to Fm. The OJIP analysis shows intermediate steps in the fluorescence induction transient such as The J step at approximately 2 milliseconds and the I step at approximately 30 milliseconds.

The advent and refinement of portable fluorometers has led to an upsurge in the use of chl fluorescence measurements under field conditions. Measurements made over a diurnal course can yield information pertaining to non-photochemical quenching, electron transport rates, quantum efficiency, and the extent of photoinhibition in response to drought, high light, elevated temperature and other single or combined environmental stresses (Maxwell and Johnson 2000). Since the capacity and responsiveness of antioxidative system remarkably contributes to the tolerance against photo-oxidative stress, investigation of these protective antioxidative metabolites has been considered to be another important approach to assess the photosynthetic capacity and photoprotection efficiency of different crops under drought stress (Tausz et al. 2003; Marron et al. 2006). As mentioned earlier, development of oxidative stress is a result of the imbalance between the formation of ROS and their detoxification (Mittler 2002, Zimmermann and Zentgraf 2005). Electron transport chains in chloroplasts and mitochondria membranes and excited chlorophyll are the most active intracellular producers of ROS such as superoxide anion radical ($O_2^{\bullet}$). and singlet oxygen ($_1O^2$). Other important sites of ROS production, especially of hydrogen peroxide (H_2O_2), are peroxisomes (sources—photorespiration and fatty acid β-oxidation), plasmalemma, and cell walls (Mittler 2002). Inhibition of photosynthesis under drought leads to exposure of chloroplasts to excess excitation energy and increased activated oxygen formation via the Mehler reaction (photoreduction of O_2 yielding $O_2^{\bullet}$) along with decrease in photorespiratory H_2O_2 production in peroxisomes (Smirnoff 1993). The mitochondrial respiration is also activated under stress (Mittler 2002). If not quenched, the above mentioned ROS can be converted to the highly toxic hydroxyl radical ($OH^{\bullet}$) which can randomly damage cell membranes, proteins, and nucleic acids. All ROS except H_2O_2 are short living (2–4 μs) so their harmful effect is mainly at the sites of their production. Only H_2O_2 (half-time 1 ms) can diffuse apart and penetrate membranes (Mittler 2002). It has a double role as ROS and as signaling molecule, a cellular indicator of stress and secondary messenger involved in the stress-response signal transduction pathway and activation of the defense systems.

Together with enzymatic detoxification cycles, the non-enzymatic antioxidants are important antioxidative defense constituents (as mentioned before). The distinct subcellular localization as well as the unique biochemical/physical properties of non-

enzymatic antioxidants renders the antioxidant defence system a versatile and efficient unit that can control ROS level in cells (Schwarz and Polle 1998; Hong-Bo et al. 2008). Low-molecular-weight metabolites which include tocopherols (α,β,γ,δ), ascorbic acid (AA) and glutathione; photo-protective pigments like carotenoids; and cellular osmoprotectants like proline are also some of the important non-enzymatic antioxidative defence constituents counteracting negative effects of ROS. These non-enzymatic metabolites play important functions in maintaining the integrity of photosynthetic membranes, protect metabolic processes, quench various ROS and lipid oxidization products, neutralize secondary products of ROS reactions and modulate signal transduction (Foyer and Noctor 2005; Hong-Bo et al. 2008). It is generally assumed that drought tolerant genotypes have higher levels of non-enzymatic antioxidants than those of drought susceptible ones. However, according to literature, in tree crops, concentration of these non-enzymatic antioxidants showed increases, decreases, or no effects, depending on duration of drought stress, the type of tree species studied and the antioxidant investigated (Tausz et al. 2003; Yanbao et al. 2006; Šircelj et al. 2007). So far, not many perennial tree crops have been investigated for their non-enzymatic antioxidative protection under water-limited conditions and undertaking such studies can considerably strengthen our knowledge to understand tree crops' responses towards drought. In a series of studies on oxidative stress responses of mulberry to water deficit, researchers have mostly concentrated on the responses of enzymatic-antioxidants (Chaitanya et al. 2003; Reddy et al. 2004; Reddy et al. 2005). However, the effects of drought on non-enzymatic antioxidants and their efficiency to quench ROS in drought tolerant mulberry genotypes were not examined in those studies. To the best of our knowledge, information is scanty regarding non-enzymatic antioxidative defence mechanisms in mulberry genotypes under water stress conditions. Kotresha et al. (2007) analyzed the genotypic variations in some of the major non-enzymatic antioxidants in mulberry leaf in response to drought and high temperature stress. However, their study mostly dealt with screening of mulberry germplasm for drought and high temperature tolerance and did not undertake detailed investigation of non-enzymatic antioxidative defense responses across different water stress regimes and also lacked insight into photosynthetic behavior of mulberry genotypes under drought stress conditions.

In contrast to other short-rotation crop species, the perennially cultivated evergreen and semi-deciduous mulberry genotypes exhibit the capacity to retain their leaves during the summer and are therefore expected to be physiologically acclimated to maintain photosynthesis during dry periods. Being an early successional species, mulberry genotypes are also known for their high gas exchange rates, and those high rates are accompanied by highly conductive xylem and leaves (Tyree and Zimmermann 2002). Such high rates might also be maintained during persisting droughts in the summer, although they may decline under extreme conditions. From a morphological point of view, plants in drought- stressed environments are expected to invest proportionately more in structures involved in water acquisition and transport. It has been proposed that leaf-level homeostasis in water status is attained due to whole-plant changes in morphology and anatomy (Bhaskar and Ackerly 2006; Maseda and Fernandez 2006). To date, studies evaluating water-use strategies in plants have been based on the analysis of diverse variables, exploring either gas exchange between leaves and the atmosphere (Acherar and Rambal 1992; Sala and Tenhnunen 1994; Medrano et al. 2009), hydraulic properties, such as vulnerability to xylem cavitation (Salleo et al. 1996; Iovi et al. 2009), or morphological adjustments (Sterck et al. 2008; Martínez-Vilalta et al. 2009). Although a number of studies on different tree species under tropical and subtropical climates have combined measurements of leaf gas exchange with hydraulic measures (Martínez-Vilalta et al. 2002a and 2002b; Bhaskar et al. 2007), no reports are available on any such study in mulberry that included diverse genotypes growing under field drought conditions and covering a whole-summer drought period.

Thus, keeping the necessity, applicability, reliability and importance of these physio-biochemical stress indices in mind, three major objectives were framed for the present work aiming to (i) evaluate the applicability of leaf gas exchange characteristics and hydraulic performance to determine drought stress responses in mulberry and distinguish drought tolerant genotype(s) from a diverse group of mulberry germplasm, (ii) to investigate and compare the photochemical performance of PSII among mulberry genotypes under drought stress conditions and (iii) to analyze and compare differential responses in non-enzymatic antioxidative protection among the mulberry genotypes and to assess whether these antioxidative metabolites share a positive correlation with the degree

of drought tolerance in mulberry. It was hypothesized that oxidative stress linked to drought could differentially alter the levels of non-enzymatic antioxidants in mulberry leaves with increasing stress intensity. Further, it was predicted that a relatively tolerant genotype could exhibit higher levels of certain non-enzymatic antioxidative metabolites that could significantly contribute protection against water stress, help to maintain better photosynthetic CO_2 fixation and might be used as markers for drought tolerance. Therefore, concomitant measurements of photosynthetic characteristics were undertaken along with important non-enzymatic antioxidative metabolites as well as stress indicators like malondialdehyde (MDA), hydrogen peroxide (H_2O_2) and superoxide anions ($O_2^{\bullet -}$) in mulberry leaves exposed to different drought stress intensities. In view of understanding various factors controlling and determining the growth and leaf yield of mulberry under water stress, it is imperative to identify certain morphological-growth characteristics which are directly associated with drought stress tolerance. Further, it is also necessary to evaluate various leaf yield components to understand their contribution in optimizing leaf yield production under drought. Thus, additionally, different growth and leaf yield characteristics were linked with the overall physiological performance of mulberry genotypes under low water regimes. The study was performed for three years in a three phasic experimental design (experiment no. 1: field assays; experiment no. 2: glasshouse assays and experiment no. 3: glasshouse assays) combining both field and glasshouse studies. In field assays, fifteen mulberry genotypes were surveyed under two irrigation regimes (well-watered and water-limited) whereas, the glasshouse studies were conducted with selected drought tolerant and drought susceptible genotypes.

Materials and Methods

Experiment no. 1: Field assays

Plant materials

The experimental material consisted of fifteen mulberry genotypes from varied agro-climatic conditions selected on the basis of putative differences in leaf yield under drought conditions (**Fig. 3.1**). The place of origin of the genotypes and the indigenous climatic

Fig. 3.1 The fifteen mulberry genotypes selected for the screening experiment for drought tolerance. The genotypes were selected based on putative differences in leaf yield under drought conditions. The genotypes belong to *M. indica* and *M. alba*. Genotype S13 was selected as a drought tolerant check. Photograph credit: A. Guha.

conditions under which they are grown are listed in **Table 3.1**. Among the tested genotypes, S13 was selected as a drought tolerant check as it was reported to perform well under water stress conditions (Sushelamma et al. 1990; Ramanjulu and Sudhakar 1997; Thimmanaik et al. 2002; Chaitanya et al. 2003; Kotresha et al. 2007). Cuttings of the tested genotypes were obtained from different sericultural research units of the country and propagated in nursery for one year, prior to the initiation of experiment.

Field assays: Experimental design and stress treatments

The study was conducted in the experimental fields of University of Hyderabad, India, located between 17.3°10´N and 78°23´E at an altitude of 542.6 m above MSL. Fifteen mulberry genotypes were evaluated under two irrigation regimes; well-watered (control) and water-limited (drought) during Feb to Jul (which constituted two dry summer seasons of the study zone) for three consecutive years (year 2007, 2008 and 2009). Precipitation during experimental time-span was sporadic and considered negligible, the mean air temperature recorded during daytime was 32.7°C, mean monthly photosynthetically active radiation (PAR), measured at peak photosynthetic time (between 09.00 -11.00 h) ranged from 1230 to 2500 µmol m^{-2} s^{-1} (**Fig. 3.2a,b**). The soil of the experimental site was sandy loam with a pH of 7.5. The experimental design was a randomized block with split plot arrangement of treatments (Chaturvedi and Sarkar 2000) including four replications in a net plot size of 14.4 m x 14.4 m (12.6 m rows, 0.9 m apart). Healthy rooted saplings were uprooted from the nursery and transplanted in the experimental field following pit system of plantation which is recommended for rainfed mulberry gardens (Dandin et al. 2003). After six months of establishment, the plants were uniformly pruned at a basal height of 30 cm. After 10 days, a dose of mixed fertilizer was applied at the rate of 50:50:50 kg NPK ha^{-1} with subsequent irrigation. Once complete leaf sprouting was achieved in all the plants, the treatments for water stress were imposed. The control plot was irrigated twice per week (20 to 24 irrigations in each growing season depending upon the edaphic and climatic conditions), whereas the stressed plot was irrigated once in a fortnight in a growing season. As genotypic variation in growth rates, leaf area, canopy size, stomatal conductance and transpirational water loss were apparent in the tested genotypes, in order

Table 3.1 List of mulberry genotypes (*Morus* spp L.) used in the study with their place of origin and climatic conditions.

Genotype	Place of origin	Mean temperature of warmest/coldest month(°C)	Mean annual precipitation (mm)	Duration of rainy season
AR12	CSR & TI†, Berhampore, India, 24°10'N, 88°25'E	34.6/16.5	1900	Jul-Sep
BOG4	Bogura, Bangladesh, 24°51'N, 89°15'E	32.6/11.9	1610	Jun-Sep
DD	Doon valley, India, 30°30'N, 78°20'E	27.7/11.6	2136	Jun-Sep
JPK	North-east India, 26°25'N, 94°36'E	36.2/17.2	2350	May-Sep
K2	Channapatna, India,12°65'N, 77°22'E	37.8/19.5	817	May-Sep, Oct-Dec
KS2	CSR & TI, Mysore, India,12°18'N, 76°42'E	26.5/18.6	700	May-Sep
MR2	Coonoor, India,11°35'N, 76°82'E	24.3/10.8	991	Jun-Sep
ML	Mysore, India,12°30'N, 76°65'E	28.6/18.4	782	May-Sep, Oct-Dec
PNG	Papua New Guinea,6°00'S, 147°00'E	34.4	2200	Throughout the year
S1	Mandalay, Myanmar,21°98'N, 96°08'E	32.9/23.2	150	May-Jun
S13	CSR & TI, Mysore, India,12°18'N, 76°42'E	28.5/18.6	700	May-Sep
S1635	CSR & TI, Berhampore, India,24°10'N, 88°25'E	34.6/16.5	1900	Jul-Sep
S36	CSR & TI, Mysore, India,12°18'N, 76°42'E	28.5/18.6	700	May-Sep
TR10	CSR & TI, Berhampore, India,24°10'N, 88°25'E	34.6/16.5	1900	Jul-Sep
V1	CSR & TI, Mysore, India,12°18'N, 76°42'E	28.5 - 18.6	700	May-Sep

†CSR & TI - Central Sericultural Research and Training Institute

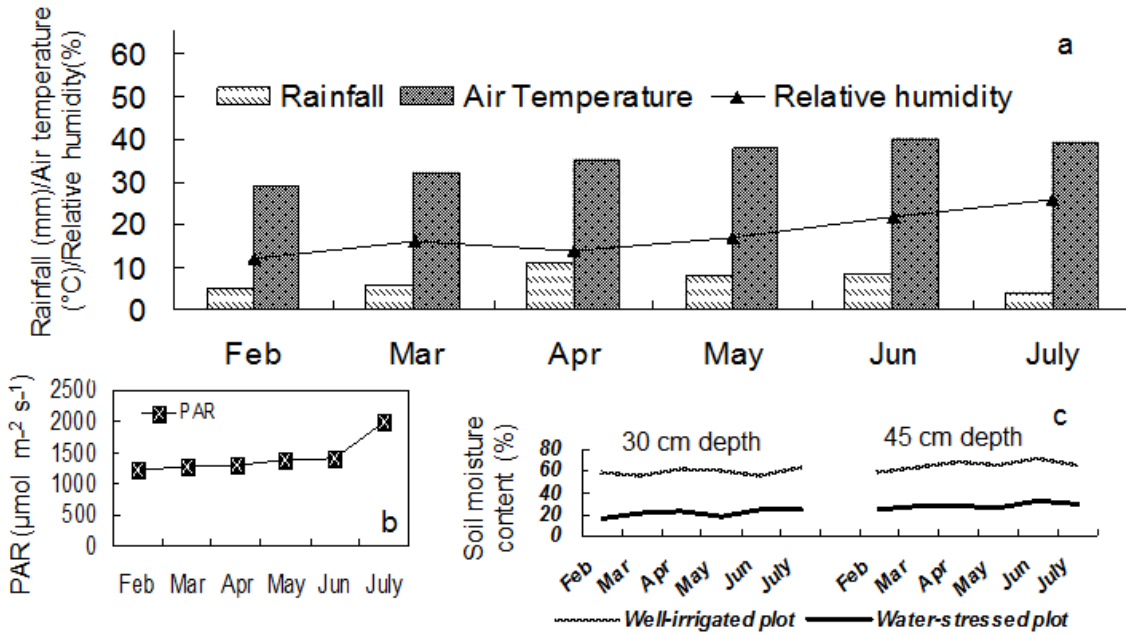

Fig. 3.2 Monthly averages of (a) rainfall, air temperature, relative humidity and (b) photosynthetically active radiation (PAR), at the study site during the experimental period (Feb to Jul) for three consecutive years (year 2007, 2008 and 2009). (c) Soil moisture contents (expressed as percentage of its oven-dried weight) recorded at two depths (30 cm and 45 cm) of the experimental site during Feb to Jul (year 2007, 2008 and 2009). Values are mean ± SD.

to prevent local differences in the degree of water availability, the duration of irrigation was increased in the control plot during the hottest months (Apr-Jun) for maintenance of soil moisture content within a range of 70 to 80%. Such treatments compensated for higher evapotranspirational moisture loss and maintained enough soil moisture in the control plot for normal growth of mulberry genotypes. To verify the degree of drought stress, soil moisture content at 30 cm and 45 cm depth of the control and stressed plots were determined periodically by taking wet weight and oven-dried (105°C for 2 days) weight of soil according to Ritchie et al. (1990) (**Fig. 3.2c**). Recommended package of practices were followed uniformly throughout the growing seasons for both the treatments which included the application of 20 metric tons farm yard manure (FYM) $ha^{-1}yr^{-1}$ (within a fortnight after first pruning) and 280:120:120 kg NPK $ha^{-1}yr^{-1}$ (within a month after each pruning) in equal splits. The plantations were maintained as bush by pruning after every experimental harvest at a basal height of 30 cm. All other agronomic practices were also kept normal and uniform for both the treatments. Measurements were made and data were collected for three years from six growing seasons *viz*., season-I (Feb 2007 - Apr 2007), season-II (May 2007 - Jul 2007), season-III (Feb 2008 - Apr 2008) and season-IV (May 2008 - Jul 2008), season-V (Feb 2009 - Apr 2009), season-VI (May 2009 - Jul 2009), covering six experimental harvests.

Field assays: Measurements of leaf gas exchange traits and leaf water status

The rate of leaf gas exchange was measured using a portable infrared CO_2/H_2O gas analyzer (IRGA) (LCpro-32070, ADC Bioscientific Ltd. U.K.) equipped with a broad leaf chamber. The air humidity in the leaf chamber was about 40%, with CO_2 concentration of 360-370 μmol mol^{-1}, air temperature of 26-28°C and flow rate of 500 μmol s^{-1}. The gas analyzer was used to measure instantaneous net photosynthetic rates (P_n), stomatal conductance (G_s) and transpiration rates (E), periodically during each growing season between 10.00 - 11.00 h on clear sunny days under natural PAR. Each measurement was made when P_n was stabilized; this process typically took 1 to 2 min. For calculating instantaneous water use efficiency ($WUE_i=P_n/E$), the values for the days on which VPD conditions were same or quite uniform were considered. All photosynthetic measurements

were performed *in-situ* on young, well-expanded and light-exposed leaves, randomly chosen from the upper half of the plant canopy of uniform plants in each replicate.

Field assays: Measurements of root-to-leaf specific hydraulic conductance (KSL)

During each experimental season, Ψ_L was measured diurnally in mature, fully expanded, upper canopy leaves from two to three apical twigs per stand using a portable pressure chamber (Plant Moisture System, SKPM 1400/40, Skye Instruments Ltd, England). All measurements were conducted within 3 min of leaf excision and minimum six leaves per genotype from the representative plants were sampled. In-situ root-to-leaf specific hydraulic conductance (KSL) was calculated by analogy to Ohm's law (Tyree 2003; Brodribb and Holbrook 2003*;* Franks 2004) : $K_{SL} = E_{max}/(\Psi_{soil} - \Psi_{md} - \rho gh)$, where Ψ_{soil} and Ψ_{md} were predawn soil and midday leaf water potentials, respectively, E_{max} was the peak transpiration rate at the midday in a leaf area basis, measured with infrared gas-analyzer system (LCpro-32070), ρ is density of water, g is acceleration due to gravity and h is tree plant. Instead of Ψ_{soil}, predawn leaf water potential (Ψ_{pd}) was used as a proxy under zero sap flow in the trees (**Box 3.3**). This equation is applicable when total rate of water uptake by the plant is equal to total rate of water lost (steady state), otherwise the capacitive (stored water) effect of adjacent tissues need to be considered. However, in the present study, the calculations of KSL were made during peak transpiration (E_{max}) when the effects of capacitance on transpiration were assumed to be minimal. Ψ_{pd} and Ψ_{md} measurements were made between 04.00–05.00 h and between 12.30-13.30 h, respectively. Based on diurnal measurements of leaf water potential at the experimental site, Ψ_{pd} and Ψ_{md} corresponded to maximum (Ψ_{Lmax}) and minimum (Ψ_{Lmin}) leaf water potentials, respectively. Leaf water status of the field grown genotypes (taking fully expanded leaves of the 3rd or 4th positions from the apex of top branches and sampled between 10.00 -11.00 h) was also determined by measuring the relative water content (RWC). The RWC was calculated by the formula: RWC(%) = [(fw-dw)/(tw-dw)]x100 where, fw is fresh weight, tw is the mass after rehydration (turgid weight) obtained by storing leaf samples for 24 h in distilled water and dw is oven dried weight (105 °C) of leaves (Castillo 1996).

Box 3.3 Diagrammatic illustration showing measurements and calculation of in-situ root-to-leaf specific hydraulic conductance (KSL).

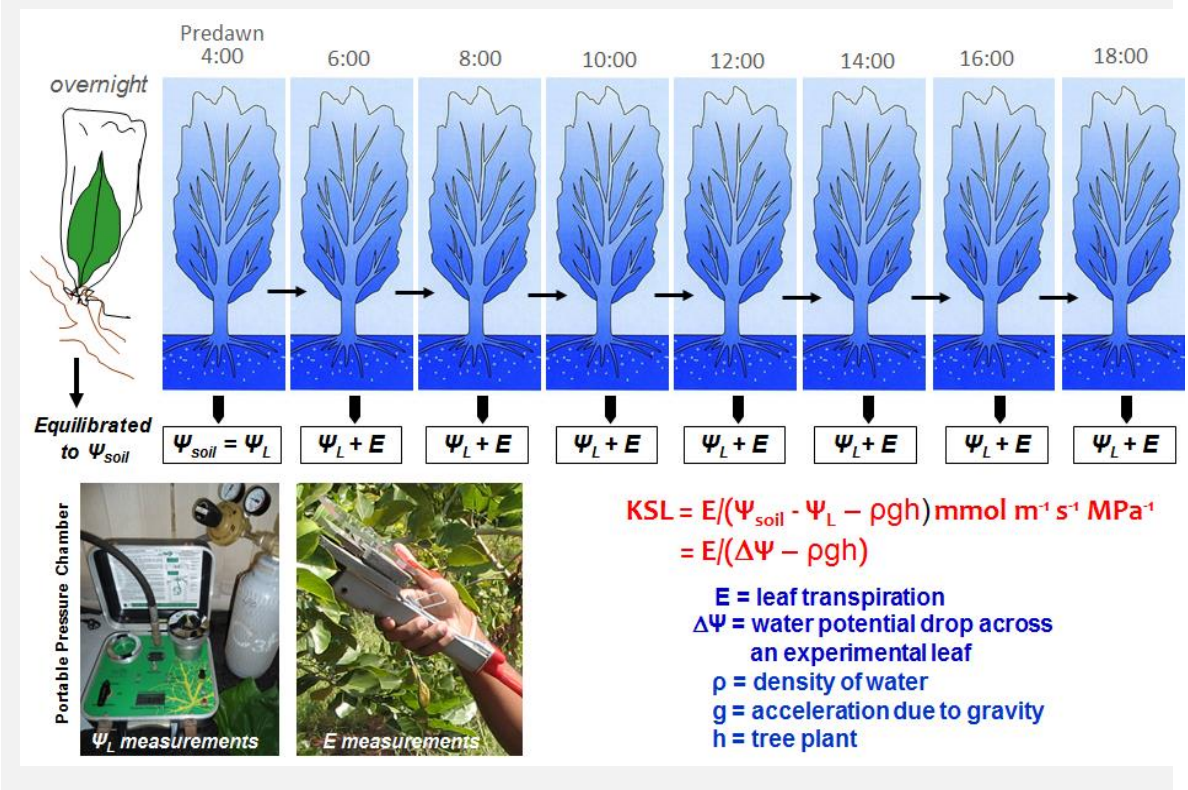

Field assays: Measurements of leaf yield (LY) and determination of tolerance index (TI)

At the end of each growing season, the plants were harvested to obtain yield measurements. Leaves of each plant were harvested separately and the weight was recorded as fresh weight (fw) of leaves in grams. For determining TI, the mean leaf yield derived from the average of four experimental harvests was considered. TI was calculated according to the formula: TI=LY(D)/LY(C) where, LY(D) and LY(C) are the leaf yields under drought (D) and control (C) conditions, respectively (Szira et al. 2008).

Experiment no. 1: Glasshouse assays

Two drought tolerant (S13 and V1) and two drought susceptible (DD and BOG4) genotypes were selected for this experiments to continue further studies (**Box 3.4**). Three

months old healthy potted (pot size 35L) saplings of the four mulberry genotypes were selected in a completely randomized block design (CRBD) with four replications. The plants were randomly submitted to two watering regimes: in stressed plants, water stress was imposed progressively by gradual decrease in pot water holding capacity (PC) (from 100% PC to 25% PC), whereas the control plants were maintained at 100% PC (Said and Hugh 2005). The water regimes maintained in the glasshouse experiments were similar to those experienced in the field trials. The study was undertaken for a time period of 71 days. Photosynthetic photon flux density (PPFD) measured (between 09.00 -11.00 h) inside the glasshouse ranged from 900 to 1200 μmol $m^{-2}s^{-1}$, air temperature ranged from 22±1°C (early morning) to 34±4°C (early afternoon) and relative humidity 36±5% to 48±2%. All the sampling and measurements were made using fully expanded leaves of the 3rd or 4th positions from the apex of top branches. Samplings were conducted periodically at an interval of 15-18 days and the results reported were the mean of all periodic data.

Box 3.4 Genotypic details of four mulberry genotypes (S13, V1, DD and BOG4) selected for drought tolerance experiments in this study. The morphological characters of the studied genotypes reported in this table are in complete agreement with the mulberry germplasm database of Central Sericultural Germplasm Resources Centre, Hosur, India (www.silkgermplassm.com).

Genotypic details	S13	V1	DD	BOG4
Germplasm accession no.	MI-0012	MI-0308	MI-0021	ME-0084
Branching nature	Erect	Erect	Semi erect	Semi erect
Phyllotaxy	Mixed	Mixed	1/2	1/3
Leaf nature	Homophyllous	Homophyllous	Homoophyllous	Homophyllous
Leaf lobation	Unlobed	Unlobed	Unlobed	Unlobed
Leaf shape	Narrow ovate	Narrow ovate	Wide ovate	Ovate
Leaf colour	Green	Dark green	Pale green	Light green
Sex expression	Unisexual male	Unisexual male	Bisexual	Bisexual
Internodal distance (cm)	4.75	4.6	4.6	5.5

Glasshouse assays: Measurements of leaf water status, leaf gas exchange and chl a fluorescence

Leaf water status was determined by calculating the RWC. Besides preliminary photosynthetic gas exchange functions *viz*., P_n, G_s, E and WUE_i, the plants were also analyzed for leaf temperature (T_L) by an integral leaf thermistor probe (ADC, M.PLC-011,

LICOR) attached to the leaf chamber. The internal CO_2 concentration (C_i) and internal to ambient CO_2 ratio (C_i/C_a) ratio were determined using IRGA. While measuring leaf gas exchange, the cuvette conditions were maintained at 40% air humidity, 360 μmol mol^{-1} CO_2 concentration and flow rate of 380 μmol s^{-1}. Each leaf was incubated for 1 to 2 min inside the microclimate of the leaf chamber until P_n was stabilized and thereafter data were recorded. All the measurements for leaf gas exchange parameters were conducted between 10.00 -11.00 h under natural PPFD inside the glasshouse. Chl a fluorescence of the non-detached leaves (carried out in the same leaves used for gas exchange records) was measured at predawn (05.00 -05.30 h) using a portable plant efficiency analyzer-fluorometer (Handy PEA-2126, Hansatech Instruments, Kings Lynn, UK). Minimal (F_o) and maximum (F_m) fluorescence yield were measured in the leaves, dark-adapted for 30 min. F_m was estimated by illuminating the dark-adapted leaves with PPFD pulse of 3,000 μmol m^{-2} s^{-1} for 1s with the help of light-emitting diodes (650 nm). Variable fluorescence (F_v) was calculated as the difference between F_m and F_o values ($F_v = F_m - F_o$). Maximum quantum yield of PSII in the dark-adapted leaves was estimated by the ratio $F_v/F_m = (F_m - F_o)/F_m$ according to Genty et al. (1989). Measurements were done in 10 replications. A single leaf per plant constituted each replicate.

Glasshouse assays: Growth and leaf yield measurements

Periodically, some of the potted mulberry plants were completely harvested (both shoots and roots) while remaining plants were harvested at the end of the experiment (75^{th} day) to obtain periodic as well as final growth and yield records. The height of all primary shoots of each plant was measured to obtain total shoot length. Relative plant height growth rate (RHGR) was calculated based on periodic data according to Hunt (1982). Leaves and stems of each plant were harvested separately and the weight recorded as fw in grams. Leaf weight and stem weight were added to get above ground biomass. Leaf area (cm^2) was recorded using a LICOR leaf area meter (LI 1600, LICOR Biosciences, USA). Root weight was recorded as fw of roots in grams. Root volume (cm^3) was measured following the water displacement method (Burdett 1979). Leaf mass ratio (LMR), stem mass ratio (SMR), root mass ratio (RMR) and root:shoot ratio were calculated using the data of leaf,

stem and root weights in the final harvest. The periodically as well as finally harvested plant tissues were oven-dried at 70 °C for 72 h to determine the dry matter of leaves, stems and roots and based on these data, the growth parameters *viz*., crop growth rate (CGR) net assimilation rate (NAR) and biomass duration (BMD) were calculated (Nagakura et al. 2004).

Experiment no. 2

Genotypes selected, stress treatments and experimental conditions in glasshouse

The experiment was conducted in the glasshouse chamber of University of Hyderabad, Hyderabad, India. Three months old, healthy potted (pot size 35L, filled with red loamy soil of pH 7.5) saplings of four mulberry genotypes (*M. indica* L. S36, MR2, K2 and V1) were selected for the study (**Box 3.5**). The experiment was established in CRBD with four replications. The different treatment pots were randomized at each water regime to avoid effects from other environmental factors, such as light conditions, temperature or humidity. Plants were submitted to four water regimes *viz*., (a) control: pots maintained at 100% PC, (b) low water stress: 75% PC, (c) medium water stress: 50% PC and (d) high water stress: 25% PC. The measured soil water content equivalent to 100% PC was 62.5% (weight basis). Accordingly, the soil water contents equivalent to 75%, 50% and 25% PC were also determined. To obtain a relatively stable soil water status, the volumetric soil water status was determined in the pots (at a depth of 25 cm midway between plant and pot rim) under each water regime, every 1-3 days prior to watering. The amount of water (W) applied at each irrigation was calculated using the following equation: $W = Y \times H \times A \times (W_t - W_o)$ where, Y = soil bulk density, H = soil depth, A = pot area, W_t = target soil water content and W_o = measured soil water content before watering (LiXin et al. 2009). The study was undertaken for a time period of 75 days calculated from the day after initiation of treatments. Chamber walls and ceiling were transparent to sunlight. Mean PAR inside the glasshouse measured between 09.00 - 11.00 h hour ranged from 1200 to 1800 µmol m^{-2} s^{-1}, mean air temperature ranged from 22±1°C (early morning) to 34±4°C (early afternoon) and relative humidity ranged from 20±5% to 41±2%. Leaf photosynthetic traits

and water status, foliar non-enzymatic antioxidants, extent of lipid peroxidation (MDA contents) and concentrations of ROS (H_2O_2 and $O_2^{\bullet -}$) were determined in fully developed young leaves of the 3rd-4th position from the shoot apex. Sampling was first conducted after 7 days of the onset of treatments. Thereafter, all samplings were periodically conducted at an interval of 10-12 days and the results reported are the mean of all periodic data.

Box 3.5 Genotypic details of four mulberry genotypes (S36, K2, MR2 and V1) selected for drought tolerance experiments in experiment no. 2. The morphological characters of the studied genotypes reported in this table are in complete agreement with the mulberry germplasm database of Central Sericultural Germplasm Resources Centre, Hosur, India (www.silkgermplassm.com). The agronomical characters are reported according to Dandin et al. 2003.

Genotypic details	S36	K2	MR2	V1
Genetic origin	Mutational selection	OPH* selection	Clonal selection	OPH selection
Germplasm accession no.	MI-0013	MI-0014	MI-0025	MI-0308
Morphological characters				
Branching nature	Semi erect	Erect	Erect	Erect
Phyllotaxy	Mixed	Mixed	Mixed	Mixed
Leaf nature	Homophyllous	Homophyllous	Heterophyllous	Homophyllous
Leaf lobation	Unlobed	Unlobed	Lobed/unlobed	Unlobed
Leaf shape	Wide ovate	Ovate	Narrow ovate	Narrow ovate
Leaf colour	Light green	Light green	Dark green	Dark green
Sex expression	Unisexual male or female	Unisexual female	Bisexual	Unisexual male
Ploidy level (n)	2n=30	2n=30	2n=28	2n=28
Agrnomical characters				
Internodal distance (cm)	4.0	4.2	3.7	4.6
Shoot height (90 days after pruning) (cm)	130	138	139	146
Fresh weight of 100 leaves (g)	518	400	377	560
Rooting (%)	> 80	> 80	> 90	> 90
Leaf yield potential (MT/ha/year)	40	35	35	60

Photosynthetic leaf gas-exchange traits and chl a fluorescence

Non-detached, young and fully expanded leaves from each genotype under each treatment were used to measure leaf photosynthetic traits during 09.00 to 11.00 h using a portable IRGA (LCpro-32070, ADC Bioscientific, UK) at a saturating PAR of 1800 µmol m^{-2} s^{-1}. Inside the leaf chamber, air humidity was about 60%, CO_2 concentration was 360 µmol mol^{-1} and air temperature was 25±2°C. Each measurement was made when the reading of net photosynthetic rate (P_n) was stabilized; this process typically took 1 to 2 min. Chl a fluorescence was determined using a portable fluorometer: Plant Efficiency Analyzer (Handy PEA-2126, Hansatech, UK). Measurements were made on dark-acclimated (30

min) leaves (same leaves used for photosynthetic studies) immediately after photosynthetic readings. The minimal fluorescence yield (F_o) and maximal fluorescence induction (F_m) were obtained by illuminating the leaves with a beam of saturating light (3,000 μmol m^{-2} s^{-1}) of 650 nm peak wave length obtained from three light-emitting diodes, focused on a circle of 5 mm diameter of the leaf sample. The first reliably measured point of the fluorescence transient is at 50 μs, which was taken as F_o. The variable fluorescence (F_v = F_m- F_o) and the maximum quantum yield (F_v/F_m) of PSII were estimated.

Leaf water status

Freshly harvested leaves were weighed immediately, then re-hydrated by immersing entire leaves in distilled water in plastic trays sealed with parafilm for 24 h at 4°C in darkness and subsequently over-dried for 24 h at 105°C. The leaf RWC was determined as 100 x [(fw-dw)/(tw-dw)] where, fw is the leaf fresh weight, tw is the turgid weight after re-hydrating the leaves for 24 h, and dw is the oven-dried weight of leaf. Leaf moisture content (LMC) was calculated as 100 x [(fw- dw)/fw].

Estimation of α-tocopherol

The extraction and analysis of α-tocopherol were carried out according to Yen et al. (1996) with minor modifications. Freshly collected leaf samples were immediately frozen in liquid nitrogen and stored at -40°C. The freeze-dried leaf tissue (1g) was homogenized with 10 ml of ice-cold 80% methanol using ultrasonication (VCX 130 Ultrasonic Processor, Sonics & Materials, Inc. USA). The leaf extract was centrifuged at 3,000 *g* for 15 min at 4ºC. The pellet was re-extracted thrice and supernatants were combined, filtered through 25 mm millipore filter and the filtrate was stored in dark at 3°C. α-Tocopherol content of the filtrate was determined by high performance liquid chromatography (HPLC) with a C_{18} reverse-phase column (Phenomenax, UK,) at a flow rate of 1ml min^{-1}, using isocratic solvent system: methanol and ethyl acetate (1:4, v/v) as an eluant. α-Tocopherol was quantified by UV detection system at 295 nm (LC-10 AT VP Shimadzu, Japan). Peak identification was performed by comparing the retention times with pure α-tocopherol standard (Sigma-Aldrich, Germany) and confirmed with characteristic spectra obtained

from the photoiodote array detector, which also permitted the confirmation of the purity of the peaks. α-Tocopherol content was expressed in µg g^{-1} fw.

Estimation of ascorbic acid (AA)

AA was determined according to Omaye et al. (1979) with some modifications. Fresh leaf tissue (0.5g) was homogenized with 5 ml of 10% (w/v) trichloroacetic acid (TCA). The extract was centrifuged at 10,000 *g* for 20 min at room temperature. The pellet was re-extracted twice, supernatants were combined and used for assay. To 0.5 ml of extract, 1 ml of 2% DNTPH (2, 4-dinitrophenyl hydrazine in 0.5 N H_2SO_4), a drop of 10% thiourea (in 70% ethanol) were added and incubated at 37ºC for 3 h. After incubation, 1.75 ml of ice-cold 65% H_2SO_4 was added, allowed to stand at 30ºC for 30 min and the absorbance of the resulting colour was detected at 520 nm in a UV-Visible spectrophotometer (Shimadzu Corporation, Tokyo, Japan). The AA content was determined from the standard curve prepared with authentic L-AA (Sigma) and was expressed in mg g^{-1} fw.

Estimation of total glutathione

Total glutathione content in mulberry leaves was determined according to Griffith and Meister (1979). Fresh leaf tissue (0.2 g) was homogenized with 0.8 ml of 10% sulphosalicylic acid and centrifuged at 15,000 *g* for 5 min at 4ºC. The supernatant was neutralized by adding 0.6 ml of 10% sodium citrate. One ml reaction mixture was prepared by adding 100 µl extract, 100 µl double distilled water (ddw), 700 µl of 0.3 mM NADPH in potassium phosphate buffer (20 mM, pH 7.5) and 6 mM 5'-dithio-bis(2-nitrobenzoic acid)(DNTB). The reaction mixture was stabilized at 25°C for 3-4 min. Then 10 µl glutathione reductase (GR) was added to the reaction mixture and the absorbance of the resulting colour was read at 412 nm in a UV-Visible spectrophotometer. The results were expressed in µmol g^{-1} fw.

Estimation of free proline

Free proline content in leaf tissue was determined according to Bates et al. (1973). Fresh leaf sample (0.5 g) was homogenized in 10 ml of 3% sulphosalicyclic acid. The homogenate was centrifuged at 9,000 *g* for 15 min at room temperature. The reaction

mixture containing 1 ml leaf extract, 2 ml acid ninhydrin and 2 ml glacial acetic acid was incubated for 1h in boiling water bath. After incubation, 4 ml of toluene was added to the reaction mixture and mixed vigorously by vortexing for 15 to 20 sec. The upper reddish pink coloured toluene layer was separated and the absorbance was read at 520 nm in a UV-Visible spectrophotometer. Proline content was determined from the standard curve prepared by using authentic proline (Sigma) and was expressed in mg g^{-1} fw.

Estimation of total carotenoids

For quantification of total carotenoids, fresh leaf sample (0.5 g) was homogenized in 10 ml of 80% (v/v) acetone. The homogenate was centrifuged at 10,000 *g* for 5 min. The supernatant was collected and the extraction was repeated twice with 80% acetone. Absorbance of the extract was read at 663.2, 646.8 and 470 nm in a UV-Visible spectrophotometer. Total carotenoid content was calculated using the extinction coefficients given by Lichtenthaler (1987) and results were expressed in mg g^{-1} fw.

Estimation of MDA

The extent of lipid peroxidation was determined by quantifying malondialdehyde (MDA) (Fu and Huang 2001). Fresh leaf sample (0.5 g) was homogenized in 5 ml of 0.1% (w/v) TCA at 4°C. The homogenate was centrifuged at 5,000 *g* for 10 min at 4ºC. The reaction mixture contained 500 µl of the supernatant and 4 ml of 0.5% (w/v) thiobarbituric acid (TBA) in 20% (w/v) TCA. The reaction mixture was incubated at 95°C in a shaking water bath for 30 min and the reaction was stopped by quickly cooling the tubes in an ice water bath. The samples were centrifuged at 5,000 *g* for 15 min and the absorbance of the supernatant read at 532, 600 and 440 nm. MDA concentration was calculated using an extinction coefficient of 155 mM^{-1} cm^{-1}.

Estimation of H_2O_2 and superoxide anion ($O_2^{\cdot -}$)

H_2O_2 was estimated according to Becana et al. (1986) with minor modifications. Fresh leaf tissue (0.5 g) was homogenized in liquid nitrogen with 5% (w/v) TCA. The homogenate was centrifuged at 12,000 *g* for 10 min at 4°C. The supernatant was collected in fresh eppendorf and once again centrifuged at 12,000 *g* for 2 min, and used immediately for

assay. H_2O_2 concentration was determined spectrophotometrically at 508 nm in a reaction mixture that contained 50 mM phosphate buffer (pH 8.4), 0.6 mM 4-(-2 pyridylazo) resorcinol and 0.6 mM potassium–titanium oxalate in 1:1 proportion.

$O_2^{\bullet -}$ accumulation was determined according to Doke (1983) with minor modifications. Fresh leaf sample (0.5 g) was placed in test tube containing 7 ml of reaction mixture which contained 50 mM phosphate buffer (pH 7.8), 0.05% nitroblue tetrazolium (NBT) and 10 mM of NaN_3. The test tubes were then incubated in dark for 5 min, and subsequently 2 ml of solution was taken from the tube and heated for 10-15 min at 85°C. The sample was cooled on ice for 5 min and the absorbance (A) was measured at 580 nm against the control.

In-situ localization of H_2O_2 and $O_2^{\cdot -}$

In-situ detection of H_2O_2 was performed using DCF (2', 7'-dichlorofluorescin diacetate; H_2DCFDA) according to Keyes et al. (2002) with some modifications. Leaf discs were transferred to petri dishes filled with water. Before treating with DCF, control leaves were incubated with catalase (1500 U ml^{-1}, Sigma) and superoxide dismutase (900 U ml^{-1}, Sigma) for 2 h in darkness. The discs were incubated in 4µM DCF in 5 mM dimethyl sulfoxide (DMSO) for 12 h in darkness on an orbital shaker. The discs were washed thrice with 50 mM potassium phosphate buffer (pH 7.4), mounted on glass slides and observed under a confocal fluorescence microscope (Leica Model DM 6000, Germany) with a filter set no. 10, excitation 475 nm, emission 520-580 nm). Histochemical localization of $O_2^{\cdot -}$ in leaf tissue was performed as described by Hernandez et al. (2001). Leaf discs were vacuum infiltrated with 0.1 mg ml^{-1} solution of NBT in 0.2 M sodium phosphate buffer (pH 7.6) for 15 min. The discs were incubated at 25°C in dark for 2 h. Controls or blanks in presence of SOD and $MnCl_2$ (scavengers of $O_2^{\bullet -}$) were also performed simultaneously by adding 100 U of SOD and 10 mM of $MnCl_2$ into the infiltration buffer. Pigments present in the leaf discs were cleared in 80% (v/v) ethanol for 30 min at 70°C. The mounted leaf discs were observed using a Leica Wetzlar light microscope.

Plant morphology, growth and biomass

At the end of experiment (on 75th day), plants were photographed to record and compare the morphological differences among the genotypes due to different drought stress intensities. All the plants were completely harvested to obtain growth and biomass data. Plant heights were recorded and number of branches per plant was counted. Leaves of each plant were harvested separately and the weight recorded as fresh weight (fw) of leaves in grams. Likewise, the stems of each plant were pruned separately and the weight recorded as fw in grams. Leaf weight and stem weight were added to get shoot weight (above ground biomass). Root weight of each plant was taken separately after washing and the weight recorded as fw of roots in grams. Root to shoot ratio was calculated using the data of root weight and shoot weight.

Statistical analyses

The significance of the differences between mean values of control and water-stressed plants was determined using the *t*-test and analysis of variance (ANOVA). Data analyses were performed using the statistical package SigmaPlot 11.0. Differences among genotypes and treatments were determined by two way ANOVA. To determine the influence of year, genotype and year × genotype (Y × G) interaction on the variance of growth and yield parameters measured across experimental seasons, the ANOVA-general linear model (GLM) analysis was performed. The XLSTAT was used to determine correlations between different pairs of variables using Pearson correlation coefficient matrix and the threshold for significance was adjusted using Bonferroni correction. Differences among genotypes and treatments in the daily course of leaf gas exchange, chl a fluorescence, leaf water status and antioxidant levels were determined by two way repeated measures analysis of variance (ANOVAR) using genotypes as between-subjects, and using 'time intervals (Tm)' as within-subject variable. Growth and biomass data were analyzed using two way ANOVA to test significant differences between the genotypes, treatments and their interactions on measured traits. Coefficients of determinations (R^2) of linear relationships between the investigated parameters were established by using linear regression. The linear regression slopes were analyzed using bivariate correlation significance tests. The statistical analyses were performed using Sigma Plot 11.0.

Results

Experiment 1 (field assays): Leaf gas exchange, leaf water relations and KSL

Significant genotypic variation was recorded for P_n among the mulberry genotypes in both water regimes (**Fig. 3.3a**). In control conditions, genotype PNG exhibited highest P_n (15.08 µmol m^{-2} s^{-1}) followed by AR12 (13.2 µmol m^{-2} s^{-1}), V1 (12.58 µmol m^{-2} s^{-1}) and BOG4 (12.52 µmol m^{-2} s^{-1}). P_n was minimum for ML (9.03 µmol m^{-2} s^{-1}) and S1 (7.98 µmol m^{-2} s^{-1}). Water stress apparently reduced P_n in all mulberry genotypes, and high reduction in P_n was observed in genotypes DD (73.6%), BOG4 (77.1%) and PNG (80.1%). However, the higher P_n under water deficit conditions was recorded in genotypes V1 (7.9 µmol m^{-2} s^{-1}), S13 (7.17 µmol m^{-2} s^{-1}) and S1 (6.32 µmol m^{-2} s^{-1}). The G_s ranged from 0.57 to 0.27 mol m^{-2} s^{-1} and from 0.19 to 0.012 mol m^{-2} s^{-1} in control and stress treatments, respectively (**Fig. 3.3b**). In well-watered conditions, S1635 exhibited the maximum G_s (0.57 mol m^{-2} s^{-1}) followed by KS2 and V1 (0.46 mol m^{-2} s^{-1}); whereas G_s was lower in JPK (0.29 mol m^{-2} s^{-1}) and S1 (0.27 mol m^{-2} s^{-1}). However, under water stress, genotype V1 (0.19 mol m^{-2} s^{-1}), S13 (0.16 mol m^{-2} s^{-1}) and S1 (0.12 mol m^{-2} s^{-1}) exhibited maximum G_s. Drought caused drastic reduction in E of all the genotypes (**Fig. 3.3c**) with an average decline of 70%. Genotypes *viz*., V1 (1.65 mmol m^{-2} s^{-1}), S36 (1.58 mmol m^{-2} s^{-1}), S1 (1.57 mmol m^{-2} s^{-1}) and S13 (1.48 mmol m^{-2} s^{-1}) maintained relatively higher rates for E under low water regimes. Relative to unstressed plants, drought led to an increase in WUE_i in most of the mulberry genotypes except in PNG and BOG4 (**Fig. 3.3d**). PNG had highest WUE_i (4.3 µmol CO_2 mol^{-1} H_2O) under well-watered conditions, however, during water stress the WUE_i decreased substantially in PNG (1.87 µmol CO_2 mol^{-1} H_2O) compared to control. In BOG4 there was a 13.4% reduction in WUE_i under water stress. Genotypes V1, S13 and S1 performed best in terms of WUE_i under drought regimes and the maximum percentage increase in WUE_i was recorded in S1 (61.2%) followed by S13 (57.9%).

Among the genotypes grown under control conditions, Ψ_L varied from -0.82 to -1.35 MPa (**Fig. 3.3e**). Genotype V1, S13 and S1 exhibited values < -1.0 MPa under well-watered conditions. Drought stress caused significant alterations in Ψ_L among the genotypes and the values ranged between -1.65 MPa in S1 and -2.96 MPa in PNG (**Fig. 3.3e**). Followed by S1, genotype V1 and S13 showed less negative Ψ_L values (-1.8 and -

1.85 MPa, respectively) when compared to other genotypes (Ψ_L values ranged from -1.94 to -2.96 MPa).

KSL varied greatly among the genotypes both under control and drought stressed conditions (**Fig. 3.3f**). Under well-watered conditions, S1, S13, V1 and TR10 recorded higher KSL (> 5 mmol MPa^{-1} m^{-2} s^{-1}), whereas the lowest value was recorded in PNG (~ 3 mmol MPa^{-1} m^{-2} s^{-1}) followed by BOG4 (~ 3.2 mmol MPa^{-1} m^{-2} s^{-1}), JPK (~ 4.1 mmol MPa^{-1} m^{-2} s^{-1}) and K2 (~ 4.2 mmol MPa^{-1} m^{-2} s^{-1}). The remaining genotypes (S36, S1635, ML, MR2, KS2, DD and AR12) had medium KSL under well-irrigated conditions (values ranging from 4.8 to 4.3 mmol MPa^{-1} m^{-2} s^{-1}). Drought stress caused significant decrease in KSL and the values on an average decreased to more than 50% in all the genotypes (**Fig. 3.3f**). In water-stressed S1, V1 and S13, the KSL values were comparatively higher (> 1.6 mmol MPa^{-1} m^{-2} s^{-1}) than compared to other genotypes (KSL values ranged from 0.5 to 1.3 mmol MPa^{-1} m^{-2} s^{-1}).

The correlations among leaf gas exchange traits, WUE_i, Ψ_L and KSL were a mixture of both positive and negative relationships and were highly significant for most of the pairwise comparisons (**Fig. 3.4**). P_n was positively correlated with G_s, E and KSL, whereas, shared negative correlation with WUE_i and $-\Psi_L$. Like P_n, G_s was also found to be positively correlated with E and KSL, but negatively associated with WUE_i and $-\Psi_L$. Variable E shared significantly strong positive correlation with KSL (R^2 = 0.80) but a negative correlation with WUE_i (R^2 = 0.70). WUEi and $-\Psi_L$ were not significantly associated, whereas $-\Psi_L$ was significantly negatively correlated with KSL (R^2 = 0.73) (**Fig. 3.4**). The RWC of the drought stressed mulberry genotypes ranged from 72.1% to 66.6% and the value was higher in V1 followed by TR10 and S1. The lower value of RWC was observed in DD and PNG (**Table 3.2**).

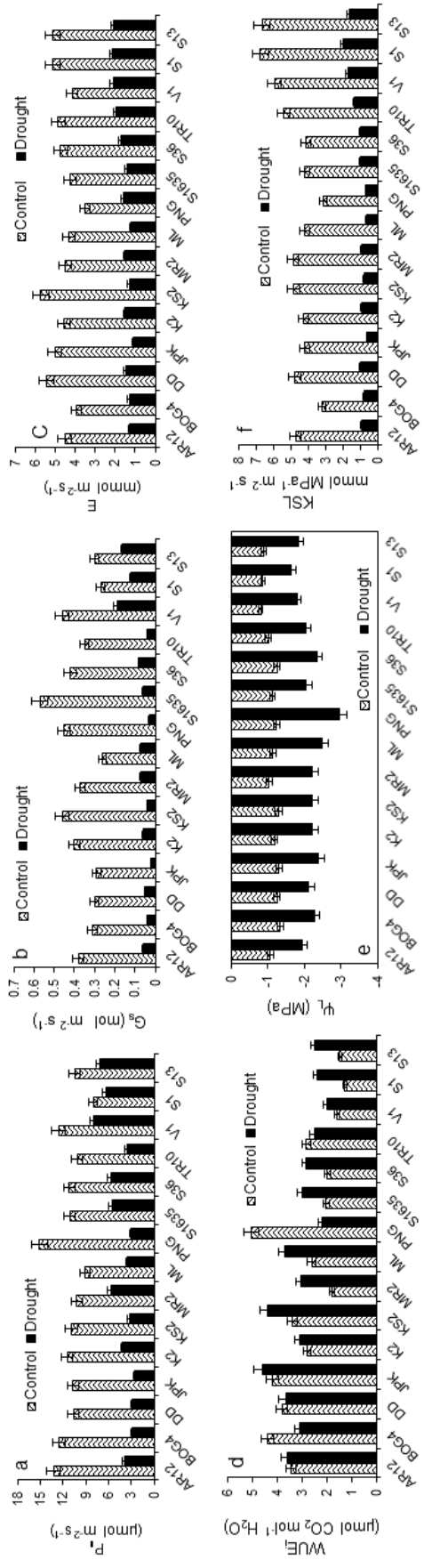

Fig. 3.3 Leaf gas exchange characteristics in cluding (a) net photosynthetic rate (P_n), (b) stomatal conductance (G_s), (c) transpiration rate (E), (d) instantaneous water use efficiency (WUE_i), (e) leaf water potential (Ψ_L) and (f) leaf-specific soil-to-leaf hydraulic conductance (KSL) of fifteen mulberry genotypes grown under two water regimes (control and drought) during Feb to Jul for three consecutive years (2007-2009). Data represented are the average over six growing seasons. Values are mean ± SD.

Table 3.2 Effect of drought stress on leaf relative water content (RWC) in the three months old leaves of mulberry genotypes grown under field conditions. Data represented are the average over six growing seasons. Values are mean ± SD. Effects of drought were tested by *t*-test. ($P < 0.001$).

Genotypes	AR12	BOG4	DD	JPK	K2	KS2	MR2	ML	PNG	S1635	S36	TR10	V1	S1	S13
RWC (%)	68.7 ± 1.8	68.8 ± 2.6	69.6 ± 1.5	66.8 ± 1.1	68.3 ± 1.4	69.2 ± 1.2	69.2 ± 1.3	70.5 ± 1.5	66.6 ± 0.8	70.5 ± 1.3	68.6 ± 0.6	71.7 ± 0.5	72.1 ± 1.1	71.6 ± 1.1	70.4 ± 1.4

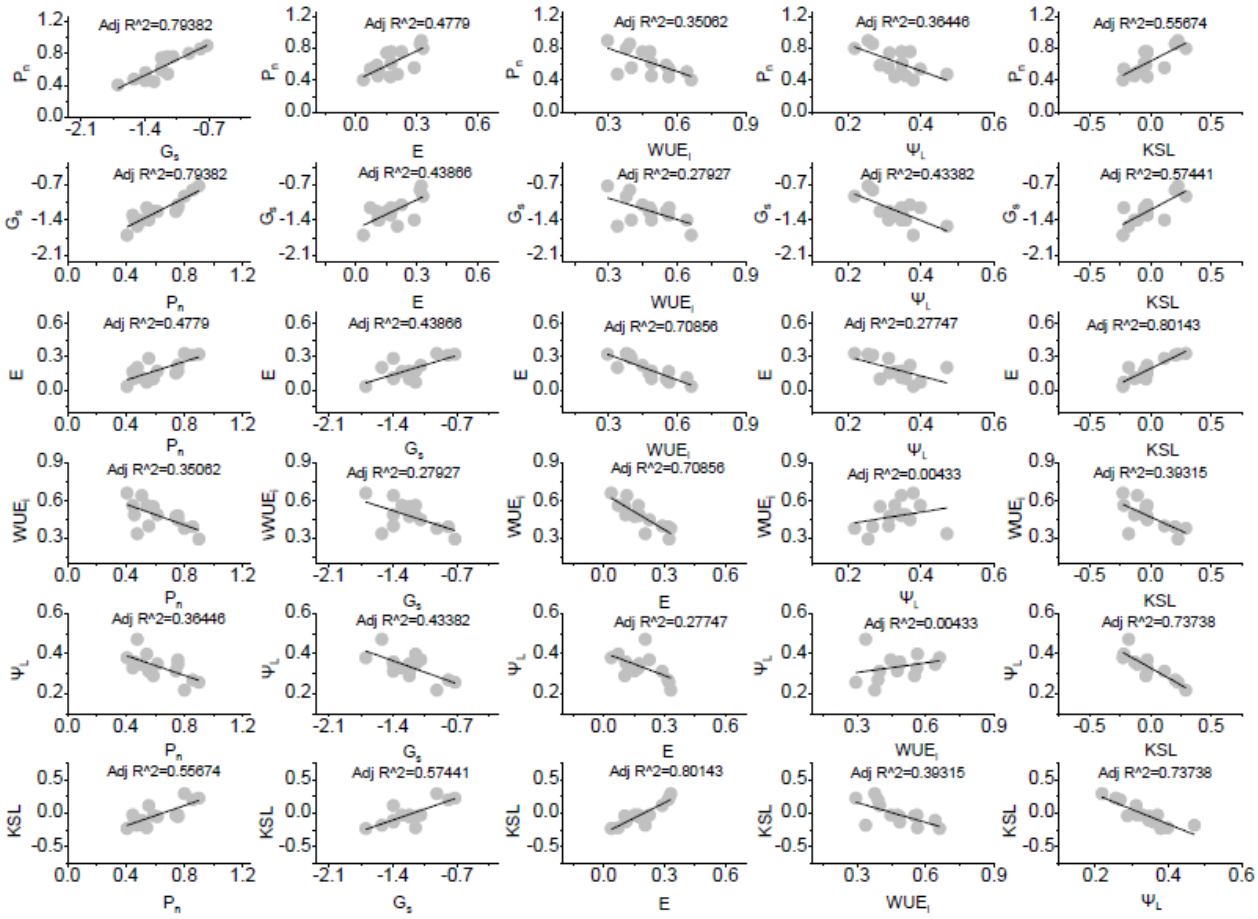

Fig. 3.4 Scatter matrix plots and regressions of multiple parameter relationships used to assess drought tolerance of mulberry genotypes. The parameters used were: net photosynthetic rate (P_n), stomatal conductance (G_S), transpiration rate (E), instantaneous water use efficiency (WUE_i), leaf water potential (Ψ_L) and leaf-specific soil-to-leaf hydraulic conductance (KSL). All values were log transformed before analysis.

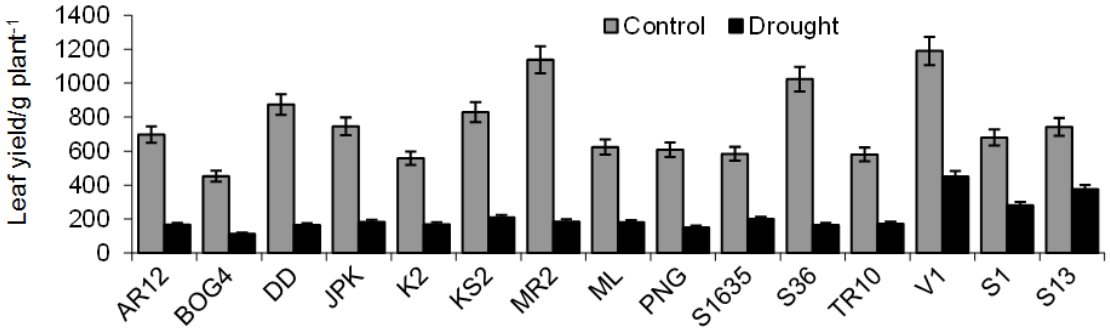

Fig. 3.5 Comparative leaf yield of fifteen mulberry genotypes grown under two water regimes (control and drought) during Feb to Jul for three consecutive years (2007-2009). Data represented are the average over six growing seasons. Values are mean ± SD.

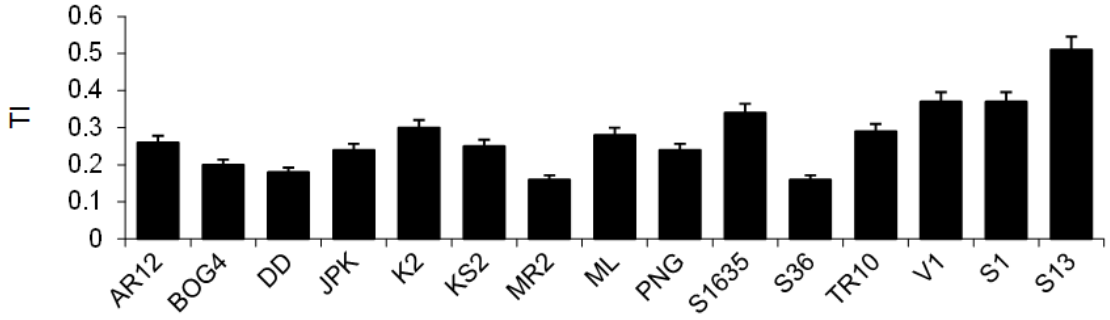

Fig. 3.6 Tolerance index (TI, based on leaf yield) of fifteen mulberry genotypes grown under drought stress conditions during Feb to Jul for two consecutive years (2007-2009). Data represented are the average over six growing seasons. Values are mean ± SD.

Experiment 1 (field assays): Leaf yield performance and tolerance index (TI)

The mulberry genotypes exhibited wide genetic variance in leaf yield production (**Fig. 3.5**). Under well-watered conditions, the highest leaf yield plant^{-1} was recorded in V1 (1190g plant^{-1}) followed by MR2 (1138g plant^{-1}) and S36 (1024g plant^{-1}). Genotypes *viz*, BOG4 (452g plant^{-1}), K2 (558g plant^{-1}) and TR10 (580 plant^{-1}) were found to be low leaf yielders amongst tested mulberry genotypes under high water availability. A marked decline in leaf yield was recorded in all the genotypes under water-stressed treatment. However, the maximum leaf yield plant^{-1} was recorded in V1 (450g plant^{-1}) followed by S13 (375g plant^{-1}) under drought, whereas the minimum leaf yield was obtained in DD (164g plant^{-1}) and PNG (150g plant^{-1}) followed by BOG4 (112g plant^{-1}). The TI calculated on leaf yield plant^{-1} basis, revealed conspicuous genotypic variation among the tested mulberry accessions in respect to the degree of drought tolerance (**Fig. 3.6**). The TI ranged from 0.51 to 0.16. Highest TI value was obtained with S13 (0.51) followed by V1 (0.4) and S1635 (0.34), whereas the value was much lower for the genotypes S36 (0.16), MR2 (0.16), DD (0.18) and BOG4 (0.2).

Experiment 1 (glasshouse assays): Leaf water status, leaf gas exchange and chl a fluorescence

Under water stress Ψ_L was reduced in all mulberry genotypes compared to control (**Fig. 3.7 a**). However, V1 presented the highest Ψ_L of -1.88 MPa, whereas the decrease in Ψ_L was stronger in BOG4 and dropped to -2.86 MPa during periods of water deprivation. Water stress caused a similar trend of inhibition in the functional gas exchange characteristics of four mulberry genotypes evaluated under glasshouse conditions. Suppression of $P_{n,}$ G_s and E was more pronounced in water-stressed leaves of drought susceptible genotypes (DD and BOG4) compared to the drought tolerants (V1 and S13). Genotype V1 and S13 exhibited less inhibition in $P_{n,}$ G_s and E and maintained better gas exchange functions during drought period (**Fig. 3.7a, b, c, d**). Compared to well-watered counterparts, a reduction in C_i was observed in the stressed leaves of all mulberry genotypes (**Fig. 3.7f**). The reduction in C_i was more conspicuous in DD (21%), whereas the ratio decreased only 12.3% and 13% in V1 and S13, respectively. The T_L under control conditions ranged between 31.4°C to 35.9°C. Among the four mulberry genotypes, V1 had minimal T_L under well-irrigated conditions. Water stress resulted in an increase in T_L for all the genotypes (**Fig. 3.7g**). The highest T_L of stressed mulberry leaves was observed in BOG4 (37.7°C) followed by DD (37°C), whilst V1 again maintained the lowest value for T_L (~32.6°C) throughout the periods of water deprivation.

Chl a fluorescence parameters were significantly affected by drought stress. Drought stress induced an increase in F_o which was significantly more in DD and BOG4, compared to V1 and S13 (**Fig. 3.7h**). Unlike F_o, a reduction in F_m was encountered in the water stressed genotypes compared to the well-watered counterparts (**Fig. 3.7i**). Reduction in F_m was more conspicuous in BOG4 (16%), followed by DD (9.7%), whereas a reduction of 2% in F_m was recorded in the stressed leaves of S13. In V1, a marginal increase in F_m (0.8%) was observed in water-stressed conditions, compared to control. The F_v/F_m ratio in four mulberry genotypes remained above 0.8 in control treatment throughout the experiment. The ratio was also practically not altered in the drought tolerant genotype V1 (0.812) and S13 (0.809) under water stress. However, significant drawdown in F_v/F_m was recorded in the susceptible genotypes, particularly in BOG4 (0.653) followed by DD (0.726) (**Fig. 3.7j**).

Experiment 1 (glasshouse assays): Growth and leaf yield characteristics

The RHGR was analyzed for the four mulberry genotypes according to the increment over periodic observations under both the watering regimes. Drought stress significantly slowed down plant height growth rate in all the mulberry genotypes compared to control. Genotype V1 and S13, however, had greater height growth rate than the drought sensitive genotypes DD and BOG4 (**Fig. 3.7k**). Drought stress also led to decrease in total biomass accumulation in both the tolerant and susceptible genotypes. In V1 and S13, there was no significant alterations in biomass allocation in shoots since LMR and SMR were unaffected by drought. By contrast, the group of drought susceptible genotypes allocated more biomass to stems and significantly less to leaves, as deduced from the decrease in LMR (~38.5%) at the expense of an increase in SMR (~28.4%) (**Fig. 3.7l, m**). No significant variation was encountered in RMR within the genotypes, however within the treatments, there was significant variation. Higher RMR was evident in all the genotypes under low moisture regimes (**Fig. 3.7n**). Water deprivation significantly increased the root:shoot ratio in the tolerant as well as in susceptible mulberry genotypes (**Fig. 3.7o**). CGR ranged from 1.5 to 2.07 g m^{-2} day^{-1} and from 0.33 to 0.61 g m^{-2} day^{-1} under control and drought treatments, respectively (**Fig. 3.7p**). Under well-watered conditions, V1 had higher CGR (2.07 g m^{-2} day^{-1}); while in BOG4 the rate was minimal (1.5 g m^{-2} day^{-1}). Deprivation in soil moisture led to a severe reduction in CGR in all the mulberry genotypes. Under well-watered conditions, the genotypes did not differ much in respect to NAR; however drought stress led to a significant drawdown in NAR in all groups (**Fig. 3.7q**). V1 exhibited relatively higher values for NAR (0.64 g m^{-2} day^{-1}) followed by S13 (0.6 g m^{-2} day^{-1}) under low water regimes, whereas in BOG4 the NAR was lowest (0.2 g m^{-2} day^{-1}). Regardless of the watering regimes, V1 maintained relatively higher values for BMD, whilst drought caused dramatic reduction of BMD in all the mulberry genotypes with an average decline of 73.1% (**Fig. 3.7r**).

The four mulberry genotypes also varied significantly in respect to root characteristics (**Table 3.3**). Genotypes differed significantly in root fw both under control and drought stress conditions. Enhancement in root fw was observed in the tolerant genotypes (~15.5%) under water stress treatments. Vertical proliferation of roots was retarded, in all the

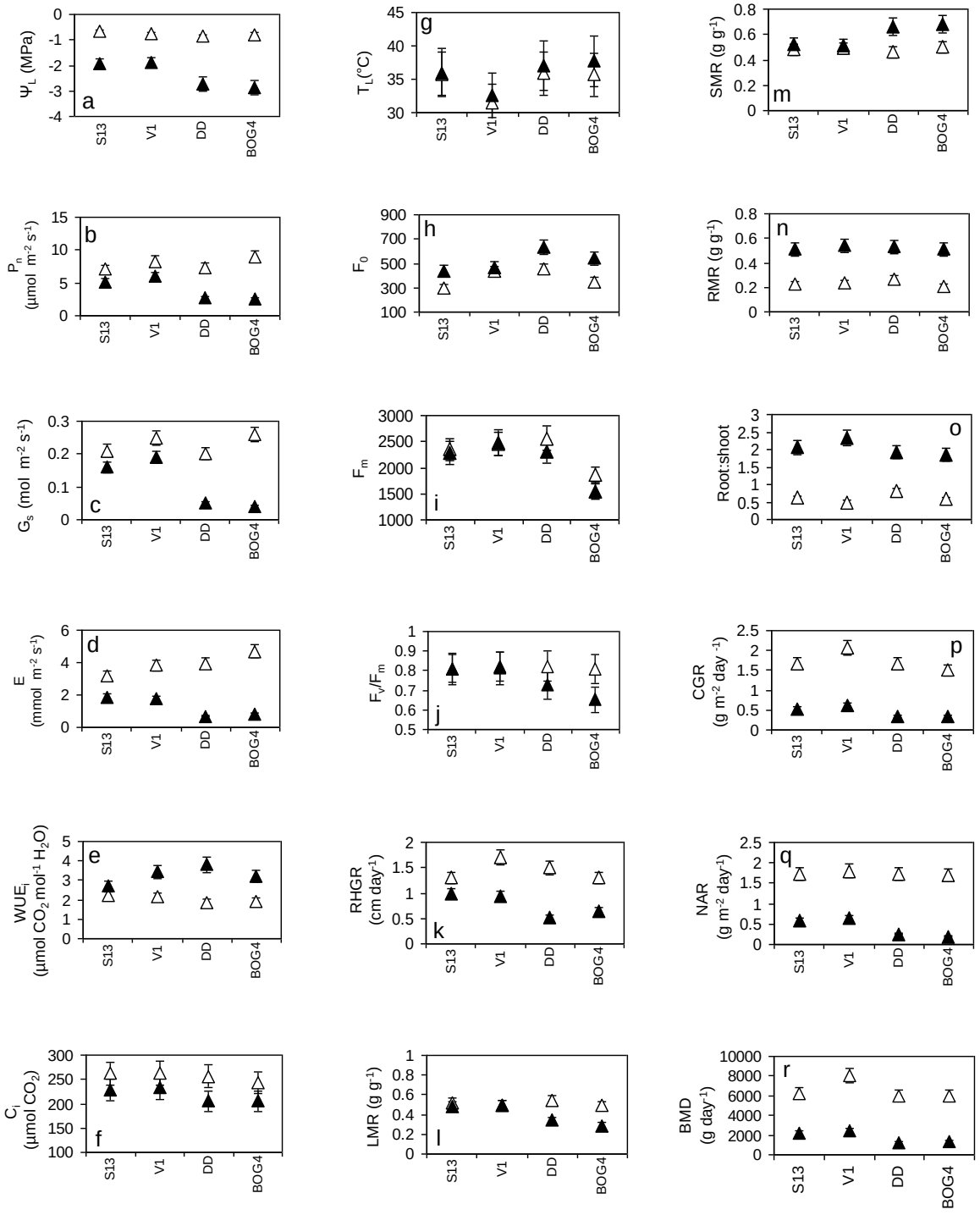

Fig. 3.7 Leaf-level physiological characteristics and plant growth dynamics including (a) leaf water potential (Ψ_L), (b) net photosynthetic rate (P_n), (c) stomatal conductance (G_s), (d) transpiration rate (E), (e) instantaneous water use efficiency (WUE_i), (f) internal CO_2 concentration (C_i), (g) leaf temperature (T_L), (h) minimal fluorescence (F_o), (i) maximal fluorescence (F_m), (j) maximal quantum yield of PSII (F_v/F_m), (k) mean relative plant height growth rate (RHGR), (l) leaf mass ratio (LMR), (m) stem mass ratio (SMR), (n) root mass ratio (RMR), (o) root:shoot ratio, (p) crop growth rate (CGR), (q) net assimilation rate (NAR) and (r) biomass duration (BMD) of four mulberry genotypes (S13, V1, DD and BOG4) grown under two water regimes (control and drought) in glasshouse conditions. Values are mean ± SD.

mulberry genotypes under low water regimes, which was reflected in reduction of root length in the mulberry genotypes of either group. However, the drought tolerant group maintained larger root length irrespective of the watering regimes. V1 had the largest root length of 104.1 and 88.9 cm in control and water stress treatments, respectively. Mulberry genotypes differed significantly in root volume both under control and drought stress conditions. A significant increase in root volume was also recorded in V1 (39%) and in S13 (49.6%) compared to control; however, the root volume was reduced to 22.2% and 48.3% in DD and BOG4, respectively in response to water stress. The genotypes differed significantly in shoot morphology and leaf yield traits regardless of watering

Table 3.3 Morphology and leaf yield characteristics of four mulberry genotypes (S13, V1, DD and BOG4) grown at glasshouse conditions under two water regimes (control and drought). Values are mean ± SD. Effects of drought were tested by *t*-test. *P< 0.05, **P< 0.01, ***P < 0.001, n.s., not significant.

Characteristics	S13		V1		DD		BOG4	
	Control	Drought	Control	Drought	Control	Drought	Control	Drought
Root weight (g)	74.4	86.5 ***	98.3	114.2 ***	92.5	54.3 ***	68.2	52.4 **
Root length (cm)	81.2	78.7 n.s	104.1	88.9 **	68.5	66.0 ***	71.1	69.8 ***
Root volume (cm^3)	55.5	110.2 ***	90.4	150.5 **	48.6	37.8 ***	59.2	30.6 **
Plant height (cm)	78.2	48.5 ***	97.7	46.3 ***	85.2	25.3 ***	76.2	31.4 **
Total shoot length (cm)	124.6	80.5 ***	196.5	113.0 **	121.7	38.5 **	126.5	36.6 ***
No. leaves $shoot^{-1}$	20.2	9.8 ***	24.5	13.5 ***	18.5	5.5 *	21.5	5.0 ***
Leaf weight $plant^{-1}$ (g)	130.2	38.6 ***	154.5	46.5 ***	132.3	16.2 ***	122.3	14.5 **
Leaf area $plant^{-1}$(cm^2)	2852.9	1153.2 ***	3041.6	1274.6 ***	2961.5	972.6 ***	2232.4	906.3 *
Above ground biomass (g)	250.2	79.8 ***	309.3	95.2 ***	244.5	47.8 **	248.0	48.8 ***

regimes (**Table 3.3**). Under well-watered conditions, V1 and DD had higher plant height of 97.7 cm and 85.2 cm, respectively. The total shoot length was also higher in V1, whereas in the remaining three genotypes no significant variation was encountered in total shoot length under well-watered conditions. Significant genotypic variation was also recorded in leaf yield both under control and drought stressed conditions. V1 and DD also performed well in leaf yield and total leaf area under control conditions. Maximum leaf weight $plant^{-1}$ was recorded in V1 (154.5 g), whereas BOG4 had lowest leaf weight of 122 g $plant^{-1}$ under high water availability. Genotype V1 and S13 had larger accumulation of above ground biomass while DD and BOG4 had the minimum values for the same.

However, in contrary to well-watered conditions, drought stress led to an apparent decrease in all leaf yield components particularly in number of leaves, leaf weight, leaf area and above ground biomass of four mulberry genotypes although to different extents. BOG4 and DD exhibited minimum leaf weight plant^{-1} with a concomitant sharp drawdown in cumulative leaf area. However, V1 and S13 maintained relatively higher leaf weight, leaf area as well as above ground biomass during water stress.

Table 3.4 Pearson correlation coefficients between each pair of variable. Significant values are indicated in bold. Negative correlations are indicated by '–' symbol.

	Ψ_L	P_n	G_s	E	WUE_i	C_i	T_L	F_o	F_m	F_v/F_m	LMR	SMR	RMR	R:S	CGR	BMD	NAR
P_n	**0.987**																
G_s	**0.993**	**0.999**															
E	**0.976**	**0.956**	**0.964**														
WUE_i	-0.435	-0.372	-0.388	-0.615													
C_i	**0.991**	**0.998**	**0.998**	**0.974**	-0.435												
T_L	-0.821	-0.890	-0.873	-0.718	-0.060	-0.856											
F_o	-0.827	-0.828	-0.827	-0.923	0.798	-0.859	0.547										
F_m	0.713	0.676	0.691	0.560	0.195	0.649	-0.705	-0.199									
F_v/F_m	**0.955**	0.915	0.930	0.887	-0.269	0.913	-0.776	-0.642	0.877								
LMR	**0.995**	**0.972**	**0.982**	**0.956**	-0.384	**0.975**	-0.813	-0.773	0.776	**0.980**							
SMR	**-1.000**	**-0.986**	**-0.993**	**-0.980**	0.450	**-0.992**	0.814	0.836	-0.702	**-0.951**	**-0.994**						
RMR	0.293	0.367	0.350	0.090	0.727	0.303	-0.720	0.186	0.690	0.404	0.332	-0.278					
R:S	0.880	0.932	0.920	0.785	-0.023	0.904	**-0.993**	-0.606	0.742	0.840	0.874	-0.874	0.668				
CGR	**0.968**	**0.996**	**0.991**	0.939	-0.350	**0.991**	-0.910	-0.829	0.635	0.879	0.947	-0.968	0.387	0.944			
BMD	**0.982**	**0.995**	**0.994**	**0.972**	-0.450	**0.998**	-0.857	-0.877	0.607	0.886	**0.959**	-0.983	0.286	0.902	**0.993**		
NAR	**1.000**	**0.988**	**0.995**	**0.973**	-0.421	**0.992**	-0.830	-0.822	0.718	**0.955**	**0.995**	-0.999	0.308	0.887	**0.971**	**0.983**	
RHGR	0.931	0.926	0.928	**0.984**	-0.689	0.948	-0.679	**-0.975**	0.409	0.792	0.893	-0.936	-0.005	0.740	0.920	**0.957**	0.927

A general PCA was performed with genotypic means of all variables using data of drought-stressed samples. The main plane of the PCA (F1 X F2) explained 96.7% of total variation estimated in all grouped variables, with F1 comprising 81.1% and F2 comprising 15.6% of total variation estimated. Axes F1 and F2 were linear combinations of the 18 variables and were built to maximize the part of the data variability that they explained (**Fig. 3.8**). P_n scaled positively with G_s (R^2 = 0.99), C_i (R^2 = 0.99), F_v/F_m (R^2 = 0.92), Ψ_L (R^2 = 0.98), NAR (R^2 = 0.98), BMD (R^2 = 0.99), E (R^2 = 0.95) and CGR (R^2 = 0.99) (see **Table 3.4** for Pearson correlation coefficients). F_v/F_m (R^2 = -0.77), F_m (R^2 = -0.70), P_n (R^2 = -0.89) and G_s (R^2 = - 0.87) scaled negatively with T_L (Table 3.4). WUE_i scaled negatively with E (R^2 = -0.62), P_n (R^2 = -0.37), RHGR (R^2 = -0.68), and C_i (R^2 = -0.43).

LMR scaled positively with P_n (R^2 = 0.97), CGR (R^2 = 0.94), NAR (R^2 = 0.99), G_s (R^2 = 0.98) and Ψ_L (R^2 = 0.99). Root:shoot (R:S) was positively correlated with P_n (R^2 = 0.93), G_s (R^2 = 0.92), C_i (R^2 = 0.90) and Ψ_L (R^2 = 0.88), whereas it was negatively correlated with T_L (R^2 = -0.99) and SMR (R^2 = -0.87) (see **Table 3.4** for Pearson correlation coefficients).

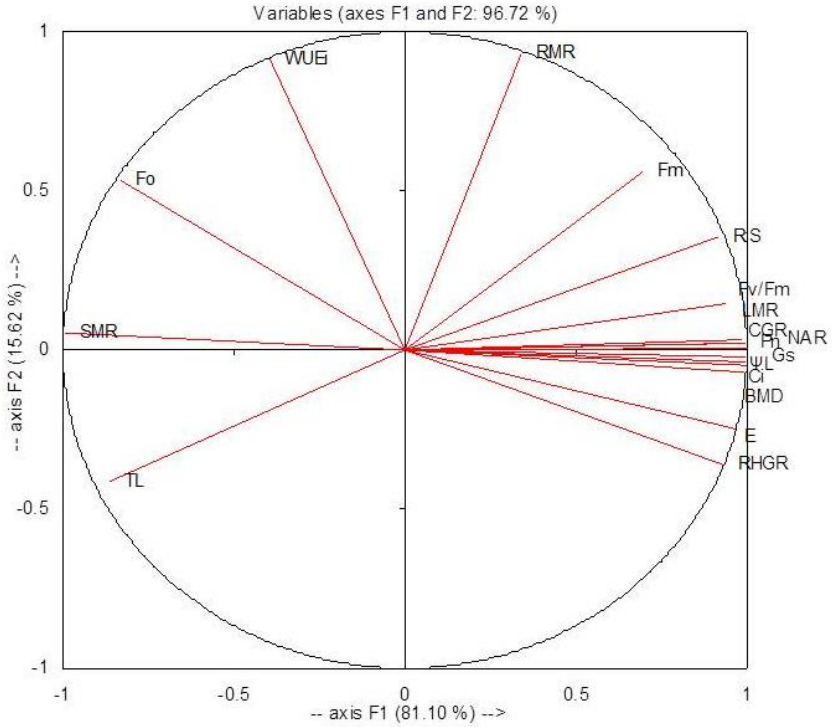

Fig. 3.8 Principal component analysis summarising the interrelationship among the parameters studied in drought-stressed mulberry genotypes (S13, V1, DD and BOG4) in glasshouse. Ψ_L = leaf water potential, P_n = net photosynthetic rate, G_s = stomatal conductance, E = transpiration rate, WUE_i = instantaneous water use efficiency, C_i = internal CO_2 concentration, T_L = leaf temperature , F_o = minimal fluorescence, F_m = maximal fluorescence, F_v/F_m = maximal quantum yield of PSII, RHGR = mean relative plant height growth rate, LMR = leaf mass ratio, SMR = stem mass ratio, RMR = root mass ratio, R:S= root:shoot ratio, CGR = crop growth rate, NAR = net assimilation rate and BMD= biomass duration.

Experiment 2 : Photosynthetic responses among genotypes at different water regimes

All mulberry genotypes, compared to their corresponding control counterparts differed significantly (P<0.05) and exhibited an apparent decline in P_n under drought conditions (**Fig. 3.9a**). At highest water stress level (25% PC), P_n declined maximum in all genotypes,

and the lowest P_n was recorded in K2 (4.1 µmol m^{-2} s^{-1}) followed by S36 and MR2 (~5.7 µmol m^{-2} s^{-1}). However, V1 exhibited the highest P_n (7.9 µmol m^{-2} s^{-1}) compared to other genotypes at the most intense drought regime (25% PC) (**Fig. 3.9a**). Stomatal conductance (G_s) declined at all drought stress regimes in all mulberry genotypes compared to their respective control counterparts and differed significantly within genotypes (G), and treatments (T) ($P<0.05$). Tm and Tm x T interaction also significantly influenced G_s (**Fig. 3.9b**). Strongest reduction in G_s was observed in plants grown at 25% PC, and the lowest G_s value was recorded in K2 (0.06 mol m^{-2} s^{-1}) followed by S36 and MR2 (~0.07 mol m^{-2} s^{-1}). V1 had highest G_s than other genotypes at low and medium drought stress regimes, and also recorded maximum value for G_s (0.19 mol m^{-2} s^{-1}) at the highest drought intensity when compared to other genotypes. Drought stress resulted in an apparent reduction of internal to ambient CO_2 ratio (C_i/C_a) in all tested mulberry genotypes, although to a different extent depending upon the genotype (**Fig. 3.9c**). The reduction in C_i/C_a was strongest at the highest water stress regime (25%PC) manifesting a reduction of 36.8% in K2, followed by S36 (28.2%) and MR2 (23.6%) compared to their respective control counterparts ($P<0.05$). V1 always maintained a higher C_i/C_a ratio in control plants as well as at all different drought regimes.

The quantum efficiency of PSII estimated by the fluorescence ratio F_v/F_m of dark-adapted leaves ranged between 0.81-0.84 in control plants of all mulberry genotypes (**Fig. 3.9d**). Unlike leaf gas exchange attributes, the F_v/F_m ratio did not show significant reduction at low water stress regime (75% PC) in any of the tested genotypes. However, at medium (50% PC) and more conspicuously at highest stress level (25% PC), F_v/F_m ratio differed significantly ($P<0.05$) within genotypes and treatments. Tm and Tm x T interaction also significantly influenced F_v/F_m. At 25% PC, F_v/F_m showed apparent reduction in K2 (F_v/F_m = 0.54) and also in S36 (F_v/F_m = 0.56) and MR2 (F_v/F_m = 0.60). The ratio was marginally altered in V1 (F_v/F_m = 0.80) in response to severe drought stress when compared to its well-watered stands (**Fig. 3.9d**).

Changes in leaf water status

LMC and RWC consistently decreased ($P<0.05$) with increase in water stress intensity in all mulberry genotypes (**Table 3.5**). V1 showed relative tolerance compared to other

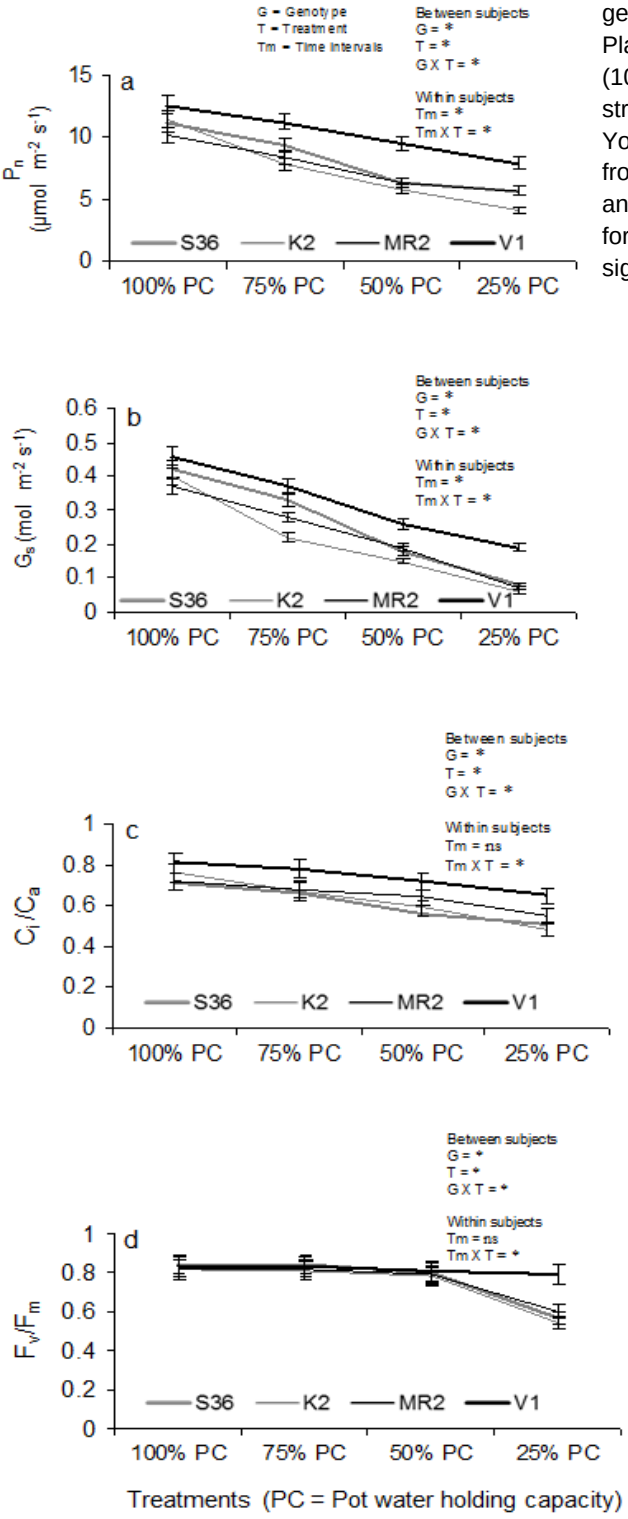

Table 3.5 Changes in leaf moisture content (LMC) and leaf relative water content (RWC) of four mulberry genotypes exposed to drought stress treatments. Plants were subjected to four water regimes: control (100% PC), low water stress (75% PC), medium water stress (50% PC) and high water stress (25% PC). Young, fully expanded leaves of the 3rd-4th position from the apical branches were used to determine LMC and RWC. Values are the means (±SE). The *F*-values for ANOVAR test are reported. *P<0.05, ns non significant.

Genotype	Treatment	LMC %	RWC %
S36	100% PC†	74.3 (1.2)	82.5 (2.0)
	75% PC	73.5 (1.5)	78.3 (1.6)
	50% PC	69.5 (0.9)	70.5 (0.8)
	25% PC	66.3 (0.7)	67.2 (1.7)
K2	100% PC	71.8 (1.5)	82.1 (3.8)
	75% PC	70.2 (1.2)	77.5 (1.2)
	50% PC	68.4 (1.2)	71.2 (0.9)
	25% PC	65.5 (1.3)	68.5 (0.9)
MR2	100% PC	72.5 (1.1)	82.1 (3.8)
	75% PC	71.1 (0.9)	76.5 (0.8)
	50% PC	68.6 (0.8)	70.4 (1.1)
	25% PC	67.5 (0.9)	68.6 (0.9)
V1	100% PC	76.1 (0.8)	84.6 (2.7)
	75% PC	74.5 (1.1)	79.8 (1.2)
	50% PC	73.2 (0.9)	76.5 (0.8)
	25% PC	72.6 (0.8)	75.4 (1.9)
ANOVAR	*F*-values		
Between	Genotype	27.77*	30.96*
subjects	Treatment	40.79*	195.70*
	Genotype x Treatment	11.40*	22.75*
Within	Time intervals	2.43ns	1.78ns
subjects	Time intervals x Treatment	22.35*	27.63*

†PC Pot water holding

Fig. 3.9 Effect of water deficit on photosynthetic characteristics: (a) net photosynthetic rate (P_n), (b) stomatal conductance (G_s), (c) internal to ambient CO_2 ratio (C_i/C_a), and (d) maximal quantum yield of PSII (F_v/F_m) in four mulberry genotypes (S36, K2, MR2 and V1) grown in glasshouse conditions under four water regimes (100% PC, 75% PC, 50% PC and 25% PC). Data are the mean ± SE. The significance level of ANOVAR is reported (*P < 0.05, ns not significant).

genotypes as evidenced by maintenance of better water status in all water stress regimes. At highest water stress (25% PC), LMC was found to be minimum in K2 (65.5%) followed by S36 (66.3%) and MR2 (67.5 %), whereas V1 maintained relatively higher LMC of 72.6% than other genotypes at the same stress level. No significant differences in RWC were recorded amongst well-watered genotypes (RWC values were invariably maintained above 80%). However, in water stress-exposed plants, RWC differed significantly ($P<0.05$) within G, among T and also in case of Tm x T interaction showing an apparent reduction. At 25% PC, RWC was estimated to be 67.2% in S36 followed by MR2 and K2 (~68.5%). V1 maintained highest RWC of 84.6% and 75.4%, at 100% PC and 25% PC, respectively.

Responses of non-enzymatic antioxidants

Exposure to different drought regimes caused substantial changes in α-tocopherol content causing significant difference ($P<0.05$) within genotypes and among treatments. **Fig. 3.10a** shows the RP-HPLC profiles of foliar α-tocopherol obtained from all four tested genotypes of two water regimes (100%PC and 25%PC). V1 and S36, inherently had low foliar α-tocopherol content compared to other genotypes under well-watered conditions which were estimated to be 12.7 μg g^{-1} fw and 16.4 μg g^{-1} fw, respectively (**Fig. 3.10b**). The control plants of MR2 possessed significantly high α-tocopherol content (48.8 μg g^{-1} fw) followed by K2 (42.4 μg g^{-1} fw) compared to remaining genotypes (**Fig. 3.10b**). Under low water stress (75% PC), no conspicuous changes were visible in the foliar α-tocopherol contents of K2 and MR2, whereas significant increment was recorded in S36 (20.2% increase) and V1 (31.4% increase) compared to their respective controls. The endogenous α-tocopherol levels of MR2, K2 and S36 were significantly ($P<0.05$) affected and a net α-tocopherol loss was encountered in those three mulberry genotypes at the highest water stress regime (25% PC) compared to their controls depicting a reduction level of 45.2% and 46.5%, respectively (**Fig 3.10a,b**). The α-tocopherol level in S36 was reduced to 7.6 μg g^{-1} fw at 25% PC which was also the minimum value of α-tocopherol obtained at highest stress level (**Fig. 3.10b**). Inspite of endogenous loss, MR2 (22.5 μg g^{-1} fw) and K2 (19.6 μg g^{-1} fw) had more foliar α-tocopherol than S36 (**Fig. 3.10b**). Interestingly, in stressed V1 leaves, α-tocopherol content showed increasing trend above control and exhibited

significantly (P<0.05) elevated accumulation (2.2 fold increase) at the highest drought stress regime (25% PC) than compared to its well-watered counterparts (**Fig. 3.10a,b**).

Foliar AA content tended to increase in all mulberry genotypes under low water stress (75% PC) resulting in significantly (P<0.05) higher values of 1.68 mg g^{-1} fw in V1, followed by MR2 (1.56 mg g^{-1} fw), K2 (1.22 mg g^{-1} fw) and S36 (1.17 mg g^{-1} fw). However, at medium (50% PC) and highest (25% PC) water stress regimes, no marked up-regulation in foliar AA content was evident in MR2, K2 and S36. In V1, compared to its control counterparts, an increment of 26.8% and 34.9% in foliar AA was observed at 50% PC and 25% PC, respectively. V1 showed highest AA content at severe water stress regime followed by MR2, K2 and S36 (**Fig. 3.10c**). Low level of water stress (75% PC) induced significant (P<0.05) enhancement in foliar glutathione content in all mulberry genotypes except K2, whereas at the highest drought stress regime (25% PC), foliar glutathione increased substantially (20.5%) only in V1 with respect to its control plants (**Fig. 3.10d**). Furthermore, in S36, K2 and MR2 no significant changes in glutathione level was determined between the plants grown at medium (50% PC) and highest water stress levels (25% PC). Overall, V1 ranked highest in glutathione accumulation amongst all genotypes at all drought stress regimes (**Fig. 3.10d**).

Genotype S36 and K2 showed maximum proline content at moderate water stress regime (50% PC) and no further statistically significant enhancement was observed in those two genotypes at the highest stress level (**Fig. 3.10e**). MR2 and V1 showed an increasing trend in foliar proline content at all the water stress regimes compared to their respective controls and also when compared to other tested genotypes of the same stress regime. However, at the highest stress level, V1 exhibited higher level of proline compared to others and accumulated significantly (57.2%, almost 3 fold increase) compared to the control stands (**Fig. 3.10e**). Total carotenoid content was slightly higher in MR2 (0.58 mg g^{-1} fw) and V1 (0.59 mg g^{-1} fw) than S36 (0.53 mg g^{-1} fw) and K2 (0.51 mg g^{-1} fw) in well-watered conditions (**Fig. 3.10f**). The level of total carotenoids increased significantly (P<0.05) in all the mulberry genotypes under drought exposure with progression in time, however, to a different extent depending upon the genotype and stress intensity. Maximum level of total carotenoid content was observed in V1 (0.71 mg g^{-1} fw) at the highest water stress regime (25% PC) followed by MR2, S36 and K2. Overall, V1 ranked highest among

all genotypes in total carotenoid content, whereas K2 scored the lowest for the same (**Fig. 3.10f**).

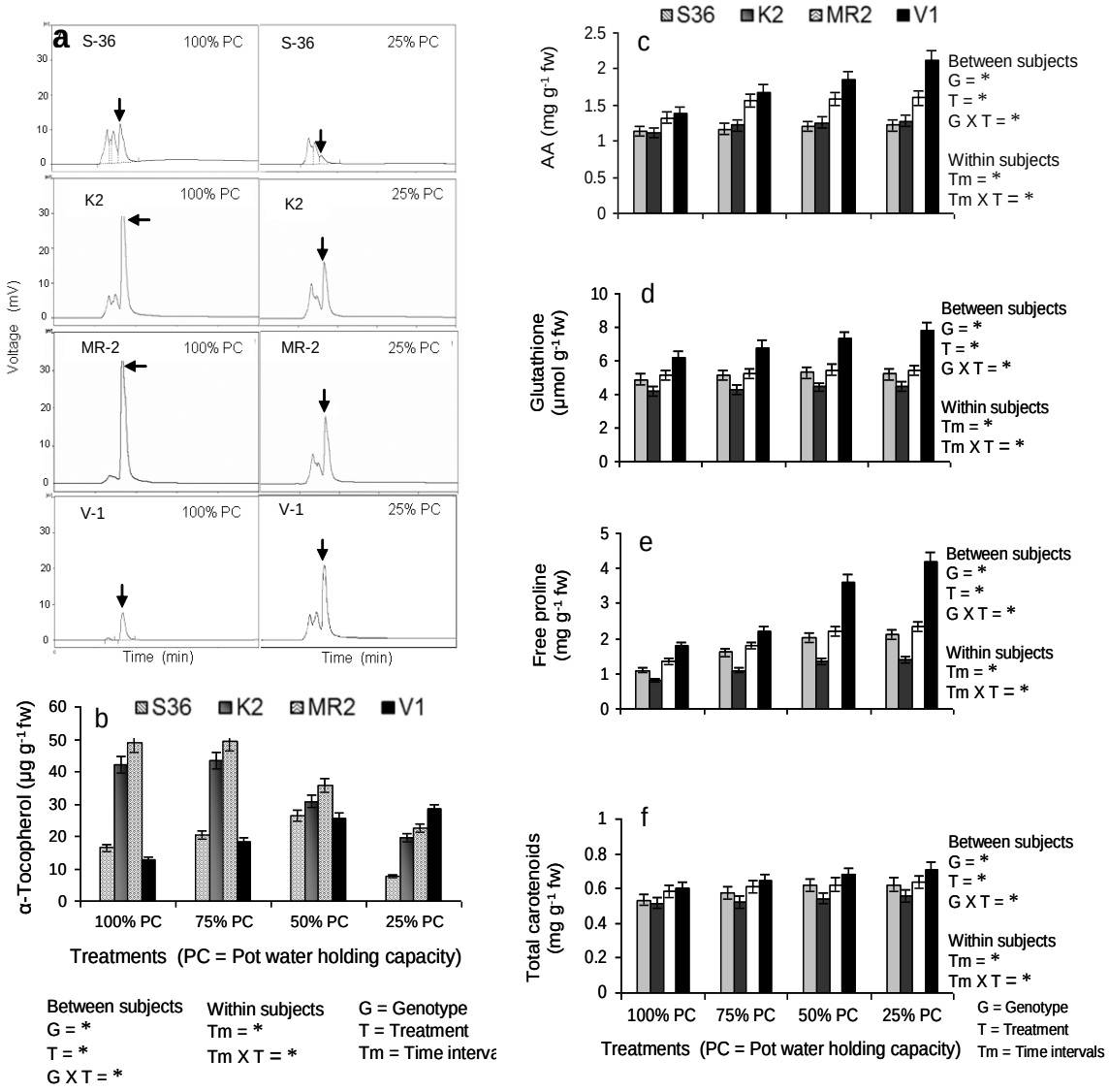

Fig. 3.10 Drought induced changes in foliar α-tocopherol content in tested mulberry genotypes: (a) reverse phase-high performance liquid chromatography (RP-HPLC) of α-tocopherol (arrows indicating α-tocopherol peaks) from the leaves of different mulberry genotypes (S36, K2, MR2 and V1). Chromatographic peaks of α-tocopherol were obtained for all the genotypes from each water regime, however, only peaks which were obtained from the plants under 100% PC and 25% PC are depicted in this figure for comparing the fate of endogenous α-tocopherol at severe water stress intensity in respect to well-watered conditions; (b) foliar α-tocopherol content of four tested mulberry genotypes grown under all four different water regimes (100% PC, 75% PC, 50% PC and 25% PC). Data are the mean ± SE. The significance level of ANOVAR is reported (*P <0.05); (c) Changes in foliar a ascorbic acid (AA), (d) glutathione, (e) free proline and (f) total carotenoid contents of four mulberry genotypes (S36, K2, MR2 and V1) grown at glasshouse conditions under four water regimes (100% PC, 75% PC, 50% PC and 25% PC). Data are the mean ± SE. The significance level of ANOVAR is reported (*P <0.05).

Lipid peroxidation and generation of ROS

Genotype S36, K2 and MR2 had considerably higher leaf MDA estimated as 38.3 nmol g^{-1} fw, 37.8 nmol g^{-1} fw and 34.2 nmol g^{-1} fw, respectively compared to V1 (21.7 nmol g^{-1} fw) at the highest water stress regime (25% PC) (**Fig. 3.11a**). K2 and S36 had higher concentrations of H_2O_2 in leaves (5.8 µmol g^{-1} fw and 5.6 µmol g^{-1} fw, respectively) compared to other genotypes at the highest drought regime (25% PC), whereas the concentration was found to be lowest in V1 (2.2 µmol g^{-1} fw) at the same stress level (**Fig. 3.11b**). A marked enhancement in $O_2^{\bullet -}$ accumulation was observed in the leaves of all mulberry genotypes due to drought stress, particularly at the higher water stress regimes (75% PC and 25% PC) with significant differences ($P<0.05$) within G, among T, within Tm and also in case of Tm x T interaction (**Fig. 3.11c**). Maximum foliar $O_2^{\bullet -}$ was recorded in S36 and K2 at the highest stress level (25% PC), whereas the concentration was lowest in leaves of V1 for the same stress regime. Accumulation of H_2O_2 was detected using green fluorescent signals of H_2DCFDA dye reacting in a concentration-dependent manner. Drought-stressed leaf samples of S36, K2 and MR2, with higher concentrations of H_2O_2, showed most conspicuous and widely distributed green fluorescence spots than the leaves from their respective control counterparts (**Fig. 3.11d**). In contrast, highly stressed leaves of V1 showed less pronounced green spots when compared to its control as well as with other stressed genotypes indicating lower accumulation of H_2O_2 in the leaf tissues. Accumulation of $O_2^{\bullet -}$ was observed as irregularly distributed round, oval and elliptical spots of blue coloured formosan on the leaf lamina. At highest water stress regime, K2, S36 and MR2 exhibited relatively higher blue spot intensities in the leaf tissues and veins compared to V1, which had less spots indicating lower $O_2^{\bullet -}$ generation (**Fig. 3.11e,f**). Significant positive correlation ($R^2= 0.90$, $P< 0.001$) was achieved and the regression slope was linear with MDA *versus* H_2O_2 relationship curve (**Fig. 3.12a**). The association between $O_2^{\bullet -}$ accumulation and MDA level was also positively correlated ($R^2= 0.76$, $P< 0.001$) and linear regression slope was achieved (**Fig. 3.11b**).

Changes in plant growth and biomass characteristics

In all water stress intensities (75% PC, 50% PC and 25%PC), drought invariably reduced plant height, stem biomass, leaf biomass and above ground biomass in all mulberry

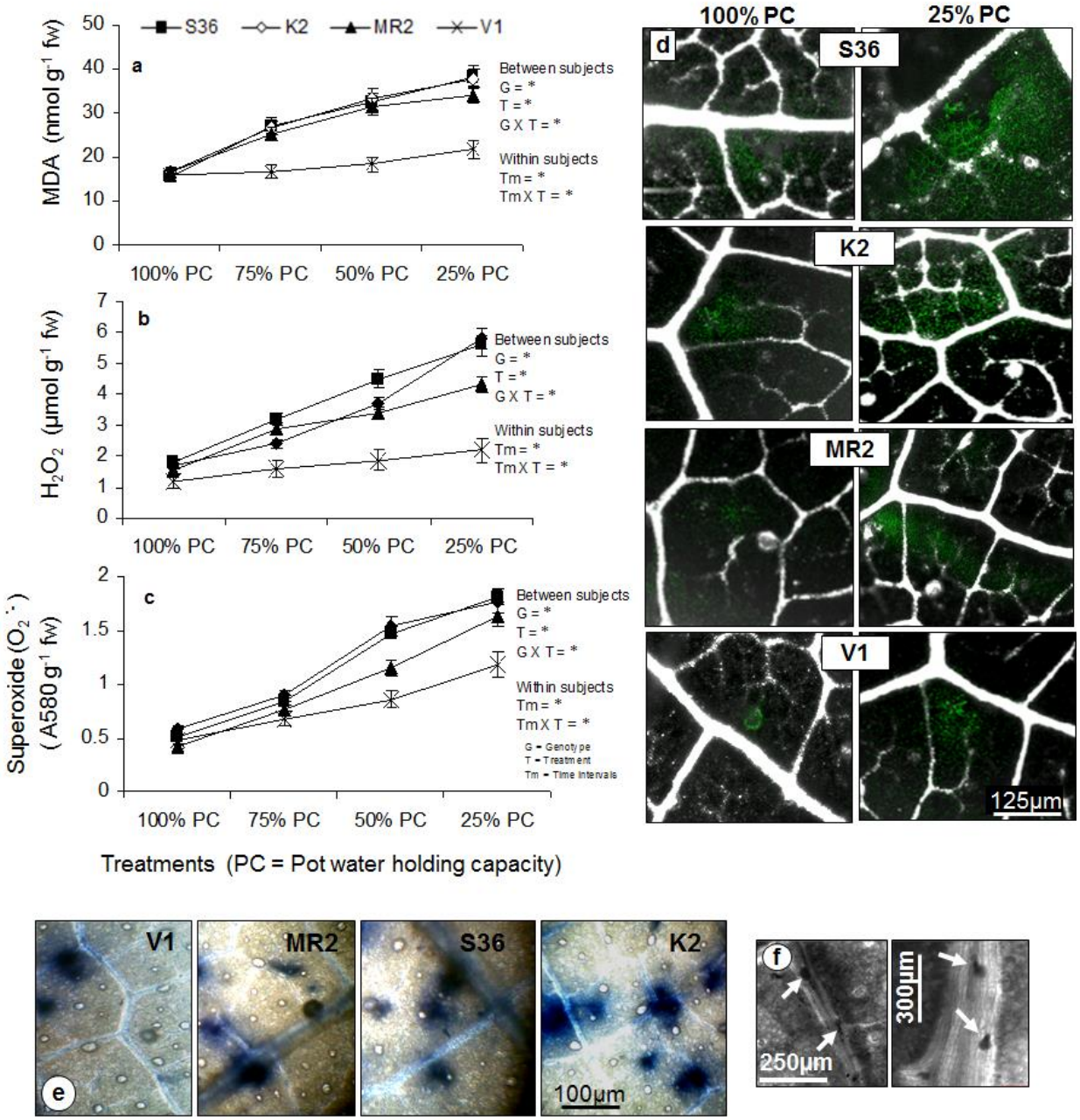

Fig. 3.11 Contents of (a) malondialdehyde (MDA), (b) H_2O_2, and (c) superoxide anions ($O_2^{\cdot -}$) in the leaves of four mulberry genotypes (S36, M5, MR2 and V1) grown at glasshouse conditions under four water regimes (100% PC, 75% PC, 50% PC and 25% PC). Data are the mean ± SE. The significance level of ANOVAR is reported (*P <0.05). Accumulation of (d) H_2O_2 in the leaves of mulberry genotypes under different water regimes were detected using green fluorescent signals of H_2DCFDA dye, however, only the control (100% PC, left panel) and high water stressed (25% PC, right panel) leaves from all the four genotypes were compared in this figure to show the relative intensity of green fluorescent signals. Accumulation of (e) $O_2^{\cdot -}$ was detected as blue coloured formosan spots on the leaf lamina and veins. The intense spots of $O_2^{\cdot -}$ accumulation in the high water-stressed (25% PC) leaves of K2, S36, MR2 and V1 were compared. Accumulation of (f) $O_2^{\cdot -}$ was also evident in the leaf veins of high water-stressed plants as observed in case of S-36 under 25% PC.

genotypes with significant differences (P<0.05) within genotypes and among treatments (**Table 3.6**). K2, S36 and MR2 suffered greater reductions in all shoot growth criteria than V1 which maintained comparatively higher above ground plant biomass at all water stress regimes when compared to others (**Fig. 3.13**). The interaction genotype x treatment was significant for most of the growth and biomass parameters. The four genotypes also varied significantly in respect to root characteristics (**Table 3.6**). Significant reduction (P<0.05) in root fw was observed in all tested genotypes at all water stress treatments; however, V1 recorded highest root fw compared to others. A substantial shift in root biomass allocation was recorded in the water-stressed plants compared to their respective control counterparts which concurrently increased the root:shoot mass ratios in all genotypes with significant differences (P<0.05) within genotypes and among the treatments (**Table 3.6**).

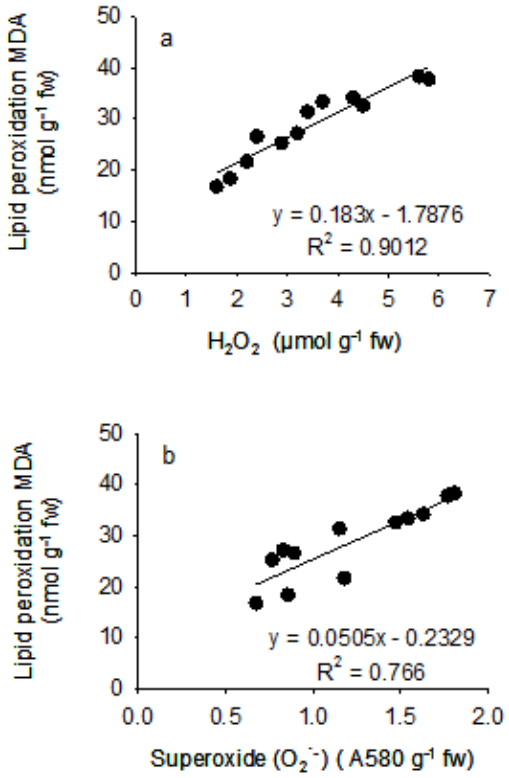

Fig. 3.12 Relationships between (a) H_2O_2 production and MDA accumulation and (b) superoxide anions ($O_2^{\cdot -}$) production and MDA accumulation in the drought stressed mulberry leaves. Linear regression analysis was performed considering the data from drought exposed (75% PC, 50% PC and 25% PC) plants of all the four mulberry genotypes (S36, K2, MR2 and V1) grown at glasshouse conditions. Each point represents mean of five independent measurements from individual plant. The correlations were significant at P<0.001.

Table 3.6 Growth and biomass characteristics of four mulberry genotypes subjected to four different water regimes: control (100% PC), low water stress (75% PC), medium water stress (50% PC) and high water stress (25% PC). Plants were completely harvested to obtain growth and biomass (fresh weight basis) data at the end of experiment (on 75th day). Values are the means (±SE). The *F*-values for ANOVA test are reported. *P<0.05, ns non significant.

	Treatment	Plant height	Leaf biomass	Stem biomass	Root biomass	Above ground biomass	Root:Shoot
S36	100% PC†	112.3 (7.8)	161.2 (4.2)	188.6 (3.2)	151.2 (4.4)	349.8 (5.9)	0.43 (0.02)
	75% PC	70.2 (4.2)	124.3 (3.5)	142.7 (4.1)	115.4 (3.8)	267.2 (7.3)	0.44 (0.03)
	50% PC	46.7 (3.7)	56.2 (5.6)	78.2 (3.3)	82.3 (4.2)	134.4 (6.4)	0.61 (0.01)
	25% PC	38.6 (1.9)	26.8 (2.4)	30.3 (6.3)	64.2 (2.8)	57.1 (2.6)	1.12 (0.07)
K2	100% PC	89.2 (6.6)	102.6 (3.3)	174.3 (4.7)	140.7 (4.3)	276.9 (4.5)	0.51 (0.02)
	75% PC	66.4 (5.2)	74.2 (5.3)	86.8 (2.6)	92.3 (3.2)	161.2 (3.9)	0.57 (0.02)
	50% PC	60.2 (4.1)	37.7 (2.4)	50.9 (3.9)	68.2 (4.7)	88.6 (5.2)	0.76 (0.04)
	25% PC	32.7 (6.8)	20.8 (4.2)	37.2 (4.6)	60.5 (2.8)	58.0 (2.5)	1.04 (0.03)
MR2	100% PC	80.7 (6.2)	138.3 (6.3)	182.4 (3.5)	160.5 (5.5)	320.7 (6.3)	0.50 (0.02)
	75% PC	58.8 (2.6)	118.5 (5.4)	102.7 (5.4)	122.4 (3.4)	221.2 (4.8)	0.55 (0.05)
	50% PC	45.3 (2.3)	39.8 (2.2)	46.8 (2.2)	86.2 (2.3)	86.6 (5.4)	1.08 (0.06)
	25% PC	36.2 (5.2)	22.2 (2.7)	32.2 (3.8)	75.8 (3.8)	54.4 (2.6)	1.38 (0.02)
V1	100% PC	116.4 (7.9)	191.7 (5.3)	221.7 (7.4)	171.1 (6.2)	412.4 (8.3)	0.37 (0.04)
	75% PC	98.2 (4.0)	172.6 (6.8)	198.6 (6.3)	138.5 (5.7)	371.2 (4.5)	0.38 (0.07)
	50% PC	76.4 (4.2)	108.3 (4.7)	63.7 (4.3)	116.7 (4.6)	172.0 (3.2)	0.67 (0.01)
	25% PC	52.4 (3.9)	56.5 (3.5)	42.7 (2.7)	108.2 (3.1)	98.2 (3.3)	1.10 (0.06)
ANOVA	*F*-values						
	Genotype	14.26*	78.41*	36.45*	37.18*	110.96*	145.33*
	Treatment	65.70*	138.85*	136.16*	138.37*	162.28*	198.03*
	Genotype x Treatment	1.96^{ns}	3.83**	11.02*	0.96^{ns}	10.30*	114.65*

Discussion

Experiment 1: Field and glasshouse assays

The present comprehensive study elucidates a wide genetic variation for drought tolerance among different mulberry genotypes. Based on growth and leaf yield productivity in the six growing seasons under drought conditions, two mulberry genotypes (V1 and S1) were considered to be drought tolerant apart from the drought tolerant check S13. Leaf yield for V1 and S1 significantly differed under well-watered and drought stress conditions, however, these genotypes were able to maintain relatively higher and stable leaf yield throughout the growing seasons under drought conditions compared to other genotypes.

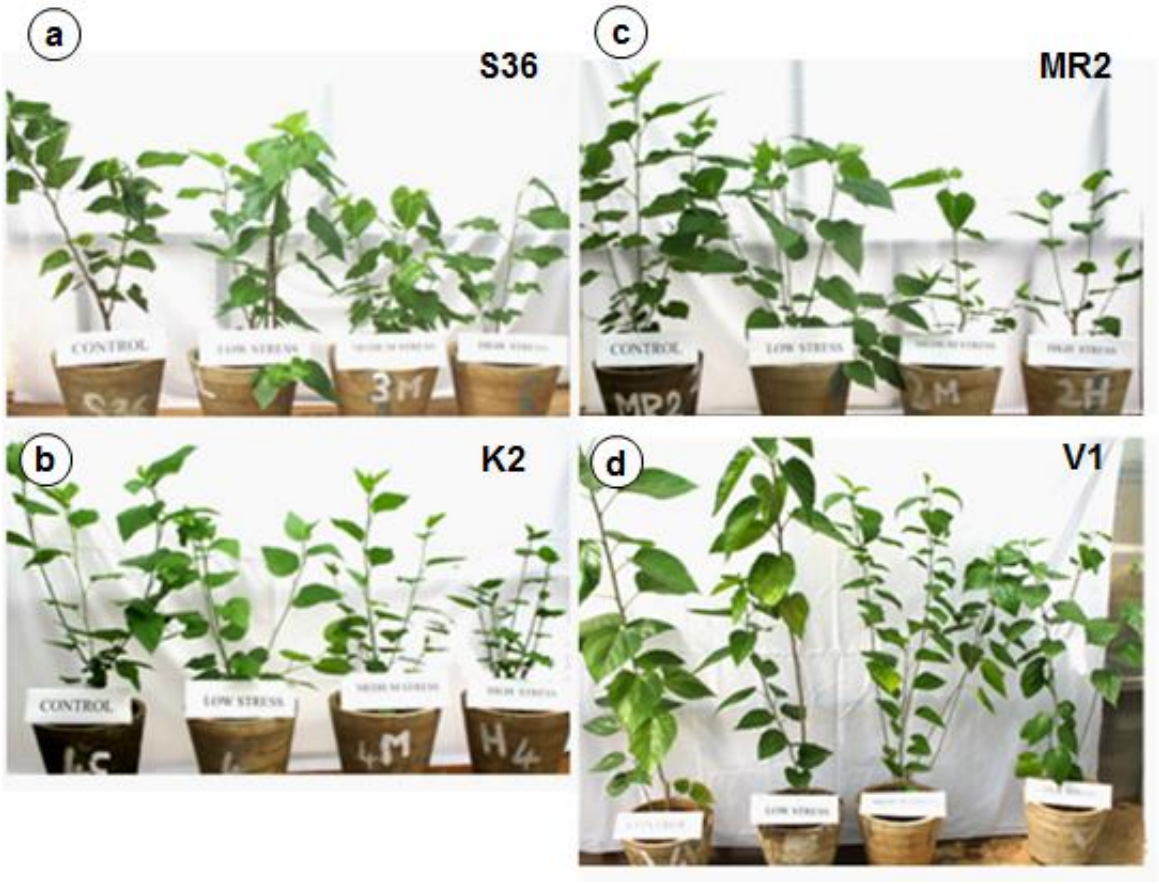

Fig. 3.13 Morphology and growth of four tested mulberry genotypes (S36, K2, MR2 and V1) grown in pots under glasshouse conditions. Plants were grown at four water regimes: control (100 % PC,), low water stress (75% PC), medium water stress (50% PC) and high water stress (25% PC). In the photographs, for each genotype, pots are sequentially arranged from left to right in the order of 100% PC, 75% PC, 50% PC and 25% PC. Plants were photographed on 70th day after the onset of stress treatment to record and compare the growth and morphological changes amongst tested genotypes after exposure to different water stress intensities with respect to well-watered control plants.

The most important and immediate response of drought stress in mulberry was the reduction in leaf surface size that co-limited leaf area as well as leaf mass and ultimately led to low leaf yield. Limitation in leaf yield due to drought stress cannot be assigned to a single physiological process rather it can be explained as a consequence of declined P_n with a concomitant down-regulation in G_s (Dias et al. 2007). As a consequence of low soil moisture availability, a significant decline in the rates of photosynthesis (P_n) and stomatal conductance (G_s) were observed in all the studied mulberry genotypes. The carbon acquisition ability of the genotypes was hampered by the greater magnitude of reduction in G_s compared to P_n under drought. Such high stomatal sensitivity can reduce the leaf gas

exchange capacity by narrowing stomatal pore or by stomatal closure and in this process, P_n is also dramatically down-regulated (Buckley et al. 2003; Medrano et al. 2002). The experimental data points out stomatal inhibition as the major cause of photosynthetic down-regulation in mulberry leaves under water stress. Although P_n and E had similar responses under drought, the relative decrease of E was greater, resulting in a significant increase of WUE_i in most of the mulberry genotypes. However, in drought tolerant genotypes, P_n was found to be higher and less sensitive to E compared to the sensitive genotypes under soil water deficit; hence, the WUE_i was consequently much improved in the tolerant genotypes. Plants preferring 'drought avoidance' minimize water loss by substantial plummet in gas exchange parameters, mainly controlling G_s. Such strategy undoubtedly leads to reduced photosynthesis which ultimately results in slow growth rate and poor leaf yield. However, a drought tolerant genotype can maintain better physiological functions like photosynthesis and stomatal conductance despite large water deficit (Tardieu 2005). The strategies noticed in V1 and S13 can be termed as 'drought tolerance' rather than 'drought avoidance' as they faced less inhibition in P_n and maintained higher leaf gas exchange rates under severe water restriction compared to other genotypes. Down-regulation in the gas exchange physiology exhibited by the drought sensitive genotypes significantly limited photosynthetic carbon assimilation affecting quantitative traits and resulted in low leaf yield productivity under drought.

In the second phase of the investigation, studies were focused on selected drought tolerant and drought susceptible mulberry genotypes and continued to investigate the evidences for yield losses in the susceptible genotypes compared to the tolerants. Gas exchange measurements demonstrated that the susceptible genotypes with significantly reduced P_n and G_s also exhibited significantly reduced C_i/C_a values under drought stress, indicating strong stomatal inhibition with negative reflexes on the photosynthetic CO_2 uptake. There are uncertainties in calculating C_i in water-stressed, heteroboric leaves such as mulberry due to stomatal patchiness (Nikolopoulos et al. 2002; Gomes et al. 2007). As patchy stomatal conductance (Terashima 1998; Mott and Buckley 2000) was not measured, it is difficult to state that the C_i values were not subjected to the patchiness problems. However, it should be noted that: (i) patchiness should not be an important problem under progressively drought exposed conditions and (ii) since G_s values

measured during the water-stressed periods were always higher than 0.03 mol m^{-2} s^{-1}, below which the patchiness phenomenon can be important (Flexas et al. 2002; Grassi and Magnani 2005). Elevated T_L (>35°C), as recorded in control and stressed leaves of drought susceptible mulberry genotypes grown under water deficit might adversely affect mesophyll conductance to CO_2 and cause damage to the photosynthetic machinery (Bernacchi et al. 2002; Salvucci and Crafts-Brander 2004). Because of impaired leaf cooling by low E, T_L of stressed leaves in sensitive genotypes showed significantly high values. Interestingly, the drought tolerant genotypes were able to maintain low T_L and therefore, heat-induced damage on the photosynthetic apparatus was presumably less critical. The overall photosynthetic gas exchange studies (including field assays and glasshouse experiments) highlight the reliability of such non-destructive, gas exchange techniques for screening mulberry genotypes for drought tolerance. Among the various leaf gas exchange parameters measured in this study, rate of photosynthesis, stomatal conductance and leaf temperature seems to be useful selection criteria for screening drought tolerant genotype(s) from a diverse group of mulberry germplasm.

Measurements on chl a fluorescence were widely monitored to evaluate the direct effects of drought stress on PSII photochemistry. Light-harvesting complexes reduced their efficiency due to drought-induced damages to the antennae, as evidenced by an increase in F_o in stressed leaves of mulberry genotypes. In the stressed leaves of drought tolerant mulberry genotypes, this increase was relatively less and was balanced by the maintenance of F_m which contributed to keep similar F_v/F_m. A decrease in F_m, as observed in the sensitive mulberry plants, may be related to the decrease in the activity of the water-splitting enzyme complex and perhaps a concomitant cyclic electron transport with or around PSII (Zlatev and Yordanov 2004). The significant increase of F_o and decrease of F_m under drought stress concurrently led to a strong decrease of F_v/F_m values in the sensitive mulberry genotypes suggesting a chronic photoinhibition due to photo-inactivation of PSII centres, possibly attributable to D1 protein damage (Ohnishi et al. 2005). The ability to maintain high F_v/F_m under moisture stress thus indicates that the drought tolerant genotypes had stabilized PSII photochemistry and better carbon assimilation capacity when compared to the sensitives. The relatively faster method of measuring photosynthetic activity via chl a fluorescence techniques seems to be promising for monitoring

photosynthetic events and rapid screening of large number of mulberry germplasm for drought tolerance.

In the present study, drought stress decreased the root length in drought susceptible mulberry genotypes. However, in the drought tolerant genotypes, root length was less affected and a significant increase in root volume with simultaneous increment in root biomass was recorded compared to the susceptible genotypes. Such phenomena indicate that low soil water availability altered root growth pattern. Instead of vertical growth, horizontal proliferation of roots was achieved in order to exploit the existing soil water in and around the rhizosphere. A better rooting vigour as observed in the drought tolerant genotypes would have facilitated higher hydraulic conductance in those genotypes which was reflected by their ability to maintain a higher RWC of their leaf tissues. It is often reported that under limited water supply the natural coherence among the growth characteristics is altered and the plants show a shift as well as selectivity in biomass allocation to specific parts (Dias et al. 2007). In the present investigation, the biomass allocation to leaves (LMR) under water deficit was severely affected in the drought susceptible genotypes which can be explained as an adaptive response in order to avoid excess irradiance and to prevent transpirational loss by dramatic reduction in leaf size and number. However, such adaptive phenotypic plasticity causing diminution of foliage cannot be linked to enhanced performance under drought as leaf yield is economically important in mulberry. In contrary to the susceptibles, the LMR was maintained in the tolerant genotypes which would attribute for higher leaf yield under low water regime. Allocation to roots remained unaffected, moreover, RMR and root:shoot ratios were improved in both tolerant and susceptible mulberry genotypes thus reflecting a common trend of higher biomass allocation to roots under water deficit conditions. A major loss in NAR, as observed in drought sensitive mulberry genotypes under water limited conditions might be ascribed to strong reduction in P_n, whilst superior photosynthetic functioning and better root characteristics of drought tolerant genotypes would enable to attain relatively higher NAR as well as CGR and BMD under water stress regimes compared to the susceptibles (Machado et al. 2002; Dias et al. 2007).

Experiment 2: Glasshouse assays

The present study demonstrated that V1 subjected to water limitation, manifested significant drought tolerance relative to other tested genotypes (K2, S36 and MR2), as judged by the maintenance of better height growth, leaf development and higher biomass accumulation at all water stress regimes. In anomaly to V1, the remaining genotypes (K2, S36 and MR2) exhibited higher degree of plasticity in growth, most compressed morphology and underwent severe loss in biomass traits (both aboveground as well as root biomass) when exposed to intense drought regimes. V1 manifested most 'optimistic' response to drought and was able to maintain relatively higher leaf water status (in terms of LMC and RWC) and better leaf gas exchange functions than the susceptibles. A better rooting vigour (determined in terms of root biomass and root:shoot ratio) as observed in V1 would have facilitated better hydraulic conductance and a higher leaf water status under drought stress situations. The drought response features manifested by V1 are fitting well with the 'drought tolerance' attributes of higher plants according to the classic drought response terms defined by Turner (1979) and Chaves et al. (2010). As indicated in **Fig. 3.9**, while water stress strongly down-regulated stomatal conductance (G_s) and net photosynthetic rate (P_n) in susceptible mulberry genotypes (K2, S36 and MR2), V1 on contrary, maintained relatively higher G_s and also exhibited higher P_n, despite severe water limitation. Further, leaf gas exchange analyses, elucidated that in case of susceptibles, G_s was more sensitive in response to drought manifesting strong stomatal regulation even at low water stress intensity before any drastic change in LMC and RWC was detectable. These findings indicate that the susceptible mulberry genotypes tried to employ physiologically drought-avoidance strategies triggered by stomatal closure which might have restricted CO_2 influx from stomata to mesophyll cells as reflected by acute reduction in C_i/C_a causing down-regulation of P_n for the same. Such drought avoiding 'pessimistic behaviour' has been reported earlier in ponderesa pine (Maherali and DeLucia 2001), olive (Connor 2005) and Populus (Cocozza et al. 2010).

It was interesting to observe that in spite of significant down-regulation in P_n of the tested genotypes, the photochemical efficiency of PSII (indicated by F_v/F_m) was not affected by low and medium water stress intensities. Such findings are in agreement with earlier reports documented in Coffea canephora (Pinheiro et al. 2004) and Mangifera

indica (Elsheery and Cao 2008) where neither PSII photochemistry nor electron flow through electron transport chain (ETC) of PSII were significantly affected by mild to moderate water stress. The phenomenon of electron transport through PSII under drought conditions has not been clearly understood in higher plants. Nevertheless, there are evidences that electron transport in PSII can continue at a considerable rate even in severely water-stressed leaf and the electrons from the excited photosystem centres are directed to the normal physiological acceptors ($NADP^+$ and ferredoxin) and to alternative electron acceptor routes such as Mehler reaction and photorespiration (Lawlor 1995). The PSII is thus considered to be much stable and relatively tolerant to drought in many higher plants including trees (Bukhov and Carpentier 2004). However, unlike low/medium water stress regimes, significantly lower F_v/F_m values were detected in drought susceptible genotypes (K2, S36 and MR2) at high water stress intensity when compared to drought tolerant V1. Such reduction in F_v/F_m indicates that the genotypic capacity of the susceptibles to maintain photochemical efficiency of PSII obviously exceeded at severe drought intensity, probably due to down-regulation in PSII ability caused by photoinactivation of PSII centres (Ohnishi et al. 2005). Interestingly, the present study the P_n values of drought susceptible genotypes were found to decline sharply even at low/medium water stress levels when the corresponding F_v/F_m values were still high. Such phenomenon might arise due to a surplus of excitation light energy as well as due to enhanced proportion of electron flow to O_2 (Mehler reaction), which might have resulted in excessive production of lethal reactive oxygen species (ROS) in chloroplasts leading to photosynthetic down-regulation in susceptibles compared to the relatively tolerant V1 (Lawlor 1995; Reddy et al. 2004; Gill and Tuteja 2010). Higher levels of ROS can lead to peroxidation and breakdown of thylakoid lipids causing oxidative damage to photosynthetic processes (Mittler 2002; Shao et al. 2008). This contention is supported by the present experimental data on MDA content and concentrations of stress indicators such as $O_2^{\bullet -}$ and H_2O_2 in water-stressed leaves of mulberry (**Fig. 3.11**). ROS (H_2O_2, $OH^{\cdot}$, $^1O_2$ and $O_2^{\bullet -}$) are known to be responsible for increased MDA accumulation in cells under drought stress (Mittler 2002; Mittler et al. 2004; Reddy et al. 2004a) and variations in MDA content has been reported as a reliable index of oxidative injury under various environmental stress conditions, including drought (Yildiz-Aktas et al. 2009). As indicated

in **Fig. 3.12**, significant positive correlations achieved between the concentrations of ROS ($O_2^{\bullet -}$ and H_2O_2) and MDA accumulation under drought affirm the contribution of $O_2^{\bullet -}$and H_2O_2 on lipid peroxidation in the water-stressed leaves of mulberry genotypes. Relatively higher oxidative damage was recorded in K2, S36 and MR2 whereas, V1 possessed low levels of ROS ($O_2^{\bullet -}$and H_2O_2) and concurrently accumulated less MDA when compared to its control counterparts as well as in respect to other genotypes of the same stress regime. Such low MDA content was also found to be a characteristic feature of drought tolerance in olive (Bacelar et al. 2006) and cotton (Yildiz-Aktas et al. 2009). From the present experimental results, it can be assumed that the drought-induced ROS accumulation and concurrent oxidative damage might have undergone a more stringent control in drought tolerant V1 compared to susceptibles which might be attributed to efficient regulatory strategies and effective operating mechanisms associated with oxidative stress metabolism.

Increased levels of foliar antioxidants were reported to be associated with drought tolerance of higher plants (Šircelj et al. 2007; Ashraf and Foolad 2007). In the present study, different drought regimes caused significant variations in the level of non-enzymatic antioxidative metabolites among different mulberry genotypes and remarkable differences in the response of non-enzymatic antioxidants were observed between drought tolerant and drought susceptibles genotypes. AA was found to be one of the major non-enzymatic antioxidants in drought tolerant V1 where a significant positive correlation was observed between drought stress intensity and foliar AA level. In case of drought susceptible genotypes, a marginal however, significant increment in AA level was detected mostly at low water stress regime (75% PC) which indicates that the AA mediated antioxidative protection might be successful in the susceptibles when drought stress was less intense. At severe water stress regime, no further increment in AA was recorded in susceptibles when compared to drought tolerant V1, indicating genotypic limitation of the susceptibles failing to trigger AA accumulation. AA is a key component in the network of antioxidants that include glutathione, α-tocopherol and a series of antioxidative enzymes (Foyer and Noctor 2005). AA can react non-enzymatically with $O_2^{\bullet -}$, H_2O_2 and $^1O_2$ and was reported to play multiple roles in plant growth including cell division, cell wall expansion, and other developmental processes (Mittler 2002; Reddy et al. 2004b; Gill and Tuteja 2010). High AA level in V1 leaves at severe water stress regime indicates that the AA mediated

quenching of ROS might be successful in this drought tolerant genotype conferring chloroplastic stability, better photosynthetic capacity and less lipid peroxidation. Besides AA, glutathione is the next key metabolite in AA-glutathione cycle which occurs in reduced form (GSH) in plant tissues and is widely considered as a marker of oxidative stress in plants under various abiotic stress conditions including drought (Xiang et al. 2001; Mullineaux and Rausch 2005). Glutathione is a potential scavenger of $^1O_2$, H_2O_2, $OH^{\cdot}$ and plays a key role in regulating AA *via* AA-glutathione cycle (Foyer and Noctor 2005; Meyer 2008). In the present study, at low and medium water stress regimes, a marginal but significant accumulation of glutathione was recorded in the susceptible mulberry genotypes. However, under severe water stress, no further increment in glutathione was recorded in the susceptibles and the level was statistically unaltered. Under low water stress, such increase in glutathione level was also reported in some cases (Zhang and Kirkham 1996; Šircelj et al. 2007). According to Tausz et al. (2001) and Šircelj et al. (2007), oxidation of GSH to GSSG (oxidized GSH) might trigger such increased glutathione concentrations during low water stress. However, severe drought obviously exceeded the adaptive capacity of GSH pool, and, therefore, no further elevation in glutathione level was observed in susceptibles when compared to tolerant V1.

Tocopherols are another major group of non-enzymatic antioxidants which efficiently trap free radicals ($^1O_2$), stabilize photosynthetic membranes, protect chloroplasts from photooxidative damage and modulate signal transduction (Schwanz and Polle 1998; Munné-Bosch 2005). Out of four isomers of tocopherols (α,β,γ,δ) found in plants, α-tocopherol is known to have the highest antioxidative properties (Kamal-Eldin and Appelqvist 1996; Wu et al. 2007). In the present study, a positive correlation was observed among foliar α-tocopherol, AA and glutathione levels under drought conditions. V1 had significantly high, efficient AA-glutathione pool and also recorded elevated levels of α-tocopherol under severe drought stress, whereas a net α-tocopherol loss was observed in other susceptible genotypes at severe water stress regime. Tocopheroxyl radicals, generated due to the chemical scavenging of $^1O_2$ by α-tocopherol are recycled back to α-tocopherol by AA. When the abundance of AA in chloroplast becomes limited, as occurred in drought susceptible mulberry genotypes (at severe water stress regime), an irreversible degradation of α-tocopherol takes place leading to severe loss of endogenous α-tocopherol

level (Munné-Bosch 2005). The drought tolerant V1, by virtue of its elevated AA-glutathione pool, was able to recycle back α-tocopherol successfully which in turn might have facilitated low MDA accumulation when compared to other susceptibles (**Fig. 3.14**). At severe water stress, the endogenous loss of α-tocopherol can also be positively correlated with apparent down-regulation in photochemical efficiency of PSII (F_v/F_m) of the drought susceptible genotypes. Trebst et al. (2002) showed the essentiality of α-tocopherol in maintaining the function of D1 protein and PS II activity which support our findings.

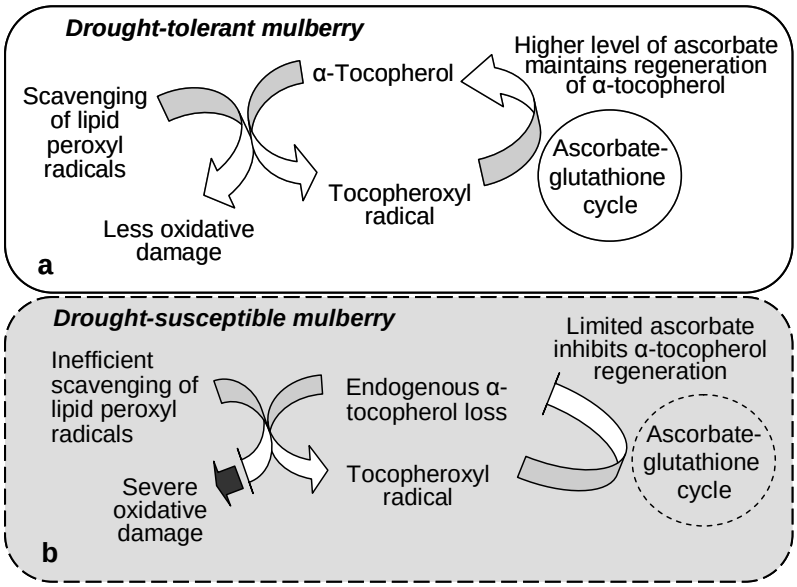

Fig. 3.14 Relationship between ascorbate-glutathione pool and α-tocopherol content in mulberry leaves: a α-tocopherol recycling by higher level of ascorbate-glutathione pool leading to less oxidative damage in the leaves of relatively drought tolerant mulberry genotype V1 whereas b endogenous loss of α-tocopherol due to limited availability of ascorbate was evident in drought susceptible mulberry genotypes S36, K2 and MR2 which caused severe oxidative damage in terms of more lipid peroxidation.

Carotenoids have received less attention compared to other non-enzymatic ROS scavengers. Carotenoids are lipohilic antioxidants which play crucial role in energy dissipation, photoprotection of chloroplasts, thylakoid membrane integrity and scavenging of ROS (Collins 2001; Niyogi et al. 2001; Edreva 2005; Yildiz-Aktas et al. 2009). The present experimental data elucidate that the mulberry genotypes tried to enhance their photoprotection by maintaining higher carotenoid level under drought. This mechanism, might have partially aided the susceptibles to minimize degradation of chlorophyll molecules and other photoinhibitory damages of their photosynthetic apparatus at low and medium water stress regimes (reflected by higher F_v/F_m). However, severe drought obviously exceeded the photoprotective capacity of carotenoids in the susceptibles as

reflected by apparent decrease in F_v/F_m with concomitant decline of P_n and substantial increment in MDA content. In contrast, under severe drought, the total carotenoid content remained at higher levels in the drought tolerant V1, indicating better photoprotection and integrity of the photosynthetic membranes of chloroplasts (Efeoğlu et al. 2009).

Analysis of free proline content in water-stressed mulberry leaves elucidated most significant differential responses among the tested genotypes. Other than an osmoprotectant, proline is regarded as an important non-enzymatic antioxidant playing important roles in stabilizing sub-cellular structures, scavenging free radicals and buffering cellular redox-potential under stress conditions (Ashraf and Foolad 2007; Yildiz-Aktas et al. 2009). Proline accumulation under water stress is generally considered as an important phenomenon involved in stress tolerance (Hare and Cress 1997; Yin et al. 2005; Shvaleva et al. 2006). In the present study, proline was found to be a major non-enzymatic antioxidative metabolite in mulberry leaves and significant positive correlation was observed between the concentration of proline and the level of drought stress intensity. The enhanced proline accumulation in water-stressed V1 leaves might have provided better osmotic equilibrium, ROS-scavenging ability and cell membrane stability. The stimulation of proline biosynthesis might be associated with an increase in glutamate dehydrogenase (GDH), Δ^1- pyrroline-5-caboxylate reductase (P5CR) and the Δ^1- pyrroline-5-caboxylate synthetase (P5CS) levels as shown by earlier workers (Savoure et al. 1995; Zhu et al. 2002; Chaitanya et al. 2009). Chaitanya et al. (2009) also reported the significance of ornithine transaminase (OT) cycle in accumulation of proline in drought-stressed mulberry.

To conclude, the results reported here indicate substantial genotypic variation in morphophysiological and leaf yield traits among the tested mulberry genotypes. The reduced leaf yield under water limitation as observed for those genotypes which otherwise yielded high when well-irrigated (in the experiments reported here) suggest that maintaining better yields in dry-land conditions can be possible through breeding strategies, specifically focused on minimizing the gap between potential yield and actual yield. Drought stress severely down-regulated leaf-level physiological variables in the susceptible genotypes resulting in poor leaf yield. However, genotypes S13, V1 and S1 performed better in terms of leaf gas exchange and proved their superiority over other genotypes in drought tolerance. Under glasshouse conditions, the combined leaf gas

exchange/chl a fluorescence measurements further dissected out stomatal and non-stomatal restrictions to P_n. As internal/ambient CO_2 ratio (C_i/C_a) decreased concurrently with G_s in non-irrigated stands, it appeared that greater stomatal limitation to P_n was associated with decreased photo-assimilation and leaf yield production. Further, higher leaf temperature (T_L) (>35 °C) and down-regulation of maximum quantum yield of PSII (F_v/F_m) were apparent in the susceptibles compared to the tolerants which indicated chronic photoinhibition due to photo-inactivation of PSII centers in the susceptible mulberry genotypes. Drought-induced trade-offs in biomass allocation was also highlighted. The 'drought tolerant' characteristics as observed in the tested genotypes, such as higher rates of photosynthesis and stomatal conductance, low leaf temperature, less photoinhibition, stabilized photochemistry, higher biomass allocation to leaves and better root growth characteristics are likely to be beneficial in breeding programs to develop drought tolerant mulberry genotypes. Overall, the results suggest that a better rooting vigor and leaf hydration status, minimal stomatal inhibition and stabilized photochemistry might play major roles in maintaining higher P_n and associated gas exchange functions in drought tolerant mulberry genotypes under water stress conditions. The minimal plasticity in foliar gas exchange traits and better quantitative growth characteristics can be accredited for higher leaf yield production in tolerant genotypes compared to susceptibles under low water regimes. In drought tolerant genotypes, the relative variation in some of these characteristics were tend to be consistent between well-watered and water-limited conditions, indicating low genotype × environment interaction, which could be exploited in breeding programs for improving drought tolerance in mulberry. The involvement of non-enzymatic antioxidants in potentiating antioxidative defense system and ameliorating oxidative damage have significant implications in mulberry in relation to drought stress tolerance. The most consistent and sensitive biochemical drought stress markers in mulberry as recorded in our study were AA, glutathione and proline with α-tocopherol and carotenoids as good additional indicators. Thus, these non-enzymatic antioxidants can be considered as reliable biochemical markers for drought stress tolerance in mulberry. The data obtained with mulberry genotypes from the present study is an important complement to understand drought-induced non-enzymatic antioxidative responses in tree crops.

Dynamics of photosynthetic and hydraulic acclimation processes in mulberry during progressive drought stress

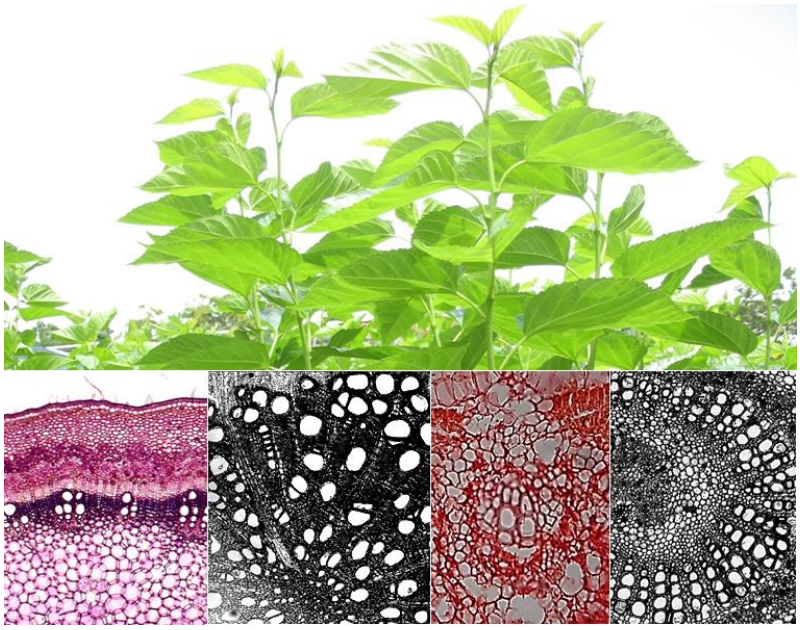

Chapter 4

Several decades of photosynthesis research have demonstrated that eukaryotes performing oxygenic photosynthesis have developed acclimation and adaptation strategies for modifying specific features of light energy conversion. The functional flexibility of the photosynthetic apparatus allows photoautotrophs to rapidly cope with fluctuating environmental conditions. Drought, one of the most prevalent environmental stress factors, can profoundly affect photosynthetic processes in plants (Flexas et al. 2006). Analyses of drought-induced photosynthetic responses have provided valuable insights to understand the mechanisms that allow plants to exert control over the energy balance of leaves during water-limitation (Yordavov et al. 2000). Data available on photosynthetic adjustments under drought stress broadly suggest two types of responses in vascular plants including rapid short-term (in a matter of seconds and minutes) and long-term (hours to days) acclimatory changes (**Fig. 4.1**). The short-term acclimation processes are mostly involved in regulation of light-harvesting capacity and rates of electron flow. During water stress, these short-term acclimatory mechanisms that regulate light harvesting and photosynthetic electron transfer (PET) facilitate the formation of remodeled photosynthetic complexes with distinct properties. The effectors that elicit these changes are most often sensitized by pH and/or redox conditions, while the new

structural/functional components may also be sensitive to redox conditions (Eberhard et al. 2008). This is illustrated by PSII minor subunit (PSII-S) and possibly LHCSR (present in *Chlamydomonas* and diatoms, but absent in land plants) which enhance the sensitivity of the non-photochemical quenching (NPQ) in response to pH and for PGR5/PGRL1 (a protein complex with regulatory role in cyclic electron flow), whose function modifies redox properties of PET downstream of the cyt b6f complex by an as-yet unknown mechanism (Munekage et al. 2002). Unlike short-term scale, on longer time scale, alterations in gene expressions and net protein synthesis processes are induced in favor of photosystem stability and to minimize photoxidative damage (Eberhard et al. 2008). This flexibility depends on key proteins currently being identified, generally as a result of genetic screens based on changes in chl fluorescence. The proteins that appear to contribute to the dynamics of the photosynthetic machinery are listed in **Table 4.1**. The list encompasses subunits of light-harvesting and electron-transfer complexes whose conditional expression may contribute to a remodeling of the photosynthetic apparatus, enzymes that control branching pathways for electron transfer or that contribute to posttranslational modification of photosynthetic targets and signaling proteins. However, the table does not include several additional proteins that participate in biogenesis and assembly of photosynthetic complexes because they have not been identified in available photosynthetic acclimation studies.

Despite a wealth of existing knowledge, our understanding of functional flexibility of photosynthetic system to environmental cues is mostly confined to unicellular model organisms (*Chlamydomonas reinhardtii*, *Synechocystis*, *Synechococcus* etc.) (Finazzi et al. 2004; Forti et al. 2005; Eberhard et al. 2008) and few higher systems like arabidopsis, barley, pea, tobacco etc. (Iturbe-Ormaetxe et al. 1998; Woo et al. 2004; Oukarroum et al. 2007). Unfortunately, trees have received less attention and little information is available on how rapidly they can cope with energy imbalance in order to protect photosynthetic apparatus under drought-stressed situations. Thus, exploring the dynamics of photosynthesis in trees during drought stress conditions still remain as highly desirable goals. Among the various screens used to probe the characteristics features of photosynthetic acclimation, use of chl a fluorescence has been invaluable due to its non-destructive nature and high sensitivity to evaluate important PSII characteristics including

energy trapping, electron transport and dissipation of excitation energy in the antenna complex etc. (Stirbet and Govindjee 2011). However, such measurements are not routinely conducted in case of trees and there is an emerging consensus to include such experimental approach for characterizing drought-

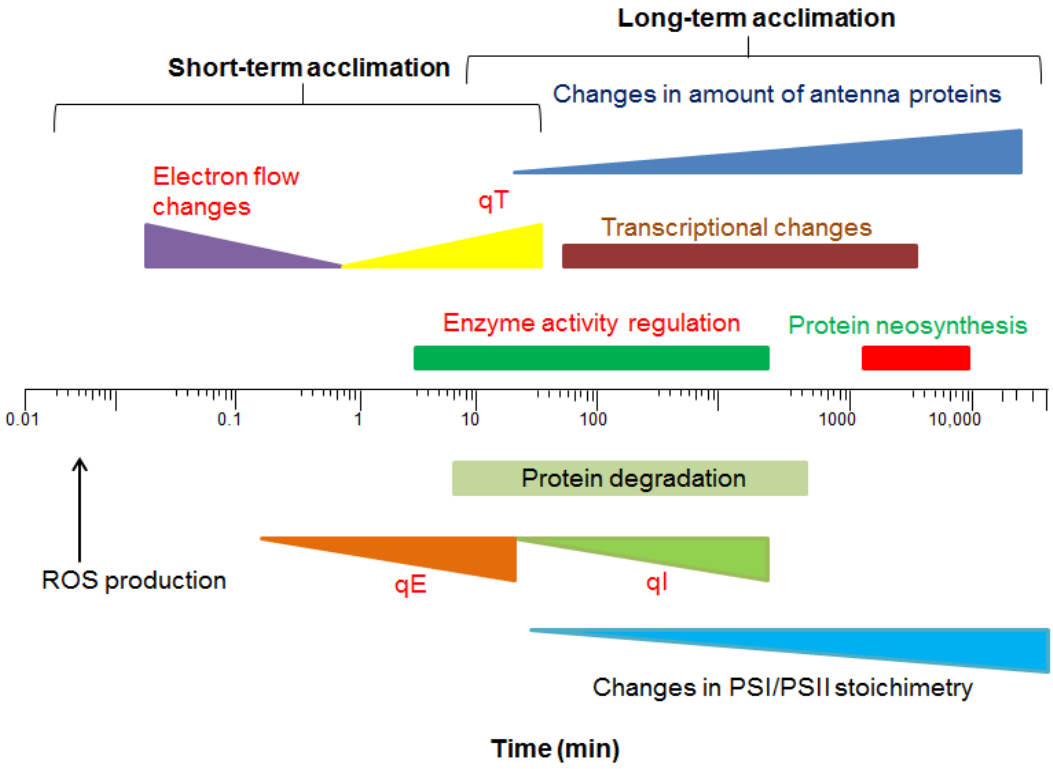

Fig. 4.1 Major short-term and long-term acclimation processes in vascular plants. The diagram represents "consensus" time scales for regulation of light-harvesting capacity (the qE, qT, and qI components of NPQ) as well as rates of electron flow. Short-term acclimation processes also include regulation of enzymatic activities e.g., via kinase-dependent phosphorylation cascades, as well as protein-degradation mechanisms involved. On longer time scales, changes in gene expression and net protein synthesis processes are induced (Eberhard et al. 2008). qE, thermal dissipation; qT, state transition and qI, photoinhibition.

induced photosynthetic responses in trees. Because long-term acclimation of photosynthesis is largely regulated at post-translational level (Eberhard et al. 2008), integration of proteomic studies with chl a fluorescence analysis can further improve our understanding on overall photosynthetic acclimation processes in trees. In general, most photosynthetic genes are down-regulated in a multitude of stress conditions including drought elucidating that down-regulation is part of the general stress response. Nevertheless, hunting drought-induced over expressed proteins that may have a

photoprotective function can be helpful in identifying environmental biomarkers and in developing strategies for genetic improvement of higher plants including trees for enhanced drought tolerance (Hashiguchi et al. 2010). In this direction, however, very few proteomics-based analyses of tree species have been carried out till date (He et al. 2008; Bedon et al. 2010; Sergeant et al. 2011; Durand et al. 2011).

Table 4.1 Proteins potentially playing significant roles in the dynamics of photosynthesis, as revealed by functional, genetic, proteomic and genomic studies (Eberhard et al. 2008).

Gene (families)	Protein	Role
APX, PTOX, NDH	Chloroplast ascorbate peroxidase, plastid terminal oxidase, NADPH dehydrogenase	Alternative electron sinks for the light reactions of photosynthesis
ELIP2	Early light-induced protein	Dissipation of excess light energy
HCF136	Lumen of stroma lamellae	PSII stability/assembly factor
LHCSR2 & LHCSR3	Chloroplast proteins of the light-harvesting complexes	Dissipation of excess light energy
PETE & FED	Plastocyanin and ferridoxin	Linear and cyclic electron flow
PGR5 & PGRL1	Chloroplast proteins	Cyclic electron flow
PSB01 & 2/PSBP1&2	Subunits of the oxygen evolving complex	Dynamic changes of subunit composition of the oxygen evolving complex involving paralog gene products
PSII-S	Photosystem II subunit	Dissipation of excess light energy
RBCS & RBCL	Subunits of Rubisco	Photosynthetic carbon fixation, alternative electron sink (through oxygenase activity)
STT7/STN7 & STN8	Chloroplast protein kinases	State transition, chloroplast to nucleus retrograde signaling
YCF37	Thylakoid bound in *Synechocystis*	Potentially implicated PSI assembly
Nuclear genes acting on chloroplast gene expression	Sigma factors involved in plastid transcription. M (plastid mRNA maturation and stability) and T factors (plastid mRNA translation)	Control of plastid gene expression

From earlier experiments (see Chapter 3: field and glasshouse data), it was evident that the drought tolerant mulberry genotypes exhibit minimal plasticity in foliar gas exchange characteristics and subsequently maintain higher rates of photosynthesis and stomatal conductance. Since the capacity of photoacclimtion and efficiency in photodamage repair can minimize oxidative damage and sustain photosynthesis, investigation of these photoacclimation strategies can be important complement to understand photosynthetic performance in drought tolerant mulberry genotypes under water-limited conditions. So

far, most of the drought experiments in mulberry have predominantly concentrated on leaf gas exchange physiology, Calvin cycle enzymes and antioxidative defense mechanisms (Ramanjulu et al. 1998; Chaitanya et al. 2003). No studies have provided yet detailed information on photoacclimation in drought-exposed mulberry under conditions of progressively increasing drought stress intensity. Moreover, we are not aware of any leaf proteomic investigations in drought-stressed mulberry in order to identify over expressing proteins that might be linked to photosystem stability and photoprotection.

Like photosynthesis, hydraulic conductance is also known to vary substantially, on both short and long time-scales, as a function of different environmental parameters such as temperature (Sellin and Kupper 2007), light (Scoffoni et al. 2008) and water availability (Scoffoni et al. 2012), as well as during leaf ontogenesis and ageing (Assama et al. 2005). Drought poses a serious threat to the maintenance of hydraulic conductance due to vulnerability of the conductive tissues towards water deficit (Nardini et al. 2003; Choat et al. 2005; Hao et al. 2008). Generally water deficiency causes reductions in stomatal and hydraulic conductance, compromising the water status of the plants (Siemens and Zwiazeck 2004). While mechanisms of stomatal closure during water deficit are well understood, mechanisms that lead to changes in hydraulic conductance during drought stress remain largely unknown. Hydraulic conductance is influenced by several internal and external factors including embolism of the xylem vessels, xylem anatomy, water availability, temperature, cellular properties etc. (Siemens and Zwiazek 2004; Aroca et al. 2005; Boursiac et al. 2005). Many of these factors regulate hydraulic conductance mainly by affecting the activity and/or abundance of water channel proteins known as aquaporins.

Earlier reports (Steudle 2000a, 2000b) have explained variation in hydraulic conductivity in terms of the composite transport model based on the composite anatomical structure of tissues, where water can move radially toward the xylem along three pathways: the apoplastic, symplastic, and transcellular. The symplastic and transcellular pathways are difficult to separate experimentally and are collectively considered as the cell-to-cell pathway (Steudle 2000b). The extent to which water flow predominates in either pathway varies according to the relative hydraulic conductances of the pathways and the relative magnitude of hydrostatic versus osmotic gradients (Steudle 2000a; Bramley et al. 2007). Apoplastic flow can be altered irreversibly by anatomical changes (Steudle and Peterson

1998), whereas the conductance of the cell-to-cell pathway can be largely determined by the activity of aquaporins within the series array of membranes, which results in changes in conductance that can be relatively rapid and reversible (Vandeleur et al. 2009) (**Fig. 4.2**).

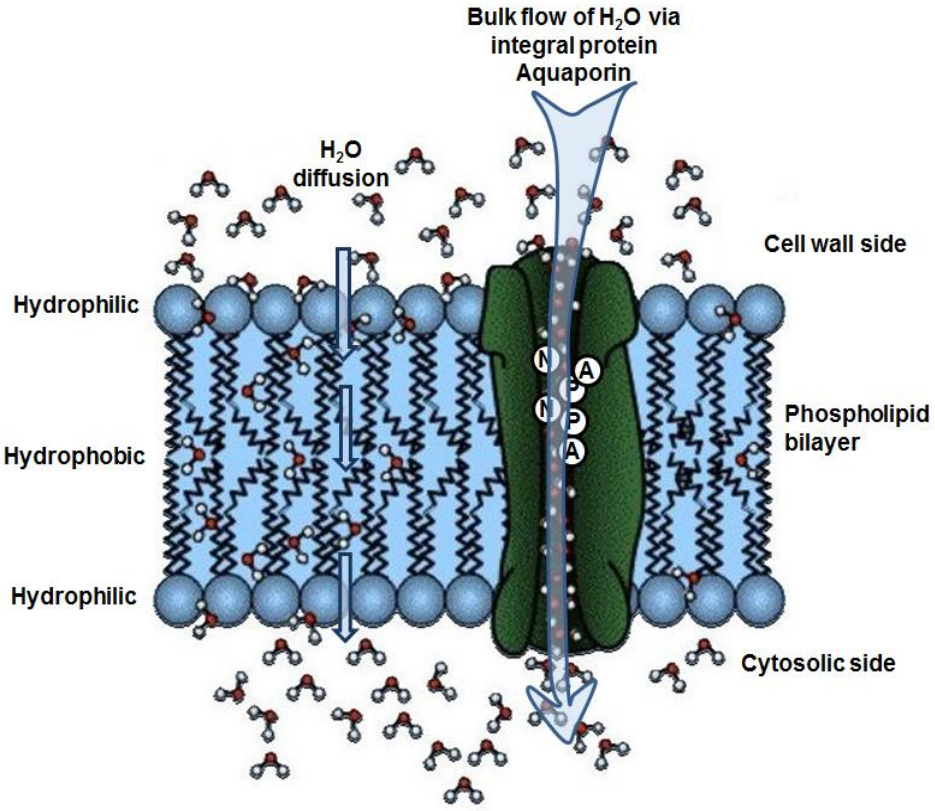

Fig. 4.2 Aquaporin facilitates the diffusion of water and small neutral solutes across plant cell membranes. Plant aquaporins similar to their animal counterparts are thought to form tetramers, each monomer being functionally independent.

In plants, aquaporins form a large gene family, comprising, for example, 35 members in Arabidopsis (Johanson et al. 2001), 33 members in rice (Sakurai et al. 2005) and at least 33 members in maize (Chaumont et al. 2001). Based on amino acid sequence comparison, plant aquaporins have been divided into four subfamilies: plasma membrane intrinsic proteins (PIPs), tonoplast intrinsic proteins (TIPs), NOD26-like intrinsic proteins (NIPs) and small basic intrinsic proteins (SIPs). The PIP subfamily can be further divided into PIP1 and PIP2 isoforms based on the sequence homology. In general PIP1s have little or no water channel activity in vitro, whereas the PIP2s show high water permeability when expressed in *Xenopus laevis* oocytes (Chaumont et al. 2001). Aquaporins are believed to be

involved in a large number of physiological functions in plants (**Fig. 4.3**), however, their functional roles during water stress remain as yet largely unknown. The over-expression of

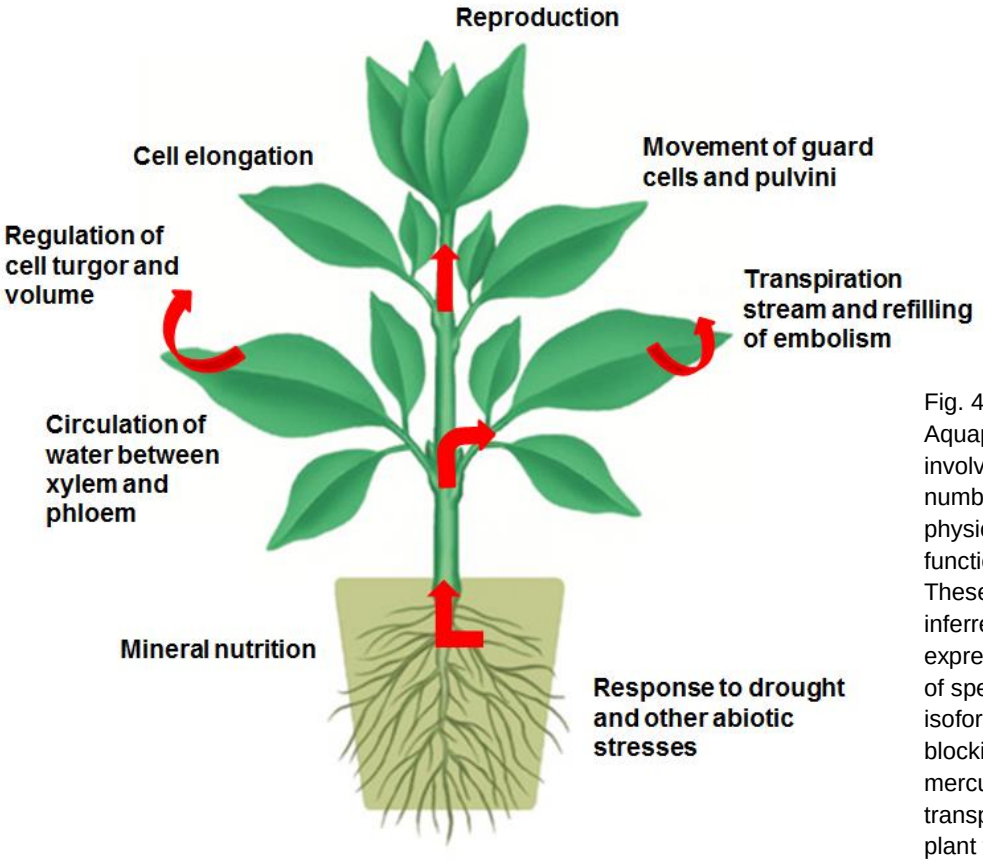

Fig. 4.3 Aquaporins are involved in a large number of physiological functions in plants. These functions were inferred from the expression patterns of specific aquaporin isoforms or from the blocking effects of mercury on water transport through plant tissues (Maurel and Chrispeels 2001).

AtPIP1;2 (PIP1b) from *Arabidopsis* in transgenic tobacco plants increased plant growth rate in control conditions. However, under water stress, transgenic tobacco plants wilted faster than wild plants (Aharon et al. 2003). In contrast, Siefritz et al. (2002) found that on knocking down the expression of the NtAQP1 gene using NtAQP1 antisense constructs, transgenic tobacco plants showed a higher sensitivity to water stress. Gene expression studies in various plant species have shown variable responses of aquaporin isoforms to water stress, with both up- and down-regulation of genes (Suga et al. 2002; Jang et al. 2004; Alexandersson et al. 2005). In leaves, roots, and twigs of olive (*Olea europaea*), OePIP1;1, OePIP2;1, and OeTIP1;1 were significantly reduced at 3 and 4 weeks after

water was withheld (Secchi et al. 2007). Water deficiency may evoke transcriptional and post-translational regulation of aquaporin activity, since aquaporin activity has been shown to be regulated by phosphorylation (Johansson et al. 1998; Luu and Maurel 2005). Under water deficit, aquaporins are likely to play important roles both at whole plant level, for transport of water to and from the vascular tissues, and at the cellular level, for buffering osmotic fluctuations in the cytosol (Johansson et al. 2000). In the last two decades, significant thrust has been given in the research for aquaporin function at whole plant level using new experimental approaches and several laboratories have started investigating aquaporin-mediated regulation of hydraulic conductance in higher plants under drought and other abiotic stress conditions.

Mulberry ideally represents the group of fast growing perennial tree crop species. There is also considerable phenotypic and genetic variation among the cultivars of mulberry that is advantageous in comparative physiology and molecular studies. In the arid and semiarid zones, the crop often experiences cycles of water deficit stress and often gets exposed to multiple environmental stresses either sequentially or simultaneously. These result in various degrees of water stress, with exposure to cycles of drying and wetting over time scales ranging from diurnal to several days or weeks. Lal et al. (2009), for the first time reported up-regulation in PIP1, PIP2, and TIP2 in mulberry leaf under dehydration stress. However, they induced water stress using PEG (10%) solution for 3 h or by air drying and thus the results did not reflect realistic water stress conditions. Moreover, no information is available yet on mulberry aquaporins regarding their response under progressive water stress conditions, their comparative expression in leaf and root tissues as well as their comparative expression in drought tolerant and drought susceptible genotypes. Thus, the present comparative study was undertaken between two mulberry genotypes: V1 (drought tolerant) and K2 (drought susceptible) for understanding how progressive water stress influence changes in the expression of aquaporins and in turn plant water status. In earlier studies, K2 exhibited a much lower transpiration rate per unit leaf area, exerted a tight regulation of stomatal aperture contributing to drought avoidance and was considered to be drought susceptible when compared to V1 (see Chapter 3). In the present experimental set-up, an integrated series of experiments were designed to examine concomitant changes in plant water status and transpiration rate under by progressive water

stress to see if changes in plant water relations are correlated with the observed changes in the mRNA expression of aquaporins. One of the most highly expressed PIP aquaporins (MIPIP1.3) in mulberry (Lat et al. 2009) was functionally characterized in the root and leaf tissues to determine the comparative response of MIPIP1.3 in V1 and K2 genotypes under progressive water deprivation. Changes in aquaporin expression were expected to match changes in leaf water status, transpiration and hydraulic conductivity broadly reflecting the different strategies to drought stress in the two contrasting mulberry genotypes.

A high degree of hydraulic capacity under water stress is also offered by constitutive anatomical features which are stable in higher plants and hence act as better-observed indicators for hydraulic efficiency (Kulkarni et al. 2008; Sophia and George 2003). Vessel diameter is perhaps one of the most important xylem parameters in relation to water flow. According to Poiseuille's law, vessel radius is proportional in the 4^{th} power to water conductance. Therefore, wider vessels can lead to significantly higher conductivity when compared to smaller ones. On the other hand, occlusion in wider vessel elements can significantly reduce water transport and wider conduits are also more sensitive to air embolisms (Zimmermann and Milburn 1982; Van Ieperen et al. 2001; Hacke et al. 2009). Xylem conduit length and number also have an impact on water conductance. Longer xylem conduits transport water more effectively (Comstock and Sperry 2000; Nijsse et al. 2001), but they are also more vulnerable to cavitation (Hacke et al. 2009). A higher conduit number signifies more redundancy in the stem structure, and therefore, might be advantageous in embolized or wounded stems. Different structural parameters of the leaf are important in relation to water use efficiency (Kulkarni et al. 2008). The stomata control transpirational water loss, and therefore, stomatal density is an important factor determining water relations. While high transpiration helps to cool the plant, it also facilitates rapid water loss. A less number of stomata per unit leaf area might allow a better control of transpirational water loss, while on the other hand would reduce evaporative surfaces. Other structural features of leaf including leaf thickness, palisade and spongy layer thickness, venation architecture and trichome density are also widely acclaimed as important traits associated with water conservation, water flow and water use efficiency (Dickison 2000; Sack and Holbrook 2006). The search for anatomical traits related to increased efficiency of xylem water transport can provide insights into the complexity of

hydraulic pathway depicting that a fine-tuned interplay of physio-biochemical factors along with in-built anatomical set-up, altogether work in close coordination in order to achieve better hydraulic conductance and in turn drought tolerance in higher plants. Hence, for a vivid understanding of hydraulic acclimation mechanisms, endeavor is needed to link physiology with molecular response and morpho-anatomty for finding out the subtle communion among these traits. Such integrated traits, expressing at a higher level of organization are suggested to be quintessential in crop improvement programs.

With this background, the present comparative study was undertaken with an integrated approach. The study included leaf-level gas exchange and polyphasic chl a fluorescence kinetics measurements combined with leaf protein analyses. On each alternate day, leaf gas exchange measurements were conducted combined with chl a fluorescence estimations. Finally, on 10^{th} day, when drought stress intensity was severe, leaf protein analyses were additionally performed along with other regular measurements. This photoacclimation study was coupled with the expression studies of MIPIP1.3 and investigation of morpho-anatomical characteristics in mulberry genotypes (V1 and K2) which differ in their drought tolerance response as mentioned earlier. The study aimed to investigate (i) drought-induced modulations in photosynthetic processes, (ii) photoacclimation strategies under progressive drought, (iii) expressional changes in MIP1P1.3 and (iv) in-built hydraulic architecture that are preferred by drought tolerant mulberry genotype for sustaining better hydraulic conductance and net CO_2 fixation during water-limited conditions.

Materials and Methods

Plant material, stress treatments and experimental conditions

One drought tolerant (V1, *M. indica* L.) and one drought susceptible (K2, *M. indica* L.) genotypes were selected for this experiment based on the earlier performance of those genotypes at field and glasshouse-level experiments (see chapter 3). Five months old, healthy potted (20 L cement pots filled with red loamy soil of pH 7.2) saplings of equal growth were procured from the nursery of Botanical Garden, University of Hyderabad

(Hyderabad, India). All experiments were conducted in semi-controlled glasshouse chamber of University of Hyderabad. Potted saplings were arranged in completely randomized block design (CRBD) with four replications (n=4). Plants transferred to glasshouse conditions were subjected to an acclimatization period of 3 weeks before the onset of experiments. During this period, all potted plants were maintained at 100% pot water holding capacity (PC) (Said and Hugh 2005) and were fertilized with 20 g standard slow release mixed fertilizer (13% N, 10% P and 14% K). At the beginning of the experiments (day 0: D0), the plants were randomly divided and subjected to two different watering treatments: well-watered (WW) and water-stressed (WS). WW plants were regularly maintained at 100% PC (as control) throughout next 10 days (i.e. from D1 to D10) of experimental period, whereas in WS plants, watering was withheld from D1 to D10. Chamber walls and ceiling of the glasshouse were transparent to sunlight. Mean photosynthetic photon flux density (PPFD) inside the glasshouse (measured between 09.00-11.00 h) ranged from 900 to 1600 µmol m^{-2} s^{-1}, mean air temperature ranged from 22±1°C (early morning) to 34±4°C (early afternoon), relative humidity ranged from 20±5% to 41±2% and ambient CO_2 concentrations of 360±10 µmol mol^{-1}. Leaf water status, photosynthetic gas exchange functions, chl a fluorescence transients and chl pigments were determined in fully expanded leaves of 3^{rd}-4^{th} position from the shoot apex. All measurements and samplings were first conducted on D0 before the onset of stress treatments. Thereafter, they were periodically conducted on each alternate day (D2, D4, D6, D8 and D10). For leaf protein analyses, youngest fully expanded leaves from WW and WS plants (five leaves from three plants per replicate, three biological replicates per treatment) were collected on D10 (when severity of drought stress was maximum) immediately after leaf gas exchange and chl a fluorescence measurements.

Measurements of leaf water status

Fresh leaf discs (1.5 cm^2) were collected from WW and WS plants between 10.00 – 10.30 h, weighed immediately, then re-hydrated by immersing them in distilled water in plastic trays sealed with parafilm for 24 h at 4°C in darkness and subsequently over-dried for 24 h at 105°C. Leaf relative water content (RWC) was determined as 100 x [(fw-dw)/(tw-dw)] where, fw is the fresh weight of leaf discs, tw is the turgid weight after re-hydrating the

discs for 24 h, and dw is the oven-dried weight of discs. Leaf moisture content (LMC) was calculated as 100 x [(fw- dw)/fw].

Measurements of photosynthetic leaf gas exchange characteristics

Leaf net CO_2 fixation rate (P_n) stomatal conductance (G_s), transpiration rate (E), intercellular CO_2 concentration (C_i) and leaf temperature (T_L) were measured in WW and WS plants during 10.00-10.30 h using a portable infra-red gas analyzer (IRGA, LCpro-32070, ADC Bioscientific Ltd. U.K.). Estimations of instantaneous leaf water use efficiency (WUE_i) were calculated as P_n/E. The gas analyzer was equipped with a broad leaf chamber (LCpro-32070, UK), a PAR sensor (silicon based sensor, LCpro-32070) and a leaf thermistor probe (ADC, M.PLC-011). Throughout the measurements, the following conditions were maintained: a saturating photosynthetically active radiation (PAR) of 1800 μmol m^{-2} s^{-1} supplied by a LED light source (LCpro Lamp 32070 - Broad, ADC Bioscientific Ltd. U.K.) attached to leaf chamber; air temperature of 25-26°C; CO_2 concentration of 370 μmol mol^{-1}; air flow rate of 340 μmol s^{-1}; and relative humidity of 55-60%. Each measurement was made when P_n and G_s readings were stabilized; this process typically took 1–2 min.

Measurements of chl a fluorescence and analyses of OJIP transients

Chl a fluorescence measurements were recorded during 11.00-11.30 h on the same leaves used for leaf gas exchange studies. Measurements were conducted using a portable Handy-PEA chl fluorometer (Handy-Plant Efficiency Analyser-2126, Hansatech Instruments, King's Lynn, UK). The leaves were first dark-acclimated for 30 min by fixing leaf clips (Hansatech, UK) to ensure that all PSII were in the dark-adapted state with open reaction centers (RCs). Then chl a fluorescence transients were recorded by illuminating the leaves with a beam of saturating light (3000 μmol m^{-2} s^{-1}, an excitation intensity sufficient to ensure closure of all PSII RCs) of 650 nm peak wave length, obtained from three light-emitting diodes focused on the leaf surface through the clips on a spot of 5 mm diameter circle. The fast fluorescence kinetics was recorded from 10 μs to 1s and the fluorometer was set using the following program: the initial fluorescence (F_O) was set as O (50 μs), L (150 μs), K (300 μs), J (2 ms) and I (30 ms) are the intermediates (F_L, F_K, F_J and F_I,

respectively) and P (500 ms-1s) as the maximum fluorescence (F_M). Measurements were taken in 4 replications and a single leaf per plant constituted each replicate. Using the Biolyzer 4HP v.3.306, the original (without normalization) chl a fluorescence intensity (F_t) curves were plotted and subsequently for detailed analysis of the whole digitized fluorescence kinetics, different normalizations, calculation of kinetic differences or ratios as well as time-derivatives were undertaken (Oukarroum et al. 2007; Strasser et al. 2004; Ronde et al. 2004; Redillas et al. 2011). The original OJIP transients were double normalised between the two fluorescence extreme O (F_O) and P (F_M) phases and the variable fluorescence between OP expressed as V_{OK} was determined. Further, chl a fluorescence transients were double normalised between F_O (30 µs) and F_K (300 µs) expressed as V_{OK} [$V_{OK} = (F_t-F_O)/(F_K-F_O)$] to reveal the possibility of fluorescence rise at an early step at about 300 µs. Subsequently, for each sampling date the difference in transients (ΔV_{OK}) with respect to a reference was calculated to reveal the so-called L-band (for details see result section). Further, the chl a fluorescence transients were double normalized between F_O and F_J expressed as V_{OJ} [$V_{OJ} = (F_t-F_O)/(F_J-F_O)$] and the difference between transients expressed as ΔV_{OJ} was determined periodically for each sampling dates to visualize and assess the so-called K-band (for details see result section). To evaluate the O-I phase, the chl a fluorescence data were normalized to the time range of 50 µs-1s expressed as V_{OI} (< 1) [$V_{OI} = (F_t-F_O)/(F_I-F_O)$] and the kinetic differences of V_{OI} (ΔV_{OI}) on each sampling date was determined with respect to a reference (for details see result section). The I-P phase was evaluated following two approaches: (i) normalization of fluorescence transients V_{OI} between the time range of 30 ms-300 ms expressed as V_{OI} (≥ 1) [$V_{OI} = (F_t-F_O)/(F_I-F_O)$] and (ii) transient normalisation to the time range of 30 ms-200 ms expressed as V_{IP} [$V_{IP} = (F_t-F_I)/(F_M-F_I)$]. From the V_{IP} data, comparison in the reduction rates of the electron acceptors of PSI was done by determining the rate constant (K_m) according to Michaelis-Menten equation in which the inverse of time to attain $V_{IP} = 0.5$ is an estimate of the reduction rates. The OJIP fluorescence transients also provided several other phenomenological and biophysical expressions leading to structural and functional information of PSII out of which we focused on selected parameters (**Table 4.1**) that permitted us to quantify and compare the PSII behavior of mulberry plants under progressive water stress (Strasser et al. 2004; Stirbet and Govindjee 2011).

Measurements of chl pigments

Fresh leaf discs were randomly collected (between 10.00-10.30 h) from leaf lamina (fully expanded leaves of 3^{rd}-4^{th} position from the shoot apex) using a cork borer with a diameter of 1 cm^2. Leaf discs were immersed in 10 ml of 80% (v/v) acetone in air-tight glass vials and kept in dark for 3 days under room temperature. Thereafter, absorbance of the extract was measured at 663.2 and 646.8 nm using UV-Visible 160A spectrophotometer (Shimadzu, Tokyo, Japan). Chl a, chl b and total chl contents were calculated using the extinction coefficients given by (Lichtenthaler 1987) and concentrations of the pigments were finally expressed in terms of µg cm^{-2}.

Leaf protein extraction

Youngest fully expanded leaves were collected on D10 (after withholding watering for 10 days) at 11.30 h from WW and WS plants. Leaf samples (about 2g fw, per sample) were

Table 4. 2 Selected JIP parameters from the fast OJIP fluorescence induction used in the present study.

Terms and formulae	Illustrations
$F_O \equiv F_{50\mu s}$	First reliable fluorescence value after the onset of actinic illumination; used as initial value of the fluorescence
$F_L \equiv F_{150\mu s}$	Fluorescence value at 150 µs
$F_K \equiv F_{300\mu s}$	Fluorescence value at 300 µs
$F_J \equiv F_{2ms}$	Fluorescence value at 2 ms (J-level of OJIP)
$F_I \equiv F_{30ms}$	Fluorescence value at 30 ms (I-level of OJIP)
$F_P (\equiv F_M)$	Fluorescence value at the peak of OJIP curve; maximum value under saturating illumination
T_{FM}	Time (ms) to reach the maximal fluorescence value F_M
Area	Area between fluorescence induction (OJIP) curve and the line $F = F_M$
$Fv = (F_M - F_O)$	Variable chlorophyll fluorescence
$M_O = (\Delta V/\Delta t)_O \equiv 4(F_{300}-F_O)/(F_M-F_O)$	Approximated initial slope (in ms^{-1}) of relative variable chl fluorescence curve V_t (for $F_O = F_{50\mu s}$)
$V_J = (F_J-F_O)/(F_M-F_O)$	Relative variable fluorescence at phase J of the fluorescence induction curve
$V_I = (F_I-F_O)/(F_M-F_O)$	Relative variable fluorescence at phase I of the fluorescence induction curve
$S_M = Area/F_V$	Normalized total complementary area above the OJIP transient (reflecting multiple turnover Q_A reduction events)
$N = S_M\ M_O (1/V_J)$	Number of Q_A redox turn overs until F_M is reached
K_N	Non-photochemical de-excitation rate constant in the excited antennae for non-photochemistry
K_P	Photochemical de-excitation rate constant in the excited antennae of energy fluxes for photochemistry
$ABS/RC = M_O (1/V_J) (1/\varphi_{Po})$	Absorption flux (for PSII antenna chls) per reaction center (RC)
$TR_O/RC = M_O (1/V_J)$	Trapped energy flux per RC (at t = 0)
$ET_O/RC = M_O (1/V_J) \psi_o$	Electron transport flux per RC (at t = 0)
$DI_O/RC = (ABS/RC) - (TR_O/RC)$	Dissipated energy flux per RC (at t = 0)
$\varphi_{Po} = TR_O/ABS = F_V/F_M = [1- (F_O/F_M)]$	Maximum quantum yield of primary photochemistry (at t = 0)
$\psi_o = ET_O/TR_O = (1 - V_J)$	Probability (at t = 0) that a trapped exciton moves an electron into the electron transport chain beyond Q_A
$\varphi_{Eo} = ET_O/ABS = [1- (F_O/F_M)] \psi_o$	Quantum yield of electron transport (at t = 0)
$RC/CS_m = \psi_o (V_J/M_O)(ABS/CS_m)$	Density of reaction centers per excited cross-section (at $t = t_{FM}$)
$ABS/CS_m = F_M$ (at $t = t_{FM}$)	Absorption flux per excited cross section, approximated by F_M
$TR_O/CS_m = \varphi_{Po} (ABS/CS_m)$ (at $t = t_{FM}$)	Trapped energy flux per excited cross section, approximated by F_M
$ET_O/CS_m = \varphi_{Eo} (ABS/CS_m)$ (at $t = t_{FM}$)	Electron transport flux per excited cross section, approximated by F_M
$DI_O/CS_m = (ABS/CS_m)-(TR_O/CS_m)$ (at $t = t_{FM}$)	Dissipated energy flux per excited cross section, approximated by F_M
$RC/ABS = [(F_{2ms} - F_O)/4(F_{300\mu s} - F_O)](F_V/F_M)$	Density of reaction centers per PSII antenna chl
$PI_{(ABS)} = (RC/ABS) (\varphi_{Po} /(1- \varphi_{Po}))\times(\psi_o /(1- \psi_o))$	Performance index on absorption basis
$PI_{(csm)} = (RC/CS_m) (\varphi_{Po} /(1- \varphi_{Po}))\times(\psi_o /(1- \psi_o))$	Performance index on cross section basis

immediately frozen in liquid N_2 and stored at -80ºC until protein extraction. Total soluble proteins were extracted using phenol extraction method (Hurkman and Tanaka 1986;

Sarvanan and Rose 2004). One gram of the frozen tissue was ground to fine powder in liquid N_2 and suspended in 4 ml extraction buffer [0.5 M Tris–HCl (pH 7.5), 0.7 M sucrose, 0.1 M KCl, 50 mM EDTA, 2% β mercaptoethanol and 1 mM PMSF]. Equal volume of phenol saturated with Tris–HCl (pH 7.5) was added, mixed for 30 min at 4ºC and centrifuged at 10,000 *g* for 30 min at 4ºC. The upper phenolic phase was collected and an equal volume of extraction buffer was added to it. The above step was repeated and the upper phenolic phase was re-extracted. Four volumes of 0.1 M chilled ammonium acetate in methanol was added to the collected phenolic phase and was kept overnight at -20ºC for protein precipitation. The samples were then centrifuged at 10,000 *g* at 4ºC for 30 min. The precipitated protein pellet was washed thrice in chilled methanol and acetone and air dried for few minutes. Protein concentrations of the samples were determined by using RC–DC protein assay kit (Bio-Rad, Hercules, CA, USA) using BSA as standard.

Two-dimensional gel electrophoresis (2D-GE)

Aliquots of 600 µg protein were solubilized in the rehydration buffer [8 M (w/v) urea, 2 M (w/v) thiourea, 4% (w/v) CHAPS, 30 mM DTT, 0.2% (v/v) immobilized pH gradient (IPG) buffer pH range 4-7 (GE Healthcare, Uppsala, Sweden)] to a final volume of 320 µl and 0.004% bromophenol blue was added as tracking dye. Proteins were separated according to their isoelectric point (pI) in the first dimension run using a 18 cm Immobiline pH gradient (IPG) strip (GE Healthcare) with linear gradient of pH 4-7. Focusing was performed in Ettan IPGphor II (GE Healthcare) by applying the following program: for active rehydration , the voltage was maintained for 12 h at 50 V, then the proteins were focused for 30 min at 500 V, 3 h gradient from 500 to 10000 V and 6 h at 10000 V (60000 Vh). During IEF, temperature was maintained at 20ºC and current was 50µA/IPG strip. IPG strips were equilibrated for 20 min initially in 10 ml of equilibration buffer-I (6 M urea, 50 mM Tris-HCl pH 8.8, 30% v/v glycerol, 2% w/v SDS and 2% DTT) and then in equilibration buffer-II (same components of buffer-I with the replacement of DTT by 2.5% w/v iodoacetamide). Protein separation in the second dimension was performed by SDS-PAGE (12% vertical polyacrylamide slab gels) at 10 mA gel^{-1} for 1 h and then 38 mA gel^{-1} for 6 h, using an EttanDalt6 chamber (GE Healthcare).

Staining and image analysis

Gels were stained with modified colloidal coomassie staining (Wang et al. 2007) and protein patterns were recorded as digitized images using a calibrated densitometric scanner (GE, Healthcare) and analyzed (normalization, spot matching, expression analyses, and statistics) using Image Master 2-D Platinum ver. 6 image analysis software (GE Healthcare). For relative quantification and comparison of spots, relative spot volume (% volume) parameter was used which can be defined as the ratio of the pixel density of the selected spot to the sum of the pixel densities of all the analyzed spots. Only those spots showing an up-regulation (% volume increase) of more than 1.5 fold were selected for protein identification through MALDI-TOF-TOF analysis.

In gel digestion and mass spectrometry (MS)

In gel tryptic digestion of the selected spots was performed according to the method described by (Shevchenko et al. 1996) with slight modifications. Selected protein spots were excised manually from colloidal coomassie stained gels and destained with 50% acetonitrile (ACN) in 25 mM ammonium bicarbonate (NH_4HCO_3) for five times. Gel pieces were then treated with 10 mM DTT in 25 mM NH_4HCO_3 and incubated at 56ºC for 1 h. After cooling, the DTT solution was immediately replaced with 55 mM iodoacetamide in 25 mM NH_4HCO_3 and incubated for 45 min at room temperature (25 ± 2ºC), then washed with 25 mM NH_4HCO_3 and ACN, dried in speed vac and rehydrated in 20 µl of 25 mM NH_4HCO_3 solution containing 12.5 ng μl^{-1} trypsin (sequencing grade, Promega, Wisconsin, USA). After 10 min incubation in ice, samples were kept at 37°C for overnight digestion. After digestion, the supernatant was collected and the gel pieces were re-extracted by continuous vortexing with 50 µL solution of 1% trifluoroacetic acid (TFA) and ACN (1:1 v/v) for 15 min. Supernantants were pooled together, vacuum dried using speed vac and then re-suspended in 5 µL of 50% ACN and 1% TFA (1:1 v/v) solution. Matrix-assisted laser desorption/ionization time of flight mass spectrometry MALDI-TOF MS) analysis was conducted with a MALDI-TOF-TOF mass spectrometer (Bruker Autoflex III martbeam, Bruker Daltonics, Germany). From the above prepared sample, 2 µL was mixed with equal volumes of freshly prepared α-cyano-4-hydroxycinnamic acid

(CHCA) matrix in 50% ACN and 1% TFA (1:1 v/v) and finally 1 µL of the sample was spotted on the target plate.

Protein identification through peptide mass fingerprinting and MS/MS analysis

Proteins were identified from the obtained monoisotropic peptide masses using MASCOT search engine (Matrix Science, London, UK; http://www.matrixscience.com) employing Biotools software (Bruker Daltonics, Germany). The following parameters were fixed for database searches: taxonomic category was set to *Viridiplantae* (green plants), modifications of carbamidomethyl (CS), variable modification of oxidation (M); enzyme trypsin; peptide charge of 1+; and monoisotropic. The similarity search for mass values was done with existing digests and sequence information from NCBInr and Swiss Prot database. According to MASCOT probability analysis ($P<0.05$), only significant hits were accepted for protein identification.

Real time RT-PCR analysis of MIPIP1.3 gene from root and leaf tissues

Total RNA was isolated from leaf and root tissues of V1 and K2 genotypes during different sampling points (D0, D6 and D10) using column based RNA isolation kit (Sigma) and equal amounts (1µg) of RNA was converted to cDNA using Revert Aid First strand cDNA synthesis kit (Fermentas, St Leon Road, Germany). Synthesized cDNA was used as template for amplification of a 369 bp fragment of MIPIP1.3 gene using forward and reverse primers (Fwd: GGAGGGGAAAGAAGAGGATG and Rev: GCCAAGAACAACCCAAATGT) which were designed based on the available EST sequence of MIPIP1.3 cDNA (EST name: Mim01-020-F10-A-089.g) from *M. indica* (genotype K2) at NCBI GenBank (gi|171461474|gb|ES448991|). Gel-purified PCR product was directly sent for sequencing (without TA cloning) and the obtained sequence was compared with the available MIPIP1.3 sequence using Multalin software for confirming the product identity. Within the obtained sequence, internal primers (Fwd: GGAGGGGAAAGAAGAGGATG; Rev: AGCTCTCCTGGCTCAAACAA) were designed to amplify a 132 bp product for real time qPCR analysis using KAPA SYBR FAST (Mastermix (2X) Universal) (KAPA Biosystems, Woburn, USA) real time PCR kit in an Eppendorf Realplex MasterCycler (Eppendorf, Hamburg, Germany). Equal amounts

(1 µg) of RNA, extracted during different sampling stages, were converted to cDNA and triplicate reactions were kept with 50 ng of cDNA as template following the program: 2 min at 95°C, followed by 40 cycles of 15 sec at 95°C, 30 sec at 55°C annealing temperature and 20 sec at 72°C, followed by the dissociation (melting) curve. Fold change in MIPIP1.3 was calculated according to the $2^{-\Delta\Delta Ct}$ formula (Livak and Schmittgen 2001) and the experiment was repeated thrice. Actin (*ACT*) gene from *M. alba* was used as the internal control and a validation experiment was performed to ensure equal efficiency amplification for target and reference genes, using different concentrations of template DNA according to Applied Biosystems User Bulletin No. 2(P/N 4303859).

Specimen preparation for scanning electron microscopy (SEM)

Freshly harvested leaves were cut into 3 × 3 mm squares and fixed in FAA (10% formalin: 0.5% acetic acid: 50% ethyl alcohol: 35% distilled water) for 4 h at 4ºC. The samples were post fixed for 2 h in 2% osmium tetroxide and dehydrated in a graded ethyl alcohol-acetone series for 4 h. Specimens were critical point dried and sputter-coated with gold at 1.5 keV for 10 min using a JEOL FC-1100 Fine Coat Ion Sputter Unit (JEOL, Tokyo, Japan). To view stomatal number, the ventral side of the square leaf pieces was mounted on copper stubs using double stick cellophane tape. To observe cross sectional area, leaf pieces were vertically mounted exposing their cut surfaces. Observation and photography were made using a Scanning Electron Microscope (FEI XL 30 ESEM, USA). All anatomical measurements were undertaken from the SEM images.

Histochemical studies of leaf, stem and root

Samples were collected from leaf, stems and roots of similar age, size and position and fixed in FAA (10% formalin: 0.5% acetic acid: 50% ethyl alcohol: 35% distilled water) for 24 h and kept in 70% alcohol until cutting. Freehand sections were made using a razor blade and the samples were stained by immersion in toluidine blue just for 20-30 sec, followed by three washes in distilled water. After washing, the sections were mounted in 50% aqueous glycerol and the cover slips sealed with DPX to make semi-permanent slides. The slides were then observed under a Leitz Diaplan light microscope and microphotographed.

Statistical analyses

Data are represented as mean ± SD of 4 replications (n=4). Data on leaf water status, photosynthetic gas exchange traits, chl a fluorescence characteristics and chl pigment contents were analyzed using analysis of variance (ANOVA) to determine treatment (T) x time (T_m) interactions. Post hoc mean comparisons were conducted using Tukey HSD test on the ANOVA. For proteomic analyses, three independent experiments with three replications of both WW and WS samples with each replication comprising of three pooled plants were considered and spot differences were analyzed using Image Master 2-D Platinum image analysis software (GE Healthcare). One-way factor ANOVA model ($P \leq 0.05$) was performed considering the values of best matched replicate gels from the three independent experiments. For qPCR analysis, three independent RNA samples were used for each sample and each reaction was run in triplicate for both control and stressed samples of each time point.

Results

Leaf water status

Imposed drought stress significantly declined LMC as well as RWC in both the genotypes (**Table 4.3**). This decline was initially moderate from D0 to D4, however, turned to be greater with further progression in stress intensity. On D4, LMC and RWC values in drought-stressed leaves were lower than the control counterparts by approximately ~13.7% and ~14.9%, respectively. In K2, the values for LMC and RWC decreased on D4 by 30.7% and 27.2%, respectively. However, from D8 to D10, a drastic loss in LMC and RWC was recorded indicating that drought stress caused a considerable reduction in leaf water status (**Table 4.3**). On D8 and D10, LMC values in drought-stressed V1 leaves were decreased to approximately 51.3% and 67%, respectively. In K2, on D8 and D10 the LMC values decreased to 59.7% and 73.5%, respectively than the corresponding controls. In drought-stressed V1 leaves, RWC was approximately ~44.4% and ~60% lower than the controls on D8 and D10, respectively. In case of K2, RWC decreased to almost 56.2% and 69.3% on

D8 and D10, respectively. The data on LMC and RWC showed significant T x T_m interaction (**Table 4.3**).

Table 4. 3 Changes in leaf moisture content (LMC) and leaf relative water content (RWC) with progressive water stress in mulberry genotype V1 and K2 (*M. indica* L.). Young, fully expanded leaves of the 3rd - 4th position from the apical branches were used to determine LMC and RWC. Values are means ± SD (n = 4). Values with different letters in a single column indicate significant difference (P<0.05).

	V1				K2			
	LMC (%)		RWC (%)		LMC (%)		RWC (%)	
	WW	WS	WW	WS	WW	WS	WW	WS
D0	77.4 ±1.9^{b}	77.6 ±1.7^{a}	82.4 ±2.2^{b}	82.2 ±2.3^{a}	76.2±1.7^{a}	72.3±1.3^{a}	80.5±2.3^{c}	80.7±2.2^{a}
D2	77.7 ±1.7^{b}	70.8 ±1.3^{b}	82.6 ±2.4^{b}	75.3 ±2.2^{b}	75.8±2.1^{b}	68.5±2.2^{b}	81.5±2.2^{b}	71.4±2.3^{b}
D4	76.8 ±2.2^{b}	66.3 ±2.1^{b}	81.8 ±2.3^{b}	69.6 ±2.2^{c}	75.5±1.4^{b}	52.3±1.5^{c}	82.7±1.7^{a}	60.2±2.0^{c}
D6	78.2 ±1.6^{a}	51.6 ±2.2^{c}	83.5 ±1.9^{a}	57.4 ±1.8^{d}	76.3±1.4^{a}	46.6±1.3^{d}	81.2±1.6^{b}	48.2±2.1^{d}
D8	77.6 ±1.8^{b}	37.8 ±2.8^{d}	82.2 ±1.8^{b}	45.7 ±2.0^{e}	75.8±2.0^{b}	30.5±1.4^{e}	82.5±1.5^{a}	36.2±1.8^{e}
D10	77.3 ±2.0^{b}	25.6 ±2.6^{e}	82.3 ±2.1^{b}	32.8 ±2.6^{f}	76.4±1.8^{a}	20.2±2.2^{f}	82.7±2.0^{a}	25.4±1.4^{f}

Photosynthetic leaf gas exchange

With progressive drought stress, photosynthetic gas exchange characteristics exhibited dramatic changes in drought-stressed leaves when compared to control in both the genotypes. On D2, no large difference in P_n and G_s values was evident between control and water-stressed plants. However, on D4 onwards, P_n and G_s decreased substantially with progressive increase in water stress intensity reaching minimum values on D10. On D4, in drought-stressed leaves, P_n declined by 28.6% with a concomitant decrease of 42.8% in G_s when compared to the corresponding controls (**Fig. 4.4a,b**). In K2, P_n decreased to 57.2% on D4 when compared to corresponding WW counterparts (**Fig. 4.5a**). On D6 and D8, drought-treated V1 plants showed 42.2% and 61.1% decline in P_n, respectively with a concurrent reduction of 64.6% and 80.2% in G_s, respectively than compared to corresponding controls (**Fig. 4.4a,b**). However, in K2, more dramatic reduction in P_n was recorded in compared to V1 and the values were reduced to 62.4% and 73.7% on D6 and D8, respectively when compared to their control counterparts (**Fig. 4.5a**). In control V1 plants, the P_n values did not differ substantially among the periodic time intervals. However, the values tended to increase slightly with progress in experimental time period, more specifically from D4 to D10 and finally on D10, the P_n was approximately ~17.3 µmol m^{-2} s^{-1} (**Fig. 4.4a**). The control V1 plants showed an increasing trend in G_s with progression in time and the G_s was finally recorded to be ~1.1 mol m^{-2} s^{-1} on D10 (**Fig.**

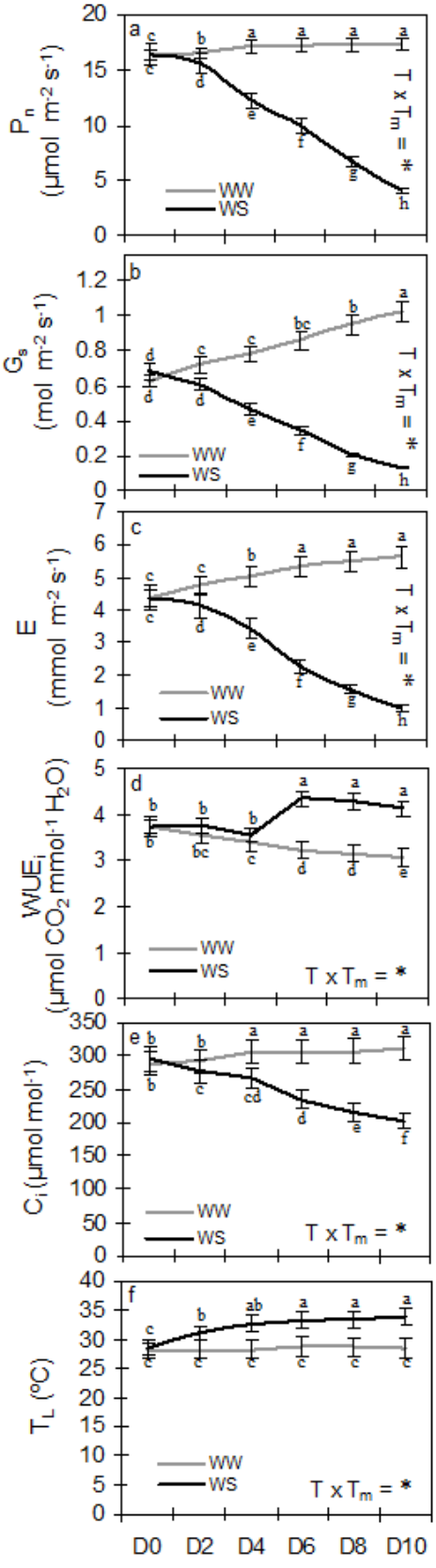

Fig. 4.4 Effect of progressive drought stress on leaf gas exchange characteristics: (A) net CO_2 fixation rate (P_n), (B) stomatal conductance (G_s), (C) transpiration rate (E), (D) instantaneous water use efficiency (WUE_i), (E) intercellular CO_2 concentration (C_i), and (F) leaf temperature (T_L) in mulberry genotype V1 (*M. indica* L.) grown in glasshouse conditions. Measurements were conducted on well-watered (WW) and water-stressed (WS) potted plants in fully expanded leaves of 3rd-4th position from the shoot apex during 10.00-10.30 h. Data are mean ± SD (n=4). Values with different letters indicate significant difference (P<0.05). Significant treatment (T) and time (T_m) interactions are indicated by * (P< 0.05).

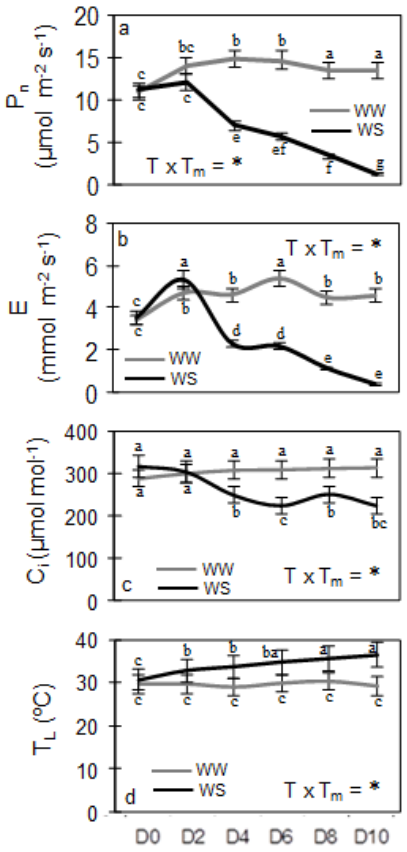

Fig. 4.5 Effect of progressive drought stress on leaf gas exchange characteristics: (a) net CO_2 fixation rate (P_n), (b) transpiration rate (E), (c) intercellular CO_2 concentration (C_i), and (d) leaf temperature (T_L) in mulberry genotype K2 (*M. indica* L.) grown in glasshouse conditions. Measurements were conducted on well-watered (WW) and water-stressed (WS) potted plants in fully expanded leaves of 3rd-4th position from the shoot apex during 10.00-10.30 h. Data are mean ± SD (n=4). Values with different letters indicate significant difference (P<0.05). Significant treatment (T) and time (T_m) interactions are indicated by * (P< 0.05).

4.4b). A similar trend of increase was also recorded in E of well-watered V1 plants with gradual increment in time and finally on D10, the recorded E value was ~5.6 mmol m^{-2} s^{-1}. However, in water-stressed V1 plants, E decreased remarkably from D4 to D10 and a reduction of 32.2%, 57.3%, 71.3% and 82.2% was recorded on D4, D6, D8 and D10, respectively in compared to corresponding controls (**Fig. 4.4c**). In water-stressed K2, E decreased significantly from D4 onwards and showed almost ~80% reduction on D10 when compared to the corresponding controls (**Fig. 4.5b**). Unlike P_n, G_s and E, the WUE_i of water-stressed V1 plants was 26.2%, 27.3% and 25.8% more on D6, D8 and D10, respectively when compared to the corresponding controls (**Fig. 4.4d**). Progressive drought stress caused significant reduction in C_i; however, the magnitude of decrease was not so apparent as it was evident with P_n, G_s and E. In drought-stressed V1 plants, C_i values declined by 23.5%, 29.6% and 34.7% on D6, D8 and D10, respectively in compared to corresponding controls (**Fig. 4.4e**). In water-stressed K2 plants a similar trend of reduction in C_i was recorded and the value decreased to ~30% on D10 in compared to corresponding controls (**Fig. 4.5c**). With advancement in drought stress intensity, a moderate but gradual rise in T_L was recorded in water-limited V1 plants more, apparently from D4 to D10. On D4 and D10, the recorded T_L in drought-stressed leaves were 32.5°C and 33.8°C, respectively, whereas in corresponding controls, T_L value was approximately maintained around 28.4°C between D0 to D10 (**Fig. 4.4f**). Rise in T_L was much higher in drought-stressed K2 leaves and the value reached to ~38.4ºC on D10, however, the control plants maintained T_L of ~30.5ºC throughout the study period (**Fig. 4.5d**). Overall, the experimental data on photosynthetic leaf gas exchange traits and T_L showed significant T x T_m interaction.

Chl a fluorescence transients: normalizations and subtraction of transients

In **Fig. 4.6a**, a comparison is made among the raw OJIP transients measured on periodic day intervals (D0, D2, D4, D6, D8 and D10) in drought-stressed V1 plants. Drought imposition induced significant variations in the shape of the transients obtained on respective sampling dates attributed to different pattern of F_t over the OJIP phases recorded at different time intervals (50µs to 1s). On D0, the F_t of the dark-adapted mulberry plants exhibited a typical OJIP transient with F_O of ~269 a.u., F_M of ~1556 a.u. and the variable

fluorescence (F_V) of ~1287 a.u. On D2, a slight increase in F_O was recorded, whereas the later part of JI and IP lost amplitude when compared to D0. On D4, the recorded F_t was also slightly higher at F_O, the amplitude rise was marginally lost in the later JI phase, however, the IP remained nearly unaffected. The recorded F_O on D6 was comparatively higher than D0, whereas the J-P steps lost amplitude when compared to D2 and D4. On D8, F_O still remained higher than compared to D0, the OJ rise gained amplitude in the later phase and was also higher in the initial JI phase, whereas fluorescence rise was low at the IP phase when compared to D0. The transient fluorescence rise recorded on D10, had highest F_O and exhibited significant attenuation over initial part of OI and later part of JI phase when compared to previous sampling dates, however, fluorescence rise was slightly delayed in the IP phase when compared to D0. In **Fig. 4.7a**, the raw OJIP transients measured on periodic day intervals in water-stressed K2 leaves were represented. Progressive drought caused significant rise in F_O, the OJ phase gained amplitude and the fluorescence rise was also higher in JI and IP phases during D2-D10 when compared to D0. To reveal detailed changes in the fluorescence kinetics in drought-stressed V1, the normalized OJIP transients between F_O to F_M (V_{OP}) are presented in **Fig. 4.6b**. The V_{OP} of WS plants as recorded on D2 and D4, exhibited marginal changes with respect to D0, however, on D6 and D8, V_{OP} was significantly altered and the fluorescence rise was faster from 1 to 10 ms covering part of the single (STP) and multiple (MTP) turn over phases. On D10, V_{OP} was slightly elevated in the beginning of the MTP, and then came down moving close with the V_{OP} of D0, D2 and D4 and thereafter again showed elevation in the later JI phase (**Fig. 4.6b**). To further elucidate the differences in fluorescence kinetics, subsequent normalizations and subtractions were carried out. The difference in chl fluorescence recorded in water-stressed V1 and K2 plants among the periodic day intervals normalized to single turnover region between 50 to 300 µs (V_{OK}) is compared in **Fig. 4.6c** and **4.7b**, respectively. The resulting kinetic difference of V_{OK} (ΔV_{OK}) was obtained as periodic differences as follows: [V_{OK} D2 - V_{OK} D0] = ΔV_{OK} D2, [V_{OK} D4 - V_{OK} D2] = ΔV_{OK} D4, [V_{OK} D6 - V_{OK} D4] = ΔV_{OK} D6, [V_{OK} D8 - V_{OK} D6] = ΔV_{OK} D8 and [V_{OK} D10 - V_{OK} D8] = ΔV_{OK} D10 (**Fig.4.6d and 4.7c**). In water-stressed V1 leaves, on D2, D4 and D6, there was marginal effect of drought on the so-called L-band as evident by the slightly higher positive peak at 0.15 ms. However, on D10, the appeared L-band showed significant

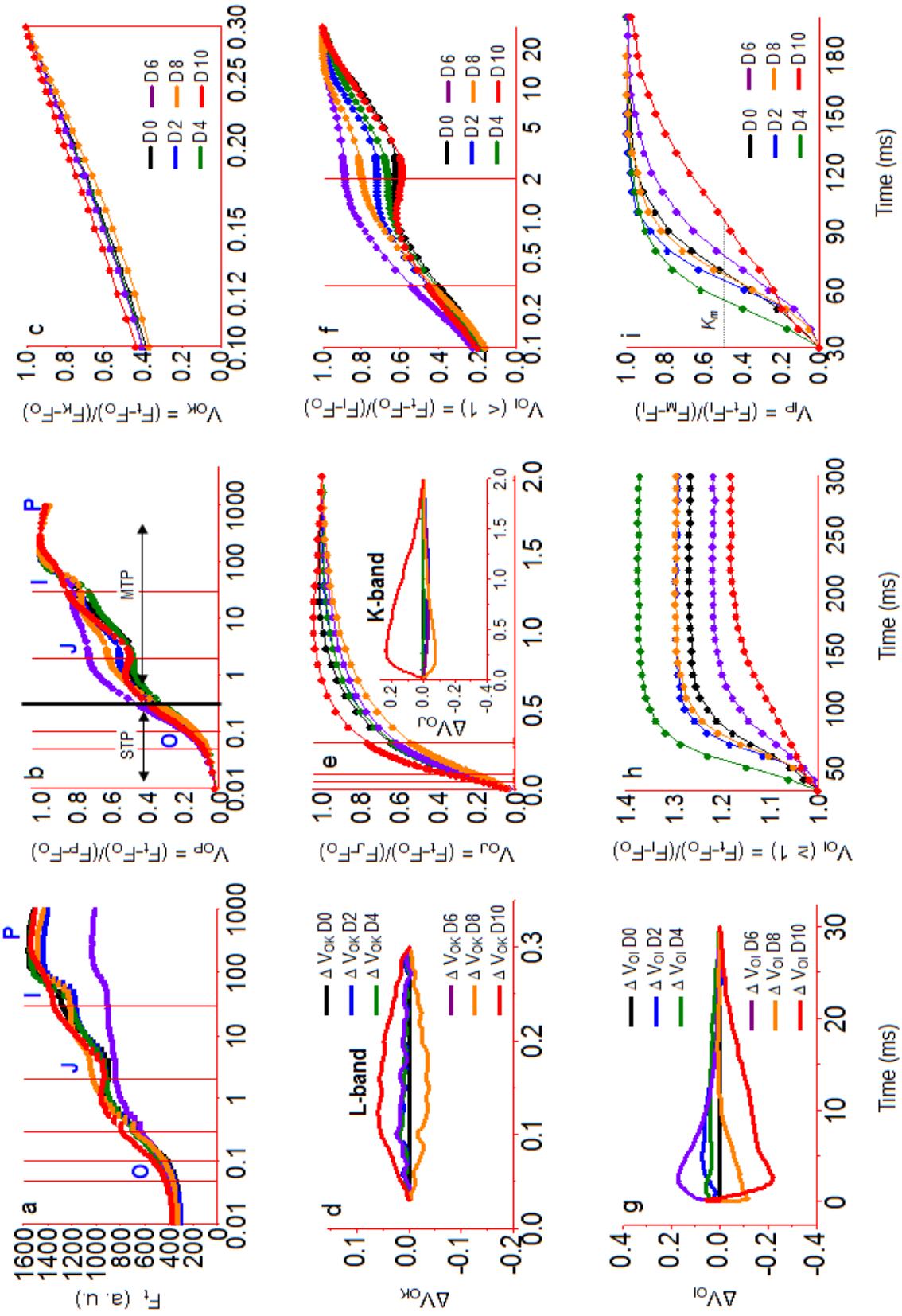
a
b
c
d
e
f
g
h
i
D0
D2
D4
D6
D8
D10
O
J
I
P
STP
MTP
L-band
K-band
Time (ms)

Fig. 4.6 The OJIP chl a fluorescence transients (log time scale) recorded in dark-adapted mulberry genotype V1 (*M. indica* L.) under progressive drought stress conditions. (a) Raw chl a fluorescence transient curves exhibiting fluorescence intensity (F_t) recorded between 0.1 to 1000 ms time period (a. u. = arbitrary unit). (b) Chl a fluorescence transients double normalized between the two fluorescence extreme O (F_O) and P (F_M) phases: $V_{OP} = (F_t-F_O)/(F_P-F_O)$. Arrows indicate the position of the single (STP) and multiple (MTP) turnover phases. (c) Chl a fluorescence transients double normalized between F_O and F_K phases: $V_{OK} = (F_t-F_O)/(F_K-F_O)$. (d) Kinetic difference of V_{OK} [$\Delta V_{OK} = (F_t-F_O)/(F_K-F_O)$] showing L - band (0.15 ms) was obtained as periodic differences as follows: [$V_{OK}D2 - V_{OK}D0$] = blue, [$V_{OK}D4 - V_{OK}D2$] = green, [$V_{OK}D6 - V_{OK}D4$] = purple, [$V_{OK}D8 - V_{OK}D6$] = orange, and [$V_{OK}D10 - V_{OK}D8$] = red. The black line represents the reference line for the D0 situation [$V_{OK}D0 - V_{OK}D0$]. (e) Variable fluorescence transients double normalized between F_O and F_J phases: $V_{OJ} = (F_t-F_O)/(F_J-F_O)$. In inset, kinetic difference of V_{OJ} [$\Delta V_{OJ} = (F_t-F_O)/(F_K-F_O)$] showing K-band was obtained as periodic differences as follows: [$V_{OJ}D2 - V_{OJ}D0$] = blue, [$V_{OJ}D4 - V_{OJ}D2$] = green, [$V_{OJ}D6 - V_{OJ}D4$] = purple, [$V_{OJ}D8 - V_{OJ}D6$] = orange, and [$V_{OJ}D10 - V_{OJ}D8$] = red. The black line represents the reference line for the D0 situation [$V_{OJ}D0 - V_{OK}D0$]. (f) Variable fluorescence transients double normalized between F_O and F_I (<1) phases: V_{OI} (<1) = $(F_t-F_O)/(F_I-F_O)$. (g) Kinetic difference of V_{OI} [$\Delta V_{OI} = (F_t-F_O)/(F_K-F_O)$] was obtained as periodic differences as follows: [$V_{OI}D2 - V_{OI}D0$] = blue, [$V_{OI}D4 - V_{OI}D2$] = green, [$V_{OI}D6 - V_{OI}D4$] = purple, [$V_{OI}D8 - V_{OI}D6$] = orange, and [$V_{OI}D10 - V_{OI}D8$] = red. The black line represents the reference line for the D0 situation [$V_{OI}D0 - V_{OI}D0$].]. (h) Variable fluorescence transients double normalized between F_O and F_I phases: V_{OI} (≥1) = $(F_t-F_O)/(F_I-F_O)$. (i) Variable fluorescence transients double normalized between F_I and F_P phases: $V_{IP} = (F_t-F_I)/(F_P-F_I)$. The horizontal dashed line at 0.5 indicates half time (K_m). All measurements were recorded on potted plants in fully expanded leaves of 3rd-4th position from the shoot apex during 11:00-11:30 h. Data are mean ± SD (n = 4).

positive peak (**Fig. 4.6d**). In water-stressed K2 leaves, there was significant effect of drought intensity on the L-band and higher positive peaks were evident at 0.15ms on D2, D4, D6 and D10 (**Fig. 4.7c**). The relative variable fluorescence normalized between 50 µs to 2 ms (V_{OJ}) for V1 and K2 genotypes are shown in **Fig. 4.6e** and **Fig. 4.7d**, respectively to elucidate changes in V_{OJ} under drought stress progression. The kinetic difference of V_{OJ} (ΔV_{OJ}) in water-stressed V1 plants on different sampling dates presented in **Fig. 4.6e** (inset) was calculated in a similar way to ΔV_{OK}. These allowed us to visualize and assess the so-called K-band which appeared as a peak between 0.25 to 0.30 ms. On D2, D4, D6 and D8, the appeared K-bands in drought-stressed V1 showed negative deviations and a positive peak was recorded only on D10. However, in drought-stressed K2, the K-band appeared and showed significant positive deviations on D2, D4, D6 and D10 (**Fig. 4.7e**). The fluorescence data normalized between 50 µs to 1s expressed as V_{OI} (<1) differed significantly among the periodic time intervals in water-stressed V1 (**Fig. 4.6f**) and the kinetic difference of V_{OI} (ΔV_{OI}: calculated in a similar way to ΔV_{OK}) showed positive deviation on D2, D4 and D6, whereas on D8 and D10, the deviation was negative (**Fig. 4.6g**). Similar trend of changes in V_{OI} and ΔV_{OI} were also recorded in drought-stressed K2 under progressive water deficit (thus data not shown). In water-stressed V1 plants, the recorded V_{OI} (≥1) on D2, D4 and D8 were higher, whereas on D6 and D10, V_{OI} (≥1) was

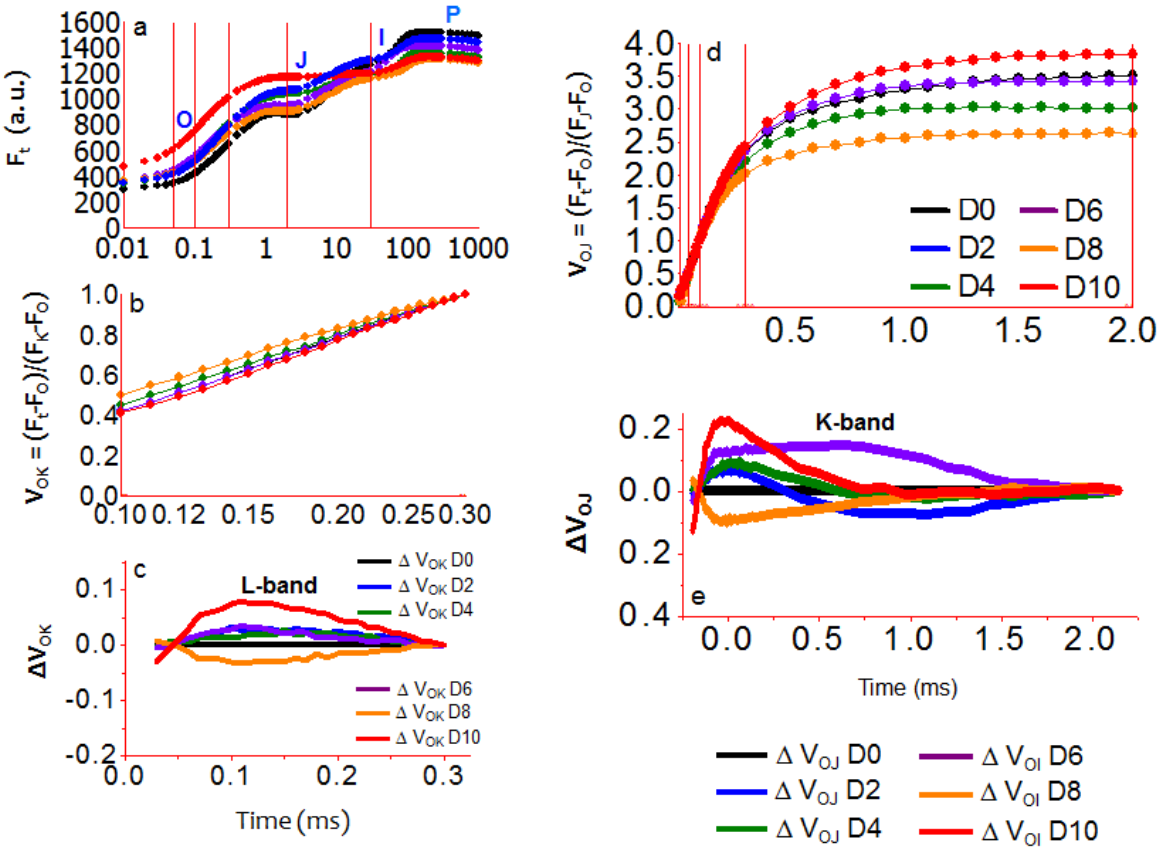

Fig. 4.7 The OJIP chl a fluorescence transients (log time scale) recorded in dark-adapted mulberry genotype K2 (*M. indica* L.) under progressive drought stress conditions. (a) Raw chl a fluorescence transient curves exhibiting fluorescence intensity (F_t) recorded between 0.1 to 1000 ms time period (a. u. = arbitrary unit). (b) Chl a fluorescence transients double normalized between F_O and F_K phases: $V_{OK} = (F_t-F_O)/(F_K-F_O)$. (c) Kinetic difference of V_{OK} [$\Delta V_{OK} = (F_t-F_O)/(F_K-F_O)$] showing L - band (0.15 ms) was obtained as periodic differences as follows: [V_{OK}D2 - V_{OK}D0] = blue, [V_{OK}D4 - V_{OK}D2] = green, [V_{OK}D6 - V_{OK}D4] = purple, [V_{OK}D8 - V_{OK}D6] = orange, and [V_{OK}D10 - V_{OK}D8] = red. The black line represents the reference line for the D0 situation [V_{OK}D0 - V_{OK}D0]. (d) Variable fluorescence transients double normalized between F_O and F_J phases: $V_{OJ} = (F_t-F_O)/(F_J-F_O)$. (e) Kinetic difference of V_{OJ} [$\Delta V_{OJ} = (F_t-F_O)/(F_K-F_O)$] showing K-band was obtained as periodic differences as follows: [V_{OJ}D2 - V_{OJ}D0] = blue, [V_{OJ}D4 - V_{OJ}D2] = green, [V_{OJ}D6 - V_{OJ}D4] = purple, [V_{OJ}D8 - V_{OJ}D6] = orange, and [V_{OJ}D10 - V_{OJ}D8] = red. The black line represents the reference line for the D0 situation [V_{OJ}D0 - V_{OK}D0]. All measurements were recorded on potted plants in fully expanded leaves of 3rd-4th position from the shoot apex during 11:00-11:30 h. Data are mean ± SD (n = 4).

significantly low when compared to D0 (**Fig. 4.6h**). The data plot of V_{IP} at the time interval of 30-200 ms showed hyperbolic pattern and by applying the Michaelis-Menten equation, the K_m was calculated (data not shown) for which the highest value was recorded on D10 (**Fig. 4.6i**). Similar changes were also observed in V_{OI} and V_{IP} of water-stressed K2 under progressive drought stress (thus data not shown).

Chl a fluorescence transients: PSII biophysical parameters derived from JIP test

To understand how progressive drought can alter energy flow in PSII of mulberry, detailed analyses of PSII biophysical parameter were undertaken. However, for this study, drought tolerant V1 was selected as a representative genotype to show the general trend of photoacclimation in mulberry leaves under progressive water deficit. Drought-induced changes in biophysical parameters in water-stressed V1 leaves derived from the transient fluorescence curves and JIP-test are presented as radar plot in **Fig. 4.8**. All the data of fluorescence parameters were normalized to reference D0 and each variable at reference D0 was standardized by giving a numeric value of 1. The M_O (a parameter expressing rate of accumulation of closed reaction centers) exhibited significant increment under progressive drought stress over the time period of D4 to D10 when compared to D0 and D2. The variable fluorescence at step J (V_J) increased significantly due to drought and was highest on D6. The V_I, which designates the variable fluorescence at step I, showed no apparent change between D0 to D8, however, on D10, V_I was highest exhibiting ~22.4% increase (significant at $P<0.05$) in compared to D0 (**Fig. 4.8**). There was no significant difference in maximum quantum yield of primary photochemistry ($\varphi_{Po} = TR_O/ABS = F_V/F_M$) on D0, D2 and D4. However, on D6, φ_{Po} was slightly decreased to ~9.6% but between D6 to D10 the φ_{Po} values remained comparatively higher in respect to D6. The multiple turnover Q_A reduction events or in other way the pool size of electron carriers (S_M) decreased marginally under progressive drought from D2 to D10 to an extent of ~7.2% with respect to D0. Similar trend was recorded in N (number of Q_A redox turnover until F_M) where the values progressively decreased with increasing drought stress. The K_N (sum of non-photochemical rate constant) remained significantly high under progressive drought and exhibited the highest increment of 26% on D6 in compared to D0. The K_P

(sum of photochemical rate constant) was significantly low under water deprivation and finally on D10, the value decreased to ~26.4% with respect to D0.

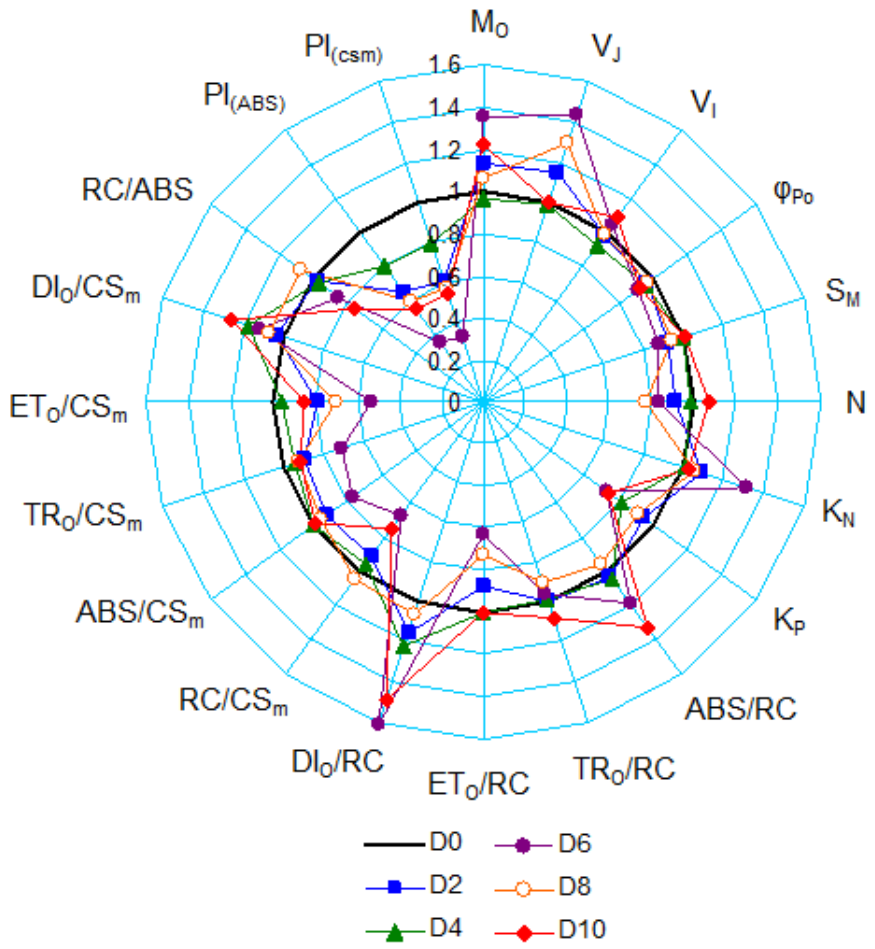

Fig. 4.8 Radar plot depicting changes in chl a fluorescence transient parameters in dark-adapted mulberry genotype V1 (*M. indica* L.) under progressive drought stress conditions. All the parameters are deduced from the OJIP-test analysis conducted on potted plants in fully expanded leaves of 3rd-4th position from the shoot apex during 11:00-11:30 h. (See Table 4.2 for the meaning of the symbols and the parameters). Data are mean ± SD (n = 4).

The ABS/RC (absorption flux per reaction center) was significantly high on the days of progressive drought and the value reached to its maximum on D10 exhibiting ~24%

increment with respect to D0. TR_O/RC was slightly decreased due to drought but deviations within the sampling dates did not exhibit significant changes, whereas ET_O/RC showed marked decrease under drought stress. Progressive drought stress significantly enhanced DI_O/RC (dissipated energy flux per reaction center) and the highest value was recorded on D6 followed by D10. Drought stress significantly ($P<0.05$) reduced RC/CS_m exhibiting 33.9 and 25.8% reductions in the recorded values on D6 and D10, respectively. The ABS/CS_m was generally not much altered under progressive drought conditions except only on D6 when a reduction of ~23% was recorded in ABS/CS_m when compared to D0. The TR_O/CS_m and ET_O/CS_m showed similar trend exhibiting significant ($P<0.05$) decrease upon progressive drought exposure. The DI_O/CS_m was substantially higher throughout the period of progressive drought over D2 to D10 and the highest DI_O/CS_m value was recorded on D10 with an increment of 20% in respect to D0. The RC/ABS was decreased due to drought exposure and on D10 a maximum reduction of ~24.8% was recorded in RC/ABS with respect to D0. Significant changes occurred in the performance indexes including $PI_{(ABS)}$ and $PI_{(csm)}$ under progressive drought stress. In compared to D0, on D10 there were ~45.2 and ~46% decrease in $PI_{(ABS)}$ and $PI_{(csm)}$, respectively.

Chl pigments and contents

The contents of chl pigments differed significantly among the sampling dates (from D0 to D10) under progressive drought conditions. In V1 leaves, chl a content did not change significantly until D2, however, showed apparent reduction in the subsequent days and finally was reduced to ~43.7% on D10 when compared to D0 (**Table 4.4**). However, water-stressed K2 plants showed significant reduction in chl a content from D2 to D10 and was finally reduced to ~54.9% on D10 when compared to D0. Like chl a, a similar trend of decrease was also recorded in chl b which was apparent from D4 to D10 in V1 and nearly ~48% decrease in chl b content was recorded on D10 when compared to D0. The content of chl b was significantly affected in K2 under progressive water stress and was nearly ~64.2% decreased on D10 when compared to D0. Total chl content was significantly reduced to ~45.6% and ~55% on D10 in V1 and K2, respectively in compared to D0 (**Table 4.4**).

Table 4.4 Changes in chlorophyll a, chlorophyll b and total chlorophyll contents in mulberry genotype V1 and K2 during progressive water stress. Young, fully expanded leaves of the 3rd - 4th position from the apical branches were used to determine the pigments. Values are means ± SD (n = 4). Values with different letters in a single column indicate significant difference (P< 0.05).

	V1			K2		
	Chlorophyll a (µg cm^{-2})	Chlorophyll b (µg cm^{-2})	Total chlorophyll (µg cm^{-2})	Chlorophyll a (µg cm^{-2})	Chlorophyll b (µg cm^{-2})	Total chlorophyll (µg cm^{-2})
D0	12.8 ± 0.10^{a}	5.2 ± 0.12^{a}	18.1 ± 0.15^{a}	10.2 ± 0.20^{a}	4.2 ± 0.07^{a}	14.6 ± 0.13^{a}
D2	12.5 ± 0.09^{a}	5.1 ± 0.08^{a}	17.5 ± 0.10^{b}	9.4 ± 0.08^{b}	3.3 ± 0.14^{b}	12.9 ± 0.11^{b}
D4	9.5 ± 0.08^{b}	3.9 ± 0.09^{b}	13.4 ± 0.08^{c}	7.3 ± 0.12^{c}	3.0 ± 0.09^{b}	10.8 ± 0.09^{c}
D6	8.2 ± 0.10^{bc}	3.5 ± 0.11^{bc}	11.6 ± 0.12^{cd}	6.2 ± 0.13^{d}	2.6 ± 0.07^{c}	9.0 ± 0.12^{d}
D8	7.6 ± 0.11^{c}	3.2 ± 0.12^{bc}	10.7 ± 0.14^{d}	5.4 ± 0.11^{e}	2.2 ± 0.09^{c}	7.7 ± 0.09^{e}
D10	7.2 ± 0.09^{c}	2.7 ± 0.08^{c}	9.8 ± 0.10^{e}	4.6 ± 0.09^{f}	1.5 ± 0.12^{d}	6.5 ± 0.09^{f}

Leaf protein expression profiles and identification of drought-induced proteins

To understand how long-term drought can induce changes in leaf protein expression profile and to know which proteins are playing significant roles in photoprotection and photoacclimation in water-stressed mulberry, 2D-GE of total soluble leaf protein was undertaken on D10. For this study, drought tolerant V1 was selected as a representative genotype to show the general trend of photoacclimation in mulberry leaves under prolonged water deficit. In the protein profiles of three independent replicates of WW and WS samples, more than 300 spots were reproducibly detected in colloidal coomassie stained control gels over a pH range of 4 to 7 and molecular weight range of 16 to 97.4 kDa. Upon image analysis of the representative standard gels, it was observed that under stress conditions, nearly half (46%) of the protein spots which were present under WW conditions disappeared or were highly down-regulated (could not be detected with colloidal coomassie staining) upon 10 days of water withholding. Nearly 21% of the protein spots were significantly down-regulated in their expression levels while 24% remained statistically unchanged and only 9% of the detected spots showed significant up-regulation in their expression patterns during WS conditions (**Fig. 4.9**). Twelve major and well-isolated (not in aggregated spot complex) protein spots showing more than 1.5 fold up-regulation were subjected to MALDI analysis and among them 9 proteins were successfully identify while the rest three showed no significant hits in the database. The representative 2D gels for control (WW) and water stress (WS) treatments indicating the 9

up-regulated spots are shown in **Fig. 4.10(a,b)**. For better visualization of the modulation in the expression patterns under WW and WS conditions, a few identified spots are magnified (**Fig. 4.10c**). The relative up-regulation of an identified spot was analyzed based on the corresponding induction factor (IF) which was calculated as the ratio of the relative spot volume (RSV) of that particular protein spot from the WW-sample gels to the corresponding RSV of the same spot from WS-sample gels. Respective RSV and IF of the 9 identified proteins during WW and WS conditions are shown in **Fig. 4.10d** and **e**, respectively. Protein identification of the 9 up-regulated spots was performed based on their mass signals using an algorithm based homology search with protein databases such as NCBInr and SwissProt through MASCOT search engine. Interestingly, most of the identified drought-induced leaf proteins were found to be photosynthesis related.

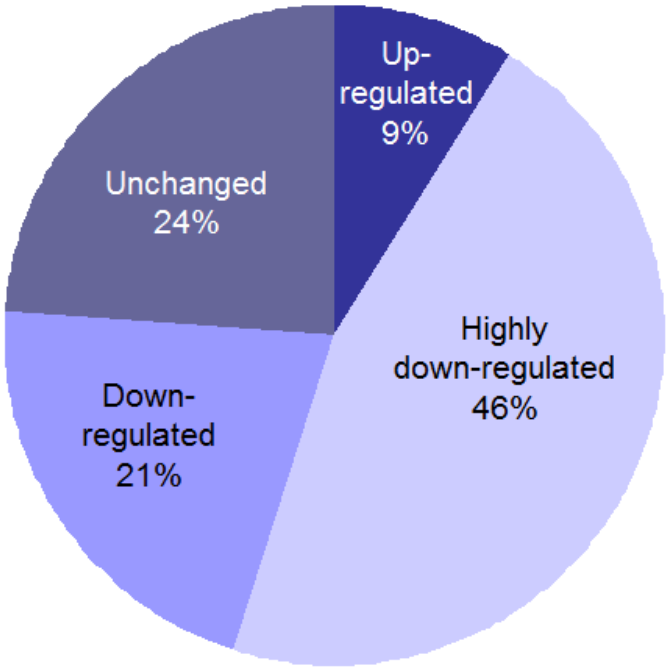

Fig. 4.9 Pie diagram representing the percentage distribution of up-regulated, unchanged, down-regulated and highly down-regulated leaf protein spots in mulberry genotype V1 (*M. indica* L.) on D10 of water withholding.

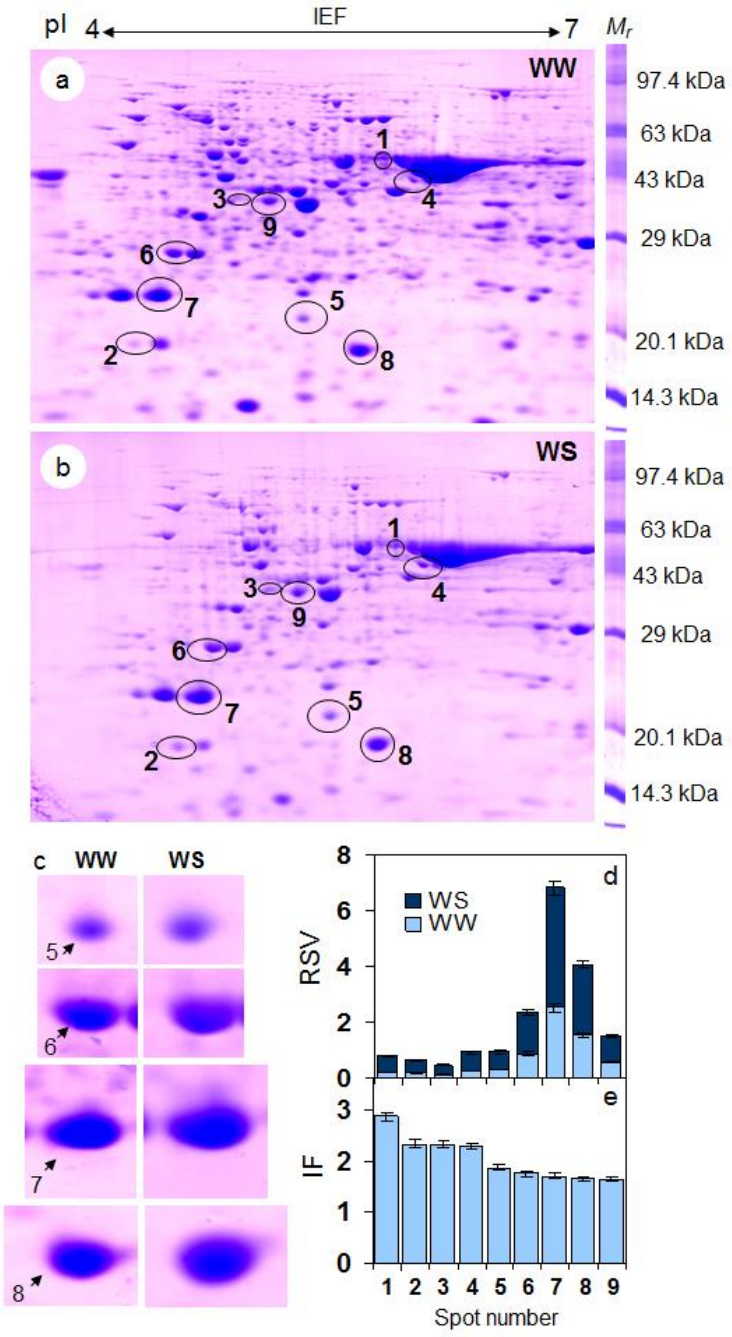

Fig. 4.10 Colloidal Coomassie-stained 2-D gels of proteins extracted from mulberry genotype V1 (*M. indica* L.) leaves on D10 of water withholding. Comparative leaf protein expression pattern is shown from (a) well-watered (WW) and (b) water-stressed (WS) conditions. For each 2D-gel, 600 µg of protein was loaded on 18 cm IPG strip with a linear gradient of pH 4-7 and 12% SDS-PAGE gels were used for the second dimension. The spot numbering shown in the 2-D gels corresponds to the spot numbers given in Table 4.5 (c) Enlarged view of the expression patterns of few spots under WW and WS conditions. (d) Relative spot volume (RSV) for each spot expressed as % spot volume indicating the normalized values of the ratio of the individual spot to the total volume of all the spots in the gel and (e) their corresponding induction factor (WS spot intensity/ WW spot intensity).

Rubisco large subunit (spot 1) exhibited the maximum IF (2.8 fold) upon WS treatment. Both the isoforms (longer and shorter) of rubisco activase (spot 3 and 9, respectively) were also found to be up-regulated under WS conditions. However, the longer isoform (also known as the α-isoform) showed comparatively higher induction level (2.3 fold) than its shorter (β-isoform) counterpart which showed only 1.6 fold up-regulation. Enhancement in the expression levels of the 33 kDa as well as 23 kDa subunit of the oxygen evolving enhancer (OEE) protein (spot 6 and 8, respectively), which were known to be associated with water-splitting complex were also observed where the former showed 1.7 fold and the latter 1.6 fold up-regulation, respectively. Moreover, two different chl a/b binding proteins (spot 5 and 7) also enhanced their expression levels (1.8 and 1.7 fold, respectively) under WS when compared to WW conditions. Apart from the above mentioned chloroplast proteins, two important drought-responsive proteins including peroxiredoxin (spot 2) and NADPH-ubiquinone oxidoreductase (spot 4) were also found to be significantly induced upon WS conditions when compared to WW plants and both exhibited an IF of 2.3 fold. The details of the 9 identified proteins with their respective accession numbers, reference organism, observed as well as theoretical molecular weight (Mr) and isoelectric points (pI), the peptide sequences matched, peptide masses, MS/MS and the scores sequence coverage (%) are given in **Table 4.5**.

Expression of MIPIP1.3 under progressive drought

To characterize the expression patterns of MIPIP1.3 genes in mulberry genotypes under progressive drought stress, mRNA expression patterns were analyzed using RT-PCR. Using primers based on MIPIP1.3 EST sequence available at NCBI gene bank (gi|171461474|gb|ES448991|), a 369 bp fragment of MIPIP1.3 was amplified from leaf and root cDNA and sequenced (**Fig. 4.11a**). Deduced sequence was compared with the existing MIPIP1.3 sequence for confirmation of the identity of the gene which showed 100% sequence similarity (**Fig. 4.11b**). In V1 leaves that experienced severe drought stress on D6 (57.4% leaf RWC) and D10 (32.8% leaf RWC), exhibited approximately 1.5 and 2.2 fold ($P<0.001$) increase in the expression level of MIPIP1.3 transcript, respectively when compared to D0 (82.2% leaf RWC) (**Fig. 4.12a**).

Table 4.5 Drought-induced proteins in mulberry (*M. indica* L; genotype V1) identified by MALDI-TOF-TOF. [a]Protein spot IDs as denoted in Fig. 4.10 [b]Protein identification (protein ID [reference organisms], accession no. and matched peptide sequences) was performed by database searches using MASCOT software (www.matrixscience.com) from NCBInr, Swiss Prot and EST databases. Molecular weight (Mr, expressed in Kilodalton) and isoelectric point (pI) of the identified proteins as [c]observed on the gel and on [d]theoretical basis. [f]MASCOT protein score from the MALDI-TOF-TOF analysis ([a] stands for statistically significant results at P<0.05). [g]Sequence coverage (SC) percentage.

Spot ID[a]	Protein identified [reference organism][b]	Accession no.[b]	Peptide sequences matched[b]	Observed Mr/pI on the gel[c]	Theoretical Mr/pI[d]	Peptide mass[e]	MS/MS score[f]	SC (%)[g]
1	RuBisCO large subunit [Dendrobium taurinum]	gi/1000936	TFQGPPHGIQVQR ELTLGFVDLLR	55/5.8	42/6.6	1465.2 1275.3	94[a]	6.3
2	Peroxiredoxin [Phaseolus vulgaris]	gi/11558242	GLFIIDKEGVIQHSTINNLAIGR	25/4.5	28.6/5.2	2508.5	171[a]	8.8
3	RuBisCO activase [Nicotiana tabacum]	gi/19988	IGVCTGIFR GLAYDISDDQQDITR FYWAPTR LLEYGNMLVQEQENVKR FYWAPTREDR	43/5.1	23/4.8	1022.6 1709.5 940 2062.9 1340.4	118[a]	17.4
4	NADH ubiquinone oxidoreductase chain 4 [Triticum aestivum]	gi/14255	VPMVPVHIWLPEAHVEAPTAGSVILAGIL LK	48/6	55.4/9.0	3273.8	68[a]	6.3
5	Type III chlorophyll a/b binding protein[Lycoris aurea]	gi/116519121	QYFLGFEK WLAYGEVINGR QGMFVIPFMTR	26/5.4	29.7/8.6	1031.4 1277.3 1358.4	80[a]	10.9
6	Oxygen evolving enhancer protein 1 (33kda subunit) [Nicotiana tabacum]	gi/11134054	QLVASGKPESFSGEFLVPSYR	33/ 4.7	35.2/5.9	2298.3	64[a]	6.3
7	Chlorophyll a/b binding protein [Pisum sativum]	gi/115788	NRELEVIHSR VASSGSPWYGPDR SAPQSIWYGPDRPK WAMLGALGCVFPELLSR	27/4.6	28.6/5.5	1252.4 1378.3 1601.3 1919.6	89[a]	20.0
8	Oxygen evolving enhancer protein 2 (23 kDa subunit) [Sinapis alba]	gi/131391	EVEYPGQVLR QYYFLSVLTR	23/ 5.7	27.9/6.8	1189.3 1289.2	88[a]	7.7
9	RuBisCO activase [Olea europaea]	gi/154259484	IVDSFPGQSIDFFGALR VPIIVTGNDFSTLYAPLIR	42/5.2	28.7/4.9	1868.6 2089.0	91[a]	13.8

In contrast to V1, genotype K2 did not show any significant increase in leaf-level MIPIP1.3 expression on D6 of water withholding when compared to D0. However, when the K2 plants experienced acute drought stress on D10 (25.4% leaf RWC), transcript level of MIPIP1.3 was significantly ($P<0.001$) increased in drought-stressed leaves to approximately 1.8 fold (**Fig. 4.12b**). Genotype V1 and K2 also significantly differed in root-level MIP1P1.3 expression response under progressive water stress. There was an approximately 4.2 fold increase in root-level MIPIP1.3 expression in drought-stressed V1 on D6 when compared to D0 and the relative expression was almost similar even on D10 when compared to D0 (**Fig. 4.12c**). In contrast to V1, genotype K2 did not show any increase in MIPIP1.3 expression on D6 and D10 of water withholding. Rather, there was an approximately 0.8 fold ($P<0.001$) decrease in root-level MIPIP1.3 expression on D6 and almost same fold of decrease was recorded even on D10 (**Fig. 4.12d**).

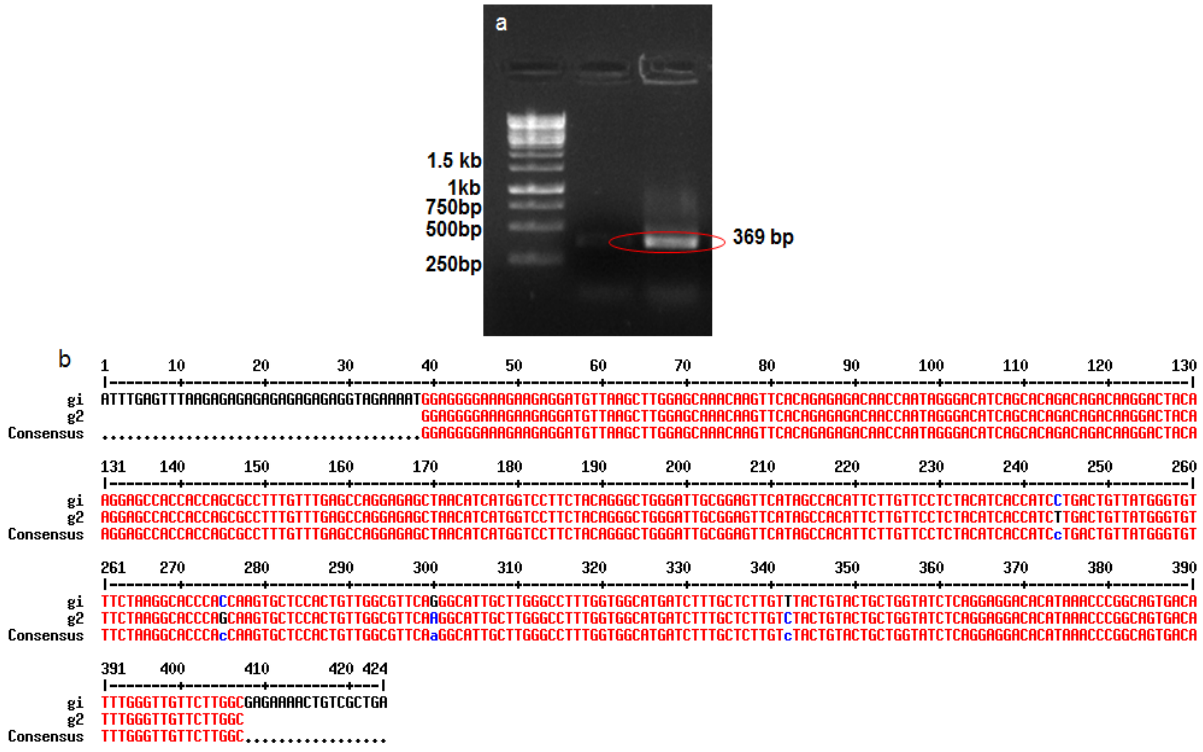

Fig. 4.11 (a) PCR amplified 369 bp fragment of MIPIP1.3 gene from *M. indica* L. (genotype V1) leaf; (b) multiple alignment of the obtained MIPIP1.3 sequence with the available EST sequence of *M. indica* L. (genotype K2) MIPIP1.3, showing 100% sequence similarity.

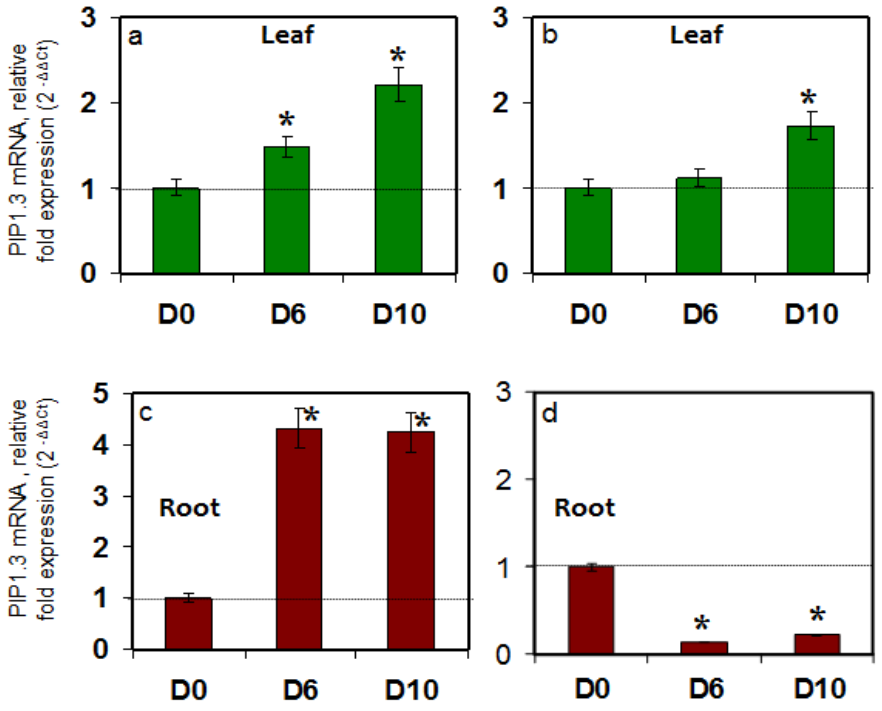

Fig 4.12 Changes in transcript level modulations in MIPIP1.3 in leaf and root tissue of the drought tolerant V1 (a and c, respectively) and drought susceptible K2 (b and d, respectively) mulberry genotypes. Values represents mean ± SD with n=3. P* <0.001 indicate significant difference (one way ANOVA).

Micromorphological, anatomical and morphological characteristics

In order to understand the contribution of in-built morpho-anatomical set-up that could probably add to drought stress tolerance, we studied several leaf, stem and root-level traits in the two compared mulberry genotypes (V1 and K2) differing widely in their response to water stress. Samples were taken from the drought stressed plants and analyzed for their innate anatomical differences. The findings are summarized in **Table 4.6**. The number of stomata per unit area of leaf was higher in V1 when compared to K2 (**Fig. 4.13a,b**). The average size of stomata was ~13.6×8.5µm and ~9.2×3.9 µm in V1 and K2, respectively. Transverse section of leaves of the two genotypes are compared in **Fig. 4.13 (c,d)**. Both the genotypes had a comparable internal structure, typical of a dorsi-ventral dicot leaf with easily distinguishable palisade and spongy parenchyma in the mesophyll. Adaxial epidermis was largely uniseriate except at the fringes of vasculature where it was biseriate.

In cross-section, the adaxial epidermal cells appeared as large, upright rectangular cells where they were uniseriate, while they appeared rhomboid in biseriate layers. The adaxial epidermis was devoid of stomata. The abaxial epidermis is uniseriate and its cells appear horizontally elongated or rhomboid in transverse sections. It is interrupted at irregular intervals by stomata. The palisade tissue is immediately below the adaxial epidermis. It consists of 1-2 layers of compactly packed cells, which appear tubular in cross section. The spongy parenchyma consists of smaller, circular or lobed cells loosely packed to form a well-developed system of intercellular spaces. There was significant variation in the thickness of lamina between the two genotypes. Leaf thickness was significantly more in V1 compared to K2 (**Table 4.6**). The height and thickness of palisade cells also showed marked variation between the two genotypes **(Fig. 4.13 c,d)**. While the V1 leaves had a palisade thickness of 55 µm, K2 possessed leaves with reduced palisade thickness of 32 µm. Moreover, the percentage ratio of palisade mesophyll was higher in V1 (48%) compared to K2 (35%). In both the genotypes, the vascular tissue of midrib consists of crescent shaped collateral vascular bundles. The support tissue is represented by collenchyma that is adjacent to the epidermis in both sides and to the sheath of fibers that surrounds the vascular bundle. However, maximum xylem poles were recorded in V1 in compared to K2 (**Fig. 4.13 e**). In each pole, the number of xylem vessels was on an average 6.5, whereas in K2, the number recorded was ~4.5 (**Fig. 4.13e,f**). In the secondary veins, a similar crescent shaped collateral arrangement of vascular bundles was evident in both the genotypes (**Fig. 4.13g,h**). In contrast to midrib, the number of xylem poles were more in K2, whereas their mean size was less in compared to genotype V1 (**Table 4.6**). The transverse section of petioles in both the genotypes is nearly crescent in shape, consists of collateral vascular bundles and scattered in the ground parenchyma in a circular manner (**Fig. 4.13i,j**). The mean vessel size in petiole was higher in V1 when compared to K2 (**Table 4.6**).

The general anatomy of stem was identical in the two mulberry genotypes studied. Young stems (during primary growth) had uniseriate epidermis, collenchymatous cortex, continuous cylinder of vascular tissue and large pith **(Fig. 4.14 a-d)**. The phloem width in the stem of V1 was apparently more (~360µm) with prominent layer of secondary phloem, whereas in K2, the phloem width was restricted to ~275 µm (**Fig. 4.14e,f**). The number

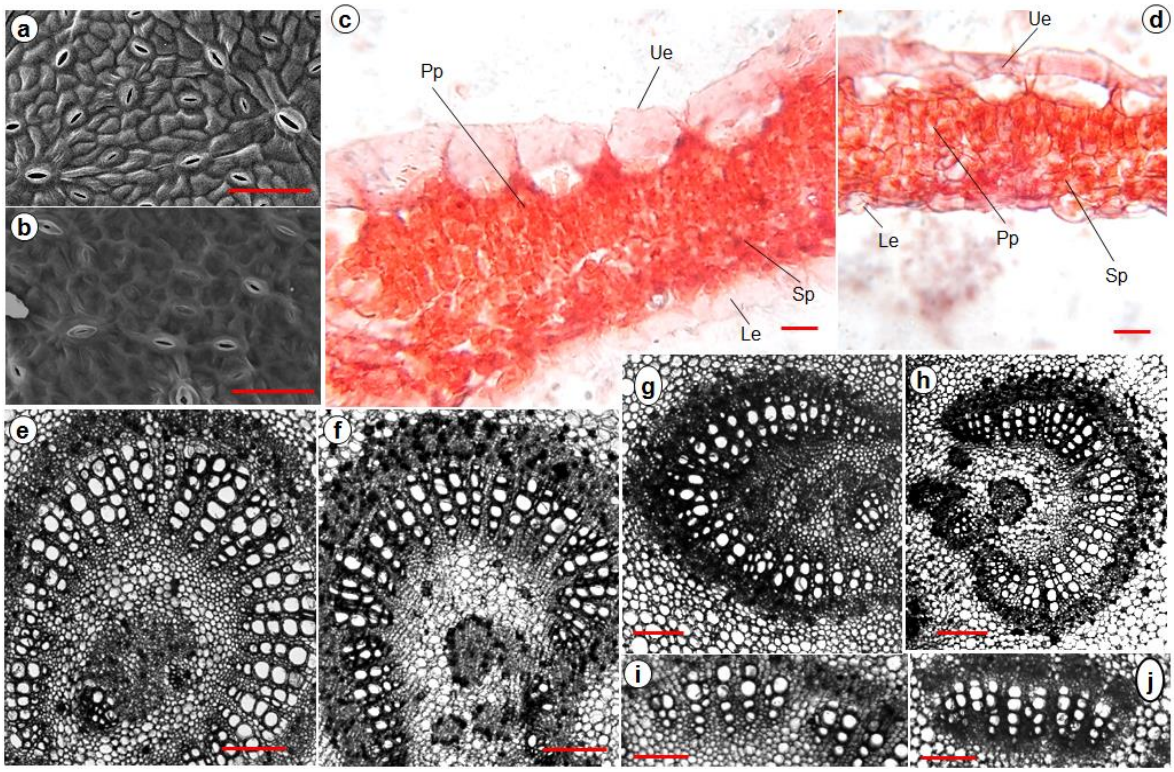

Fig. 4.13 Comaparative micromorphological and anatomical characteristics of mulberry leaf recorded in drought tolerant genotype V1 and drought susceptible genotype K2. Scanning electron micrographs of leaf samples showing stomatal distribution and size in abaxial leaf surface of mulberry genotype (a) V1 and (b) K2 (scale bar = 50 µm). Genotype V1 exhibits more no. of stomata per unit leaf area and also possesses higher stomatal size in compared to K2. Cross-sections of the leaf blade of genotype (c) V1 and (d) K2. The genotypes have a leaf cross-section of a typical dorsi-ventral dicot leaf with distinguishable palisade (Pp) and spongy parenchyma (Sp) in the mesophyll. Upper epidermis (Ue) appears as large, upright rectangular cells where they were uniseriate (V1), while they appeared rhomboid in biseriate layers (K2). Cells in the lower epidermis (Le) are smaller and are devoid of stomata. The lower epidermis is uniseriate and the cells appear horizontally elongated or rhomboid in transverse sections. The palisade tissue is immediately below the upper epidermis. It consists of 1-2 layers of compactly packed cells, which appear tubular in cross section. The spongy parenchyma consists of smaller, circular or lobed cells loosely packed to forms a well-developed system of intercellular spaces. Note the contrasting anatomical differences in respect to length, size and distribution of palisade mesophyll cells between the two genotypes. There is also significant variation in the thickness of leaf blade between the two genotypes. Leaf blade thickness is significantly more in V1 in compared to K2 (scale bar=20 µm). Leaves were stained with a 1% aqueous solution of Congo red ($C_{32}H_{22}N_6O_6S_2Na_2$ [MW:696.67]). Cross-sections of mid rib vein of genotype (e) V1 and (f) K2. The vascular tissue of midrib consists of crescent shaped collateral vascular bundles and the support tissue is collenchyma. Note the number of xylem poles in V1 and K2 (scale bar = 150 µm). Cross-sections of secondary vein of genotype (g) V1 and (h) K2 representing similar crescent shaped collateral arrangement of vascular bundles as evident in midrib. In contrast to midrib, the number of xylem poles is more in K2, whereas their mean vessel size is less in compared to genotype V1(scale bar = 200 µm). Cross-sections of petiole of genotype (i) V1 and (j) K2 showing crescent shaped collateral vascular bundles (scale bar = 100 µm). For all micromorphological anatomical measurement, 3rd – 4th positioned leaves from the tallest shoot were sampled.

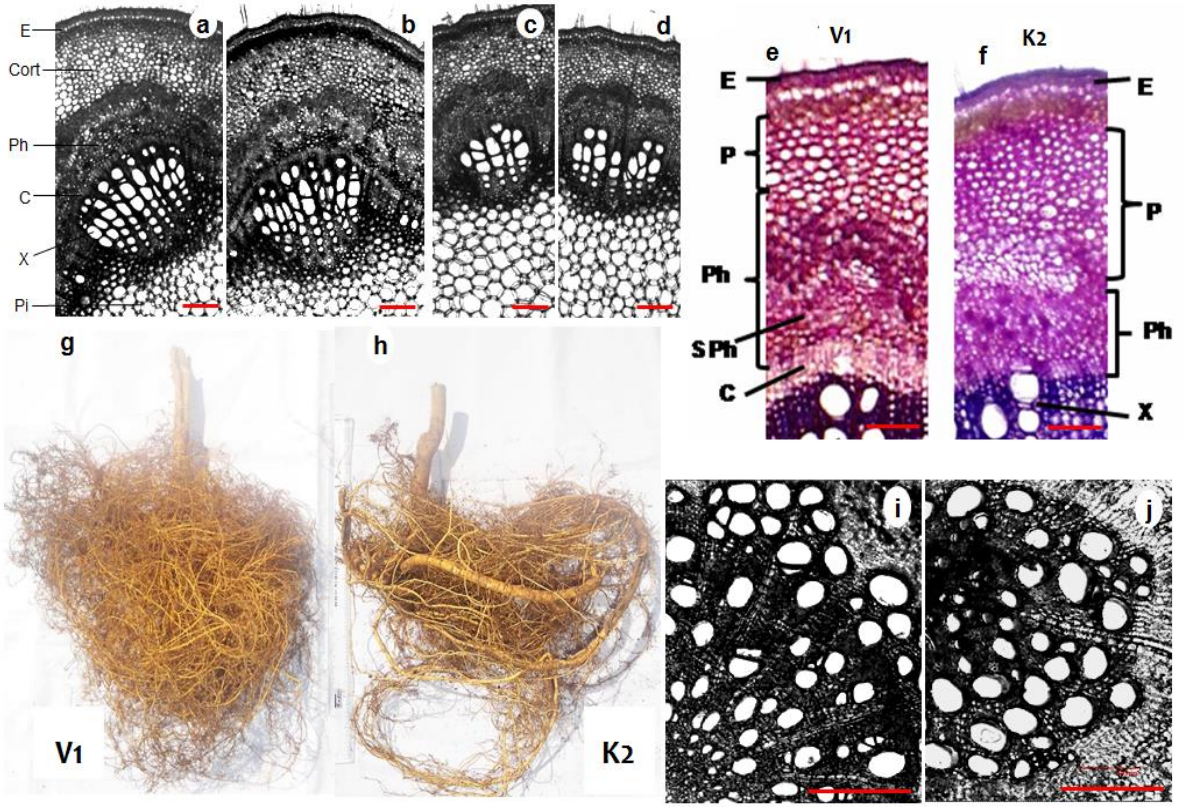

Fig. 4.14 Comaparative anatomy of mulberry stem and root tissues and general differences in root morphology recorded in drought tolerant genotype V1 and drought susceptible genotype K2. Transverse sections (T.S.) of stem portions of genotype (a,b) V1 and (c,d) K2 showing different layers of epidermis (E), cortex (Cort), parenchyma (P), phloem (Ph), secondary phloem (S Ph), cambium (C), xylem vessels (X) and pith (Pi) (scale bar = 150 µm). The general anatomy of stem is identical in the two mulberry genotypes. Young stems (during primary growth) have epidermis, collenchymatous cortex, continuous cylinder of vascular tissue and large pith. Epidermis is the outermost uniseriate layer, made of living parenchymatous tabular cells joined end to end. Epidermis is provided with multicellular hairy outgrowths. Epidermis is followed by several rows of cortex composed of oval parenchyma cells. Note the conspicuous difference in phloem width within the two genotypes (scale bar = 60 µm). The phloem width in the stem of (e) V1 is apparently more with prominent layer of secondary phloem, whereas in (f) K2, the phloem width is narrow. Vascular bundles are collateral, open, arranged in ring. Cambium is present between outer phloem and inner xylem. Xylem is endarch, metaxylem elements with larger cavities are situated towards the circumference and protoxylem elements with smaller cavities are situated towards the center. The number of xylem poles are more in V1 as well as the number of xylem vessels per pole is also higher in V1 (a, b) when compared to K2 (c,d). However, the mean vessel size is more or less similar in both the genotypes. Pith is very distinct and large, situated in the center of the stem and consists of thin-walled, oval or polygonal parenchyma cells. The black and white photographs of stem T.S. were taken using confocal microscope, whereas the T.S stained with toluidine blue (e, f) are light microscopic images. Differences in root morphology showing better rooting vigor and higher density of secondary and tertiary roots (also called feeder roots) in (g) V1 in compared to (h) K2. Such higher density of feeder roots as recorded in V1 is a crucial growth feature associated with better hydraulic conductance and drought stress tolerance. T.S. of root portions of (i) V1 and (j) K2 showing secondary growth and consisting both secondary (bigger sized) and primary (smaller sized) xylem vessels (scale bar = 100 µm). Secondary xylem is the major constituent of the secondary vascular tissues of the plant, especially the entire bulk in case of woody plants. It performs two main functions including mechanical support and conduction of water and other inorganic materials dissolved in water absorbed by roots. The T.S. of roots exhibited contrasting differences in the number of xylem vessels between the two genotypes and higher xylem vessel density was recorded in (i) V1 in compared to (j) K2. The black and white photographs of root T.S. were taken using confocal microscope.

Table 4.6 Comparative analysis of selected micromorphological, anatomical and morphological traits in two mulberry genotypes (V1 and K2). Means ±1 SE. (n=3), P<0.05.

Morpho-anatomical traits	V1	K2
Leaf		
Length of stomata (µm)	13.6±0.2	9.2±0.3
Width of stomata (µm)	8.5± 0.3	3.9±0.4
Stomatal density (no. mm^{-2})	722±15.2	540±13.4
Leaf thickness (µm)	116 ± 2.6	93 ± 4.0
Upper epidermal cell (µm)	23.2±0.4	15.3±0.3
Lower epidermal cell (µm)	13.4±0.2	8.2±0.3
Palisade parenchyma cell thickness (µm)	55 ± 6.0	32 ± 4.7
Spongy parenchyma cell thickness (µm)	15.8±0.2	10.4±0.3
% palisade tissue/leaf cross section	48 ± 4.5	35 ± 5.1
Mid rib (mid vein)		
Xylem poles/cross section	52.5±2.3	34.5±3.2
No. of xylems/pole	6.5±0.5	4.5±0.6
Vessel diameter (µm)	38.5±1.0	34.2±1.2
Secondary vein		
Xylem poles/cross section	34.5±2.2	37.5±1.5
No. of xylems/pole	3.5±0.8	4.5±1.0
Vessel diameter (µm)	30.3±2.4	26.6±1.7
Petiole		
Xylem poles/cross section	60.5±2.5	56.2±2.2
No. of xylems/pole	5.5±0.7	4.5±0.5
Vessel diameter (µm)	32.2±2.5	30.6±2.2
Stem		
Xylem poles/cross sectional group	10.5±1.5	5.5±0.9
No. of xylems/group	7.5±0.6	4.5±0.8
Vessel diameter (µm)	35.5±1.8	36.4±2.3
Phloem width of stem (µm)	360 ± 4.0	275 ± 6.5
Root		
Xylem poles/cross section	35 ± 5.8	22 ± 4.7
Root length (cm)	35 ± 5.6	38 ± 5.0
Root weight (g)	174 ± 6.8	132 ± 16.6

of xylem poles were more in V1 as well as the number of xylem vessels per pole was also higher in V1 (**Fig. 4.14 a, b**) when compared to K2 (**Fig. 4.14 c,d**). However, the mean vessel size was more or less similar in both the genotypes (**Table 4.6**). The transverse section of roots also exhibited contrasting differences in the number of xylem vessels between the two genotypes and maximum xylem poles were recorded in V1(**Fig. 4.14i**) in compared to K2 (**Fig.4.14j**). The genotypes also varied significantly in respect to root morphology and growth. Better rooting vigor was recorded in V1 with maximum root weight compared to K2. The V1 root system had more density of secondary roots with

innumerable entangled mass of tertiary roots (also called feeder roots) in compared to K2 (**Fig. 4.14g,h**).

Discussion

Progressive drought reinforced negative impact on leaf water status as exhibited by significant gradual depletion in LMC and RWC and thus one can conclude that the effects of soil drought on photosynthesis are mainly as a consequence of the higher level of dehydration of leaf tissue. The highly significant correlations observed among P_n, G_s and E suggest stomatal closure to be the primary factor responsible for reduced G_s and E, which in turn down-regulated P_n (Cornic 2000). The initial response of leaves to water stress is generally manifested by stomatal closure restricting stomatal diffusion of CO_2 coupled with a decrease in mesophyll conductance to CO_2 (internal CO_2 diffusion) which is apparently a much greater limitation during drought stress as reported recently (Medrano et al. 2002; Gomes et al. 2007). However, unlike previous report (Thimmanaik et al. 2002) on mulberry genotypes where progressive drought elevated the C_i level (an indication of mesophyll limitation), the present study on genotype V1 and K2 elucidated a progressive decline in C_i with increasing drought intensity suggesting no major involvement of mesophyll limitation to internal CO_2 diffusion (Flexas et al. 2002). The present data indicate that G_s played a strong control over P_n and stomatal closure might have largely restricted the supply of CO_2 to the site of carboxylation in drought-stressed V1 and K2 leaves. Nevertheless, a much greater reduction in P_n and G_s when compared to C_i clearly indicates that stomatal restriction to CO_2 was not the only mechanism associated with reduction of photosynthesis; rather many other photosynthetic processes might have co-limited P_n in water-stressed mulberry plants.

Chl a fluorescence technique elucidated important alterations in PSII bioenergetics and simultaneously reflected changes in many photosynthetic processes. The marginal, however, significant elevation in F_O recorded during water stress in both the genotypes might be due to several reasons including increased number of inactive RCs which could slow down the primary reduction of quinone A (Q_A) and thereby increase the fluorescence rise at F_O. It could also be due to structural damage leading to decreased excitation energy

transfer from antenna complex towards RCs, leading to increased F_O (Kalaji et al. 2011). Further, increased V_J recorded in the genotypes under water stress conditions can occur due to accumulation of the reduced Q_A (Q_A^-) pool restricting electron transport beyond Q_A^- (Haldiman et al. 1999; Redillas et al. 2011). Under drought stress such phenomenon is a typical response in higher plants where the efficiency of electron transfer towards PSI is minimized as a part of photoprotection strategy (Redillas et al. 2011). The extremes Fo and F_M were tightly associated with the conformational parameters including K_N and K_P. The reduction in F_M corresponded to the increase in non-photochemical de-excitation constant (K_N) and simultaneous decrease in photochemical de-excitation rate constant (K_P). Chl a fluorescence data double normalized between F_O and F_M (V_{OP}) further permitted us to analyze the single and multiple turn over phases for localization of other action sites of water stress in the electron transport chain. Starting with the O-J phase (represents the photochemical reduction of Q_A in PSII reaction centers), the gradual changes in fluorescence transients under progressive drought were compared for V_{OK} (between 50 to 300 µs) (**Fig. 4.6c**). The recorded marginal change in the L-band amplitude (150 µs) in water-stressed V1 till D8 suggests that the drought-stressed plants were capable to prevent dissociation of LHCII from PSII complex by virtue of which maintenance of energetic connectivity persisted (Strasser and Stirbet 1998; Oukarroum et al. 2007; Oukarroum et al. 2009). However, an attenuated L-band recorded in water-stressed K2 plants starting from the initial days of stress exposure indicates loss in energetic connectivity which might be due to its narrow threshold level of drought acclimation. The ΔV_{OJ} under progressive drought stress exhibited no positive K-band (at 300 µs) in water-stressed V1 till D8 suggesting the ability of genotype V1 to resist drought-induced imbalance between the electrons at the acceptor and donor sides of PSII. However, the accentuated K-bands recorded in K2 starting from the initial days of stress exposure might be due to the reduced efficiency of oxygen-evolving complex (OEC) resulting in an imbalance between the electron flow from the OEC to the RC and towards the PSII acceptor side in the direction of PSI (Strasser 1997; van Heerden et al. 2007). As reported earlier, elevated temperature conditions can also cause attenuation in K-band (Srivastava et al. 1997; van Heerden et al. 2007). In the present study, drought stress led to lower E and a concomitant increment in T_L was recorded in the leaves scoring highest value on D10 in both the genotypes which

might have also contributed to the positive rise in K-band. The O-I part denotes the kinetic properties for reduction/oxidation of the plastoquinone (PQ) pool (**Fig. 4.6f**), whereas the I-P phase elucidates changes in the electron flux from reduced plastoquinone (plastoquinol (PQH_2)) to the final electron acceptor of PSI. The negative ΔV_{OI} peaks recorded only at the later phase of increasing drought intensity (D8 and D10) indicate that drought-stressed V1 was able to maintain the reduction rate of PQ (capture of the exciton to the reduction of PQ) under progressive water stress and the process was only affected to some extent at the stage of severe drought intensity. A positive increase in I-P phase gives an indication of higher pool of the final electron acceptors of PSI (Tsimilli-Michael and Strasser 2008; Stirbet and Govindjee 2011; Adamski et al. 2011). A decreased I-P phase on D6 and again rise in same on D8 might be a part of an acclimation process of genotype V1 attempting to cope up with the progressive drought to maintain PQ pool size. However, an apparent decrease in I-P phase on D10 in V1 occurred due to drastic decline in leaf water status which might have reached the threshold level of drought acclimation. Involvement of PSI-dependent control of PSII activity under drought-stressed conditions has been demonstrated previously. The appearance of a clear attenuated peak on D10, support this, since the I-P phase of the OJIP transient is apparently caused by PSI associated limitations (Munday and Govindjee 1969; van Heerden et al. 2007).

Getting in more detail with the impact of drought stress on PSII, it was evident that the decrease of the maximum quantum yield of primary photochemistry φ_{Po} ($\approx F_V/F_M$) occurred to a lesser extent. The decrease of chl pigments could not cause any significant reduction in F_V/F_M which indicates that pigment breakdown was not associated to the maximum photochemical efficiency. Other authors explained such phenomenon to be a part of photoprotection mechanism for reduction of light absorbance by decreasing pigment contents (Munne-Bosch and Alegre 2000; Galmes et al. 2007). The insensitivity of F_V/F_M to drought stress is a well-known phenomenon in many plants as the parameter only considers changes in the values of F_O and F_M and if one increases with respect to a decrease in the other or *vice versa*, the ratio F_V/F_M might not change considerably (Elsheery and Cao 2008). The increased ABS/RC under drought stress refers only to the active PSII RCs which might be due to inactivation of some PSII RCs as reported earlier (Lu et al. 2001). Regrouping of antenna from inactive PSII RCs to active PSII RCs can

also lead to such observed increment in ABS/RC (Strasser et al. 1995; van Heerden et al. 2003). In spite of high ABS/RC, very high rate of effective dissipation (as evident by high DI_O/RC) of untrapped excitations (TR_O/RC values under drought stress did not vary much from control) occurred due to low level of electron transport per PSII RC i.e. ET_O/RC. This down-regulation might have prevented overreduction of the electron transport chain (ETR) as well as facilitated dissipation of excessive energy in order to minimize photooxidative damage in the thylakoid membrane (van Heerden et al. 2007). Further, acclimation responses to drought stress were also manifested in the form of increment in DI_O/CS_m and decrease in active RCs per leaf cross section area (RC/CS_m). Recent results indicate that under these type of conditions, changes in the functionality of PSII RCs can reduce the free energy gap between $S_2Q_A^-$ and $S_2Q_B^-$ (S2: state 2 transition), contributing to photoprotection of PSII through RC quenching (decrease in the active RC density, RC/CS_m) (Ivanov et al. 2006; van Heerden et al. 2007). The behaviour of other phenomenological flux parameters per leaf cross-section (ABS/CS_m, TR_O/CS_m and ET_O/CS_m), particularly ET_O/CS_m was highly reduced due to water stress which might have significantly affected the performance indexes ($PI_{(ABS)}$ and $PI_{(csm)}$). The specific (per RC basis) and phenomenological flux (per CS_m basis) parameters as a whole indicated a procreated down-regulation in overall processing of light energy per leaf sample cross-section under water stress conditions. Overall, the results obtained from the present study on chl a fluorescence showed that the OJIP transients could be very sensitive indicators to reflect changes in the PSII photochemistry in mulberry leaves under drought stress. The observed changes in PSII photochemistry might appear to be contradictory to some of the earlier reports (Lu and Zhang 1998; Lu and Zhang 1999) which demonstrated that the water stress has no effects on PSII photochemistry. However, the present study exhibits that the PSII structural integrity in drought-stressed V1 leaves was almost well-maintained and not substantially damaged until severe drought exposure (as demonstrated by ΔV_{OK}, ΔV_{OJ} and ΔV_{OI} plots), but the photochemical processes were rather down-regulated for photoacclimation and photoprotection of PSII.

The afore mentioned photoacclimation responses identified in mulberry might depend on *de novo* transcription and translation that are involved in regulation of light harvesting and photosynthetic electron transport (PET) processes. Such type of regulations are

sensitized by pH and/or redox conditions and occur by virtue of remodelled photosynthetic complexes with distinct properties whose function modifies redox properties of PET for preventing photodamage. Drought-induced photoacclimation processes also rely on alterations in stoichiometry between photosynthetic proteins achieved by controlling the relative amount/activities of regulatory proteins that play prominent roles in the dynamics of photosynthesis. In drough tolerant V1, rubisco large subunit was up-regulated by 2.8 fold, whereas two isoforms of rubisco activase were up-regulated by 1.6 and 2.3 fold. Over-expression in rubisco large subunit protein is associated with PSII stability and considered to one of the biochemical markers for drought tolerance in plants (Pääkkönen et al. 1998; Pancović et al. 1999; Pelloux et al. 2001; Demirevska et al. 2008). Rubisco and rubisco activase are the rate limiting enzymes in the carbon fixation cycle in C_3 plants and their activities are essentially interrelated. Rubisco activase is a nuclear encoded, ATP dependent chloroplast protein which enables rubisco to function by removing sugar phosphates from rubisco catalytic sites and facilitates CO_2 binding (Campbell and Ogren 1995). Enhanced levels of rubisco large subunit might have a role in increasing the proportion of workable active sites, whereas an increased expression of rubisco activase as evidenced in our study might be radical in coping up with the accelerated inactivation of rubisco catalytic sites due to low stromal CO_2 levels (Sengupta and Majumder 2009). Also, a dual function of rubisco activase under heat stress has been reported wherein it acts as a molecular chaperone in association with thylakoid bound ribosomes, protecting the thylakoid protein synthesis machinery against heat stress (Rokka et al. 2001). Hence, the stability of PSII as recorded in the stressed V1 leaves could largely be attributed to higher expression in the Rubisco large subunit and rubisco activase protein. Oxygen evolving enhancer proteins 1 and 2 (OEE1 and OEE2) are required for high levels of photosynthetic oxygen evolution and loss of these proteins can affect PSII functioning. In our study, reduction in the efficiency of OEC was recorded on D10 of water withholding which might have triggered up-regulation in both OEE proteins 1 and 2. Such changes might be associated with the repair of the stress damaged oxygen evolving systems for sustaining its physiological functions (Sugihara et al. 2000; Abbasi and Komatsu 2004). Under stress conditions fragmentations of OEE proteins may occur resulting in more than one spots in the 2D gel with different molecular weights. However, in the present experiment, the

observed molecular weight of both OEE1 and 2 corresponds to the intact (un-fragmented) protein ensuring that the reported up-regulation in its relative abundance in V1 leaves under drought stress is accurate. Up-regulation in OEE proteins without fragmentation in response to drought stress is also reported in other plants (Abbasi and Komatsu 2004; Blönder et al. 2007). Enhanced levels of the chl a/b binding proteins was also recorded in V1 leaves subjected to drought stress. Though the major function of these proteins are collecting and transferring light energy to photosynthetic RCs and some earlier reports have shown down-regulation of chl a/b binding genes under different abiotic stress conditions (Hazen et al. 2005; Guo et al. 2009), however, some recent studies have demonstrated over-expression in chl a/b proteins under drought conditions which was linked to enhanced tolerance of crop plants to dehydration stress (Guo et al. 2009; Loukehaich et al. 2012). Such up-regulation in chl a/b binding proteins under drought stress is postulated to keep PSII antenna complex intact ensuring its functional involvement in photosynthesis and was also linked with stomatal sensitivity to ABA playing a positive role in guard cell signaling, however, the actual mechanisms are yet to be understood (Guo et al. 2009; Loukehaich et al. 2012; Xu et al. 2012). In drought-stressed V1 leaves, 2.3 fold up-regulation of the peroxiredoxin protein was recorded which is a recently identified group of H_2O_2, alkyl hydro peroxides and peroxinitrite decomposing antioxidative enzyme that helps in mitigating the harmful effects of reactive oxygen species (ROS). The enzyme is also shown to function as modulator of cell signaling pathways and a redox sensor (Dietz et al. 2006). In the present study, around 2.3 fold increment was recorded in the expression level of NADH ubiquinone oxidoreductase chain 4 protein which is also known to have a protective role in plants against oxidative damage due to temperature stress (Wang et al. 2006). As drought-exposed leaf tissues are succumbed to high temperature (due to increased T_L) and oxidative stress, the observed increase in the levels of the NADH ubiquinone oxidoreductase protein in the water-stressed mulberry leaves could be beneficial for similar protective role against oxidative damage. The cellular location and physiological functions of all the above mentioned foliar proteins have been summarized in **Table 4.7**.

Table 4.7 Protein location, role in cellular metabolism, molecular function and number of spots identified under the protein ID.

Protein ID	Location	Role in metabolism	Molecular function	Number of spots identified
RuBisCO large subunit	Chloroplast	Calvin cycle	Carbon/oxygen fixation	One
Peroxiredoxin	Chloroplast Mitochondria	Antioxidative defence (protection of thylakoids and photosynthetic process) and modulation of redox signalling	Peroxide detoxification	One
RuBisCO activase	Chloroplast	Calvin cycle	Reactivation of RuBisCO for carboxylase reaction, protective energy dissipation by photorespiratory oxygenase reaction and protection of chloroplast protein synthesis as a chaperon	One
NADH ubiquinone oxidoreductase chain 4	Mitochondria	Mitochondrial respiration	Catalyses oxidation of NADH and reduction of ubiquinone, coupled to translocation of four protons across mitochondrial inner membrane and contributing to proton motive force	One
Oxygen evolving enhancer protein	Chloroplast	Photosynthetic oxygen evolution	Stabilizes manganese cluster which is primary site of water splitting, regulates dephosphorylation and turnover of the PSII reaction center D1 protein	Two
Chlorophyll a/b binding protein	Chloroplast	Photosynthetic light harvest	Balancing excitation energy between PSII and PSI and keeping PSII functional complex intact.	Two

The present study investigated the response of MIPIP1.3 to progressive water stress and its functional role in maintaining water balance in mulberry. It is commonly accepted that, under active transpiration, water flow from soil reaches the xylem of roots mainly via the apoplastic pathway governed by a hydrostatic pressure gradient. However, the more strongly transpiration is restricted due to stresses such as drought, the more water tends to flow via cell to cell pathways crossing plasmamembrane of cells. In the present study, it was observed that the transpiration rate was significantly reduced in both V1 and K2 plants under progressive water stress and thus enhancing the probability of transmembrane water flow across cells. Further, it was also evident that the reduction of transpiration is higher in K2 in compared to V1 plants under drought stress indicating that the K2 plants limited their symplastic water transport and hence their transpiration rate as an avoidance mechanism to prevent excessive water loss under water-deficit conditions. In a similar way like K2 plants, previous work on the transgenic tobacco over expressing BjPIP1 exhibited lower G_s and E in compared to wild type upon drought exposure suggesting that BjPIP1 might decrease transpiration and water loss through increasing stomatal resistance and

therefore contribute to drought avoidance (Zhang et al. 2008). However, it was interesting to note that in contrary to transgenic tobacco that showed up-regulated BjPIP1, the drought-stressed K2 plants showed the same functional leaf gas exchange response but exhibited down-regulation in the root-level MIPIP1.3. The results shown in **Table 4.3** and **Fig. 4.12** suggest that cell to cell water transport in roots might be strongly down-regulated in K2 compared to V1 in response to progressive drought stress, indicating that MIPIP1.3 could be significantly involved in transpiration rate and associated to better plant water relations in mulberry under drought. The present experimental data corroborate with Hanba et al. (2004) who demonstrated that over expression of HvPIP2.1 in transgenic rice enhanced the stomatal conductance and in turn allowed increased transpirational water loss. In this study, the obtained data on mulberry differed from previously reported transgenic tobacco (Zhang et al. 2008). One possible reason for this contradiction is that the expression pattern of aquaporins in plants is different. To maintain a reasonable water status under drought stress requires both increased water transport via aquaporins in some cells and tissues as well as reduced water transport via aquaporins in other cells and tissues (Comparot et al. 2000) and accordingly the expression of aquaporins will be regulated to perform such functions (Zhang et al. 2008).

The highly variable response to water stress of aquaporins at the transcript level depends on species, type of water stress, degree of water stress, and the plant organ (Tyerman et al. 2002; Bramley et al. 2007). Individual isoforms also vary in their response, all of which makes interpretation of the role of aquaporins during water stress rather difficult. However, in the present study, the expression data do assist in the interpretation of differential responses between V1 and K2 to water stress. Like drought tolerant V1which over-expressed MIPIP1.3 under drought, a number of researchers have previously observed the up-regulation of aquaporins in response to water stress in other plants species (Jang et al. 2004; Alexandersson et al. 2005; Aroca et al. 2006). The present data on mulberry support the view that increased MIPIP1.3 aquaporin levels can be associated with acclimation to water stress. In the present investigation, differential level of MIPIP1.3 expression was recorded between leaf and root tissues with higher over expression recorded in roots than leaves in drought tolerant V1. These findings corroborate with earlier reports on olive where OePIP1.1 accumulated to high levels in roots and twigs

with low levels in leaves (Secchi et al. 2007). NtAQO1 expressed in almost all organs of tobacco with highest levels in roots, and the plants impaired in NtAQP1 expression showed reduced root hydraulic conductivity and lower water stress resistance (Otto and Kaldenhoff 2000). The transcripts of BjPIP1 were mainly expressed in roots and were up-regulated in leaves due to osmotic stress, salt, low temperature, $CdCl_2$, or $ZnCl_2$, indicating that BjPIP1 was involved in root development and the response to various stress signals (Zhang et al. 2008). These findings elucidate that the dominant expression of a single aquaporin gene in specific organ or tissue seemed to be a consequence of the water requirement of organ development or tissue specialization.

The correlation of anatomical structures with physiological traits also support the superior performance of V1 when compared to K2 under drought stress. In the present study, a significant relation was found between stomatal density and size and drought tolerance. The results obtained imply that higher stomatal density, stomatal length and stomatal width were linked to drought stress tolerance in mulberry genotype V1. A review by Nebelsick et al. (2001) reported a number of studies describing leaf conducting tissue systems enormously variable in the number, size, and geometry of the vascular bundles in the veins and of the xylem conduits within the bundles. In the present study, the xylem number per mid vein and petiole cross sections was higher in V1 in compared to K2. These differences might be associated with significantly higher LMC, RWC and E in genotype V1 under drought stress. Although, leaf hydraulic conductivity was not measured in the present experiment, xylem diameter and density in the petiole and mid rib were reported to be positively related to hydraulic conductivity of leaves (Sack and Frole 2006; Sack and Holbrook 2006). Mulberry genotype V1 with significantly higher xylem diameter and xylem number per mid-vein and petiole cross sections possibly lead to better maintenance of leaf hydraulic conductance under drought stress. It was also reported earlier that greater xylem area is associated with the ability to maintain functional conductance under stress, ensuring better water potential and ‘stay-greenness’ (Oosterhuis and Wullschleger 1987). V1 possessed innate anatomical architectures like thicker leaves, well developed palisade tissues which would contribute to remain ‘stay-green’ and retain higher photosynthetic pigments with highest magnitude of photosynthetic performance (Charilaos et al. 2006; Kulkarni et al. 2007). The larger phloem area observed in V1stem in comparison with K2

could be an extra capacity to conduct photosynthates in higher amounts during moisture stress situation (Kulkarni et al. 2006). The higher number of xylem vessels recorded in V1 roots and stem would improve the capabilities for water transport and be more directly associated with greater potential for improved lateral root growth.

To conclude, the present integrated study was largely effective in tracking the dynamics of photosynthetic and water relation performances in mulberry genotypes under progressive water stress. Modulation of photosynthesis in mulberry genotypes under progressive drought involved an integrated down-regulation of the leaf assimilation physiology and PSII performance in a manner that the intrinsic balance between PET reactions and reductive carbon metabolism was maintained. Simultaneous leaf gas exchange and chl a fluorescence measurements revealed the stomatal and non-stomatal regulations involved in photosynthetic down-regulation. Performance of PSII was decreased *via* increment in inactive RCs, slowing down of the reduction of Q_A, decrease in electron transport beyond Q_A^-, regulation of electron transport activity (S_M, N, ET_O/RC, ET_O/CS_m), and increased energy dissipation (K_N, DI_O/RC, DI_O/CS_m). Nevertheless, the structural integrity and stability of PSII were largely maintained in the drought tolerant V1 as reflected by the L and K-bands and ΔV_{OJ}, ΔV_{OI}, and V_{IP} plots. Photostability was conferred by enhancing the expression of oxygen evolving enhancer and chl a/b binding proteins as well as rubisco and rubisco activase to protect the thylakoid membrane. Up-regulation in antioxidative enzymes like peroxiredoxin and NADH ubiquinone oxidoreductase were beneficial against oxidative damage under severe water stress conditions. In the drought tolerant V1, at root and leaf level, the significant over-expression of MIPIP1.3 was comparable with the concomitant higher leaf water status and transpiration rates of the same when compared to the susceptible genotype K2. V1 appeared to be an ‘optimistic’ genotype exhibiting less plasticity in leaf gas exchange and traits associated with water relations. Such over-expression in root and leaf-level aquaporins in V1 might be important in sustaining hydraulic and photosynthetic performance under drought. Further, leaf, stem and root level anatomical traits such as wider palisade mesophyll tissue, higher xylem number and area per mid vein, petiole, stem and root cross-sections were striking features of genotype V1 exhibiting better photosynthetic and hydraulic efficiency as confirmed by physiological measurements.

Characterizing Stomatal Regulation and Hydraulic Behavior in Mulberry under Water Deficit

Chapter 5

Stomata generally close in response to the steep concentration gradient of water vapor between the leaf and the air and therefore have great influence over plant water status. Stomata are involved in preventing damages caused by plant water deficits (Jones and Sutherland 1991), xylem cavitations and embolisms (Tyree and Sperry 1988) and have evolved to balance maximum carbon gain with minimum water loss, averting dehydration and physiological damage. While there have been advances in understanding the mechanics of stomatal opening and closing, the corresponding physiological mechanisms remain incompletely understood (Buckley 2005; Wilkinson and Davies 2008). There is evidence, however, that both chemical and hydraulic signals appear to regulate stomatal conductance (G_s) (Comstock 2002). For example, in grapevines, the control of G_s in response to soil water deficits is related to chemical signals mediated by ABA, travelling from the roots to the shoots in the transpiration stream (Stoll et al. 2000). It was also reported that during partial root zone drying, production of ABA by the drying roots reduced G_s, despite the maintenance of favorable shoot water status (Loveys et al. 2000). G_s can also be regulated by the hydraulic properties of the soil–root–shoot pathway, with a positive correlation between stomatal and hydraulic conductance of plant (K_{plant}) (Schultz 2003). Nevertheless, the mechanisms behind such a functional response of G_s to

K_{plant} remain uncertain. According to Whitehead (1998), rapid and reversible short-term changes in G_s following a perturbation to the water potential gradient in the flow pathway suggest that stomata respond directly to hydrostatic signals. Other authors (Saliendra et al. 1995; Sperry et al. 1993; Hubbard et al. 2001) have also suggested that stomata should not respond directly to changes in hydraulic conductivity, but to the consequent change in the leaf water status. Small localized changes in leaf water status, often not detected by pressure bomb measurements, can cause a stomatal response without necessarily causing observable changes in bulk leaf water status (Sperry et al. 1993; Salleo et al. 2000; Hubbard et al. 2001). Stomata should be capable to detect these small changes in leaf water status and function like a pressure regulator that controls the flow rate and maintain Ψ_L within a limited and safe range (Sperry et al. 2002). Stomatal control over conductance of water in the vapor phase within the leaf air spaces is highly dependent on the vapor pressure gradient (i.e. VPD) between the leaf and air. In most species, increasing VPD reduces G_s, but responsiveness ranges widely (Oren et al. 1999; Bunce 2006). For instance, under well-watered conditions, temperate deciduous trees undergo a greater reduction in G_s in response to increasing VPD than herbaceous species (Franks and Farquhar 1999). Variables such as irrigation and soil moisture interact with Ψ_L and often add a tier of complexity while predicting stomatal response to VPD. In order to gain a better understanding of plant's stomatal responsiveness to VPD and soil moisture, it is necessary to investigate the water relations under contrasting irrigation regimes.

Due to the diurnal and seasonal fluctuations in leaf-to-air VPD, one of the key regulatory roles of stomata is to limit transpiration-induced leaf water deficit. Different types of plants are known to vary in the sensitivity of G_s to VPD with important consequences for their survival and growth. Plants that minimize any increase in transpiration with increasing VPD have a tight stomatal regulation of a constant minimum Ψ_L; these plants are termed as 'isohydric', whereas plants that have less stomatal control of Ψ_L have been termed as 'anisohydric' (Tardieu and Simonneau 1998). Isohydric plants maintain a constant Ψ_L by reducing G_s and transpiration under drought stress. Therefore, as drought pushes soil water potential (Ψ_{soil}) below this Ψ_L set point, the plant can no longer extract water for gas exchange. On the other hand, anisohydric plants allow Ψ_L to decrease with rising VPD, reaching a much lower Ψ_L in drought-stressed plants relative to well-

watered plants (Tardieu and Simonneau 1998). This strategy produces a gradient between Ψ_{soil} and Ψ_L and allows gas exchange to continue over a greater decline in Ψ_{soil}. Thus, anisohydric plants sustain longer periods of transpiration and photosynthesis, even under large soil water deficit, and are thought to be more drought tolerant than isohydric species (McDowell 2011). A third mode of behavior was also suggested by Franks et al. (2007), in which the difference between soil and midday water potential ($\Psi_{soil} - \Psi_L$) is maintained seasonally constant but Ψ_L fluctuates in synchrony with soil water availability and is known as isohydrodynamic behavior of stomata. Plant species classification based on isohydric and anisohydric behaviors have been shown in **Table 5.1**.

Table 5.1 Classification of several species according to isohydric and anisohydric behaviors.

Species	Growing conditions	Behavior	References
Lupin	Pot	Isohydric	Henson et al. 1989
Maize	Field, pot	Isohydric	Tardieu et al. 1993
Pea	Field	Isohydric	Ben Haj Salah and Tardieu 1997, Bates and Hall 1981
Poplar	Pot	Isohydric	Tardieu and Simonneau 1998
Sugarcane	Pot	Isohydric	Saliendra and Meinzer 1989
Almond tree	Field	Anisohydric	Wartinger et al. 1990
Barley	Pot	Anisohydric	Borel et al. 1997
Peach tree	Field	Anisohydric	Xiloyannis et al. 1980, Steinberg et al. 1989
Soybean	Pot	Anisohydric	Allen et al. 1994
Subterranean clover	Pot	Anisohydric	Socias et al. 1997
Sunflower	Field, pot	Anisohydric	Tardieu et al. 1996
Wheat	Pot	Anisohydric	Henson et al. 1989
Grapevine	Field, pot	Isohydric, anisohydric	Schultz 2003, Vandeleur et al. 2009, Rogiers et al. 2011, Pou et al. 2012
Balsam poplar	Pot	Anisohydric	Larchevêque et al. 2011

The apparent differences in stomatal control of isohydric and anisohydric plants are thought to be due to differences in the perception of ABA, the chemical signal coming from the roots and the most likely candidate for root-to-shoot signaling in stomatal control (Tardieu and Simonneau 1998). Such differences in stomatal behavior may be related to the presence or absence of a sensitivity with respect to high evaporative demand and high temperature, frequent environmental cofactors of developing water deficit, or Ψ_L itself, which can modify the response of stomata to ABA (Davies and Zhang 1991; Tardieu and Simonneau 1998). ABA has been demonstrated to act on G_s of grapevines (Loveys et al. 2000; Lovisolo et al. 2002), yet a definite control has only be shown for midmorning

maximum G_s (G_{smax}) (Correia et al. 1995). However, G_s as well as leaf water status can undergo large diurnal fluctuations without substantial changes in soil water content and the controlling mechanism may not be directly related to (ABA) (Assmann et al. 2000). For example, the rapid decrease in Ψ_L in grapevines observed in the field after sunrise, even in well-watered plants (Schultz 1996), suggests the development of substantial water potential gradients in the soil-plant system, which, despite the increased transpiration rates, indicate large hydraulic resistances in the water-conducting pathway (Schultz and Matthews 1988). Differences in the diurnal behavior of Ψ_L of different grape cultivars under drought was also related to the water-conducting capacity and stomatal behavior was linked to hydraulic signal (Hubbard et al. 2001; Comstock 2002). Jones and Sutherland (1991) have proposed that stomata act primarily to avoid damaging water deficits causing cavitation in the xylem. Although at first glance, this would only fit to isohydric behavior (Jones 1998), depending on the hydraulic capacity and the proportion of conducting tissue which could be sacrificed for embolisms to maximize stomatal aperture and, hence, short-term productivity (Jones and Sutherland 1991), it would be applicable also to plants with anisohydric behavior (Hubbard et al. 2001; Comstock 2002). Woody plants such as *Quercus* (Cochard et al. 1996), *Juglans regia* (Cochard et al. 2002) or *Piper auritum* (Schultz and Matthews 1997) can achieve control of cavitation by stomatal closure, and this has also been suggested for grapevines in pot studies (Lovisolo and Schubert 1998). There have also been observations of reduced G_s in response to reduced hydraulic conductance but at a relatively constant Ψ_L suggesting a feedback link between G_s and some form of hydraulic signal (Meinzer et al. 1999; Salleo et al. 2000; Nardini et al. 2001). The mechanisms underlying such a response are not clear, but may be related to localized water potential differences as a result of the hydraulic properties of the water pathway (Nonami and Boyer 1993), or through pressure-volume changes in sensing cells or localized cavitations (Salleo et al. 2000; Nardini et al. 2001). The analysis of hydraulic constraints can improve our understanding of how changes in K_{plant} can affect G_s and in turn limit water use and carbon gain. In recent years, several studies have investigated the effects of directly manipulating root-to-leaf hydraulic conductance on gas exchange and bulk Ψ_L, using different approaches including root pruning (Teskey et al. 1983), defoliation (Meinzer and Grantz 1990; Pataki et al. 1998), cutting transverse notches in

stem (Sperry et al. 1993; Saliendra et al. 1995), root pressurization (Saliendra et al. 1995), shading lower canopy (Whitehead et al. 1996), air-injection technique (Salleo et al. 1992; Hubbard et al. 2001), and root chilling (Bloom et al. 2004). These studies have suggested that the reduction in K_{plant} results in stomatal closure, while increasing K_{plant} increases G_s.

Tree performance in dry habitats cannot be evaluated without considering constraints within the plant that influence carbon gain (Ehleringer 1994). For example, trees with an effective water supply system may lack specific adaptations for controlling water loss, resulting in low tissue water status that affects plant performance (Kramer 1980, Levitt 1980). Low maximum stomatal conductance and high stomatal sensitivity to changes in water status may be required to maintain Ψ_L above a critical threshold and to avoid xylem cavitation (Tyree and Sperry 1989; Jones and Sutherland 1991). In certain tree species, however, G_s declines long before there is a noticeable change in soil water content, imposing an early restriction to CO_2 uptake (Sperry 2000). Optimally, stomatal regulation of water loss should balance transpiration with water supply to the leaves so that a dangerous decrease in Ψ_L is avoided without unnecessary restriction to carbon gain (Meinzer 2002). Differences among species in the diurnal fluctuations in Ψ_L may reveal differences in soil water uptake or the flow of water between roots and shoots, or both, which in turn influences stomatal responses. Differences in stomatal behavior depend not only on differences in sensitivity to environmental factors associated with the development of water deficit, but also on root system development (Larcher 2003). Such differences in stomatal sensitivity between species, expressed during the development of drought, would serve to limit transpiration and compensate for differences in vulnerability to xylem cavitation (Tyree and Sperry 1988; Jones and Sutherland 1991). Because gaseous exchange, primary productivity and plant fitness are related, monitoring transpiration through sap flux measurements, coupled with instantaneous measurements of gas exchange activity during the development of water stress, should provide reliable information about species performance and ecological potentials. In certain tree species, water loss is reduced through reduction of total leaf area (LA) (Munné-Bosch and Alegre 2004). Reduction in LA as soil water becomes limiting is achieved through reduction in leaf size, leaf rolling or leaf shedding, thus reducing the transpiring leaf surface, but with significant negative

impact on carbon gain and overall plant productivity (Jones 1992). Thus, monitoring leaf phenology may also provide valuable information about species fitness.

The pioneering mulberry trees have shown adaptability to a wide range of soil water conditions and can tolerate drought by developing deep rooting system, optimizing leaf gas exchange functions, through osmotic adjustments and by up-regulating antioxidative defence systems (Chaitany et al. 2003). Although mulberry trees are generally considered to be rustic, nevertheless, large interspecific and ecotypic differences in rooting characteristics, leaf water-relations and gas exchange functions have been associated with the selection of genotypes for varying cultivation sites differing in soil water availability (Susheelamma et al. 1990; Ramanjulu et al. 1998). Mulberry genotypes belonging to *M. indica* and *M. alba* species have been recently introduced in the non-traditional moriculture sectors located in the semi-arid agroecosystems of Southern India including Andhra Pradesh and Karnataka which are broadly referred as the peninsular hot semi-arid zones (Narasaiah 2003). Besides survivability, sustainable yield, biomass productivity and higher physiological responsiveness of genotypes to take advantage of intermittent precipitation events are important requirements, particularly in hot semi-arid steppe environments which are subjected to high temperature, low air humidity, excessive solar irradiance and mild rainfall events during summer. The Telangana region on Deccan Plateau situated in northwest of Andhra Pradesh state, possesses a typical hot semi-arid steppe climate (according to Köppen climate classification) that remains fairly warm throughout the year and receive mild to moderate rainfall in monsoon. During summer (March to June), mean daily temperature of this region varies from 30-36ºC, sometimes rising as high as 42ºC accompanied by extreme hot wind waves and excessive solar irradiance (Yadav et al. 1997). Present rainfall events during summer rarely meet potential evapotranspiration and expected climate change over the course of the 21st century is likely to increase the frequency of drought events causing plant water stress with which the introduced mulberry species must cope. Farmers in this hot semi-arid steppe region primarily grow mulberry as a subsidiary crop (occasionally as major) for sericulture in conjugation with other major crops like paddy, jowar, bajra, maize, sugarcane, cotton etc and also as an intercrop with horticultural tree crops like coconut, mango and jackfruit etc (Kapoor 2009). Because most of the mulberry genotypes cultivated in this region are relatively drought tolerant, they are

still able to provide yield, when other crops fail due to the frequent drought events. Thus, mulberry trees have gained an important component of life support in this hot semi-arid steppe region and can be regarded as model system to study drought tolerance. However, such ecological importance of this tree species has not been acknowledged yet.

The previous studies (see chapter 3 and 4) depicted that the drought tolerant mulberry genotypes exhibit minimal plasticity in foliar gas exchange characteristics and subsequently maintain higher rates of transpiration and stomatal conductance displaying a characteristic behavior which can be ecologically termed as 'optimistic'. Such behavior is analogous to the anisohydric physiology of plant that exert less stomatal control on leaf gas exchange in spite of high evaporative demand. In order to establish and model such anisohydric functionality, knowledge about the operational range of Ψ_L is essential along with concurrent leaf gas exchange measurements throughout a diurnal as well as temporal course of field study (Tardieu and Simonneau 1998). Since photoacclimtion capacity of photosystem-II (PSII) contribute to the ability of plants to minimize oxidative damage and sustain photosynthesis; investigation of this protective strategy can be important complement to understand drought tolerance responses in mulberry under hot semi-arid steppe agroclimate. Such comprehensive complex studies considering stomatal regulation to Ψ_L, leaf gas exchange, hydraulic conductance and photoprotection have been successfully employed to analyze the responses of different model woody tree species in other drought-prone ecosystems under variable soil moisture conditions (Schultz 2003; Brodribb and Holbrook 2004; Sofo et al. 2008). However, such framework of analysis is still lacking in mulberry, particularly in summer drought conditions of hot semi-arid steppe agroclimate where stomatal control to leaf gas exchange, transpiration efficiency and plant water use can be critical in determining crop growth and yield. However, parameterization of these comprehensive models is difficult, rather simplified approaches combining leaf gas exchange and xylem sap flow, chlorophyll fluorescence and leaf water potential measurements can be used successfully to predict regulation of stomatal and hydraulic behavior in mulberry under field-drought conditions and such an explicit framework of analyses has rarely been applied in hot semi-arid steppe agroclimatic conditions.

The seasonal and diurnal transpiration efficiency of trees grown in the field is a complex character affected by plant water status, and the combined analysis of

relationships amongst transpiration, xylem sap flow, atmospheric evaporative demand, soil moisture, diurnal stomatal behavior and whole-tree hydraulic conductance can provide a powerful tool to assess the response of trees to drought. Through gaining an understanding of these parameters, we will be better in scheduling water supply, allowing trees some buffering against water stress. At field-level, water use in trees can be estimated from the soil water balance, but with temporal resolution of a few days at best, and difficulties arise because estimates of drainage and surface runoff are usually uncertain. Micrometeorological methods, such as the Bowen ratio technique and eddy covariance, can be used to measure evapotranspiration with much better temporal resolution, but these methods are complex, the equipment is expensive and they can only be used in large areas of flat, uniform terrain. Both water balances and micrometeorology can provide estimates of evapotranspiration, which includes soil evaporation and plant water use, while sap flow techniques measure transpiration alone; thus sap flow methods are a useful tool in studies of the water or energy budgets of land surfaces, as they can be used to partition evapotranspiration between plant and soil evaporation and to divide estimates of transpiration among the component species of plant mixtures. It is therefore important to understand how sap flow in trees is affected by restricted water availability, particularly if rain-deficient years occur more frequently in coming decades.

The general objective of this study was thus to understand and characterize drought-induced leaf gas exchange, xylem sap flow and photoacclimation responses in mulberry stands under the hot-semi arid steppe environment of Telengana. We addressed the following three questions in the present chapter: (i) Are leaf water potential (Ψ_L), stomatal conductance and associated gas exchange data consistent with the hypothesized anisohydric functionality of field-grown drought tolerant mulberry trees under water stress circumstances? (ii) How xylem sap flow respond to field-level drought stress in mulberry genotypes varying in drought stress tolerance? (iii) As short-term adjustment, which photoacclimation strategies are preferred by the drought tolerant mulberry genotypes during summer drought conditions of hot semi-arid steppe agroclimate? Finally, mulberry trees were also assessed for biomass yield and the yield sustenance capacity under drought was linked with the leaf-level functional traits of the drought-exposed stands. The present study was undertaken in two experimental phases including exp phase-I and II.

In phase-I experiment, selected field-grown mulberry genotypes were subjected to a 1-month summer drought conditions under moderate drought stress. The genotypes (chosen based on putative variability in diurnal response) were compared to determine differences in diurnal leaf gas exchange, instantaneous water use efficiency, leaf water potential, whole plant hydraulic conductance and PSII efficiency. In phase-II experiment, only a single drought tolerant genotype was assessed using the same set of physiological parameters but under two irrigation regimes including well-irrigated (control) and high water deficit (drought). We conducted all experiments (both exp phase-I and II) within 4 months spanning the peak summer period (exp phase-I: Mar and exp phase-II: Apr to Jun) for two consecutive years (2009 and 2010) and phase wise, the mean of data are presented for each variable. According to Indian Meteorological Department, the experimental summer months of Apr and May 2009 recorded the warmest temperature in Telangana since 1901, with maximum air temperature touching 45ºC.

Materials and Methods

Site description, experimental season and mulberry plantation

The present work was conducted in the experimental farm of University of Hyderabad (UH) (17.3°10´N and 78°23´E at an altitude of 542.6 m above MSL). Experiments were conducted on SRC plantations of mulberry established in experimental plots of 14.4 x 14.4 m^2 (12.6 m rows, 0.9 m apart) in RBD (with three blocks per genotype). The soil of the experimental plots was shallow alfisol with a pH of 7.5, organic carbon content of 5.2% and characterized by low water retention capacity. For exp phase-I, two drought susceptible genotypes (KL and MR2) and two drought tolerant genotypes (S13 and V1) were selected, whereas for exp phase-II, all studies were conducted on drought tolerant genotype V1. Some of the important morphological-growth features of the selected mulberry genotyeps are shown in **Fig. 5.1**.

Fig. 5.1 Important morphological-growth features of four mulberry genotypes**.** (a) Genotype Kollegal is named after the Kollegal district of Karnataka. Growth is erect, simple branches, green colored lobed leaves, acute triangle buds and with female inflorescence. High rooting ability and moderate leaf yield. (b) MR2 genotype is one of the open pollinated hybrid selections which were introduced in Nilgiri Hills. Branches simple, acute triangle buds, vertical, greyish leaves, dark-green, unlobed, elliptic, palmately veined, leathery, with smooth and irregular whitish blotches of variable sizes at intersections of veins and veinlets. This genotype is good in rooting, leaf yield (30 MT/ha/yr) under irrigated condition and growth. Recommended for South India (Tamil Nadu, especially in Salem district. The genotype is resistant to powdery mildew disease caused by *Phyllactinia corylea* and is very popular in the plains of Tamil Nadu and also better suited for high altitude areas where high temperature prevails. (c) S13 is a fast growing genotype with straight branches, short internodes and spindle shaped buds. Leaves are medium in size, entire, ovate, thick, unlobed, with dark green color, succulent, smooth and glossy, high rooting ability (>90%), staminate (male), 2n=2x=28 (diploid).The genotype is recommended for red soil regions of South India under rainfed cultivation practices. The genotype can produce 13-16 MT/ha/yr leaf yield under soil moisture stress conditions. (d) Genotype V1 is the most productive mulberry genotype. Erect stem, acute triangle buds and fast growing with large, entire, unlobed, dark green leaves, predominantly male, 2n=2x=28 (diploid). Leaves are succulent and thick with very high moisture content (78%). The genotype can produce 50-60 MT/ha/yr leaf yield under irrigated conditions. V1 is responsive to high fertilizer doses. Rooting ability is excellent and moderately resistant to leaf spot and also suitable for tree plantation.

Meteorological monitoring and drought treatments

Automatic data loggers (Neogenesis, India) installed in the experimental plots recorded daily maximum (T_{max}) and minimum (T_{min}) air temperature, relative humidity (RH), precipitation (PP), atmospheric CO_2 concentration and photosynthetically active radiation (PAR: between 06.00-18.00 h). The vapor pressure deficit (VPD) was calculated using Murray's formula (Murray 1967). During exp season-I, the experimental plot was irrigated 2-3 times in a fortnight and this water stress level had previously been calibrated to ensure moderate water stress when compared to the drought stress treatments mentioned in the field assays for screening genotypes for drought tolerance (chapter 3). In exp phase-II, control plot was irrigated whenever SWC tended to drop below 60% (weekly 2-3 times irrigation), whereas the drought-stressed plot received irrigation only once in a fortnight and the SWC was more or less maintained within 20 to 25%. Crop irrigation demands were determined according to daily crop reference evapotranspiration, calculated according to Penman-Monteith equation (Allen et al. 1998), and crop factor based on the time of the year (Allen et al. 1998). The duration of irrigation was increased in control plot during the hottest weeks to compensate higher evapotranspirational moisture loss. At periodic intervals (7 ± 2 days), SWC at two different soil depths (30 and 45 cm) was determined gravimetrically (% v/v) as the relative change in weight between fresh and dry soil samples. Regular agronomic practices were kept normal and recommended package of practices were followed uniformly throughout the growing seasons for both the treatments including application of 3 metric tonnes farm yard manure (2^{nd} week of Apr) and 46:20:20 kg NPK (1^{st} week of May), and no weeds were allowed to grow within the experimental plots.

Measurements of leaf-level gas exchange functions

Six representative trees (two from each block with uniform height and canopy growth) located in the inner rows of the blocks were tagged from each treatment to investigate leaf gas exchange, PSII efficiency and leaf water relations. Gas exchange functions were measured between 09.30 and 10.00 h on each alternate week and also throughout the day on six different sunny days to record the diurnal pattern. Net photosynthesis (P_n), transpiration (E), stomatal conductance (G_s) sub-stomatal CO_2 (C_i) and leaf temperature

(T_L) were measured accessing fully-expanded mature upper canopy leaves (4 leaves per tree at the 3rd-4th position from shoot apex) using a portable infrared CO_2/H_2O gas analyzer (IRGA) (LCpro-32070, ADC BioScientific, UK) at ambient irradiance, temperature and air humidity and at constant external CO_2 concentration (C_a = 378 μmol mol^{-1}) with a flow rate of 340 μmol s^{-1}. The gas analyzer was equipped with a broad leaf chamber (LCpro-32070, UK), a PAR sensor (silicon based sensor, LCpro-32070) and a leaf thermistor probe (ADC, M.PLC-011). Measurements were made after steady state condition was obtained, typically requiring around 2 min under standard conditions. To calculate instantaneous water use efficiency ($WUE_i = P_n/E$), we considered the values for the days on which VPD conditions were same or quite uniform.

Measurements of leaf water relations, visual assessments and record of leaf wilting and stomatal opening/closure

Leaf water potential (Ψ_L) was measured periodically in fully expanded, upper canopy leaves (3 leaves per tree at the 3rd-4th position from shoot apex) using a portable pressure chamber (SKPM 1400/40, Skye Instruments, England) during predawn (Ψ_{pd}: 04.00 h), midday (Ψ_{md}: 12.30-13.30 h) and immediately after gas exchange measurements during the diurnal course of study. Before leaf harvesting for Ψ_L measurements, the leaf angle (angle of inclination) relative to the horizontal of the petiole and lamina of each leaf was measured using a transparent plastic protractor and a plumb line according to Foot and Morgan (2005). Wilting and leaf angle changes were photographed between 10.00 and 18.00 h on each alternate week throughout the experiment. To view stomatal opening/closure during the diurnal course of a day, 2–3 square pieces of about 0.25 cm^2 were randomly (between 08.00 to 18.00 h) cut from the upper canopy leaves (same leaves used for gas exchange measurements) and were put into small cryo-bottles and thereafter quickly placed into liquid N_2 and stored. The time from cutting in-vivo samples to immersing them into liquid N_2 was less than 1 min. Leaf samples were then transferred under vacuum to the specimen stubs and sputter-coated with gold at 1.5 keV for 10 min using a JEOL FC-1100 Fine Coat Ion Sputter Unit (JEOL, Tokyo, Japan) and were examined using a Scanning Electron Microscope (FEI XL 30 ESEM, USA).

Measurements of root-to-leaf specific whole plant hydraulic conductance (KSL)

In-situ KSL from the soil through the leaf was calculated for all measurement periods after Wullschleger et al. (1998): $KSL = E_{max}/(\Psi_{pd} - \Psi_{md})$, where Ψ_{pd} and Ψ_{md} were predawn and midday leaf water potentials, respectively. Although stored water can uncouple the close relationship between transpiration and leaf water potential, our calculations of KSL were made during peak transpiration at midday (E_{max}) when the effects of capacitance on transpiration were minimal. Water potential measurements were made on exposed shoots around the lower third of the crown of each tree. A single shoot was sampled at each of three points (in 60º intervals around the tree) at each measurement period and the value for each tree calculated as the mean of these three samples. Predawn water potential measurements were made between 04.00-05.00 h and midday measurements were made between 12.30-13.30 h using a portable pressure chamber (Plant Moisture System, SKPM 1400/40, Skye Instruments Ltd, England). Based on diurnal measurements of leaf water potential at our experimental site, Ψ_{pd} and Ψ_{md} corresponded to maximum (Ψ_{Lmax}) and minimum (Ψ_{Lmin}) leaf water potentials, respectively.

Xylem sap flow measurements using heat ratio method (HRM)

Midday xylem sap flow was measured in-situ in the stem at breast height. All measurements (sap in and sap out) were made at periodic intervals with the heat ratio method (Burgess et al. 2001) using HRM-30 sensors (ICT International, Armidale Australia) coupled to an experimental wireless sensor network (provided by ICT International) that collated data on a Zaurus SL-C3000 PDA (Sharp Corporation, Japan) (**Box 5.1**). Data were then averaged. The area containing the probes was protected from direct solar radiation.

Measurements of PSII efficiency

Diurnal responses in PSII efficiency was measured immediately after the leaf gas exchange measurements on dark-acclimated (for 30 min) upper canopy leaves (same leaves used for gas exchange analyses) using a portable Plant Efficiency Analyser (Handy PEA-2126, Hansatech, UK). Changes in fluorescence intensity were measured between 10 μs and 1s by illuminating leaves with a beam of saturating light (3000 μmol m^{-2} s^{-1}) of 650 nm peak

Box 5.1 Measurements of stem xylem sap flow using heat ratio method (HRM).

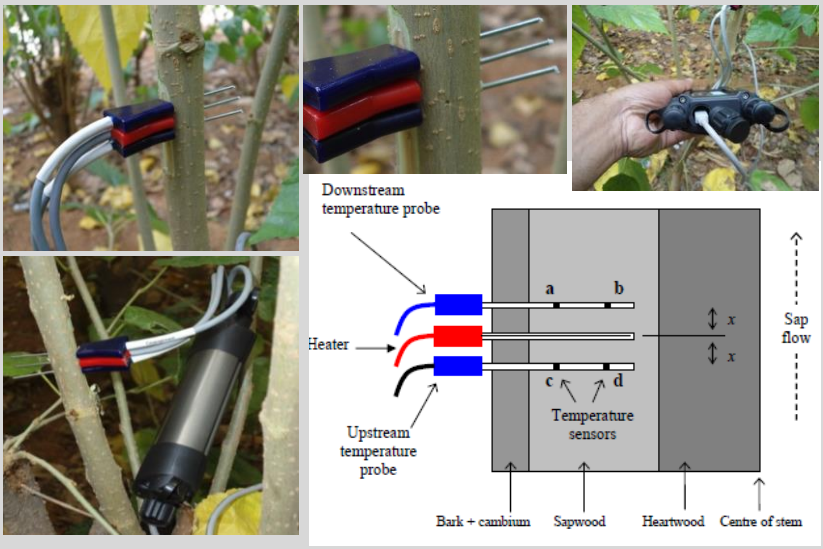

The Heat Ratio Method (HRM) is a modification of the Compensation Heat Pulse Method (CHPM). The HRM improves on the CHPM by allowing **very slow flow rates** and even **reverse sap flow** to be measured. This allows water flows to be monitored in stems and roots of a wide range of different species, sizes and environmental conditions, including drought. HRM is a thermometric method of measuring sap flow in xylem tissue which uses a short pulse of heat as a tracer. By measuring the ratio of heat transported to two symmetrically placed temperature sensors, the magnitude and direction of water flux can be calculated. The HRM sensor consists of three 35 mm long needles or probes integrally connected to a 16-bit microprocessor. The upstream and downstream probes contain two thermistors located at 7.5 mm and 22.5 mm from the tip of each probe. The third and centrally located probe is a line heater that runs the full length of the probe to deliver a uniform pulse of heat through the sapwood. The integrated microprocessor forms the heart of the HRM sensor making it a fully autonomous, Plug & Play Smart Sensor.

wave length, obtained from three light-emitting diodes focused on the leaf surface through leaf clip on a leaf spot of 5 mm diameter circle. On the basis of these measurements, maximal (F_M) and minimal (F_O) fluorescence yields, variable fluorescence ($F_V = F_M - F_O$), maximum quantum yield of PSII (F_V/F_M) and phenomenological flux parameters (per excited leaf cross-section: CSm) including ABS/CSm (light energy absorption), TR_O /CSm (trapping of excitation energy), ET_O/CSm (conversion of excitation energy to electron transport), DI_O/CSm (energy amount dissipated from PSII), PI(CSm) (overall performance index of PSII), driving force (D.F.) and structure-function index (SFI) were calculated from JIP-test based on the theory of energy flow in PSII using Biolyzer 4HP v.3.306 (Strasser et al. 2004).

Measurements of biomass yield and yield attributing traits

All the six representative trees (same six, used for studying leaf-level functional traits) per treatment were used to record growth and biomass yield characteristics. Plant height (H_t) from ground to the canopy top was measured using measuring tapes. The shoots of all the representative trees were coppiced using a sharp pruner and the aboveground compartments (leaves, branches and stems) were separated, immediately weighed fresh in the field to undertake the following measurements per plant basis: total number of stems

(T_{STM}), number of branches (axillary shoots) (T_B), total shoot length (T_{SL}), leaf fresh biomass (L_f), stem fresh biomass (S_f) and total aboveground fresh biomass (AG_{fw}). From a sub-sample of leaves, leaf dry biomass (L_d) was determined after oven-drying at 70ºC for 72 h. Subsamples from stems and branches were chipped, mixed evenly and were oven-dried at 80 ºC for several days until constant weight. Aboveground woody biomass (AG_w) was calculated as the sum of dry weights of all stems and branches and the dry weights of both wood and bark were included in the AG_w. Total above ground dry biomass (AG_{dw}) was calculated as the sum of total L_d and AG_w of a plant.

Statistical analyses

For each variable, measurements for each date or time of day (under each treatment) were repeated with the six representative trees (n= 6 trees i.e. 6 replicates) and data represented as mean ± standard error. Normality and variance homogeneity were checked by Shapiro-Wilk and Levene tests. Mean (of 6 trees per treatment) comparison over weekly time intervals was analysed with repeated measures analysis of variance (ANOVAR), whereas for diurnal time course, one-way analysis of variance (ANOVA) was followed.

Results

Exp phase-I: Meteorological conditions and soil drought

Climatic conditions recorded during exp phase-I were typical for hot semi-arid steppe conditions and the differences were not large between periods throughout the month and thus the mean of diurnal climatic conditions are presented in **Fig. 5.2**. Daily irradiance peaked at midday between 12.00 to 14.00 h and maximum PAR at midday was around 2000 µmol m^{-2} s^{-1} (**Fig. 5.2a**). The air temperature (T_{mean}) ranged from 26 to 40ºC, mean atmospheric CO_2 concentration was 365±5 µmol mol^{-1} and RH showed a narrow range (18 to 25%) (**Fig. 5.2a,b**). SWC during the experimental season did not differ between the 30 and 45 cm depth (ranging around 45.9 ± 3.6% by volume).

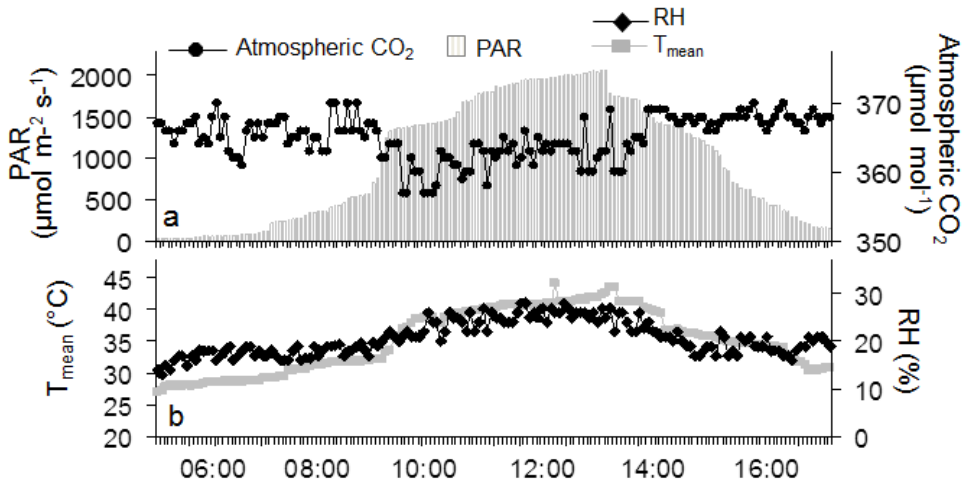

Fig. 5.2 Trend of diurnal meteorological conditions at the experimental site of University of Hyderabad monitored during the summer month of March. The presented data for each variable are mean of year 2009 and 2010. Data were recorded for (a) photosynthetically active radiation (PAR), atmospheric CO_2 concentration and (b) mean air temperatures and relative humidity (RH). All meteorological parameters were recorded using automatic data logger installed in open field at a distance of 50 m from the plantation stands.

Exp phase-I: Leaf gas exchange functions

All four genotypes of *M. indica* showed a significant ($P<0.05$) reduction in P_n during midday elucidating a clear midday depression (**Fig. 5.3a**). However, S13 and V1 showed higher P_n than KL and MR2 throughout the diurnal time period except the early hours of the day (06.00-07.00 h) when they all had almost similar P_n values. Reductions in G_s were more pronounced in S13 (approximately 56.4%) than V1 (~36%) during midday, however, S13 maintained highest G_s (values ranging from 0.04 to 0.39 µmol m^{-2} s^{-1}) during most of the time throughout the diurnal time period. Genotype KL and MR2 exhibited significantly less G_s values during morning and midday time period, however, the values were somewhat higher after 14.00 h (**Fig. 5.3b**). The genotypes differed significantly in response to diurnal pattern of E (**Fig. 5.3c**). KL and MR2 recorded very less E (~0.23 and ~1.2 mmol m^{-2} s^{-1}, respectively) when compared to S13 and V1 (~6.8 mmol m^{-2} s^{-1}) during peak photosynthetic time (10.00 h). The genotypes also differed widely in E during midday depicting a conspicuous draw-down of E in V1 and S13, whereas in KL and MR2 transpiration was almost ceased and values were slightly higher during 14.00 h. In relation to WUE_i, both V1 and S13 had almost similar WUE_i values

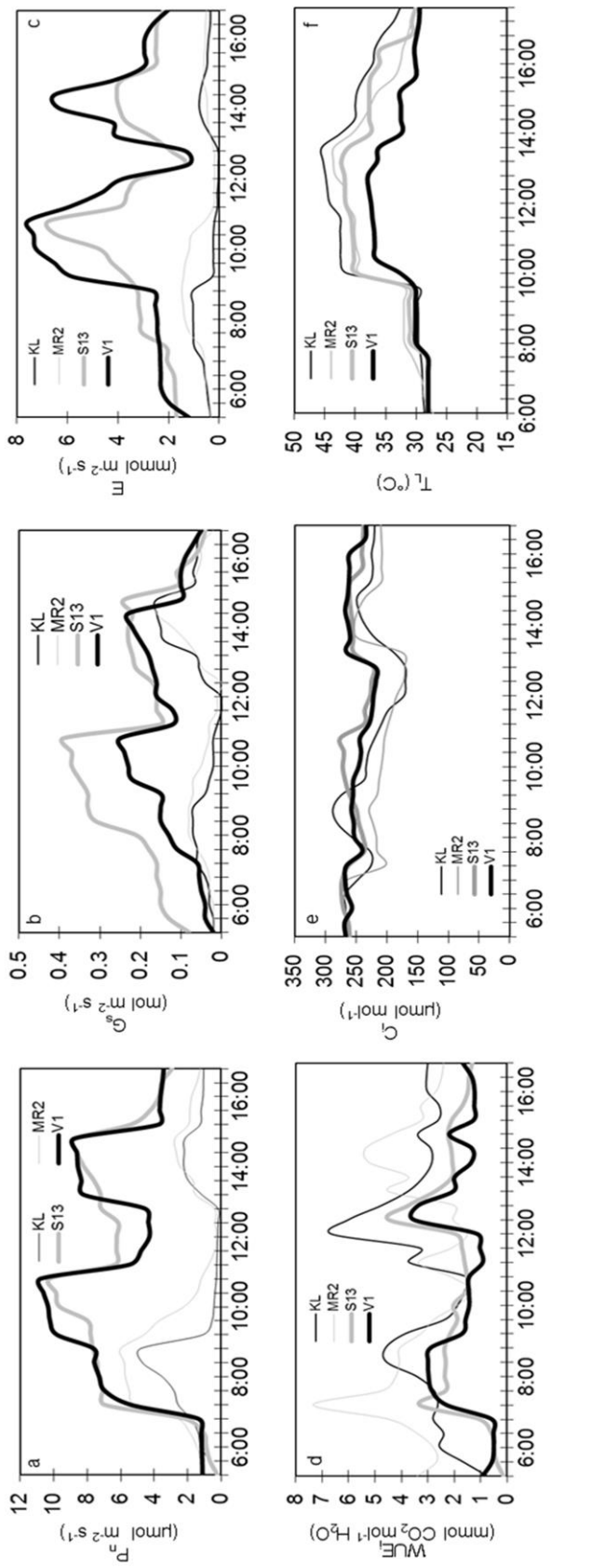

Fig. 5.3 Comparison of diurnal photosynthetic leaf gas exchange characteristics among four drought-stressed mulberry genotypes (*M. indica*: KL, MR2, S13 and V1) grown at the experimental plots of University of Hyderabad. Data were recorded during the summer month of March (for two consecutive years: 2009 and 2010) to track differences diurnal trends of (a) net photosynthetic rates (P_n), (b) stomatal conductance (G_s), (c) leaf transpiration rate (E), (d) instantaneous water use efficiency (WUE_i), (e) sub-stomatal CO_2 concentration (C_i) and leaf temperature (T_L). Values are mean ± SD of repeated measurements from six representative trees. Data represented for each variable are mean of year 2009 and 2010. At each sampling point (throughout diurnal course), ANOVA was used to compare values obtained from different genotypes. All measurements were done using upper canopy sun-exposed leaves.

which were significantly less when compared to KL and MR2 (**Fig. 5.3d**). Compared to other leaf gas exchange traits, a marginal decrease in C_i was recorded during midday in all the four mulberry genotypes. However, the C_i values were slightly higher in S13 and V1 when compared to KL and MR2 (**Fig. 5.3e**). Significant increment in T_L was recorded with increase in solar hour in all the four genotypes and the highest T_L was recorded in KL (~45ºC), followed by MR2 (~43.5ºC) at around 14.00 h. The T_L values were significantly less in S13 and V1 (<40ºC), but also showed an increasing trend during midday and then again came down at the later part of the day (**Fig. 5.3f**).

Exp-phase I: Whole plant hydraulic conductance (KSL) and xylem sap flow

Mulberry genotypes differed significantly ($P<0.05$) in KSL as recorded during midday (**Fig. 5.4**). V1 (1.9 MPa^{-1} m^{-2} s^{-1}) and S13 (1.8 MPa^{-1} m^{-2} s^{-1}) exhibited significantly higher KSL when compared to other two genotypes. The lowest KSL value was recorded in KL (0.7 MPa^{-1} m^{-2} s^{-1}) followed by MR2 (0.9 MPa^{-1} m^{-2} s^{-1}). The drought-tolerant S13 and V1 exhibited approximately 56% higher KSL during midday when compared to drought susceptible KL and MR2. The midday patterns of xylem sap flow showed significant ($P<0.05$) genotypic difference (**Fig. 5.5**). The sap flow data obtained from all the four genotypes have been segregated into two groups representing drought tolerant (**Fig. 5.5a**) and drought susceptible (**Fig. 5.5b**) genotypes and likewise graphs were plotted where the sap flow rates are expressed in terms of cm^2 h^{-1} and kg h^{-1} (see the figure legend for details). The drought tolerant genotypes (V1 and S13) exhibited significantly higher (approximately 30%) sap flow with values ranging from 35.2 to 48.5 cm^2 h^{-1}, whereas in drought susceptible genotypes (KL and MR2), the sap flow ranged from 23.6 to 36 cm^2 h^{-1}. The sap flow rates were strongly and positively correlated with midday transpiration rates (E) (**Fig. 5.5c**) as evident from the considerably steeper slope ($R^2 = 0.71$).

Exp-phase I: Changes in PSII characteristics

In **Fig 5.6**, a comparison is made among the raw OJIP transients measured during midday. Drought imposition induced significant variation in the shape of transients among the genotypes. The amplitude rise in OJIP was significantly lost in KL and MR2 affecting all the phases in OJIP transients and no attenuation in fluorescence rise could be recorded in

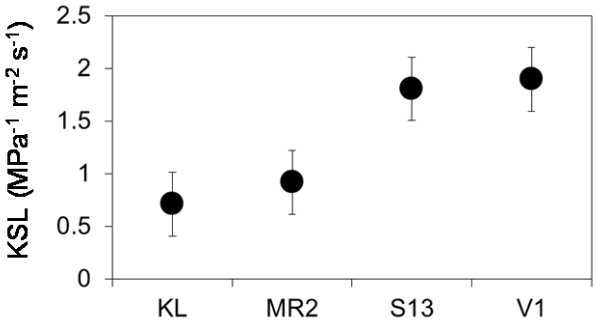

Fig. 5.4 Leaf-specific whole plant hydraulic conductance (KSL) of four mulberry genotypes (KL, MR2, S13 and V1) grown at the experimental plots of University of Hyderabad. Data were recorded during the summer month of March (for two consecutive years: 2009 and 2010) Values are mean ± SD of repeated measurements from six representative trees. ANOVA was used to compare values obtained from different genotypes. All measurements were done using upper canopy sun-exposed leaves.

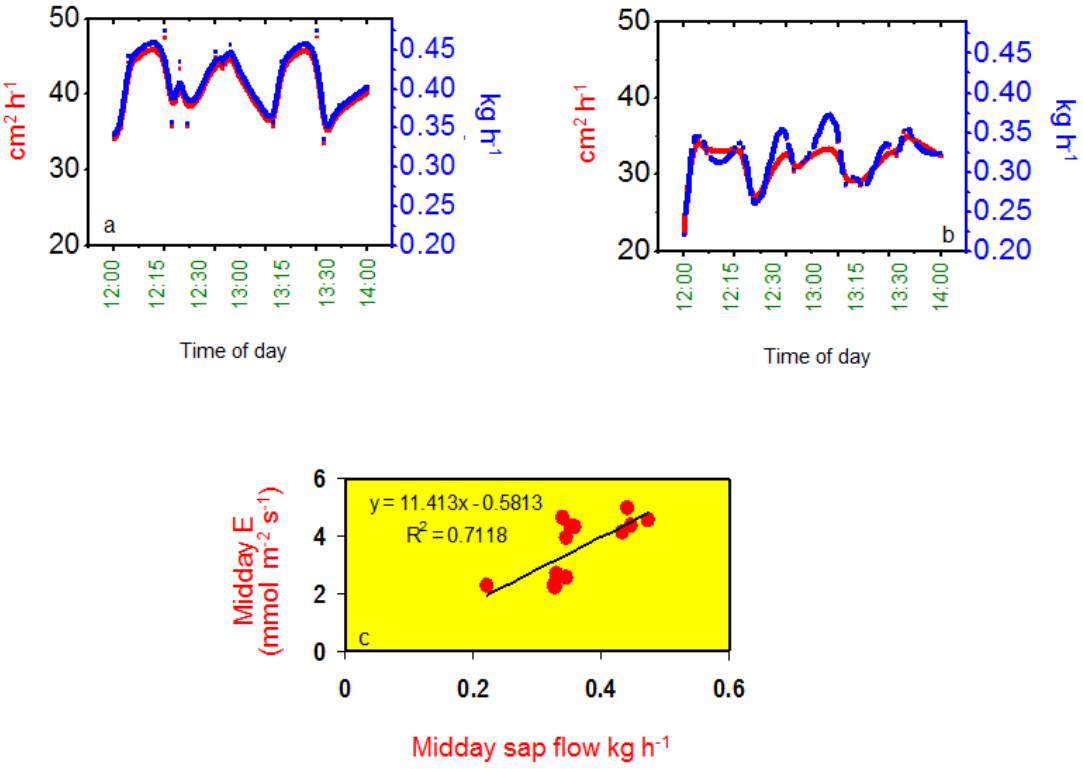

Fig. 5.5 Midday (between 12.00 to 14.00 h) xylem sap flow recorded in (a) drought tolerant (S13 and V1) and (b) drought susceptible (KL and MR2) mulberry genotypes grown at the experimental plots of University of Hyderabad. Data were recorded during the summer month of March (for two consecutive years: 2009 and 2010) Values are mean ± SD of repeated measurements from six representative trees. ANOVA was used to compare values obtained from different genotypes. The sap flow rates are expressed in terms of $cm^2\ h^{-1}$ (red line) and kg h^{-1} (blue line). Relationship was established (c) between midday transpiration (E) and xylem sap flow rates (data from four mulberry genotypes were used and each dot represents mean of six data) using linear regression analysis.

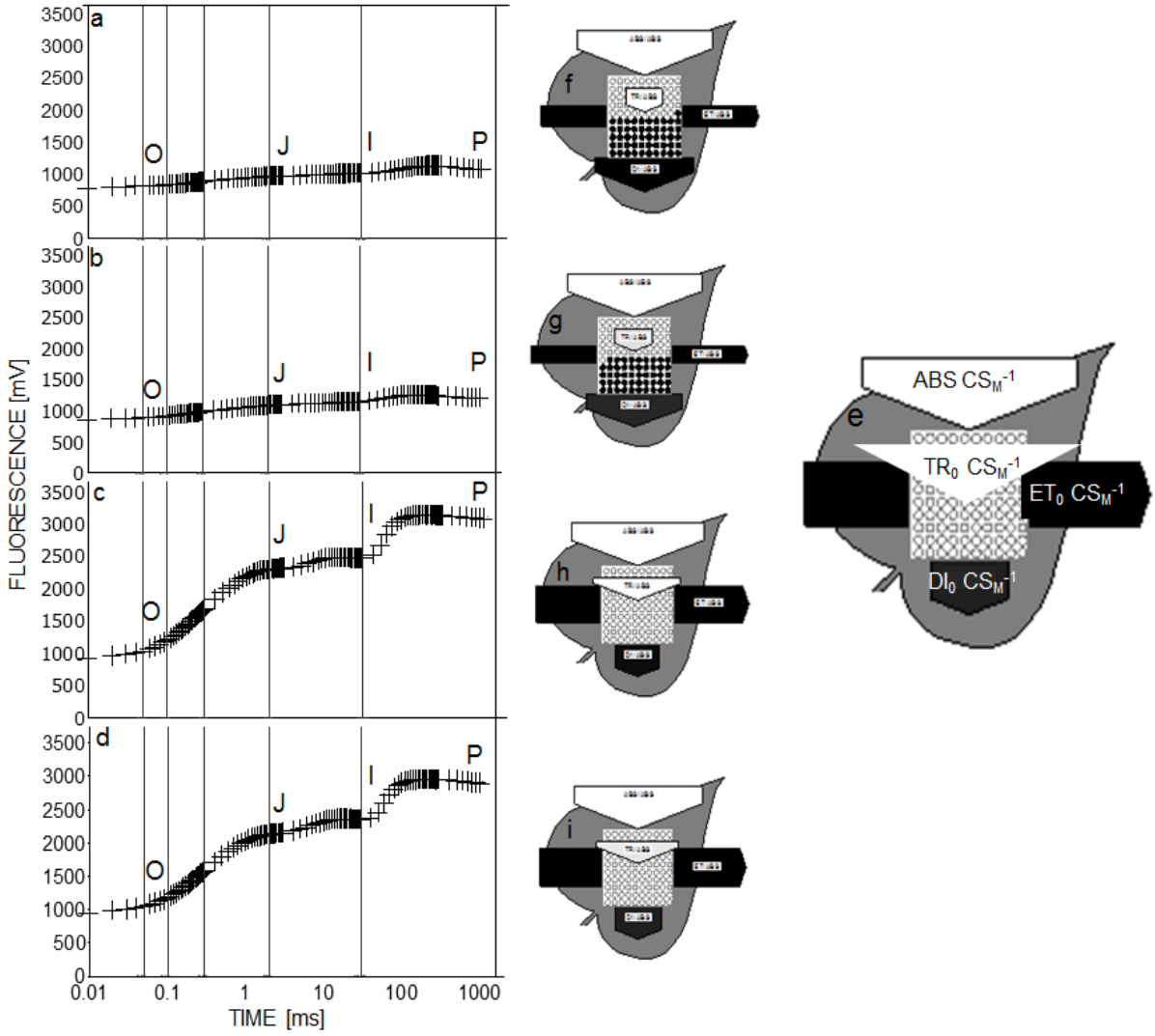

Fig. 5.6 The OJIP chl *a* fluorescence transients (log time scale) recorded in dark-adapted mulberry genotypes (a) KL, (b) MR2, (c) S13 and (d) V1 grown at the experimental plots of University of Hyderabad. Data were recorded during midday at the summer month of March (for two consecutive years: 2009 and 2010). Each fluorescence transient is mean of transients from six representative trees. Raw chl *a* fluorescence transient curves exhibiting fluorescence intensity (expressed in mV) were recorded between 0.1 to 1000 ms time period. All measurements were recorded on fully expanded leaves of 3rd-4th position from the shoot apex. Energy pipeline models (leaf model) of phenomenological fluxes were developed using Biolyzer software version vl 31. All flux parameters including (e) ABS (light energy absorption), TR (trapping of excitation energy), ET (conversion of excitation energy to electron transport) and DI (energy amount dissipated from PSII) were expressed per excited leaf cross-section (CSm). Here, the phenomenological fluxes during midday were presented for all four mulberry genotypes including (f) KL, (g) MR2, (h) S13 and (i) V1. The leaf model provides a visualization of the activation of the reaction centers (RCs) and clearly shows functioning of light energy absorption, trapping of excitation energy, energy conversion and energy dissipation from PSII per leaf cross section.

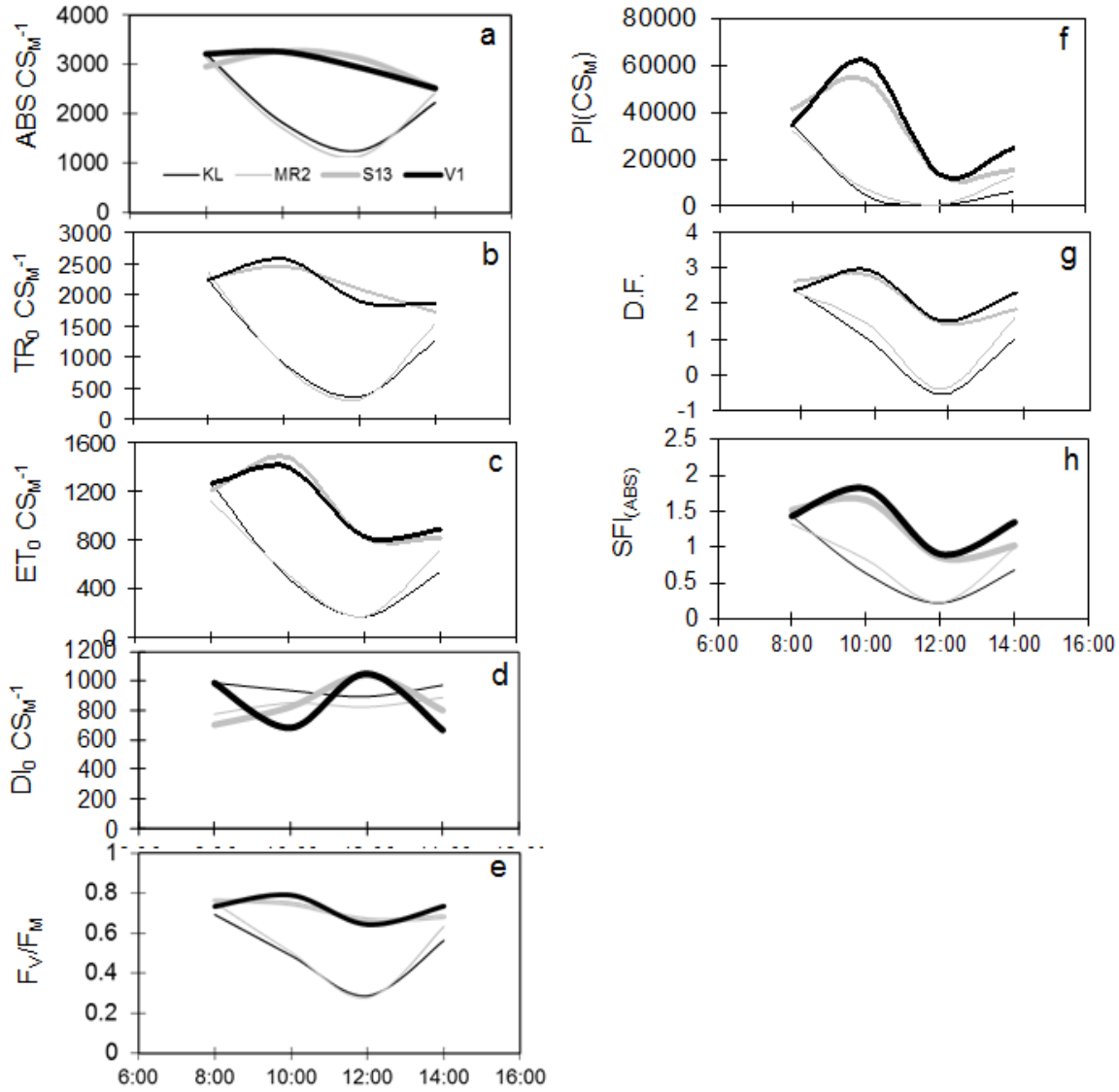

Fig. 5.7 Phenomenological fluxes per leaf cross section (CSm) and performance index measured diurnally in four drought-stressed mulberry genotypes (KL, MR2, S13 and V1) grown at the experimental plots of University of Hyderabad, Hyderabad. Data were recorded during the summer month of March (for two consecutive years: 2009 and 2010) Values are mean ± SD of repeated measurements from six representative trees. ANOVA was used to compare values obtained from different genotypes. The flux parameters recorded include (a) light energy absorption per leaf cross section (ABS CSm^{-1}), (b) trapping of excitation energy per leaf cross section (TR CSm^{-1}), (c) electron transport per leaf cross section (ET CSm^{-1}) and (d) energy dissipation per leaf cross section (DI CSm^{-1}). Genotypic differences were also recorded in diurnal (e) F_v/F_m (f) overall performance index (PI(CSm)) of PSII per leaf cross section, (g) driving force (D.F.) and (h) structure-function index (SFI) of PSII. Data were calculated from JIP-test based on the theory of energy flow in PSII using Biolyzer 4HP v.3.306 (according to Strasser et al. 2004). All fluorescence measurements were taken *in-situ* on upper canopy leaves (same leaves used for gas exchange analyses).

P-step (**Fig. 5.6a,b**). However, the drought tolerant S13 and V1 exhibited typical OJIP transients where all the phases of fluorescence rise were observed with significant attenuation in JI and IP phases (**Fig. 5.6c,d**). Diurnal changes in phenomenological flux parameters recorded among the four genotypes are presented in **Fig. 5.7**. During midday, ABS/CSm was significantly higher (~30%) in drought tolerant S13 and V1, when compared to drought-susceptible KL and MR2. TR_O/CSm showed gradual draw-down with increase in solar hour and recorded the minimum value during midday (12.00 h) in KL and MR2, however, in S13 and V1, the decrease was minimal. Same trend was also recorded in case of ET_O/CSm, where midday values of ET_O/CSm in KL and MR2 was ~55% lower than the values recorded during 10.00 h. However, S13 and V1 had higher ET_O/CSm throughout the diurnal timespan when compared to other genotypes. Unlike TR_O and ET_O/CSm, DI_O/CSm values were significantly ($P<0.05$) higher during midday particularly in S13 and V1, when compared to KL and MR2. Genotype V1 and S13 also maintained significantly higher F_v/F_m values throughout the diurnal timespan when compared to KL and MR2. Significantly strong midday depression was recorded in PI/ CSm and D.F. in all four mulberry genotypes with higher draw-down in KL and MR2 when compared to S13 and V1. The $SFI(_{ABS})$ values were significantly higher in S13 and V1 and also showed a marginal midday depression in those genotypes, whereas a strong decrease in $SFI(_{ABS})$ was recorded in KL and MR2 and overall the $SFI(_{ABS})$ values were also much lower in those genotypes than compared to S13 and V1.

Exp phase- II: Meteorological conditions and soil drought

During exp phase-II, the meteorological variables including T_{max}, T_{min}, RH, PP, PAR and VPD did not differ between the treatments (i.e. between control and water-stressed plots) and therefore, for each variable, the mean value was calculated and presented. Monthly T_{max} and T_{min} values ranged from 41.9ºC to 19.8ºC, 43.1ºC to 18.4ºC and 40.2ºC to 20ºC in Apr, May and Jun, respectively (**Fig. 5.8a**). Apr and May months were warmer than Jun with ~15 days >40ºC. RH values were generally less during Apr and Jun (ranged between 15 and 56%). However, recorded RH values were relatively higher in Jun (ranged between 33 and 64%) (**Fig. 5.8b**). During the study period, several spell of drought i.e. periods of

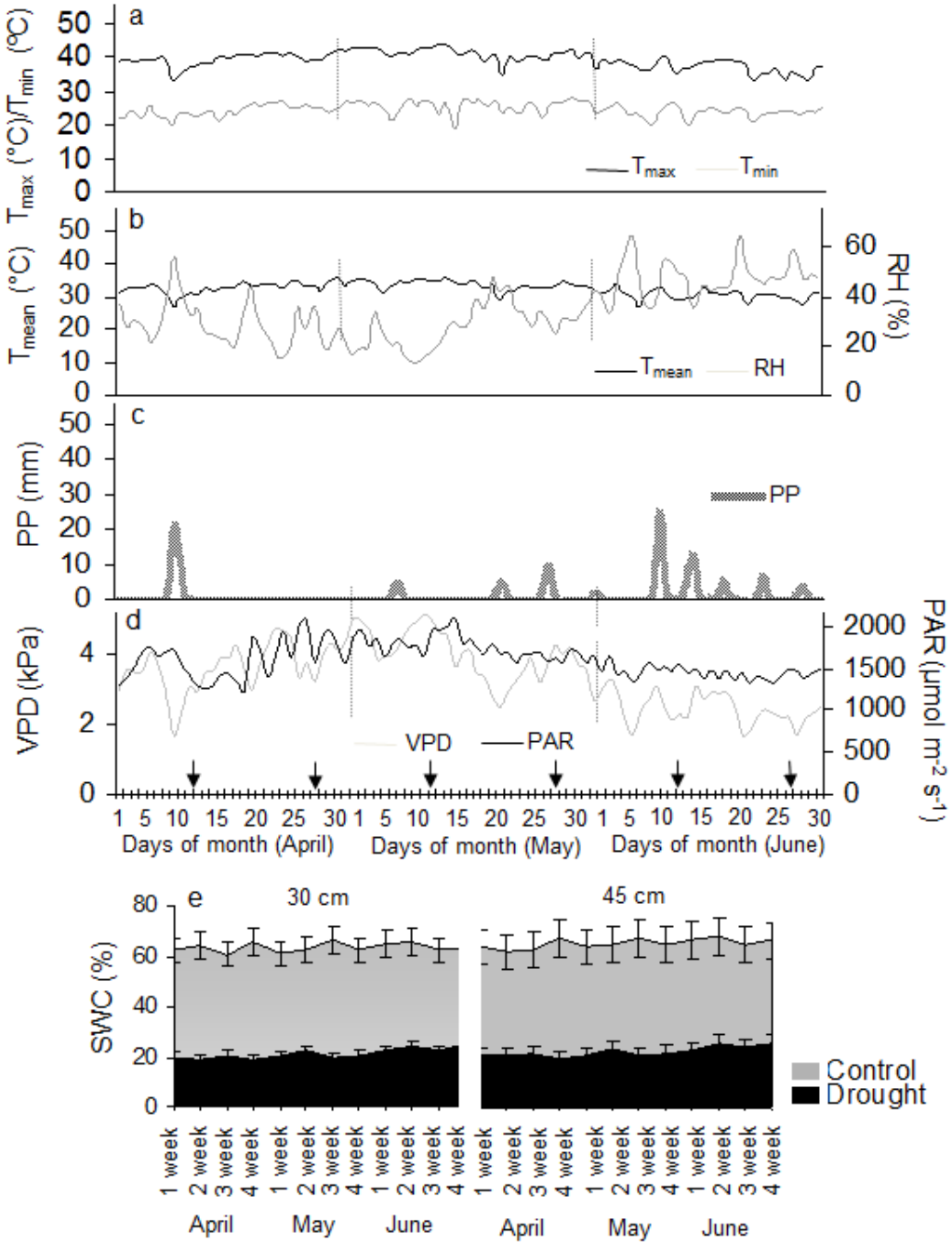

Fig. 5.8 Trend of meteorological conditions at the experimental site of University of Hyderabad monitored throughout the peak summer season from Apr to Jun (year 2009 and 2010). Data represent daily averages of (a) maximum (T_M) and minimum (T_m) air temperatures, (b) mean air temperature (T_{mean}) and relative humidity (RH), (c) precipitation (PP), (d) vapour pressure deficit (VPD) and photosynthetically active radiation (PAR). All meteorological parameters were recorded using automatic data logger installed in open field at a distance of 50 m from the plantation stands. Sampling dates are indicated by arrows. (e) Gravimetric soil water contents (SWC, expressed as percentage of oven-dried weight) were recorded at two soil depths (30 and 45 cm) at the study sites during the experimental period (Apr to Jun) of year 2009 and 2010. Values are mean ± SD of 5 soil samples taken beside each of the 6 studied trees.

10-20 days without significant rainfall occurred in Apr and May. In Jun, PP was relatively more than the previous two months, however, scanty and not intense enough (maximum PP recorded was only 24.8 mm) to balance the high seasonal evapotranspiration (**Fig. 5.8c**). The VPD remained in the range of 4.73 to 1.60 kPa and 5.14 to 2.15 kPa during Apr and May, respectively, whereas decreased in Jun and remained in the range between 3.29 and 1.61 kPa as a consequence of higher atmospheric RH (**Fig. 5.8d**). Excessive solar irradiance was recorded between Apr 3rd week and 2nd week of May when mean PAR (between 10.30-12.00 h) frequently roused above 1600 µmol m^{-2} s^{-1} and sometimes crossed 2000 µmol m^{-2} s^{-1}. The PAR values in Jun ranged between 1309 and 1643 µmol m^{-2} s^{-1}. (**Fig. 5.8d**). In drought-stressed plot, SWC was relatively less during Apr and May months (~20.2 ± 2.4%) when compared to the month of Jun (~24.6 ± 1.4%) (**Fig. 5.8e**). The few mm of PP during Apr, May and Jun months influenced only the top soil layer for a limited time period and could not be retained longer due to poor water holding capacity of the soil. Overall, the present data elucidate that the soil in the water-stressed plot contained significantly lower levels of moisture (~64% less) than the control plot (~62.5% SWC). The SWC did not differ significantly at 30 and 45 cm soil depths in both control and drought-stressed plots.

Exp phase-II: Leaf gas exchange functions in genotype V1

Photosynthetic leaf gas exchange functions during representative weeks as well as on diurnal basis are shown in **Fig. 5.9**. Drought stress significantly ($P<0.05$) reduced P_n in water-stressed stand when compared to control counterparts (**Fig. 5.9a**). Mean P_n values recorded during Apr were 7.2 and 12.3 µmol m^{-2} s^{-1} in dry and control plots, respectively. During May, P_n roused higher (~8.2 µmol m^{-2} s^{-1}) in drought-stressed stands, while in control (~12.8 µmol m^{-2} s^{-1}) no significant change was recorded. With the advent of Jun (when VPD and T_{mean} were comparatively less than previous two months), P_n values were slightly enhanced in drought-stressed stand (~8.6 µmol m^{-2} s^{-1}), however, in control stand no significant change in P_n was detected (**Fig. 5.9a**). The diurnal course of P_n showed clear difference between two treatments (**Fig. 5.9b**). P_n values in both treatments increased in the morning between 08.00 and 10.00 h, thereafter, mean P_n was more or less stable in control stands until 11.00 h and then started to show drawdown during midday (42% reduction)

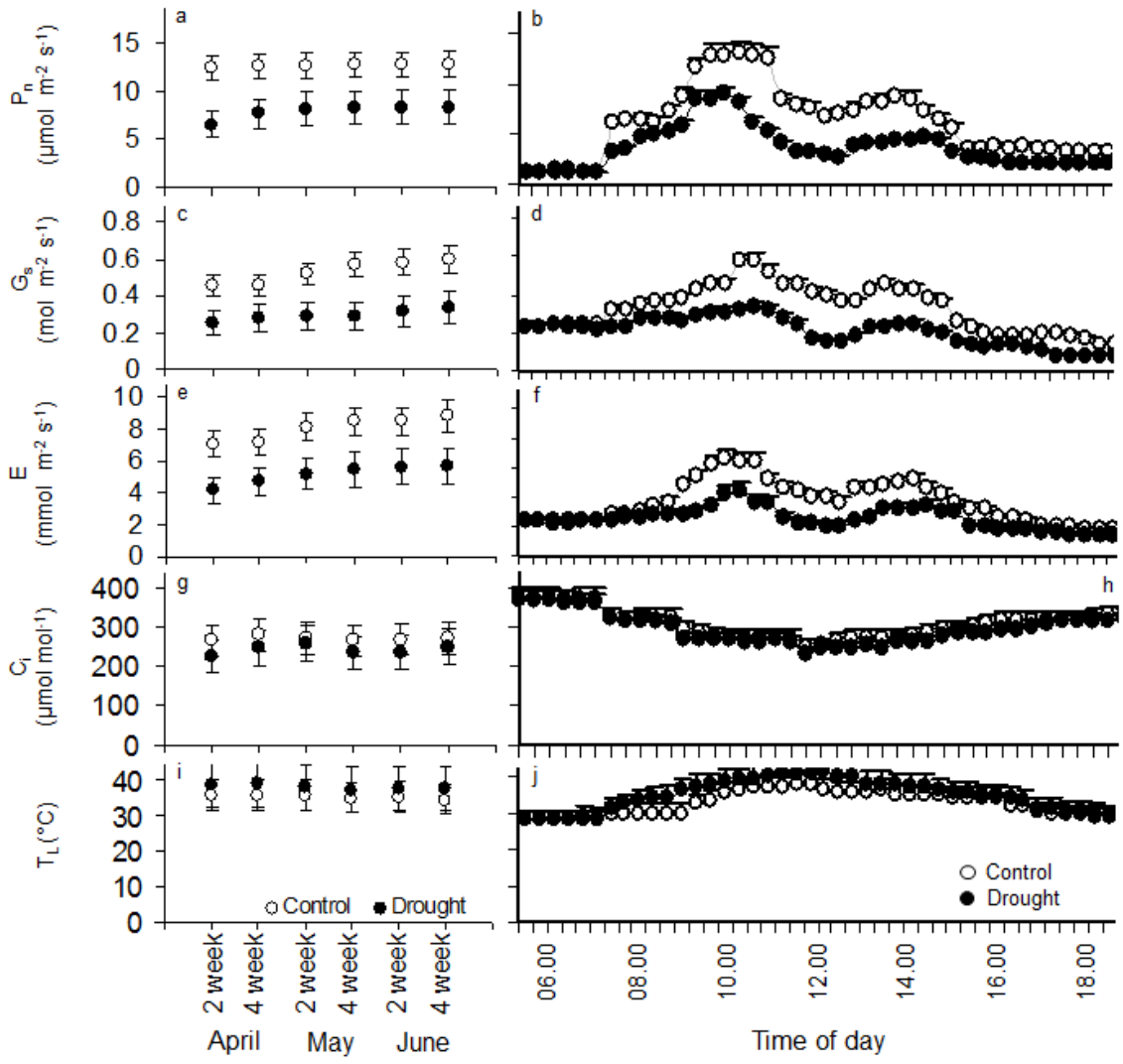

Fig. 5.9 Comparison of photosynthetic leaf gas exchange characteristics between control and drought-stressed mulberry trees (genotype V1, *M. indica*) grown at the experimental plots of University of Hyderabad. Values presented are mean of data recorded during peak summer months (April to June) of year 2009 and 2010 to track differences in (a) weekly and (b) diurnal trends of net photosynthetic rates (P_n), (c) weekly and (d) diurnal trends of stomatal conductance (G_s), (e) weekly and (f) diurnal trends of leaf transpiration rate (E), (g) weekly and (h) diurnal trends of sub-stomatal CO_2 concentration (C_i) and (i) weekly plus (j) diurnal trends of leaf temperature (T_L). Diurnal trends were analyzed on six different sunny days. Values are mean ± SD of 6 studied trees (n = 6).

followed by afternoon recovery (approximately 66% of maximum P_n), however not to a full extent (**Fig. 5.9b**). However, in drought-stressed stands, P_n values started decreasing soon after 10.00 h and showed gradual down-regulation during midday (56% reduction) followed by late afternoon recovery to approximately 52% of maximum P_n. Following the

monthly trend of P_n, the G_s and E variables in drought-stressed trees also showed moderate but significant ($P<0.05$) increment gradually from Apr to Jun. During Apr, G_s recorded in drought-stressed plants was ~0.25 mol m^{-2} s^{-1} and by the end of Jun, the value increased to ~0.36 mol m^{-2} s^{-1} (**Fig. 5.9c**), whereas in control counterparts, G_s was always higher than the drought-stressed stands and ranged from 0.42 to 0.58 µmol m^{-2} s^{-1} between Apr and Jun. During Apr, E values were approximately 38% less in the drought-stressed trees (~4.6 mmol m^{-2} s^{-1}) when compared to controls (~7.4 mmol m^{-2} s^{-1}), while in Jun end, the values increased to 5.7 and 8.8 mmol m^{-2} s^{-1} in drought-stressed and control trees, respectively (**Fig. 5.9e**). From the diurnal pattern, it was evident that G_s peaked in the morning (around 10.00 h) reaching maximum values of 0.34 and 0.58 mol m^{-2} s^{-1} for water-stressed and control plants, respectively, but declined at midday and resumed moderately in later part of the day after 13.30 h (**Fig. 5.9d**). Control and drought-stressed stands did not differ significantly in C_i on the representative weeks as well as during diurnal course of study (**Fig. 5.9g,h**). Nevertheless, in both treatments, a slight reduction in C_i was recorded during midday, however, the magnitude was not comparable with P_n and G_s. T_L was moderately higher in drought-stressed leaves than compared to controls ranging from 37.0ºC to 39.1ºC and 34.3ºC to 35.8ºC, respectively (**Fig. 5.9i**). The diurnal time course showed moderate but gradual progression in T_L in both the treatments starting from 08.00 h and reaching to maximum during midday (**Fig. 5.9j**). T_L values recorded in drought-stressed plants at midday was higher (~40.8ºC) when compared to the controls (~36.4ºC), however, in the later part of day (from 15.00 h onwards), T_L of drought-exposed trees decreased steadily and thereafter no significant difference could be determined between the values recorded for both treatments.

Exp phase-II: Operational range of Ψ_L, leaf wilting and stomatal response in genotype V1

Trends in Ψ_L did not show large differences under control conditions either in Apr, May or Jun. The only significant difference found in Apr was at midday (12.00 to 13.00 h) when Ψ_L was significantly ($P<0.05$) lower in controls compared to other two months. In case of drought-stressed trees, diurnal time course of Ψ_L showed that Ψ_{pd} and Ψ_{md} values were always significantly ($P<0.05$) lower than the control counterparts and the decrease in Ψ_L was more substantial for Ψ_{md} than for Ψ_{pd} ($\Delta\Psi_L$ was more) (**Fig. 5.10a**).

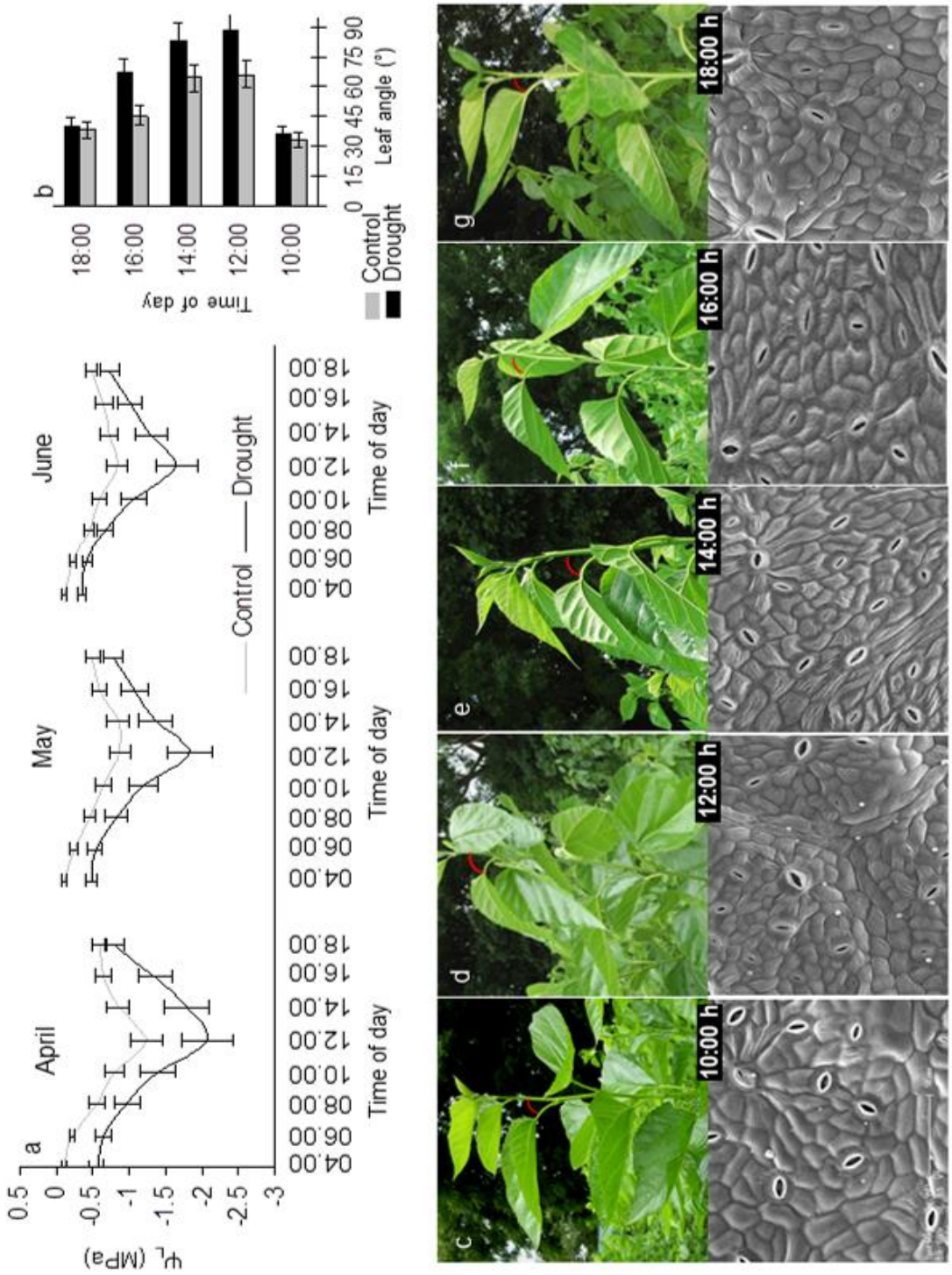

Fig. 5.10 Leaf water relations, visual assessment of leaf wilting and SEM studies of stomatal opening/closure in control and drought-stressed mulberry trees (genotype V1, *M. indica*) grown in the experimental plots of University of Hyderabad, Hyderabad. All data collection and samplings were conducted during peak summer months (Apr to Jun) for studying (a) diurnal course of leaf water potential (Ψ_L) and (b) diurnal changes in leaf angle recorded in control and drought-stressed V1 stands. For measuring Ψ_L, fully expanded, upper canopy leaves were sampled. Values presented are mean ± SD of data obtained from year 2009 and 2010. Diurnal course of leaf wilting was visually assesses and photographed both in control and drought-stressed trees, however, only photographs from (C-G) drought conditions taken at 10:00, 12:00, 14:00, 16:00 and 18:00 h are represented here. Likewise, the scanning electron micrographs of only drought-stressed leaf samples showing stomatal opening/closure conditions in abaxial leaf surface on respective solar hour are represented here.

Monthly means of Ψ_{md} recorded in drought-stressed trees were -2.0, -1.8 and -1.6 MPa for Apr, May and Jun, respectively, whereas in well-watered controls the values were -1.2, -0.88 and -0.84 during Apr, May and Jun, respectively (**Fig. 5.10a**). The recorded gas exchange and Ψ_L values were in similar range to those reported for *Quercus cerris* at Mediterranean forest climate which also showed mid and late season Ψ_{md} values more negative than isohydric *Q. pubescens* (Tongnetti et al. 2007). In early part of day until 10.30 h, both control and drought-stressed trees did not show much wilting sign (~35° leaf angle). However, with progression in solar hour, particularly between 12.00 to 14.00 h, leaf wilting was recorded in drought-stressed trees (~85.5° leaf angle), more conspicuously than controls (~65° leaf angle) (**Fig. 5.10b-e**). During later part of the day, both control as well as water-stressed plants revived gradually from wilting stage and by 18.00 h the leaves came back to their normal conditions (**Fig. 5.10b,f,g**). SEM studies of leaf abaxial surface showed that both in control and drought treatment, stomata were closed in the morning and gradually opened with increase of ambient irradiance and temperature. Between 10.00 to 11.00 h, the mean stomatal aperture reached its maximum (data not shown) in leaves of both treatments. During midday (around 12.00 to 13.00 h) the mean stomatal aperture size was slightly reduced in drought-stressed leaves compared to controls (data not shown), nevertheless, most of them were open showing no significant patchiness. Till 15.00 h stomata were all open in the drought-stressed stands thereafter, in both control and water-stressed plants gradual stomatal closing occurred.

Exp phase-II: Changes in PSII characteristics in genotype V1

Diurnal changes in F_V/F_M were moderate in both drought-stressed and control stands (**Fig. 5.11a**). During midday (12.00 h), however, a slight depression in F_V/F_M was recorded in the mulberry stands under both the treatments and the water-stressed stand exhibited slightly higher F_V/F_M values when compared to the controls. Throughout Apr and May, the midday F_V/F_M values was moderately, however, significantly ($P<0.05$) higher in drought-stressed trees (ranging from 0.688 to 0.706) throughout Apr and May, when compared to controls (ranging from 0.657 to 0.696) (**Table 5.2**). During Jun, no significant difference was recorded in F_V/F_M between the two treatments (**Table 5.2**). ABS/CSm was significantly less (~55.9%) in drought-stressed trees when compared to controls, however,

no apparent changes in the diurnal pattern of ABS/CSm was recorded in the stands under both the water regimes (**Fig. 5.11b**). The drought-stressed stand exhibited a reduction of 55.5% in TR_O/CSm when compared to the controls; however, no significant midday depression in TR_O/CSm was recorded in the drought-exposed stand as it was evident in well-watered trees (**Fig. 5.11c**). A strong reduction in ET_O/CSm was recorded in the water-stressed trees; however, no significant changes in ET_O/CSm occurred throughout the diurnal time span. In contrary to drought-stressed stand, the controls even though always maintained higher ET_O/CSm, underwent apparent midday depression and the ET_O/CSm value was recovered only at 18.00 h (**Fig. 5.11d**). Unlike drought-stressed trees, DI_O/CSm was substantially greater in the well-watered trees throughout the diurnal course of time and the DI_O/CSm values were higher during midday, whereas in water-stressed stand, no significant diurnal alterations occurred in the DI_O/CSm (**Fig. 5.11e**). The controls maintained a higher PI(CSm) in compared to the drought-stressed stands, however, exhibited an apparent reduction in PI(CSm) during midday and the values only recovered after 16.00 h. Unlike controls, the water-stressed stand exhibited only a mild midday depression in PI(CSm) and the values recovered after 16.00 h (**Fig. 5.11f**). In controls, midday PI(CSm) values were remarkably less throughout Apr and May when compared to Jun, whereas in water-stressed trees, the midday values did not differ significantly from Apr 4th week to Jun 2nd week and thereafter showed significant increment on Jun 4th week (**Table 5.2**).

Table 5.2 Weekly F_v/F_m and PI(CSm) recorded in control and drought-stressed V1 stands. Values are means ± SD.

	Fv/Fm		PI(CSm)	
	Control	Drought	Control	Drought
Apr 2 week	0.65 ± 0.02	0.68 ± 0.03	3658.5 ± 233.2	2345.3 ± 156.5
Apr 4 week	0.66 ± 0.01	0.69 ± 0.04	5862.5 ± 312.4	5245.5 ± 286.4
May 2 week	0.66 ± 0.03	0.70 ± 0.03	8008.7 ± 325.4	5537.4 ± 303.4
May 4 week	0.69 ± 0.03	0.70 ± 0.02	8800.9 ± 343.4	5825.3 ± 323.4
Jun 2 week	0.71 ± 0.02	0.71 ± 0.02	10156.3 ± 497.3	5957.5 ± 358.4
Jun 4 week	0.71 ± 0.02	0.71 ± 0.03	12224.3 ± 512.7	6956.8 ± 367.4

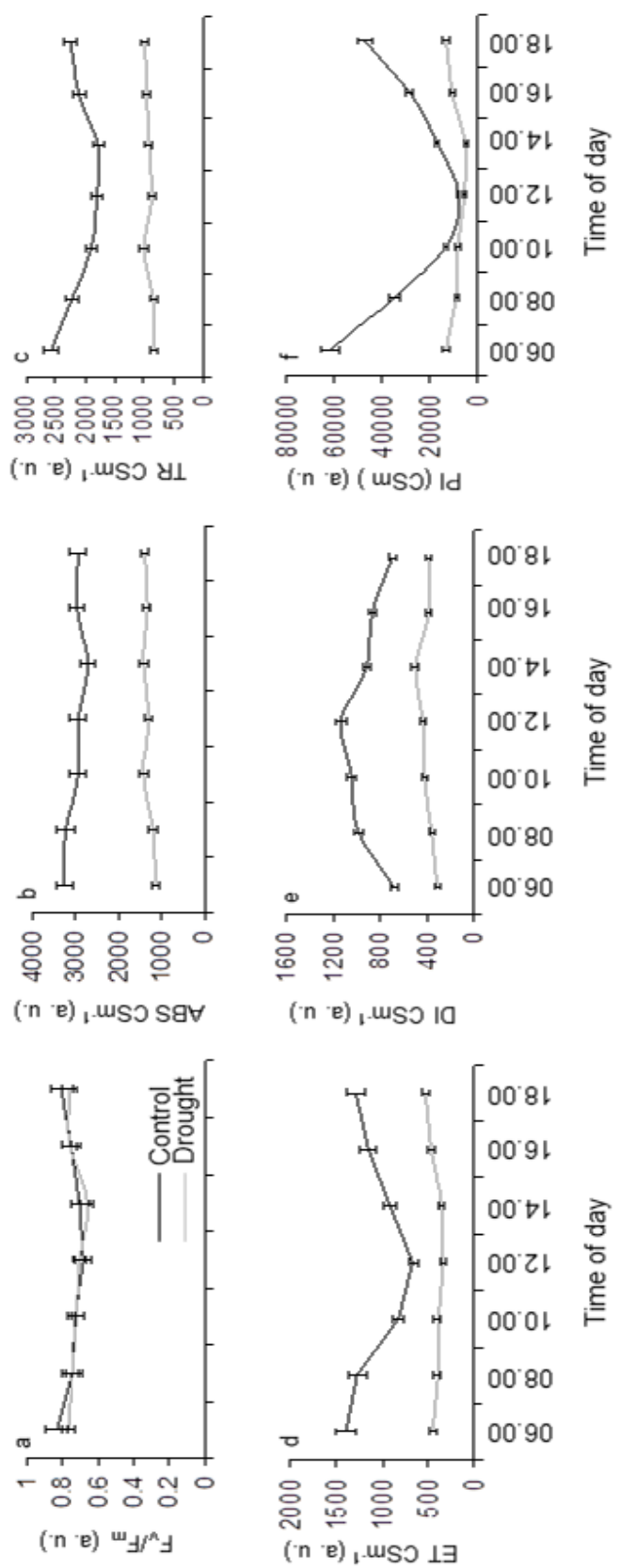

Fig. 5.11 Diurnal changes in different PSII characteristics recorded in control and drought-stressed V1 stands. Photochemical efficiency of PSII, phenomenological fluxes per leaf cross section (CSm) and performance index measured diurnally in control and drought-stressed mulberry genotype V1 grown at the experimental plots of University of Hyderabad, Hyderabad. Data were recorded during the paek summer months of Apr to Jun (for two consecutive years: 2009 and 2010) Values are mean ± SD of repeated measurements from six representative trees (n = 6). ANOVA was used to compare values obtained from different genotypes (*P*-value for comparison of treatments: < 0.05). a.u., arbitrary unit. The parameters recorded include (a) F_v/F_m (b) light energy absorption per leaf cross section (ABS CSm^{-1}), (c) trapping of excitation energy per leaf cross section (TR CSm^{-1}), (d) electron transport per leaf cross section (ET CSm^{-1}) (e) energy dissipation per leaf cross section (DI CSm^{-1}) and (f) overall performance index (PI(CSm)) of PSII per leaf cross section. Data were calculated from JIP-test based on the theory of energy flow in PSII using Biolyzer 4HP v.3.306 (according to Strasser et al. 2004). All fluorescence measurements were taken *in-situ* on upper canopy leaves (same leaves used for gas exchange analyses).

Exp phase-II: Growth and biomass

Drought stress caused reduction in above ground biomass and associated variables with significant differences between the treatments (**Table 5.3**). H_t was reduced to 23.2% in the drought-stressed stands when compared to the controls. In drought-stressed trees, T_{STM} was reduced to 19%, whereas T_B was substantially high (42.6% more) when compared to the well-watered trees. Drought stress caused significant reduction in T_{SL} as well as in L_f, S_f and AG_{fw}. In drought-exposed stands, almost 25.8%, 27.3% and 26.5% reductions were recorded in L_f, S_f and AG_{fw}, respectively when compared to well-watered counterparts. Drought-stressed stands exhibited 36.8% and 32% reductions in L_d and AG_w, respectively when compared to the controls. The AG_{dw} was reduced to 31.6% upon drought exposure.

Table 5.3 Growth and biomass yield characteristics in SRC grown V1 stands under control and drought stress treatments in the experimental plots of University of Hyderabad.

Yield variables	Control	Drought	*P*
H_t (cm)	324.2 ± 16.0	248.9 ± 7.79	0.002
T_{STM} (no. plant^{-1})	10.5 ± 0.67	8.5 ± 0.76	ns
T_B (no. plant^{-1})	15.2 ± 0.94	26.5 ± 1.85	<0.001
T_{SL} (cm plant^{-1})	2680.3 ± 49.2	1883.3 ± 36.2	<0.001
L_f (g plant^{-1})	1076.2 ±23.3	798.5 ±16.5	<0.001
S_f (g plant^{-1})	906.4 ±21.2	658.5 ±9.4	<0.001
AG_{fw} (g plant^{-1})	1982.9 ±17.2	1457.0 ±17.3	<0.001
L_d (g plant^{-1})	463.8 ±12.3	292.7 ±8.5	<0.001
AG_w (g plant^{-1})	497.4 ±11.2	337.8 ±8.8	<0.001
AG_{dw} (g plant^{-1})	940.8 ±22.1	642.6 ±11.8	<0.001

Discussion

Leaf gas exchange characteristics of drought-exposed mulberry trees demonstrated clear down-regulation in gas exchange functions and the quantitative changes in P_n, G_s and E were quite similar as documented in our earlier reports from field observations (see chapter 3). The present study ascertains that a common and close coupling among P_n, G_s and E exists, which can account for the recorded concomitant increment in all those three traits when the summer drought conditions became less intense during Jun. It is the first time that the drought-stressed mulberry trees of *M. indica* have been shown to undergo diurnal cycles of loss and recovery of leaf gas exchange functions. The diurnal variation of P_n was

characteristic of typical midday depression and a recovery in the afternoon. The lower P_n peak recorded in afternoon than compared to morning can be attributed to high solar radiation, air temperature and VPD conditions of the hot semi-arid steppe climate and might also be due to reduced water flow from soil to roots which altogether can potentially impose stomatal and non-stomatal limitations to P_n (Fu et al. 2006; Chaves et al. 2009). The recorded pattern of C_i in drought-stressed stands elucidates that if the main limitation to P_n was stomatal closure, then we would expect a draw-down in G_s with concomitantly decreased C_i values (Cornic 2000), however, the magnitude of decrease in C_i as recorded in the present study was much less than the decrease in P_n indicating prevalence of non-stomatal factors which might have limited P_n in drought-stressed mulberry leaves (Medrano et al. 2002; Chaves et al. 2009). There are possibilities to overestimate C_i in water-stressed, heterobaric mulberry leaves due to stomatal patchiness (Gomes et al. 2007). However, in the present field study, the effect of patchy stomatal closure on C_i estimation might be less in mulberry as the trees were not suddenly exposed to intense drought, rather maintained at a specific low water regime conditions. In our study, no significant decrease in C_i was observed. It is likely that an increased CO_2 efflux from photorespiration, due to an increased T_L, is responsible for the difference in extent of decline in P_n and C_i. Increased photorespiration is a common response to water stress, and may be a mechanism to avoid photoinhibitory damage when photosynthesis is reduced by carbon availability (Rodríguez et al. 2005). The drought tolerant genotypes maintained significantly higher G_s and during midday, the G_s values were not so less to reduce substantially leaf carbon gain when compared to the drought susceptible genotypes. The diurnal pattern of E showed that throughout the course of day, the drought-stressed V1 trees tended to maintain E more than 50% of the normal rate shown by controls preventing rapid increment in T_L which further affirm less stomatal regulation to leaf gas exchange and elucidate non-conservative use of water under field drought conditions. The drought tolerant genotype S13 and V1 had higher E among others under moderate field-drought conditions, which may come from their ability to increase root biomass and associated water uptake under drought when compared with other drought susceptible genotypes (Larchevêque et al. 2011).

WUE_i is a parameter often used when comparing water use efficiency of different species or genotypes because it allows comparisons at different leaf-to-air vapor pressure

deficit. It is important to remember that what matters in terms of carbon and water balances is P_n/E (WUE_i), i.e. the carbon gain per unit real water loses (Pou et al. 2012). The drought tolerant genotypes kept opened stomata and active transpiration, even at peak summer time when compared to the drought susceptible genotypes which exhibited a more conservative strategy, by rapidly reducing transpiration. The drought tolerant genotypes has a more risky strategy by keeping high P_n, G_s and E rates under drought conditions which resulted in less WUE_i when compared to the drought susceptible genotypes having opposite strategies. Obviously, unlike control stand, the drought-stressed V1 trees could not maintain higher values of P_n and associated leaf gas exchange functions, nevertheless, the trees showed tolerance against drought and did not restrict gas exchange to a degree that highly elevated two-peaked diurnal curve (indication of strong 'midday depression') would be observed as reported earlier in drought avoiding *Acacia* and *Quercus* species (Otineo et al. 2005; Tognetti et al. 2007). The KSL decreased significantly in the drought susceptible mulberry genotypes than the drought tolerants when drought was moderate, suggesting early cavitation, which might have also led to simultaneous decrease in G_s. the drought susceptible genotypes exhibited an exaggerated dehydration avoidance mechanism associated with stomtal closure that must be linked to low KSL, and with the disadvantage that declining Ψ_L might have approached the threshold for xylem cavitation. Hydraulic conductance is associated with water uptake at the root surfaces, root:leaf surface area ratio or inherent absorption capacity, root permeability and an effective water transport system (Tyree and Sperry 1988; Ni and Pallardy 1990; Otineo et al. 2005). At high soil water content, soil resistance to water flow is small and any observed differences in hydraulic conductance should be largely attributed to differences in plant resistance. The rooting vigor of the tested mulberry genotypes depicts that the drought tolerant genotypes have a more robust water-conducting system than the drought suscpetibles. Generally hydraulic conductance is expected to decline with increasing water stress as a result of increasing resistances along the conducting pathway (Sack and Holbrook 2006). There might be two possible reasons associated with higher KSL as observed in the drought tolerant mulberry genotypes: (1) a more competent transport system developed following the imposition of water stress and (2) there was an improved balance between the absorbing root and transpiration leaf surface area in the water-stressed plants. The midday day xylem sap flow

showed significantly higher values in the drought tolerant genotypes when compared to the drought susceptibles. Such low sap flow rate as recorded in drought susceptible genotypes can be correlated to their rooting pattern which might be not sufficiently vigorous to explore water from soil depth. The presence of roots in dry edaphic zones might provide sufficiently strong signals for trees to adopt prudent strategies to limit water usage. Integration of such information along with knowledge of hydraulic conductance might be useful to infer the onset, or severity of water stress in mulberry farms.

The trend in diurnal Ψ_L recorded in drought-stressed V1 was characterized by large fluctuation in midday Ψ_L and the obtained Ψ_L values were in similar range to those reported for *Quercus cerris* at Mediterranean forest climate which also showed midday Ψ_L values more negative than morning (Tongnetti et al. 2007). Genotype V1 presented the highest Ψ_L values at predawn and the lowest during midday, the value that integrates and reflects all environmental influences on the plants' internal water balance, indicating least favorable condition for the plant (Himmelsbach et al. 2012). Plant can make up its water deficit during night, that is why many authors consider Ψ_{pd} values as a true equilibrium of soil water potential (not measured in the present study) and plant water status (Bucci et al. 2004b; Himmelsbach et al. 2012). Furthermore, minimum Ψ_{pd} values are considered to express the static water stress (Sellin 1998). The midday water potential can be split into the base water potential (Ψ_{pd}) and diurnal depression (Ψ_d), which is mainly influenced by atmospheric conditions and plant hydraulic capacity, indicating the level of dynamic water stress (Himmelsbach et al. 2012). This was clearly confirmed from the significant correlations between Ψ_d and daily mean RH, and VPD. Weak stomatal control at low Ψ_{md} could lead to excessive water loss particularly during dry summers, resulting in low P_n because of non-stomatal limitation and xylem cavitation during drought (Donovan et al. 2000). However, a greater efficiency in hydraulic transport by the xylem of drought tolerant genotypes might have allowed higher E in those genotypes, thus facilitating higher P_n. Such leaf-water relations recorded in drought-stressed mulberry trees are consistent with the established theory of anisohydric control of water use where plants exert less stomatal control and Ψ_L fluctuates with evaporative demand (Schultz 2003; Chaves et al. 2010). According to the visual assessment categories prescribed by Engelbercht et al. (2007), between 12.00 to 14.00 h the observed wilting stage of the water-stressed mulberry

leaves can be included under category 3 (strong leaf angle change but no cell death) whereas, leaf wilting in control plants (photograph not shown) matched to category 2 (moderate change in leaf angle). These findings further strengthen the anisohydric functionality of V1 depicting less stomatal control over leaf moisture loss under soil water stress conditions. At water potentials lower than -2 MPa, it is like that severe vessel embolism might occur due to the lack of conservative pattern and could cause hydraulic failure. But according to McDowell et al. (2008), genotype V1 should be more resistant to long-term drought as it is the most anisohydric among the tested genotypes and thus has the highest ability to avoid carbon starvation under drought not too intense to cause hydraulic failure. It was also recorded that the water-stressed V1 trees were able to restore Ψ_L again in the evening time during sunset indicating that severe xylem cavitation did not occur during the period of high evaporative demand and the effective water transport to the shoots was restored (Otieno et al. 2005). The stomatal response further strengthened the anisohydric strategy of V1 depicting less stomatal control over G_s under decreasing soil water conditions. Such lower sensitivity of stomata in anisohydric species was recently correlated to lower concentrations of ABA which is in anomaly to the isohydric plants that possess higher stomatal sensitivity owing to high ABA concentrations (Chaves et al. 2010; Lovisolo et al. 2010). Although iso- and anisohydric behaviors have been reported to depend on ABA physiology Tardieu and Simonneau 1998; Soar et al. 2006), it was previously suggested to also strongly depend on plant and leaf hydraulics in woody species (Vandeleur et al. 2009; Lovisolo et al. 2010). Moreover the dependency between whole plant hydraulic conductivity estimated from Ohm's law and Ψ_{md} was also shown previously as well as strong linear dependency was also recorded between leaf hydraulic conductance and G_s (Schultz 2003; Pou et al. 2012). The present study is the first documentation of anisohydric behavior in water-stressed *M. indica* species under hot semi-arid steppe climate of south India and further work is required to resolve the roles and interactions of chemical (ABA mediated) and hydraulic signals in controlling stomatal behavior in such anisohydric mulberry species.

Under the climatic scenarios of warmer and drier summer at our hot semi-arid steppe experimental site, we focussed on drought, high air temperature and irradiance induced effects on the light processing events through PSII. Several chl fluorescence characteristics

showed pronounced diurnal changes that are most probably caused due to different photoacclimation and photoprotection strategies. These changes in PSII apparently represent a regulatory adjustment of PSII to the demand for products of electron transport, and are unlikely to limit photosynthetic productivity. In drought tolerant genotypes, the marginal change in F_V/F_M recorded in water-stressed leaves were almost similar with our earlier reports from glasshouse experiments (see chapter 3 and 4) depicting that even at midday, the summer drought conditions of field also could not induce severe loss in photochemical efficiency of PSII. Although F_V/F_M values at midday were slightly lower in the drought tolerant genotypes than those obtained early in the morning and late afternoon, they were always in the range considered normal for healthy non-stressed plant. The maintenance of constant F_V/F_M values at midday throughout the study demonstrates the lack of drought-induced damage to PSII photochemistry, as has been reported also for many other species (Jimenez et al. 1999; Rodríguez et al. 2005). The role of carotenoids in protection of PSII under such conditions of excessive light which are enhanced in drought conditions is well-known (Rodríguez et al. 2005). To maintain such photostability of PSII photochemistry under drought stress, short-term acclimation strategies are crucial to control the imbalance between the absorbed light energy through the light harvesting complex and the amount of energy that is dissipated (Strasser and Tsimilli-Michael 2001). Analyses of phenomenological flux parameters derived from chl a fluorescence characteristic of PSII is an important complement to measure such short-term photoacclimatory responses in higher plants (Stirbet and Govindjee 2011). Our study for the first time documents the changes in phenomenological flux parameters in water-stressed *M. indica* trees. ABS/CSm that signifies absorption of photo flux by antenna chlorophyll molecules of PSII RCs, recorded moderate decrease in drought-stressed V1 which might be due to reduction in active RC/CSm as recorded in the present study. Moreover, the recorded decrease in TR_O/CSm also occurred mainly due to the decrease in the density of RCs. It is suggested that such changes in PSII reaction centers, can protect PSII apparatus from excess excitation energy enhancing photoprotection and photostability (Zhang et al. 2010; Slabbert and Krüger 2011). Altogether, the changes are harmonized with the responses that are usually induced in photosynthetic apparatus of higher plants when exposed to excessive light and drought conditions (Wilhelm and Selmar 2011). The

strong decrease in ET_O/CSm (during peak summer months) can be ascribed as compensatory strategy for the less pronounced decrease in ABS/CSm and TR_O/CSm and might have potentially contributed to photosynthetic down-regulation as recorded in our study. However, a gradual increment in the rates of ET_O/CSm during further time course indicates the inherent capacity of drought-exposed V1 trees to recover the same. Higher DI_O/CSm in drought-exposed stand indicates increased rate of thermal energy dissipation in the antennae of PSII which might have enhanced the protection of photosynthetic apparatus and prevented over-excitation of PSII reaction centres (Demetriou et al. 2007).

In fast growing plantations like mulberry, sustenance of yield is essential to profitability. However, in hot semi-arid steppe agroclimatic zones of south India, mulberry plantations often encounter seasonal summer drought as the crop is grown either under complete rainfed system or provided with very few irrigations and do not always receive optimal agronomical inputs including fertilizers and manures. Under such conditions, the cultivated mulberry genotypes should sustain their growth despite water limitation and maintain the integrity of photosynthetic processes so that the trees will be able to resume growth when water is once again available. In the present experiment, the drought tolerance characteristics of mulberry trees exposed to atmospheric and soil drought conditions have been successfully analyzed in the framework of plant ecophysiological behavior. Field investigations were undertaken on leaf gas exchange, photoacclimation and midday xylem sap flow characteristics associated with the sustenance of crop yield in drought-stressed mulberry genotypes cultivated under hot semi-arid steppe agroclimate of southern India. During drought-exposed conditions of the hot dry season, mulberry trees down-regulated leaf gas exchange functions, however, not at severe extent which would largely compromise with net CO_2 fixation. The drought tolerant genotypes maintained comparatively better hydraulic conductance which largely attributed to their high photosynthetic rates when compared to the drought susceptibles. Midday stem xylem sap flow was considerably higher in the drought tolerant genotypes compared to drought susceptibles and xylem sap flow rate scaled positively with transpiration and photosynthetic performance. Drought-stressed trees showed more negative Ψ_L values and less stomatal control over G_s depicting anisohydric water status regulation which is of advantage during seasonal summer drought in sustaining photosynthetic CO_2 fixation and

maintenance of tree growth and productivity. Further, SEM studies on diurnal stomatal opening/closure also confirmed low stomatal sensitivity of the studied tree species. Investigation of photochemical efficiency of PSII clearly indicated that drought stress coupled with excessive solar irradiance was a stress factor lowering the potential flux of electron per leaf cross section and substantially increasing the thermal dissipational loss of energy. Nevertheless, such photoacclimation strategies indicate controlled plant response to excessive light and might be crucial for photoprotection against overreduction of electron transport chain which might generate ROS. The present work highlights the scope of incorporating new parameters describing photosystem functioning, xylem sap flux and structure-function relationships of hydraulic system in various tree crop productivity models including mulberry, which currently are being implemented in a limited agroecosystems and holds potential to further fine tuning simulation-models of tree-soil-water interactions under global climate change scenario.

Genotypic Variation in Stem Wood Hydraulic Architecture in relation to Anisohydric Behavior

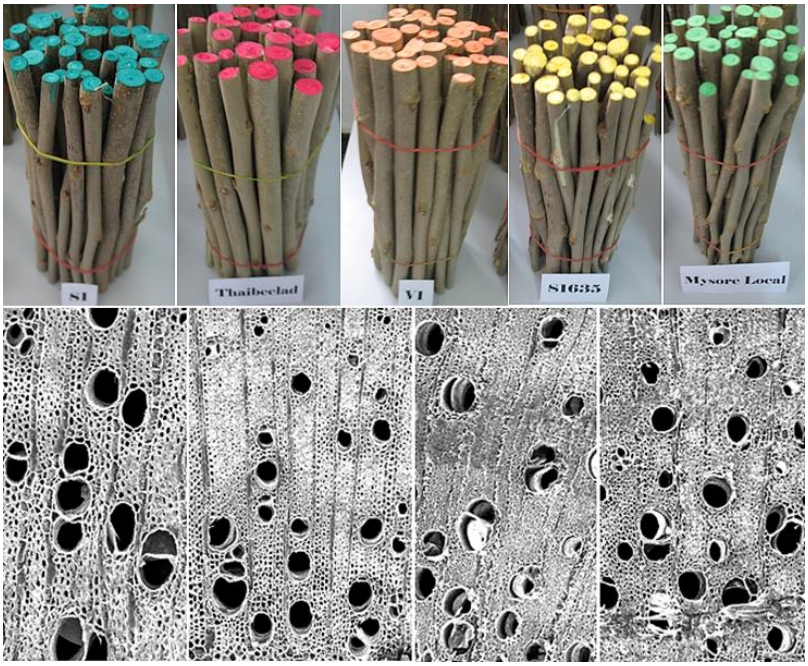

Chapter 6

Recently, stem traits in higher plants are emerging as core plant functional traits because of their immense importance in stability, defense, architecture, hydraulics, carbon gain and growth potential (Santiago et al. 2004; Chave et al. 2009). Stems of higher plants are generally considered to serve four major functions including mechanical function of supporting the plant in an upright position, conduction of water and soil nutrients from roots to leaves, conduction of carbohydrates and other assimilates from leaves to stem and roots and storage of assimilates (usually as starch) for future use. In arborescent monocotyledons, these four functions are distributed more or less evenly throughout the transverse section of the stem with quantification that the mechanical function is primarily at the stem periphery in the area of greatest stress where the fibrous sheaths of vascular bundles are most highly developed. Xylem and phloem serve the two respective transport functions, and the ground parenchyma is storage area. In conifers and most dicotyledonous trees, phloem and xylem are morphologically separate. Water transport and mechanical function are located in the woody cylinder, the xylem and storage takes place in vertical and radial parenchyma of xylem and phloem (**Fig. 6.1**).

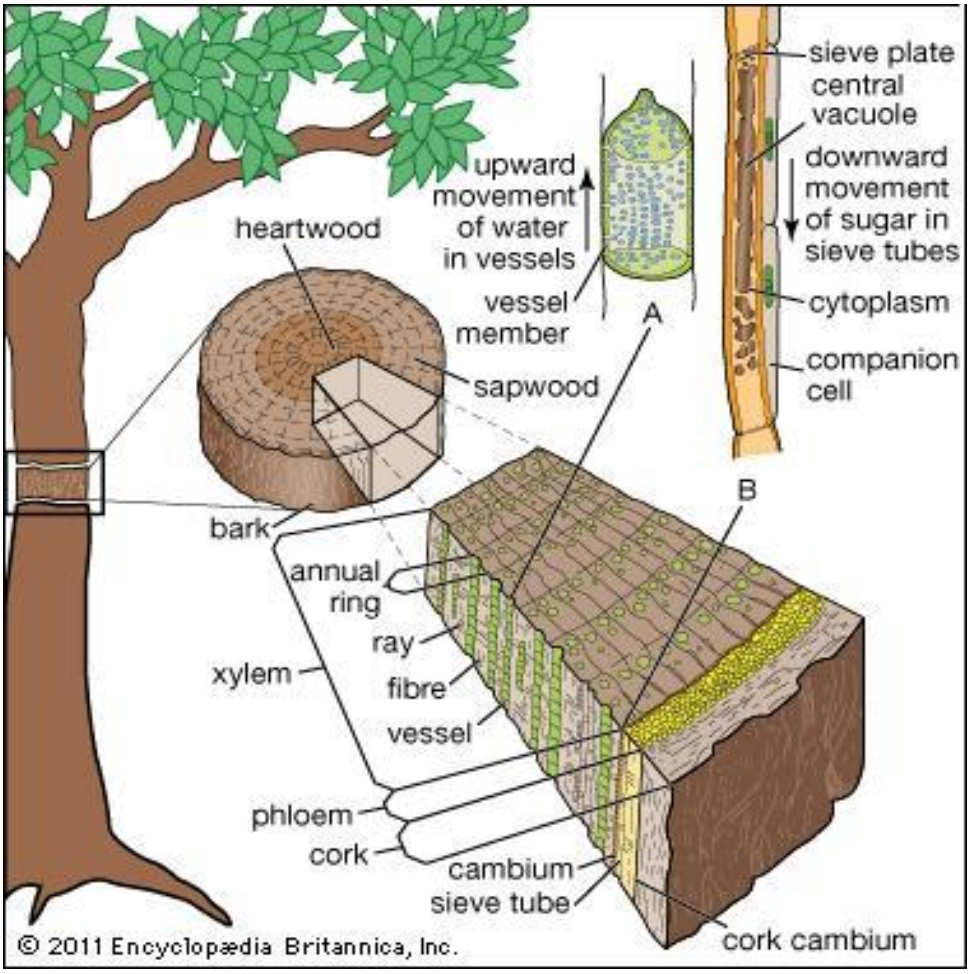

Fig. 6.1 Internal transport system in a tree. (A) Enlarged xylem vessel and (B) enlarged mature sieve element (*Credit: Encyclopædia Britannica, Inc.).*This image shows a typical cross-section of an woody stem. As a woody stem or tree trunk continues to grow, most of the cross-sectional area will be filled with secondary xylem. New vascular tissue is added at the vascular cambium, which is one of the two lateral meristems. The vascular cambium continually adds new secondary xylem to the outside of the existing xylem (just inside the vascular cambium), so the xylem area grows thicker and thicker. However, this stretches out the band of phloem, which must continue to add new cells to fill in the phloem band. The new secondary phloem cells are added to the inner part of the ring of phloem. The annual rings of phloem are not as clearly defined as those of xylem. The vascular cambium produces vascular tissue inside the stem (xylem and phloem); the cork cambium produces new cells on the outside, forming a protective layer for the stem. Since stems grow from the inside, the outer layers tend to get stretched thinner and thinner; the cork cambium fills in additional cells to ensure that the protective cork and epidermis form a continuous layer of bark around the stem.

Structurally, xylem is a network of interconnected conduits (Cruiziat et al. 2002; Tyree and Zimmermann 2002). The structure of xylem vessel has been known for decades (Braun 1959; Burggraaf 1972; Zimmermann, 1971) and was again presented recently by 3D-images of X-ray computed microtomography (Steppe et al. 2004) and series of cross-

sections taken with epifluorescence microscope (Kitin et al. 2004). In the xylem, connectivity corresponds to the average number of different neighbor conduits to which a conduit is connected. For instance, the capacity of a conduit to transport water will be limited by its own resistance only if there is no constraint to its water supply elsewhere in the network. Like a motorway without any access roads would be empty - never mind how many lanes it has, a xylem conduit will not conduct sap if it is not connected to a conducting cluster that connects roots to leaves (Loepfe et al. 2007). Following this logic, it seems reasonable to expect that the more conduits a conduit is connected to (i.e., the greater its connectivity), the higher will be the flow through it.

The main function of the xylem is to provide a low resistance pathway for water transport within the soil–plant–atmosphere continuum (SPAC). According to the cohesion-tension theory, water ascent in plants takes place in a metastable state under tension. This negative pressure in the xylem makes it vulnerable to cavitation, i.e., the expansion of gas bubbles in the conduits (Tyree and Zimmermann 2002). The two main properties that determine the overall transport efficiency of the xylem are its maximum hydraulic conductivity and its vulnerability to cavitation. A high maximum conductivity lowers its probability to become a bottleneck in the pathway between the soil and the leaves when plenty of water is available and, therefore, a limiting factor to photosynthetic capacity and plant growth (Brodribb and Feild 2000; Stiller et al. 2003). On the other hand, when water is scarce, the resistance to cavitation (and embolism) is crucial. A number of studies have shown that vulnerability to embolism is related to drought tolerance (Maherali et al. 2004; Martinez-Vilalta et al. 2002a; Sperry et al. 2002). Some experimental data suggest that these two goals (high maximum conductivity and high resistance to embolism) cannot be achieved independently, implying that there is a trade-off between maximum hydraulic conductivity and safety in the xylem, at least when comparing tissues within the same individual. However, the principles underlying this trade-off and knowledge of intermediate trait values are still poorly understood (Hacke et al. 2000; Lo Gullo and Salleo 1993; Mencuccini and Comstock 1997; Martinez-Vilalta et al. 2002b; Pockman and Sperry 2000; Tyree et al. 1994).

The conductivity of the xylem was classically estimated by adding up the conductivities of the conduits found in a cross-section of wood, using the Hagen-Poiseuille

equation to calculate the conductivity of each conduit (Zimmermann 1983). However, this calculation consistently overestimates the conductance measured experimentally on wood segments. The discrepancy (about 20-70% of measured conductivity) is universally attributed to the resistance of inter-conduit pit pores (Chiu and Ewers 1993; Lancashire and Ennos 2002; Tyree and Zimmermann 2002), as sap has to cross a porous membrane to flow from one conduit to the next. The overall hydraulic resistance is thus considered to be the sum of lumen resistance and inter-conduit resistance in series. Based on this assumption, it is possible to estimate inter-conduit resistance by substracting the calculated lumen resistance (using the Hagen-Poiseuille equation) from the resistance measured experimentally. By doing that, Sperry et al. (2005) concluded that inter-conduit resistance and lumen resistance are co-limiting, i.e., each is responsible for about half of the total resistance of a wood segment. But Schulte et al. (1987) showed that even after dissolving the porous membrane of the inter-conduit connections, the measured conductivity was still 30% lower than the conductivity predicted by the Hagen-Poiseuille equation. On the other hand, drought-induced embolism is believed to spread between conduits as a function of the maximum size of the pores in the inter-conduit membrane connecting them (air-seeding hypothesis; Zimmermann 1983). Pit pore size has often been estimated from vulnerability curves making direct use of the capillarity equation (e.g., Sperry and Tyree 1990) and a direct relationship between air-seeding pressure and pit pore size has been measured (Jarbeau et al. 1995). However, Choat et al. (2003) could not establish any direct correspondence between pit pore size and vulnerability to embolism, as pores large enough to fit the predicted values could not be detected. This suggests that this relationship is at least not as straightforward as previously thought and that pit-pore dimensions may not be the only characteristics that determine the spread of embolism in the xylem.

There has been much interest in investigating the structure and arrangement of vessels using new scientific approaches. The 3-D architecture of vessel networks in secondary xylem has been investigated at the microscopic level in a few studies and in very small segments of wood (Fujii et al. 2001; Tyree and Zimmermann 2002). A cinematographic method has facilitated 3-D reconstructions and proved very useful in studies of vessel networks (Zimmermann and Tomlinson 1966; Tomlinson et al. 2001). Other techniques for the rapid tracing of vessel networks include injection of dye and insertion of wire (Kanai et

al. 1996). The cinematographic and the wire-insertion methods allow studies of larger specimens but fail to provide detailed anatomical information about features such as the structures of pit contacts and of perforation plates, which play important roles in the patterns of water movement. However, the architecture of vessel networks in most dicotyledonous species and the pathways via which water is conducted, in particular, in the radial direction in xylem, remain poorly understood. The frequency of contacts between vessels on the two sides of a growth-ring boundary remains poorly characterized and the type of xylem element (vessel or tracheid) that is predominantly involved in the apoplastic transfer of water in the radial direction remains to be identified (**Fig. 6.2**).

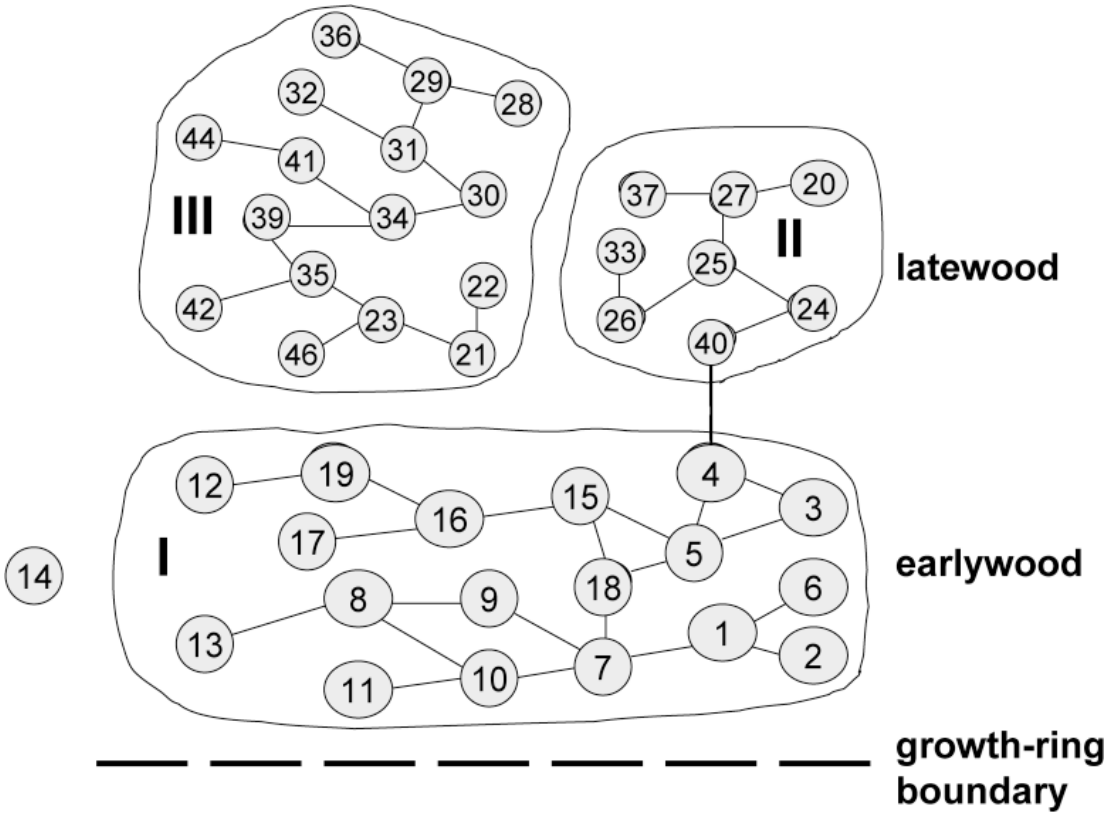

Fig. 6.2 Schematic representation of part of the vessel network within a growth ring in a segment of *Fraxinus lanuginosa* wood. The three-dimensional (3-D) arrangement of vessels and the vessel-to-vessel connections in the secondary xylem of the stem of *F. lanuginosa* were studied in series of thick transverse sections with epifluorescence microscope and confocal laser scanning microscope. Vessels were traced in sequential sections, and vessel networks were reconstructed in two segments of wood with dimensions of 2 × 1.4 × 21.2 mm^3 and 2 × 1.4 × 5.8 mm^3 (tangential × radial × axial) (Kitin et al. 2004). This study was undertaken with an effort to characterize the 3-D network of vessels in *F. lanuginosa*, a ring-porous hardwood from the temperate forests in East Asia to understand how the vessels might communicate to provide a continuous network.

Direct visualization of the vessel-to-vessel connections along the course of individual vessels requires the microscopic analysis of large specimens. Epifluorescence microscopy allows observations of the details of cell structure on the surface of a specimen (Donaldson et al. 1999; McManus et al. 2002), and confocal laser scanning microscopy (CLSM), allows, in addition to the dimensions (x, y) for conventional optical resolution, higher resolution in the third (z) dimension, that is useful for studies of the internal structure of thick histological sections (Donaldson and Lausberg 1998; Kitin et al. 2000, 2003; Funada, 2002). The use of such recently developed anatomical methods, supported by powerful computer software, should facilitate the understanding of vessel networks in longer segments of stem and, at the same time, should allow detailed analysis of anatomical structures, such as inter-vessel pits. Besides investigating xylem anatomy, concomitant measurements of leaf-specific hydraulic conductance (KSL) is another appropriate measure to compare patterns of hydraulic architecture among species because it integrates the hydraulic conductivities of individual plant parts across the organism and has been shown to be proportional to stomatal conductance and photosynthetic rate (Meinzer and Grantz 1990; Sperry and Pockman 1993; Meinzer et al. 1995; Hubbard et al. 2001).

The picture that emerges is that trees can solve strength and hydraulic limitations in several ways and a better characterization of the hydraulic architecture of whole mature trees would improve our understanding of its ecological consequences. However, very little is known how anatomical traits vary across the genotypes of mulberry tree species. Moreover, it is not clear how these wood traits relate to whole-plant hydraulic performance in mulberry under field drought conditions. Initial results (see Chapter 4) suggested that the drought tolerant mulberry genotype V1 had higher vessel density and better hydraulic conductance, while drought susceptible K2 had a low vessel density; although the study was conducted with only two genotypes and also under potted conditions by comparing the tissues mostly at their primary growth stage. Thus, in the present study, 13 coexisting mulberry genotypes were compared for quantitative xylem traits. The primary goal was to explore wood traits important for the hydraulic system. Xylem anatomical traits were related to each other, then to leaf gas exchange and KSL, and finally to anisohydric mode of drought tolerance. The rationale behind this approach is that xylem vessel traits should affect plant performance and that traits together with plant performance might confer

variation in the degree of drought tolerance across the genotypes. The following three corresponding questions were addressed: (1) How does in-built stem wood hydraulic architecture vary among the genotypes? (2) Are stem-wood hydraulic architectural traits correlated with the KSL of anisohydric mulberry stands? (3) Can we postulate an ideal hydraulic architecture for anisohydric mulberry with intermediate trait values?

Materials and Methods

Study site and experimental setup

The experiment was conducted at the SRC plantations of mulberry, University of Hyderabad, India, located between 17.3°10´N and 78°23´E at an altitude of 542.6 m above MSL. Mulberry genotypes were evaluated under field drought conditions during Mar to Jul, year 2012 (which constituted the dry summer season of the study zone). Precipitation during experimental time-span was sporadic and considered negligible; the highest air temperature recorded during day time was 41.7°C, mean air temperature recorded during daytime was 33.7°C, mean monthly PAR measured at peak photosynthetic time (between 9.00-11.00 h) ranged from 1320 to 2200 µmol m^{-2} s^{-1}. The soil of the experimental site was sandy loam with a pH of 7.5. The experimental design was a randomized block including four replications in a net plot size of 14.4 m x 14.4 m (12.6 m rows, 0.9 m apart). The experimental plot was irrigated once in a fortnight. To verify the degree of drought stress, soil moisture contents at 30 cm and 45 cm depth of the plot were determined periodically by taking wet weight and oven-dried (105°C for 2 days) weight of soil according to Ritchie et al. (1990). The timing of the start of irrigation was based on the threshold values of soil water content (<15%) and predawn leaf water potential (<-2.0 MPa). Recommended package of practices were followed uniformly throughout the experimental period which included the application of 20 metric tons FYM $ha^{-1}yr^{-1}$ and 280:120:120 kg NPK $ha^{-1}yr^{-1}$ in equal splits.

Mulberry genotypes selected

Thirteen genotypes were studied for xylem anatomical characteristics including AR12, JPK, K2, KS2, MR2, ML, PNG, S1635, S36, TR10, S1, S13 and V1. Total twenty six trees

were selected, comprising the tallest two from each genotype. The genotypes varied in adult stature and light requirements. At the end of the experiment, adult height (H_{max}) was estimated along with stem diameter (D_{100}: at a height of 100 cm from stem base) for individual tree. For calculating D_{100}, the third-thickest stem coming out from a single stump was used, thus avoiding outliers caused by incorrect measurements or rare thick 'champion' stems. For selecting the two representative trees from each genotype, in a separate study, mulberry stands were analyzed for crown exposure in relation to the height of individual trees. To this end, on average 224 individuals were measured over their whole size range for their height and crown exposure (CE). The CE had the following categories (C): C1- tree does not receive any direct light; C2- it receives lateral light; C3- it receives overhead light on 10-90% of the crown; C4- it receives full overhead light on > 90% of the crown; C5- it has an emergent crown. The CE was measured repeatedly (mean difference between two independent observers is 0.1 ± 0.01 SE) and there was a good relation between CE and both canopy openness and incident radiation. For each species the CE was related to tree height, using a multinomial regression analysis (Poorter et al. 2005). The trees selected for the present study belonged to either C4 or C5. The mean H_{max}, D_{100}, number of primary, secondary and tertiary branches for each genotype recorded at the end of the experimental period is presented in **Table 6.1**.

Table 6.1 Maximum stand height (H_{max}), stem diameter (D_{100}), no. of primary stems per stump and wood density (D_w) of the 13 mulberry genotypes recorded under field drought conditions and used for measurements of different stem wood vessel traits. Values are ± SD.

Genotype	Height (H_{max}) (cm)	Stem diameter (D_{100}) (cm)	No. of primary stems/stump	Wood density (D_w) (g cm^{-3})
AR12	198.2 ± 3.4	1.76 ± 0.01	3.0 ± 3.4	0.46 ± 0.04
JPK	192.4 ± 2.5	1.72 ± 0.02	3.0 ± 4.4	0.42 ± 0.05
K2	206.3 ± 4.3	1.82 ± 0.01	3.5 ± 2.3	0.48 ± 0.02
KS2	234.4 ± 5.3	2.03 ± 0.03	3.0 ± 3.8	0.56 ± 0.04
MR2	254.6 ± 3.3	1.96 ± 0.05	4.0 ± 5.5	0.48 ± 0.03
ML	264.2 ± 6.4	1.98 ± 0.04	4.5 ± 4.2	0.45 ± 0.02
PNG	218.3 ± 4.2	2.02 ± 0.02	3.5 ± 3.8	0.40 ± 0.05
S1635	212.3 ± 5.6	1.83 ± 0.01	3.0 ± 2.5	0.44 ± 0.06
S36	222.7 ± 7.2	1.82 ± 0.03	3.5 ± 2.5	0.46 ± 0.04
TR10	208.2 ± 4.6	1.68 ± 0.02	3.0 ± 4.7	0.33 ± 0.03
V1	297.3 ± 4.4.	3.20 ± 0.01	5.5 ± 5.3	0.56 ± 0.04
S1	312.1 ± 3.8	2.32 ± 0.03	6.0 ± 3.2	0.60 ± 0.05
S13	302.5 ± 2.5	2.22 ± 0.02	5.5 ± 4.2	0.49 ± 0.03

Collection of stem samples for xylem anatomy

Stem wood samples were collected from twigs in the canopy at periodic intervals during Apr, May, Jun and Jul months of year 2012. Three or four branches were collected from the upper crown of each individual at a stem height of 150 cm from base, except few genotypes including AR12, TR10, JPK and S1635 because they had very few branches. Instead, for those genotypes, stem samples were collected from the upper crown of each individual at a stem height of 100 cm from base from individual trees in an attempt to minimize damage. Branches for all twenty six trees from thirteen genotypes were accessed and taken from morphologically equivalent locations (i.e., the same number of branch junctions proximally from the leaves) for all species except JPK, which had very few junctions. For JPK, branches were taken from roughly the same distance proximally from the leaves as the other genotypes. Two to three stem segments were collected per tree. Initial samples were collected in Mar 3rd week, 2012. Analysis of the material revealed the need for additional collection dates, so additional materials were collected in Apr and May of 2012 and finally on last week of Jul 2012. For each collection date, new samples were taken from the same trees. Although 2-3 samples were made per tree, no stresses were observed in the trees nor abnormal wood in the samples. Samples 2-3 cm wide, 4-5 cm height and of variable depth, depending on bark thickness, were collected from the stem using a secature, chisel and drill. The samples were immediately fixed in methanol/glacial: acetic acid fixative (3:1, v/v) and was preserved in 1:1 (v/v) ethanol/glycerol for long-term storage (2 months) to undertake wood anatomical studies (**Fig. 6.3**).

Sap wood anatomy and density

Vessel dimensions from preserved stem wood segments were assessed in all genotypes listed in **Table 6.1**. Preserved samples were rinsed and rehydrated in several changes of lukewarm water. The samples were then air dried in a dust free environment and were trimmed to small blocks or sections. Thereafter, exposing transverse, radial or tangential surfaces, the samples were glued to specimen stubs using adhesive carbon tape and sputter coated with gold to a thickness of 15 mm at 1.5 keV for 10 min using a JEOL FC-1100 Fine Coat Ion Sputter Unit (JEOL, Tokyo, Japan) (**Fig. 6.3**).

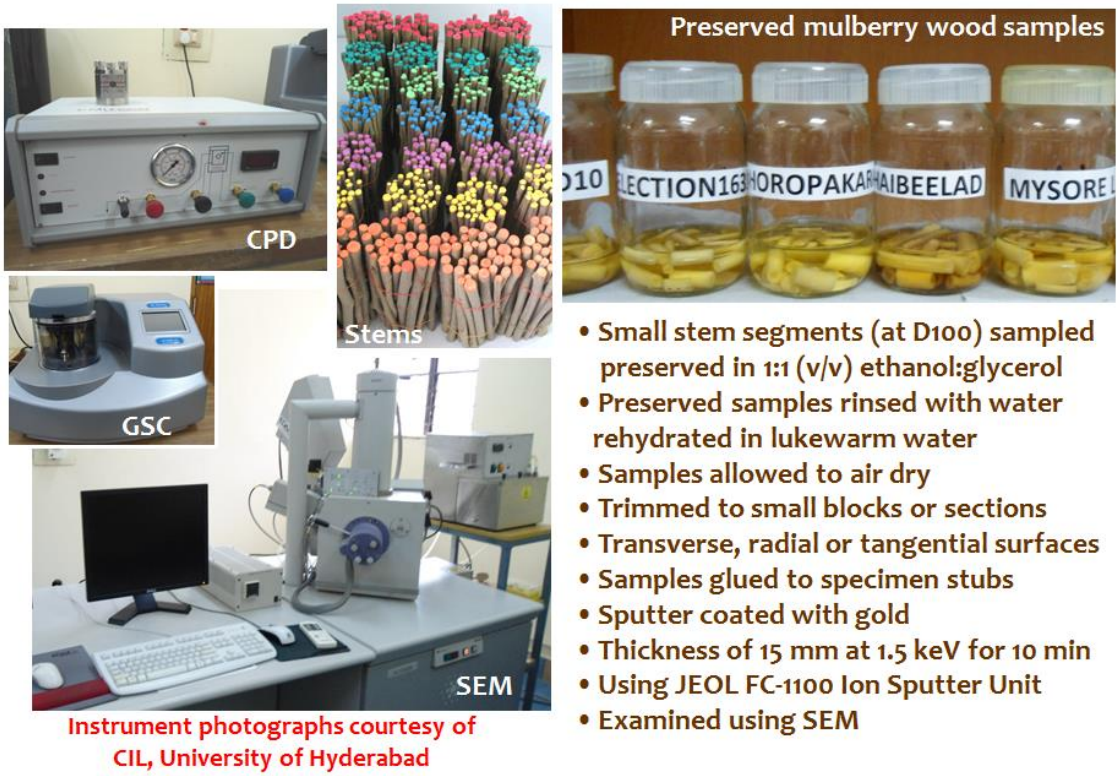

Fig. 6.3 Different steps in stem wood sample processing including collection, color coding, preservation, and preparation for viewing under scanning electron microscope (SEM). Before viewing under SEM, the samples were dried using critical point drier (CPD) and coated with gold using gold sputter coater (GSC). Important steps in sample preparation are listed in bullets.

Wood specimens were then examined using a Scanning Electron Microscope (FEI XL 30 ESEM, USA) and photographed. Total cross-sectional area of wood (W_A) and the area of pith (P_A) within the wood were calculated. The xylem vessel diameter (V_d), density of xylem vessels (V_D), proportion of stem-cross sectional area occupied by xylem vessels (V_A), vessel grouping index (VGI), solitary vessel percentage (SV), pitting pattern, number of pits, pit shape, pit size, horizontal (Pd_H) and vertical (Pd_V) diameter of pit, vessel wall thickening and the types of perforation plates were recorded. Images were analyzed using the freeware software ImageJ (NIH, USA, http://rsb.info. nih.gov/ij/). Xylem vessel lumen areas were measured on all vessels within three pie piece-shaped areas spanning from the bark to the pith. If fewer than 100 vessels were measured in three combined areas, more pie piece-shaped areas were added until 100 vessels had been measured (McCulloh et al.

2011). For all sampling locations, each vessel diameter (V_d) was determined by calculating the diameter of a circle of the given lumen area. Terminology of wood anatomical characters follows the recommendations of the IAWA list (IAWA Committee 1989).

Wood density (D_w) was measured fresh using major primary stems coming out directly from the stumps for all genotypes. Generally 3-5 cm fresh stem segments cut out uniformly at a stem height of 100 cm from base of all the tested genotypes. To avoid any shrinkage in volume, the fresh stem segments were kept in shade and the green mass and volume were measured on the same day of stem cutting. The bark and pith were carefully removed, discarded and each stem segment was impaled on a thin needle. The green wood volume (V_w) was measured immediately by submerging the stem sample in a beaker of distilled water of known mass placed on a digital balance (Sartorius GD103, Germany) sensitive to 0.1 mg and the change in balance reading was recorded. The mass of the displaced water in grams was taken to correspond closely to sample volume in cm^3. Necessary precautions were undertaken to minimize movement of the wood sample while measuring on the balance. Measurements were quickly completed within 10s of immersion to minimize entry of water into the cut ends of the wood sample. Samples were then dried for 3-5 days in an oven at 103°C to obtain a constant weight and weighed for dry mass (M_s). In the present study, D_w is defined as 'basic density' which is calculated as the ratio between the oven dry mass and the fresh volume of the green wood ($D_w = M_s / V_w$) (Hacke et al. 2000).

Whole tree root-to-leaf specific hydraulic conductance (KSL)

On five different sunny days during the experimental period, whole tree soil-to-leaf hydraulic conductance (KSL; mmol MPa^{-1} m^{-2} s^{-1}) was estimated according to the ratio of branch transpiration per unit leaf area to the difference between soil and leaf water potentials during the same time period and on the same days as the transpiration measurements. Leaf water potential (Ψ_L) was measured in mature, fully expanded, upper canopy leaves from two to three apical twigs per stand using a portable pressure chamber (Plant Moisture System, SKPM 1400/40, Skye Instruments Ltd, England). All measurements were conducted within 3-4 min of leaf excision and minimum 6 leaves per genotype from the representative plants were sampled. KSL was calculated by analogy to

Ohm's law (Tyree 2003; Brodribb and Holbrook 2003): KSL = $E_{max}/(\Psi_{soil} - \Psi_{md} - \rho gh)$, where Ψ_{soil} and Ψ_{md} were predawn soil and midday leaf water potentials, respectively, E_{max} was the peak transpiration rate at the midday in a leaf area basis, measured with infrared gas-analyzer system (LCpro-32070), ρ is density of water, g is acceleration due to gravity and h is tree plant. To obtain the net driving force for transpiration, the KSL values were corrected to ground level based on the estimated height (h) of branches above the ground and a vertical gravitational gradient (g) of 0.01 MPa m^{-1}. Instead of Ψ_{soil}, predawn leaf water potential (Ψ_{pd}) was used as a proxy under zero sap flow in the trees. There are possibilities that stored water can uncouple the close relationship between transpiration and leaf water potential, however, the present calculations of KSL were made during peak transpiration (E_{max}) at midday when the effects of capacitance on transpiration were assumed to be minimal. Ψ_{pd} and Ψ_{md} measurements were made between 04.00–05.00 solar hours and between 12.30-13.30 solar hours, respectively. Based on diurnal measurements of leaf water potential at our experimental site, Ψ_{pd} and Ψ_{md} corresponded to maximum (Ψ_{Lmax}) and minimum (Ψ_{Lmin}) leaf water potentials, respectively.

Statistical analyses

For stem wood density and xylem vessel characteristics, analysis of variance (ANOVA) was carried out on data obtained from the representative trees. Data were averaged on a plant basis and the individual means were used for the analysis. The *compare many groups* statistical procedure of SigmaPlot11.0 was used to perform one way ANOVA (significant threshold set at $P<0.05$) and whenever there was statistically significant difference, pair wise multiple mean comparison was conducted using Fisher's LSD method (alpha=0.050). The XLSTAT (ver. 7.5.2) was used to determine correlations between different pairs of variables as well as among genotypes using Principal component analysis (PCA). The values for vessel traits, D_w and KSL were $\log_{10}$ transformed prior to PCA. Pearson correlation coefficient matrix analysis was performed and the threshold for significance was adjusted using Bonferroni correction, where 0.05 divided by the number of paired correlation assessed the adjusted significant level.

Results

General observations

The following features were mainly based on SEM studies. All mulberry genotypes examined in this study were ring-porous to semi-ring porous, with distinct growth rings boundaries distinct (**Fig. 6.4**). Vessels were in tangential/diagonal and / or radial pattern. Vessel clustering was common (**Fig. 6.5**) and the intervessel pits were mostly alternate. Shape of alternate pits was polygonal and ranged from medium (7-10 µm) to large (>= 10 µm) (**Fig. 6.6**). Vessel-ray pits were with much reduced borders to apparently simple and the pits were rounded or angular in shape. Helical thickenings were present in vessel elements either throughout body of vessel element or only in narrower vessel elements. The xylem conduits were with simple perforation plates (**Fig. 6.7**). Fibers were thin- to-thick-walled with simple to minutely bordered pits.

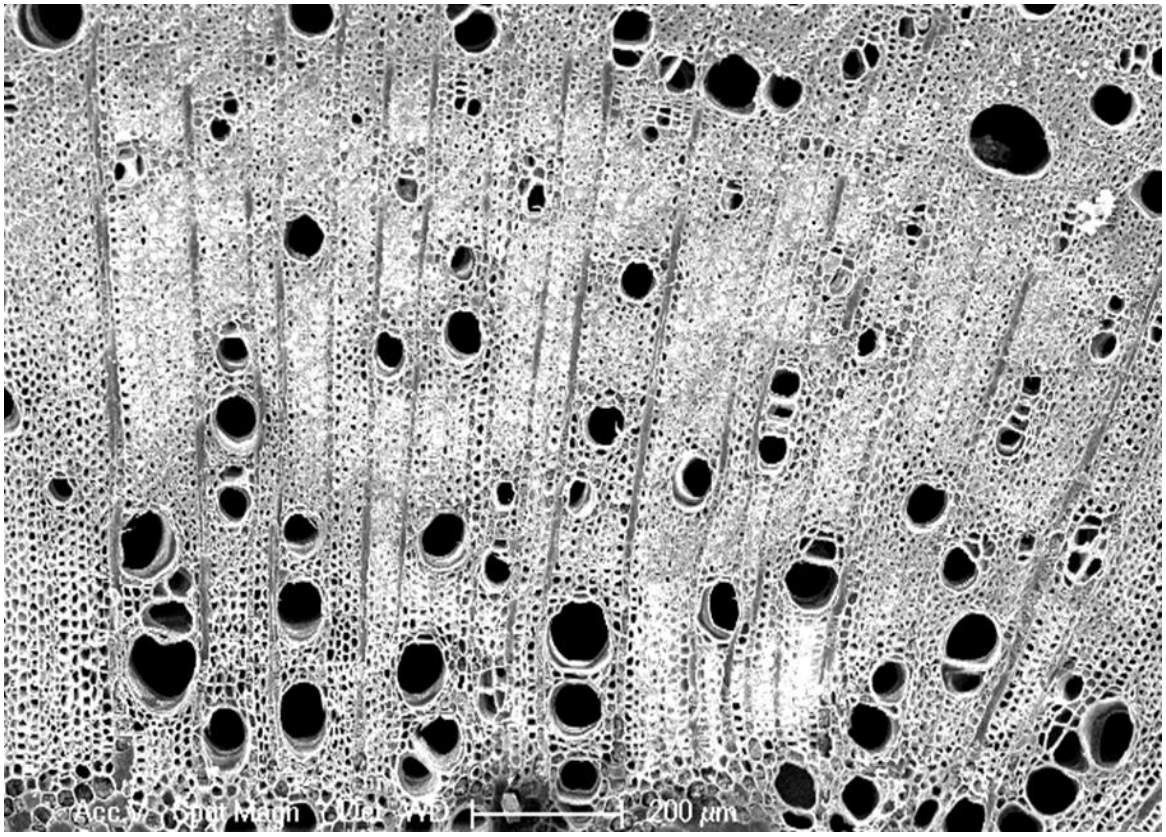

Fig. 6.4 Transverse section of stem wood from mulberry genotype S1 to represent a ring-porous feature, under low magnification. In this ring-porous mulberry genotype, pores in the earlywood portion of a growth ring are large compared with those in the latewood portion.

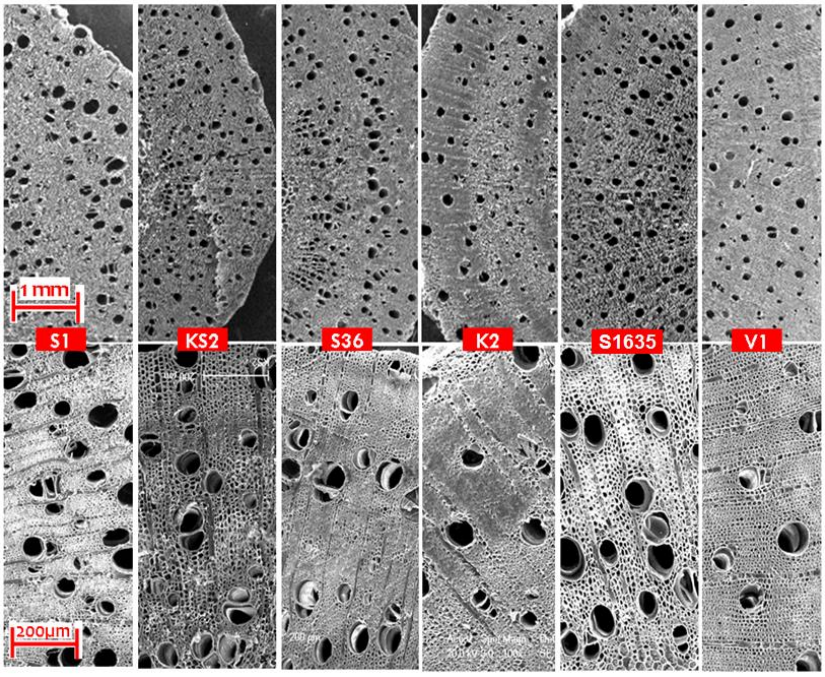

Fig. 6.5 Scanning electron photographs of woody stem transverse sections (T.S.) in selected mulberry genotypes. T.S. of stem showing ring porous and semi-ring porous patterns of vessel formation and showing enlarged view of vessel distribution pattern, vessel size variation and types of vessel grouping. Rays composed of ray parenchyma cells and fibres are also visible. Vessels are elliptic, generally solitary, sometimes in multiples of 2 to 3.

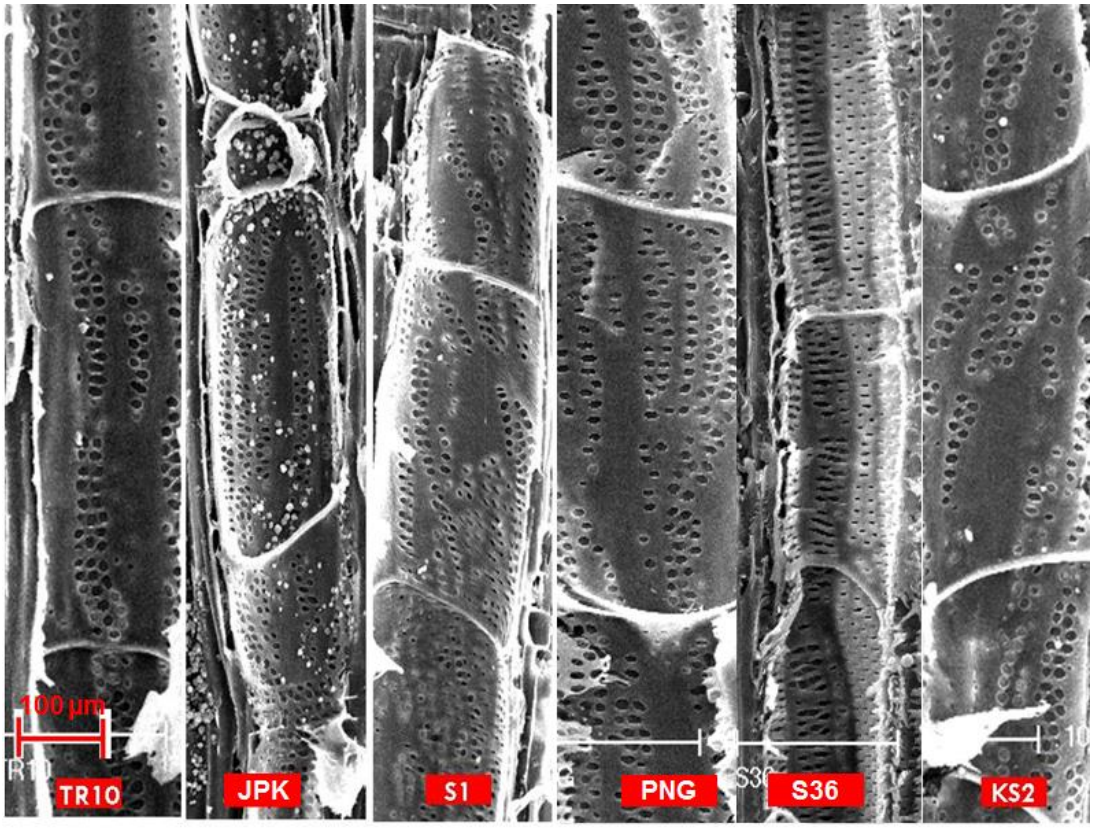

Fig. 6.6 Scanning electron photographs of vessel elements in the secondary xylem of selected mulberry genotypes. Magnified part of vessel elements showing pits with membranes or retaining some remnants and perforation plates between adjacent cells.

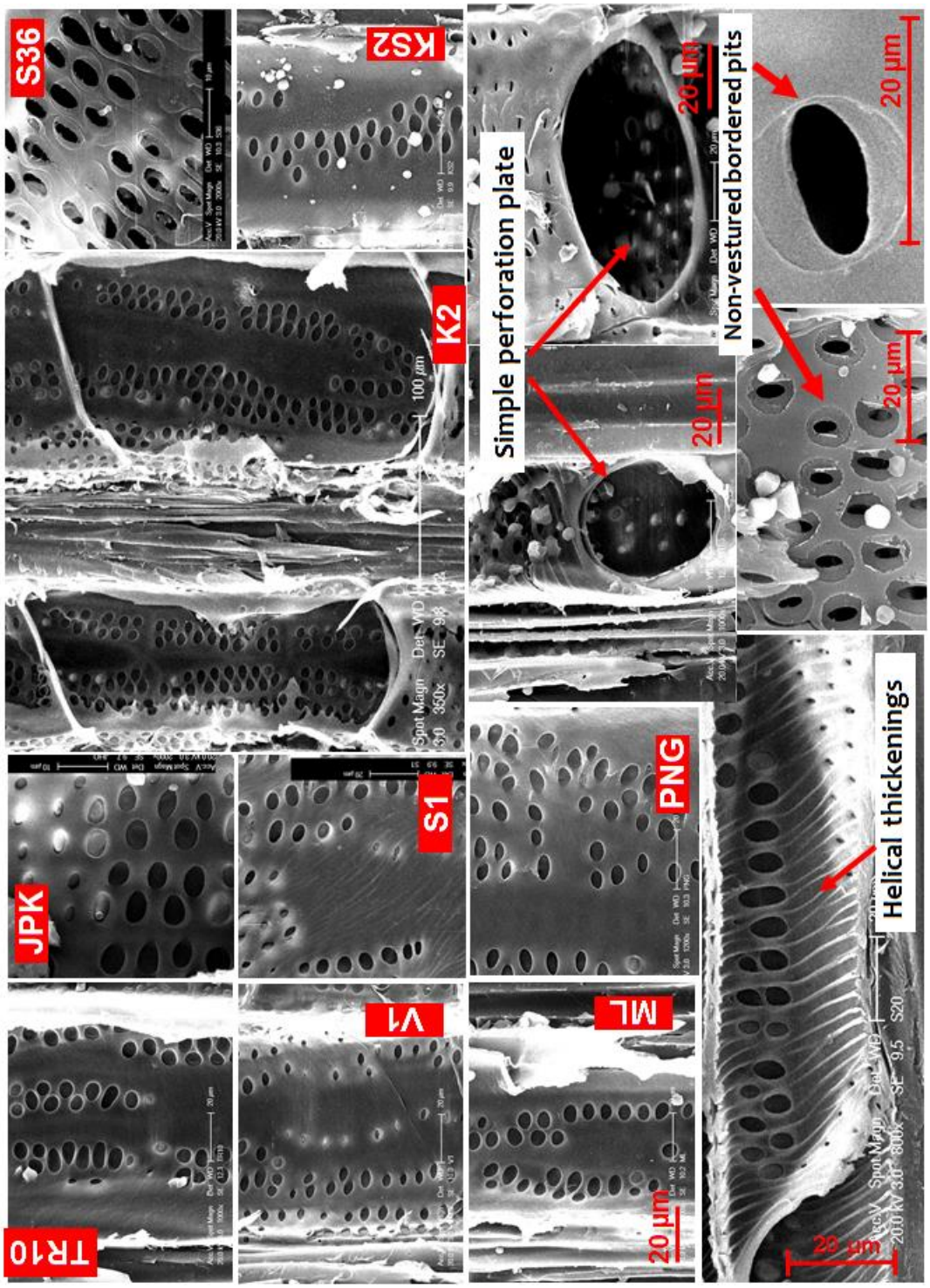

Fig. 6. 7 Scanning electron photographs of xylem vessel pits viewed from outer and inner surfaces in different mulberry genotypes. Views of vessel elements from the outer side showing alternate inter vessel pitting and simple perforation plates (genotype V1). Tangential longitudinal view (from genotype V1) of surface showing helical vessel wall thickenings on the inner wall which depicts thick and dense sculpturing patterns. The slender helical thickenings are not completely horizontal but slightly oblique and they never run midway between two pit apertures. Magnified view of a non-vestured bordered pit viewed from outer wall of the vessel.

Xylem vessel density (V_D)

The V_D differed significantly ($P<0.05$) among the mulberry genotypes as evident from ANOVA and Fisher's LSD test results (**Fig. 6.8**). Genotype KS2 (68.2 mm^{-2}), S36 (59.4 mm^{-2}) and AR12 (56.8 mm^{-2}) had the maximum V_D amongst all. Genotype S1, V1, S1635, PNG and JPK had V_D < 40 mm^{-2} but >30 mm^{-2}. Genotype K2, MR2, ML, TR10 and S13 had intermediate V_D and the values ranged from 40.1 to 44.9 mm^{-2} (**Fig. 6.8**).

Vessel lumen diameter (V_d)

The V_d varied among the tested mulberry genotypes and significant ($P<0.05$) differences were noted. V_d values were obtained from stem cross-sections and the values were determined from secondary xylem vessels in the most recent growth increment. Measurements were taken at the widest region of the lumen. V_d values of most genotypes were relatively small, with mean values between 1.03 and 1.62 µm (**Fig. 6.9**). Genotype S13 recorded the smallest V_d of 1.03 µm followed by genotype KS2 (~1.26 µm). There was no significant difference in lumen diameter between V1 and S1 and the mean V_d value recorded for those two genotypes was ~1.28 µm. Genotype S1635 recoded the highest value for V_d (~2.20 µm) followed by TR10 (~1.62 µm), AR12, JPK and MR2 (~1.50 µm). The ANOVA and Fisher's LSD tests showed significant differences in V_d among the genotypes (**Fig. 6.9**).

Percentage area occupied by xylem vessel (V_A)

The selected mulberry genotypes also differed significantly in V_A. The results of ANOVA and Fisher's LSD test yielded statistically significant differences in V_A among the genotypes (**Fig. 6.10**). The V_A values ranged from 10.5 and 37.8%. The highest value for V_A was recorded in JPK (~37.8%) followed by PNG (~34.5%). There was no large difference in V_A among genotype MR2, S13, S36 and KS2 and the values recorded for those genotypes were 26.9%, 25.8%, 23.3% and 22.5%, respectively. The lowest value for V_A was recorded for ML (~10.5%), however, no statistically significant difference was recorded in V_A values of genotype ML, V1, S1635 and K2 (**Fig. 6.10**).

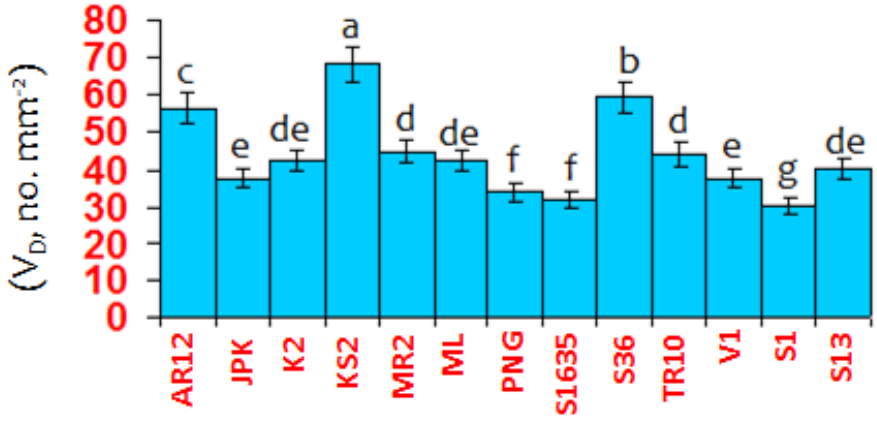

Fig. 6.8 Genotypic differences in vessel density (V_D) recorded among 13 mulberry genotypes grown under field drought conditions. The differences between means were separated by Fisher's LSD test. Values followed by the same letters are not statistically different.

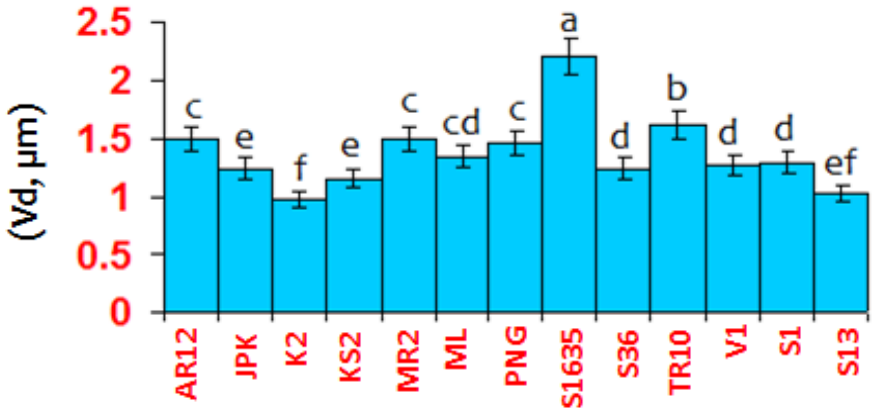

Fig. 6.9 Genotypic differences in vessel diameter (V_d) recorded among 13 mulberry genotypes grown under field drought conditions. The differences between means were separated by Fisher's LSD test. Values followed by the same letters are not statistically different.

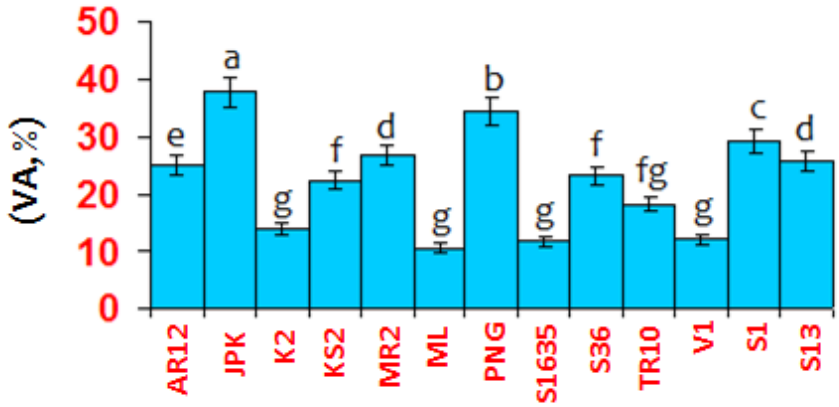

Fig. 6.10 Genotypic differences in vessel area (V_A) recorded among 13 mulberry genotypes grown under field drought conditions. The differences between means were separated by Fisher's LSD test. Values followed by the same letters are not statistically different.

Vessel grouping index (VGI) and solitary vessel percentage (SV%)

VGI varied moderately, however, significantly amongst the mulberry genotypes in the present study as evident from the results of ANOVA followed by Fisher's LSD test (**Fig. 6.11**). Genotype JPK, K2, KS2, ML and TR10 had the same VGI value (~1.75). PNG showed the highest VGI of ~4. Higher grouping index was also recorded in genotype S13 (~3), V1 (~2.3) and AR12 (~2.2) (**Fig. 6.11**). Mulberry genotypes also differed significantly in SV% as recorded from the ANOVA results followed by Fisher's LSD test (**Fig. 6.12**). The highest value for SV% was recorded in ML (~90%) and V1 (~85%) followed by K2, KS2 and MR2 (~81%). Mulberry genotype TR10 had lowest value (~57%) for SV% followed by PNG (~64%) and S13 (~68%) (**Fig. 6.12**).

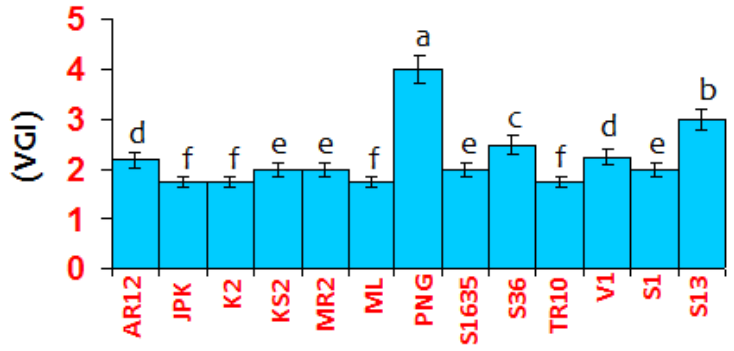

Fig. 6.11 Genotypic differences in vessel grouping index (VGI) recorded among 13 mulberry genotypes grown under field drought conditions. The differences between means were separated by Fisher's LSD test. Values followed by the same letters are not statistically different.

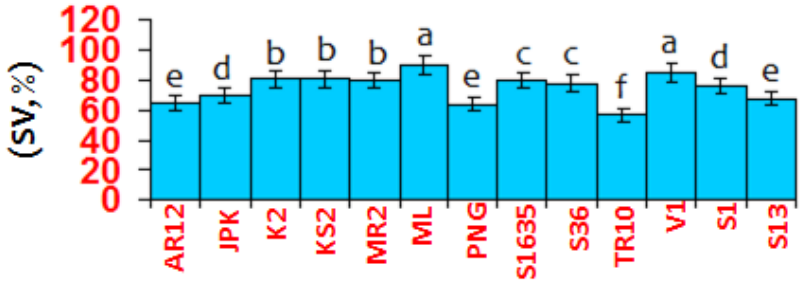

Fig. 6.12 Genotypic differences in solitary vessel percentage (SV %) recorded among 13 mulberry genotypes grown under field drought conditions. The differences between means were separated by Fisher's LSD test. Values followed by the same letters are not statistically different.

Horizontal (Pd_H) and vertical (Pd_V) diameters of vessel pit

The Pd_H of xylem vessels varied considerably among the genotypes (**Fig. 6.13**). The Pd_H ranged from 10.8 to 5.2 µm. Because of this wide variation, the ANOVA and Fisher's LSD test showed statistically significant ($P<0.05$) genotypic differences. Maximum Pd_H was recorded in TR10 (~10.8 µm) followed by MR2 (~10.2 µm), PNG (~9.7 µm) and K2 (~9.4 µm). The lowest Pd_H value was recorded in S1635 (~5.2 µm) followed by S1, S13 and V1 (~5.8 µm) (**Fig. 6.13**). Genotype AR12 had significantly higher Pd_V value (~6.8 µm) followed by S1635 (~6.8 µm), K2 (~5.9 µm) and PNG (~5.4 µm) and TR10 (~5.4 µm). The lowest value for the same was recorded in S36 and V1 (~3.8 µm) followed by S1 (~4.3 µm) and S13 (~4.5 µm) (**Fig. 6.14**).

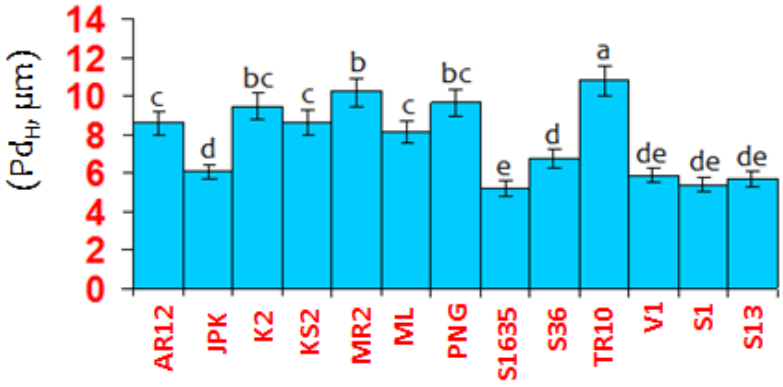

Fig. 6.13 Genotypic differences in horizontal pit diameter (Pd_H) recorded among 13 mulberry genotypes grown under field drought conditions. The differences between means were separated by Fisher's LSD test. Values followed by the same letters are not statistically different.

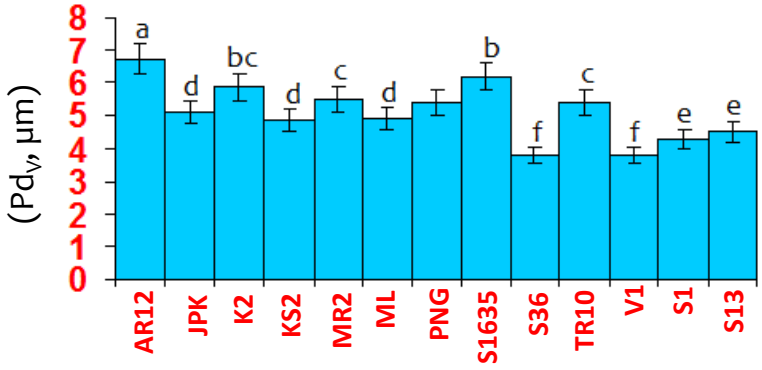

Fig. 6.14 Genotypic differences in vertical pit diameter (Pd_V) recorded among 13 mulberry genotypes grown under field drought conditions. The differences between means were separated by Fisher's LSD test. Values followed by the same letters are not statistically different.

Associations amongst vessel traits

The relationships amongst stem xylem anatomical characteristics and hydraulic conductivity (KSL) were analyzed using scatter plot matrix (**Fig. 6.15**). KSL was not significantly related to V_A but was positively related to VGI (highlighted in blue colored box). However, KSL behaved independently with V_d and V_D. Both Pd_V and Pd_H, showed significant negative correlations with KSL (highlighted in yellow boxes). V_d behaved independently with SV% and Pd_H but interestingly showed strong positive correlation with Pd_V (highlighted in blue colored box). V_D showed no significant correlation with V_A, S_V, Pd_V and VGI, however, exhibited a weak positive correlation with Pd_H. SV showed significantly strong negative correlation with V_A and VGI and a weak negative correlation with Pd_H and Pd_V. The R^2 value for each pairwise correlation was obtained from Pearson correlation coefficient analysis and presented in **Table 6.2**.

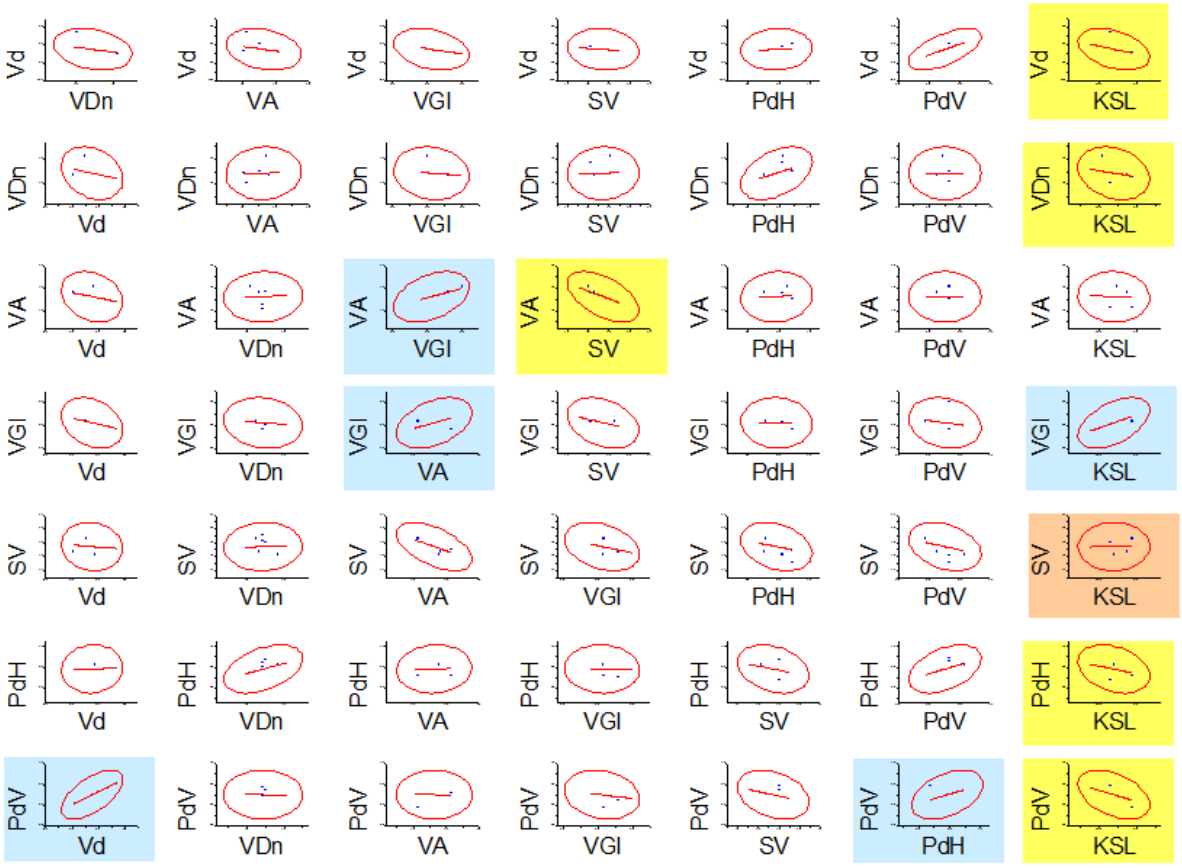

Fig. 6.15 Scatter plot matrix of selected xylem vessel characteristics and hydraulic conductance (KSL) data from 13 mulberry genotypes to investigate the relationships amongst these variables.

Table 6.2 Pearson correlation coefficients between each pair of variables including vessel characteristics, leaf gas exchange and water relation traits. For abbreviations see Materials and Methods. The P_n, G_s, E and $-\Psi_L$ data included in this correlation analysis were taken from the field screening data of Chapter 3. Significant values are indicated in bold. Negative correlations are indicated by '–' symbol.

	VD	VA	VGI	SV	PdH	PdV	Pn	Gs	E	$-\Psi_L$	KSL
Vd	-0.254	-0.247	-0.285	-0.099	0.064	**0.615**	-0.030	-0.115	0.015	0.396	-0.378
VD		0.050	-0.117	0.037	0.433	-0.009	0.048	0.144	-0.068	0.219	**-0.531**
VA			**0.564**	-0.546	0.067	-0.008	-0.316	-0.440	-0.104	0.046	-0.038
VGI				-0.316	-0.043	-0.186	0.150	0.163	**0.596**	-0.474	**0.560**
SV					-0.289	-0.317	0.029	0.200	-0.214	0.006	0.011
PdH						**0.535**	-0.228	-0.277	0.028	0.358	**-0.523**
PdV							-0.265	-0.244	0.096	0.519	**-0.534**
Pn								**0.924**	**0.635**	**-0.567**	0.548
Gs									0.570	-0.514	0.481
E										**-0.673**	**0.751**
$-\Psi_L$											**-0.970**

The leaf gas exchange, the vessel anatomy, leaf water potential and hydraulic conductance were compared together in Principal component analysis (PCA) in order to explain the variation in all the data set (13 genotypes under field drought conditions). PCA, as an unsupervised clustering method, acts to reduce the dimensionality of multivariate data while preserving most of the variance with it. Coefficients (eigenvector values), by which the original variables must be multiplied during transformation procedure to obtain the principal components, show the weight of the contribution of each variable in the variation. In this study, a PCA model constituted by two principal components explaining 54.20% of the total variance (eigenvalue) was investigated. Axis F1 (1^{st} PC) explained 35.93% and Axis F2 (2^{nd} PC) explained 18.27% of the total variance in the data and the eigenvector values of the parameters studied in the two axes are shown in the **Table 6.3**. Furthermore, the correlations for each parameter with axes F1 and F2 were investigated and the data were represented graphically (**Fig. 6.16**) showing the association among the parameters in terms of their position along the two axes.

Taking into account the eigenvector values (**Table 6.3**), it can be assumed that Ψ_L is the trait with the greater weight (load) in the total variation (0.446) to the 1^{st} PC. The traits KSL, P_n, G_s, E, Pd_V and V_d showed a strong contribution with a range of eigenvector values from 0.441 to 0.180 (**Table 6.3**). The traits including KSL, E, VGI, P_n and G_s clustered almost together and loaded on the 1^{st} PC. Accordingly, the genotypes S13, S1, S34 and V1 were located in the same direction, indicating a strong positive effect of these

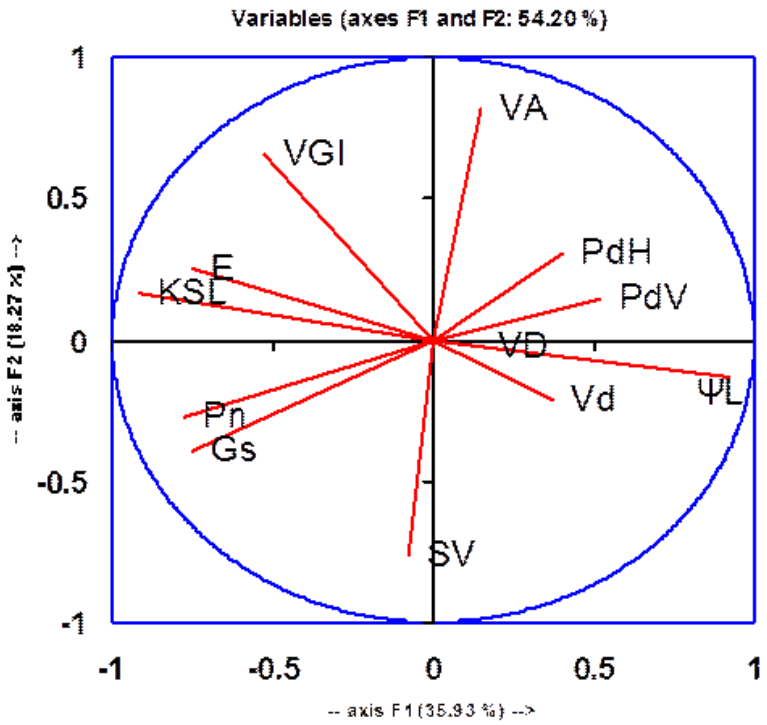

Fig. 6.16 Principal component analysis (PCA) of 12 traits of 13 mulberry genotypes. All data were $\log_{10}$-transformed before analysis. For abbreviations see Materials and Methods.

Table 6.3 Eigenvector values of all 12 variables (for all 13 mulberry genotypes) on the first two PCA axes in Fig. 6.16. Values are ranked in order of absolute magnitude along 1st PC. The higher value for each parameter between the two axes is in bold.

	F1	F2
$-\Psi_L$	**0.446**	-0.087
KSL	**-0.441**	0.111
P_n	**-0.372**	-0.186
G_s	**-0.361**	-0.267
E	**-0.361**	0.171
VGl	-0.252	**0.445**
Pd_V	**0.250**	0.097
Pd_H	0.194	**0.209**
V_d	**0.180**	-0.144
V_A	0.072	**0.554**
V_D	**0.067**	-0.018
SV	-0.036	**-0.516**

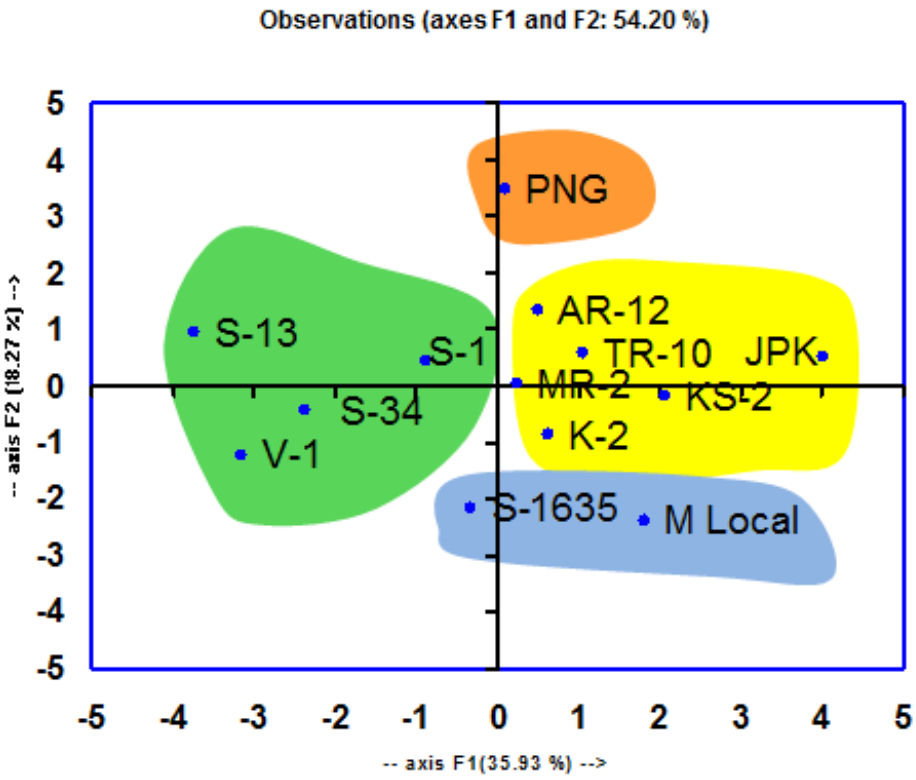

Fig. 6.17 Principal component analysis (PCA) of 13 mulberry genotypes. Genotype positioning within the multivariate space, with genotype grouped into different functional groups shown by differentially colored highlighted background.

traits in determining their position (**Fig. 6.17**). V_A and SV showed low contribution in the variation of the 1st PC, although in the 2nd PC their contribution in the variation was the highest among the other traits, with eigenvector values 0.554 and 0.545, respectively. Additionally, in the 2nd PC, the traits with strong contribution in the variation were VGI and Pd_H. Overall, the 1st PC was well associated with parameters of leaf gas exchange, water relations, Pd_V and V_d (**Table 6.3**), whereas the 2nd PC was well associated mainly with VGI, Pd_H, VA and SV (**Table 6.3**). The Pd_H, Pd_V, V_D and V_d clustered together and loaded strongly (**Fig. 6.16**); accordingly, genotype AR12, TR10, JPK, KS2, MR2 and K2 were located in the same direction, indicating a strong positive effect of these traits in determining their position (**Fig. 6.17**).

Discussion

The present study demonstrates that the stem-wood vessel traits of mulberry stands differed significantly among the genotypes. All the vessel characteristics assessed, had significant influence on the overall wood anatomy of the genotypes and concomitantly gave rise to visually observable trends in diverse vessel architecture. It is remarkable that the vessel features of the studied mulberry genotypes, mostly from the same species (all the genotypes except PNG and S1 belong to *M. indica*) growing under similar agroclimate, on a very small geographical scale, is significantly different. Plant hydraulic architecture concerns the spatial distribution of various xylem properties throughout the individual. Properties of the xylem that have received considerable attention include vulnerability to embolism, hydraulic conductivity and wood density. Nevertheless, vessel characteristics, especially adaptively-changing vessel traits, can partially explain how perennial trees survive in their environment. Intervessel pit characteristics also appear to play significant roles in safeguarding the water transport in the dynamic environment (Lopez-Portillo et al. 2005; Schmitz et al. 2007; Schmitz et al. 2008). We are, however, far from understanding the full spectrum of the vessel anatomy and functioning in relation to plant survivability under water deficit environment. The present study on stem wood anatomy of mulberry genotype can throw some light into the explanation of the varying agronomical performances of the genotypes and their performance potentialities in future climate change scenario. Tissue traits such as wood density and the hydraulic architecture of plant species are informative for land-plant ecology (Westoby and Wright 2006; Swenson and Enquist 2007). With respect to water transport, wood properties such as vessel dimensions and lumen area are considered to be crucial when compared to other vessel traits (Preston et al. 2006). Conductivity increases with the fourth power of radius and only linearly with vessel number. Therefore, vessel size is a far more important parameter determining hydraulic characteristics than vessel number (Tyree and Zimmermann 2002). Previous studies have indicated the importance of larger xylem vessels for greater hydraulic conductance and increased plant growth under well-watered conditions (Rodriguez-Gamir et al. 2010). Further, a high vessel density was also reported to optimize the water transport capacity of plants under stressful conditions by allowing a more efficient bypass of air-filled vessels and by leaving more vessels functional for the same number of embolized

vessels (Schmitz et al. 2006). In non-stressful conditions such as under adequate water regime, this safety solution is however unnecessary and weighed against more advantageous characteristics of the vessel network. However, in the present study, both vessel density and vessel size were found to be negatively associated with hydraulic conductance under summer drought conditions. The osmotic stress due to drought causes low water potential (causing a high tension or negative pressure) in the xylem sap of tree species (Robert et al. 2009). This tension in turn causes a higher probability for cavitation events (Tyree and Sperry 1989; Hacke and Sperry 2001; Naidoo 2006). Thus, small vessel diameters are reported to be advantageous in various tree species under more stressful conditions for the water transport (Lo Gullo et al. 1995; Villagra and Juñent 1997; Corcuera et al. 2004; Choat et al. 2005). In the present study, the drought tolerant mulberry genotypes (V1, S13 and S1) seem to deal with the higher cavitation risk at water deprivation by virtue of less V_d and low V_D.

From the comparison between drought tolerant and drought susceptible genotypes based on the vessel characteristics studied, it can be inferred that the water transport systems of the tested mulberry genotypes were highly different under field drought conditions. Former studies on wood characteristics in some of these mulberry genotypes (see Chapter 2) have already proven the potentialities of these vessel characteristics in influencing KSL of the genotypes. The present study further provided additional evidence for such diverse hydraulic efficiency of the mulberry genotypes. However, one should be aware that besides the in-built genetic background of the genotypes, their plasticity in wood characteristics under field drought conditions could also influence their hydraulic structure and efficiency. Yet, under short-term drought as experienced in the present study when the chances of phenotypic plasticity of the observed wood characteristics turns out to be low, the highly diverse in-built structure of the co-occurring genotypes growing in the same habitat can have a major effect on the physiological performance under soil drought, thus defining genotypic tolerance. In the present study, drought tolerant mulberry genotypes exhibited dominance of smaller vessel diameters when to others genotypes where vessels of intermediate size were more frequent. Although, a link between vessel diameter and cavitation sensitivity is not generally accepted, some earlier reports showed smaller vessels to be less prone to cavitation (Lo Gullo and Salleo 1991; Hargrave

et al. 1994; Lo Gullo et al. 1995; Choat et al. 2003). As drought tolerant V1 not only possessed smaller vessels than the drought susceptibles but also had a larger proportion of the tiniest vessels, a link between small vessel diameter and low vulnerability to cavitation would predict that the water transport system of genotype V1 was double safe.

Intervessel pit characteristics are however supposed to explain differences in vulnerability to cavitation better than vessel diameters (Jarbeau et al. 1995; Hacke and Sperry 2001; Wheeler et al. 2005; Hacke et al. 2006; Choat et al. 2008). Pits play an important role in the movement of sap in living trees and in the penetration of liquids or gases into timber; therefore intensive efforts have been made to clarify their structures (Sano and Jansen 2006). In the present study, a safety difference between drought tolerant and drought susceptible genotypes is evident in the architecture of their intervessel pits. The drought tolerant genotypes mostly exhibited intervessel pits with smaller horizontal (Pd_H) and vertical (Pd_V) diameters and further Pd_H and Pd_V were also negatively associated with KSL under field drought conditions. Schmitz et al. (2007) also reported that several pit characteristics including smaller pit-field fractions, smaller inner and outer pit apertures, smaller individual pit size, thicker pit membranes and the presence of vestures could be linked to a safer water transport system. Observations of more circular small sized vessels in different *Rhizophora* species growing on locations with lower annual rainfall and longer dry seasons (Schmitz et al. 2006) also provided a clear indication that more circular smaller vessels can offer an additional advantage in stressful conditions. The present study demonstrates that the diameter of intervessel pit aperture differed significantly among the mulberry genotypes and the differences might be closely associated to the hydraulic efficiency of the genotypes under field drought conditions though further data would be needed to explain this observation.

Vessel grouping, one the important xylem characteristics, is also found to differ among the mulberry genotypes. Within drought tolerant genotypes, vessel grouping was higher in the conditions of field drought, whereas the vessels of drought susceptibles were less grouped. One way to mitigate the trade-off between vessel size and vulnerability is to have small vessel for safety, but to minimize the xylem/vessel area ratio by packing the maximum number of small vessels in xylem. Thus, high vessel grouping does not only increase hydraulic efficiency, it also safeguards the water transport system (Mauseth and

PlemonsRodriguez 1997; Villar-Salvador et al. 1997). High vessel grouping, more probable with high vessel density, can also bring a functional advantage because it allows water to bypass air-filled vessels by alternative pathways created by the intervessel pits of touching vessels in a vessel group (Zimmermann 1983; Yáñez-Espinosa et al. 2001; Lopez et al. 2005). On the contrary, there may be limits to high vessel grouping. A higher vessel grouping can also increase cavitation probability as vessel contact, influencing the spread of embolisms, is more intense (Wheeler et al. 2005; Hacke et al. 2006; Choat et al. 2008). We, however, do not know whether either the safety aspect or the cavitation spread is the more important in the present context. As we observed higher vessel grouping and smaller pit field fractions in the drought tolerant genotypes, both safety and cavitation spread might be balanced, giving the drought tolerant genotypes a functional advantage. Apart from vessel diameter, vessel shape, vessel grouping and vessel density, the vessel element length was also significantly different among the mulberry genotypes studied. Vessel length and not vessel element length is generally considered the more important hydraulic characteristic (Robert et al. 2009). However, vessel length was not quantified in the present study and further research need to be conducted to investigate if smaller vessel elements (i) obstruct the spreading of embolisms by their perforation plates and hence are functionally advantageous, (ii) on the contrary, a functional disadvantage causing increased embolism spread due to higher resistance to xylem sap flow (Ellerby and Ennos 1998; Schulte 1999) and thus larger pressure differences across intervessel pits, or (iii) do not have a functional significance and behave independently.

Although validation is needed, the interpretation of all wood anatomical characteristics studied does not contradict the statement that the water transport systems of drought tolerant mulberry genotypes were most probably safer and highly advantageous than that of drought susceptibles. In this respect, the agro-ecological success of these anisohydric drought tolerant genotypes (discussed in Chapter 5) can be related to the characteristics of their water transport system. As this safety and efficiency of the water transport is reflected in the leaf gas exchange and KSL of the drought tolerant anisohydric genotypes (**Fig. 6.18**), it can be concluded that the vessel traits of these genotypes explain at least partially the better photosynthetic productivity of those genotypes under field drought conditions. Not only locally, but also within the country, V1, S13 and S1 have a

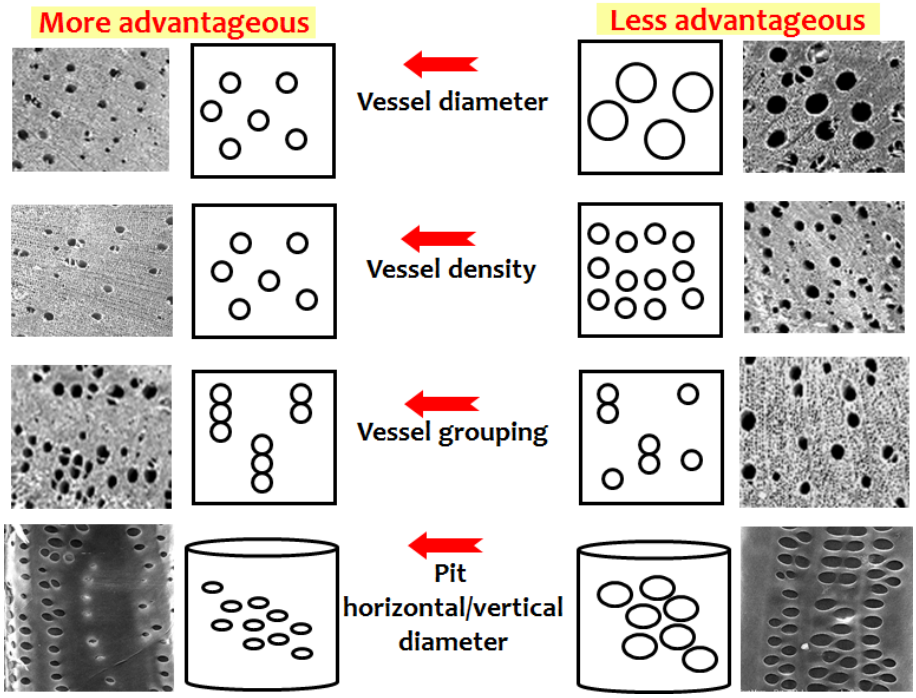

Fig. 6.18 Overview of the observed wood anatomical characteristics of mulberry genotypes. Anisohydric genotypes showing drought tolerance under field drought conditions that are more challenging for the water transport system, are characterized by a water transport system composed of low vessel density, high vessel grouping, small vessel diameters and small sized pit aperture. Taking the functional interpretation of all these wood anatomical characteristics together, the water transport system of anisohydric mulberry trees at the agroclimatic location of the present experiment is considered safer and advantageous. Arrows showing ecological gradients from less advantageous to more advantageous water transport systems.

wider distribution when compared to many other genotypes (Dandin et al. 2003). Thus, it can be expected that the characteristic vessel anatomy of these genotypes can also contribute to the explanation of their wider distribution in different moriculture regions across the country. Across the ecological gradient from semi-arid to arid, we can expect a transect of environmental conditions that are less and less suitable for perennial tree crops like mulberry. The intermediate vessel traits were associated with safety and efficiency of the water transport system of mulberry trees and have a high potential to explain crop yield sustainability under future climate change, at least partially. We clearly demsonstrate that the water transport system of drought tolerant mulberry genotypes with a low vessel density, a high vessel grouping, small vessel diameters and small sized pit, is in contrast with the water transport system of drought susceptible genotypes and is expected to be safer and physiologically efficient as recorded in our present study.

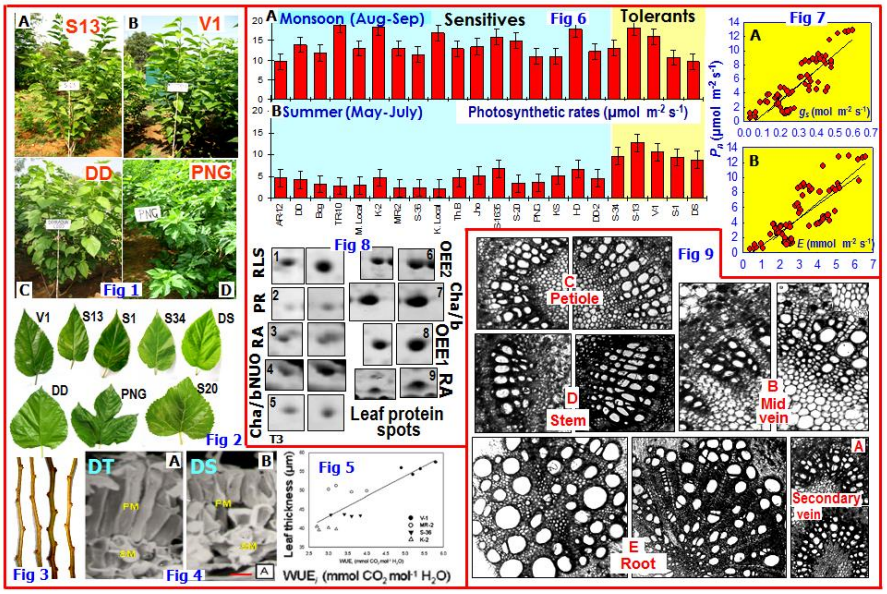

Chapter 7

The present study estimated leaf-level functional traits and stem wood characteristics of mulberry stands aiming to identify key traits that are linked to high biomass productivity. Mulberry trees were cultivated in SRC system under well-irrigated optimum farming conditions. Data were collected on biomass yield along with several leaf-level physiobiochemical characteristics and wood quality parameters. Significant genetic variation was recorded amongst the genotypes in most of the studied parameters. Fifteen out of total 22 traits, used in computing correlation coefficient matrix, were found to correlate with above ground biomass yield. Light-saturated rate of photosynthesis, performance index, leaf nitrogen content, minimum leaf water potential and leaf-specific hydraulic conductance showed strong positive correlation with biomass productivity. Wood density, wood cross-sectional area and fiber cell density exhibited tight correlation with woody biomass yield. Fifteen key parameters were identified which were correlated with above ground biomass yield, whereas remaining traits showed either negative, weak or no correlations with productivity. Those fifteen traits could be most appropriate indicators to select mulberry genotypes with higher photosynthetic efficiency and biomass yield.

The study was aimed to screen drought tolerant genotypes and to investigate whether photosynthetic leaf gas exchange traits scale with hydraulic conductance in mulberry. In a

two phasic experimental design combining field and glasshouse observations, mulberry genotypes were surveyed under two irrigation regimes: well-watered and water-limited. The genotypes were assessed for variation in key leaf gas exchange characteristics including net photosynthetic rates (P_n), stomatal conductance (G_s), transpiration rates (E) and instantaneous water use efficiency (WUE_i). Leaf yield/plant was considered to determine the tolerance index (TI). Drought stress severely down-regulated leaf-level physiological variables in the susceptible genotypes resulting in poor leaf yield. However, genotypes S13 and V1 performed better in terms of leaf gas exchange and proved their superiority over other genotypes in drought tolerance. Leaf photosynthetic traits scaled with hydraulic conductance in the DT genotypes and better KSL resulted in higher G_s and E values even under water stress conditions. The combined leaf gas exchange/chl a fluorescence measurements dissected out stomatal and non-stomatal restrictions to P_n. Overall, the results indicated that a better rooting vigor and leaf hydration status, minimal stomatal inhibition and stabilized photochemistry might play major roles in maintaining higher P_n and associated gas exchange functions in drought tolerant mulberry genotypes under water stress conditions. The drought tolerant V1 showed significantly higher accumulation of α-tocopherol and AA-glutathione pool in association with higher carotenoids and proline contents. Susceptible S36, K2 and MR2 could not induce any significant up-regulation in AA-glutathione pool leading to endogenous loss of α-tocopherol and more lipid peroxidation. The study demonstrated that proline, AA and glutathione were the major non-enzymatic antioxidants in mulberry with α-tocopherol and carotenoids as good additional indicators for drought stress tolerance.

Modulation of photosynthesis and the underlying mechanisms were studied in mulberry genotypes under progressive drought stress conditions. The OJIP transients and other associated biophysical parameters elucidated the events of photoacclimatory changes in PSII with progressive increase in drought stress. Down-regulation of PSII activity occurred predominantly due to increase in inactive reaction centers (RCs), decrease in electron transport per RC (ET_O/RC) as well as per leaf cross-section (ET_O/CS_m) and enhanced energy dissipation. The L and K- bands appeared only in the stage of extreme drought severity indicating the ability of drought tolerant genotype V1 to resist drought-induced damage on structural stability of PSII and imbalance between the electrons at the

acceptor and donor sides of PSII, respectively. Drought-induced changes in leaf protein analyses revealed significant up-regulation of important proteins associated to photostability of thylakoid membrane including oxygen evolving enhancer, chlorophyll a/b binding proteins, rubisco and rubisco activase. Further, the antioxidative defense proteins including peroxiredoxin and NADH ubiquinone oxidoreductase were also enhanced. The study demonstrated an integrated down-regulation of the photosynthetic process to maintain intrinsic balance between electron transfer reactions and reductive carbon metabolism without severe damage to PSII structural and functional integrity. In the drought tolerant V1, at root and leaf level significant up-regulation of MIPIP1.3 was recorded which was comparable with the concomitant higher leaf water potential and transpiration rates of the same when compared to the susceptible genotypes. The correlation of anatomical structures with physiological traits also supported the superior performance of V1 when compared to other drought susceptible genotypes under water stress. Genotype V1 possessed innate anatomical architectures like thicker leaves, well developed palisade tissues which would contribute to remain 'stay-green' and retain higher photosynthetic pigments with highest magnitude of photosynthetic performance. The higher number of xylem vessels recorded in V1 root and leaf would improve the capabilities for water transport.

In the present study, measurements were undertaken on diurnal leaf gas exchange, photoacclimation and midday xylem sap flow characteristics associated with the sustenance of crop yield in drought-stressed mulberry genotypes cultivated under hot semi-arid steppe agroclimate of southern India. In spite of significant down-regulation in leaf gas exchange, the drought-stressed stands still exhibited considerable rate of photosynthesis along with significant concomitant decrease in leaf water potential (Ψ_L), more conspicuously during midday (12.00 to 13.00 h) depicting less stomatal control on Ψ_L, a behaviour known to be typically 'anisohydric'. The diurnal course of P_n showed clear difference between two treatments. The CO_2 fixation rates in both treatments increased in the morning between 08.00 and 10.00 h, thereafter, mean P_n was more or less stable in control stands until 11.00 h and then started to show drawdown during midday followed by afternoon recovery, however not to a full extent. However, in drought-stressed stands, P_n values started decreasing soon after 10.00 h and showed gradual down-regulation during

midday followed by late afternoon recovery. In order to prevent over-excitation of the reaction centers, apparent photoacclimatory changes in PSII were recorded in drought-exposed stands which included decrease in the electron transport and enhanced thermal dissipation from PSII when compared to the controls. Midday stem xylem sap flow was considerably higher in the drought tolerant V1 when compared to drought susceptibles. Such higher xylem sap flow was positively correlated with higher transpiration rate and better photosynthetic performance of V1. Overall, the data demonstrate some of the important driving mechanisms adapted by mulberry to tolerate drought stress and sustain yield.

Analyses of stem wood hydraulic architecture in mulberry revealed interesting vessel traits which were associated with optimization of hydraulic conductance as well as conferring safety from cavitation under soil moisture stress conditions. The tested genotype seems to deal with higher cavitation risk at soil dehydration mainly by optimizing V_D. A less but more number of functional vessels can optimize the water transport under drought conditions by facilitating a more efficient bypass of cavitation-affected vessels. Besides V_D, vessel grouping is also considered to be an important xylem characteristic. High vessel grouping can induce functional advantage by allowing water to bypass air filled vessels through alternative pathways created by the intervessel pits of adhering vessels in a vessel group. The experimental findings elucidates that maintenance of higher vessel grouping index (V_{GI}) is a preferred strategy in drought tolerant mulberry genotypes by virtue of which the genotypes might balance both safety and cavitation spread. Apart from vessel architecture, inter-vessel pit characteristics also played significant roles in safe-guarding and optimizing the water-transport functions, which are predicted to be adaptive strategies in optimally balancing trade-offs among conductive efficiency, mechanical strengths and resistance to cavitation. SEM images of vessel elements from the outer side of lumen showed dominancy of simple perforation plates in the end wall of vessel elements in drought tolerant genotypes which is suggested to be an effective characteristic feature of dry arid and/or semi-arid climates with a seasonal or permanent demand of greater hydraulic efficiency. The size of pit chamber aperture was minute in drought tolerant genotypes and such shallow pit chamber aperture and especially thick pit membrane as observed V1 stands could play a substantial role in the prevention of

excessive pit membrane stretching or deflection. Moreover, the dense helical thickening observed in the inner vessel walls of drought-stressed V1 could also contribute to a high safety factor.

Major conclusions

- Leaf functional traits including net CO_2 fixation, light-saturated rates of photosynthesis, performance index, leaf nitrogen content and hydraulic conductance (KSL) could be the most appropriate indicators to select high yielding mulberry.
- Wood density, stem wood cross-sectional area and fibre cell number should be useful to screen mulberry genotypes for high woody biomass productivity.
- Substantial genotypic variation exists in physiological and biomass yield traits in mulberry under water stress.
- Photosynthesis rate, stomatal conductance, KSL, PSII photochemistry and root to shoot ratio are likely to be appropriate markers for assessing drought stress tolerance in mulberry.
- Leaf photosynthetic traits scaled with hydraulic conductance in the drought tolerant genotypes and better KSL resulted in higher Gs and E values, even under water stress conditions.
- Modulation of photosynthesis in drought tolerant genotype under progressive drought involved an integrated down-regulation of the leaf assimilation physiology and PS-II performance.
- Decreased PS-II performance under drought stress was due to increment in inactive RCs, slowing down of QA reduction, decrease in electron transport beyond QA^- and increased energy dissipation.
- The structural integrity and stability of PSII were largely maintained in the DT genotype as reflected by the L - and K-bands.

- The inbuilt efficient leaf and root-level hydraulic architecture and hydraulic acclimations resulted in better photosynthetic performance of the drought tolerant genotype.

- For the first time, the present study reports that the drought-stressed *M. indica* showed diurnal cycles of loss and recovery in leaf gas exchange characteristics.

- Anisohydric behaviour, associated with efficient KSL in mulberry, is advantageous during seasonal summer drought in sustaining photosynthetic CO_2 fixation.

- KSL and xylem sap flow measured in drought tolerant genotype scaled with its leaf transpiration and net CO_2 fixation rates.

- The study elucidates that the drought-stressed mulberry achieved necessary PSII photoprotection and substantially increased thermal dissipation of energy during the peak summer time.

- Stem wood hydraulic architecture including vessel size, vessel density and percentage of area occupied by vessels significantly varied among the mulberry genotypes.

- The anatomical data demonstrate that stem wood xylem vessel architecture largely influences KSL and in turn leaf water status, photosynthetic carbon gain, growth rates and biomass yields both under optimal as well as limited soil moisture conditions.

- Simple perforation plates and dense helical thickening in the inner vessel walls could play a substantial role in maintaining better hydraulic efficiency and prevention of excessive pit membrane deflection, respectively.

- At stem wood level, small vessel diameter, less vessel density, high vessel grouping index and small pits can positively scale with better KSL and photosynthetic performance of the anisohydric mulberry genotypes under field drought conditions.

Aasamaa K, NiinemetsU, Sober A. 2005. Leaf hydraulic conductance in relation to anatomical and functional traits during *Populus tremula* leaf ontogeny. *Tree Physiology* 25: 1409-1418.

Aasamaa K, Sober A, Rahi M. 2001. Leaf anatomical characteristics associated with shoot hydraulic conductance, stomatal conductance and stomatal sensitivity to changes of leaf water status in temperate deciduous trees. *Australian Journal of Plant Physiology* 28: 765-774.

Abbasi FM, Komatsu S. 2004. A proteomic approach to analyse salt-responsive proteins in rice leaf sheath. *Proteomics* 4: 2072-2081.

Acherar M, Rambal S. 1992. Comparative water relations of four Mediterranean oak species. *Plant Ecology* 99-100: 177-184.

Ackerly DD. 2004. Functional strategies of chaparral shrubs in relation to seasonal water deficit and disturbance. *Ecological Monograph* 74: 25-44.

Adams HD, Guardiola-Claramonte M, Barron-Gafford G, Camilo Villegasa J, Breshears D, Zou C, Troch P, Huxman T. 2009. Reply to Sala: Temperature sensitivity in drought-induced tree mortality hastens the need to further resolve a physiological model of death. *Proceedings of the National Academy of Sciences of the Unites States of America* 106: E69.

Adamski JM, Peters JA, Danieloski R, Bacarin MA. 2011. Excess iron-induced changes in the photosynthetic characteristics of sweet potato. *Journal of Plant Physiology* 168: 2056-2062.

Addington RN, Donovan LA, Mitchell RJ, Vose M, Pecot SD, Jack SB, Hacke UG, Sperry JS, Oren R. 2006. Adjustments in hydraulic architecture of *Pinus palustris* maintain similar stomatal conductance in xeric and mesic habitats. *Plant, Cell & Environment* 29: 535-545.

Agastian P, Vivekanandan M. 1997. Evaluation of mulberry genotypes for saline tolerance by chemo and bio-assays. *Indian Journal of Sericulture* 36:142-146.

Aguilar-Rodríguez M, Abundiz-Bonilla L, Barajas-Morales. 2001. Comparación de la gravedad específica y características anatomicas de la madera de dos comunidades vegetales en México. Anales del Instituto de Biología, Universidad Nacional Autonoma de México. *Serie Botánica* 72:171-185.

Aharon R, Shahak Y, Wininger S, Bendov R, Kapulnik Y, Galili G. 2003. Overexpression of a plasma membrane aquaporin in transgenic tobacco improves plant vigor under favorable growth conditions but not under drought or salt stress. *The Plant Cell* 15: 439-447.

Ahmad P, Sharma S. 2010. Physio-biochemical attributes in two cultivars of mulberry (*Morus alba* L.) under $NaHCO_3$ stress. *International Journal of Plant Production* 4: 79-86.

Alexandersson E, Fraysse L, Sjovall-Larsen S, Gustavsson S, Fellert M, Karlsson M, Johanson U, Kjellbom P. 2005. Whole gene family expression and drought stress regulation of aquaporins. *Plant Molecular Biology* 59: 469-484.

Allen CD, Macalady A, Chenchouni H, Bachelet D, McDowell N, Vennetier M, Gonzales P, Hogg T, Rigling A, Breshears D *et al*. 2010. A global overview of drought and heat-induced tree mortality reveals emerging climate change risks for forests. *Forest Ecology and Management* 259: 660-684.

Allen CD. 2009. Climate-induced forest dieback: an escalating global phenomenon? *Unasylva*, 231/232, 43-49.

Allen LH, Valle RR, Mishoe JW, Jones JW. 1994. Soybean leaf gas-exchange responses to carbon dioxide and water stress. *Agronomy Journal* 86: 625-636.

Allen RG, Pereira LS, Raes D, Smith M. 1998. Crop evapotranspiration: Guidelines for computing crop requirements. Irrigation and Drainage Paper No. 56, FAO, Rome, Italy.

Alpert P, Simms EL. 2002. The relative advantages of plasticity and fixity in different environments: when is it good for a plant to adjust? *Evolutionary Ecology* 16: 285-297.

Amthor JS. 2000. The McCree-deWit-Penning de Vries-Thornley respiration paradigms: 30 years later. *Annals of Botany* 86: 1-20.

Angelopoulos K, Dichio B, Xiloyannis C. 1996. Inhibition of photosynthesis in olive trees (*Olea europaea* L.) during water stress and rewatering. *Journal of Experimental Botany* 47: 1093-1100.

Aranda I, Gil L, Pardos JA. 2005. Seasonal changes in apparent hydraulic conductance and their implications for water use of European beech (*Fagus sylvatica* L.) and sessile oak [*Quercus petraea* (Matt.) Liebl] in South Europe. *Plant Ecology* 179: 155-167.

Aroca R, Amodeo G, Fernádez-Illescas S, Herman EH, Chaumont F, Chrispeels MJ. 2005. The role of aquaporins and membrane damage in chilling and hydrogen peroxide induced changes in the hydraulic conductance of maize roots. *Plant Physiology* 137: 341-353.

Aroca R, Ferrante A, Vernieri P, Chrispeels MJ. 2006. Drought, abscisic acid and transpiration rate effects on the regulation of PIP aquaporin gene expression and abundance in *Phaseolus vulgaris* plants. *Annals of Botany* 98: 1301-1310.

Asada K. 1999. The water–water cycle in chloroplasts scavenging of active oxygens and dissipation of excess photons. *Annual Review of Plant Physiology and Plant Molecular Biology* 50: 601-639.

Ashraf M, Foolad MR. 2007. Roles of glycine betaine and proline in improving plant abiotic stress resistance. *Environmental and Experimental Botany* 59: 206-216.

Aspinwall MJ, King JS, McKeand SE, Domec JC. 2011. Leaf-level gas-exchange uniformity and photosynthetic capacity among loblolly pine (*Pinus taeda* L.) genotypes of contrasting inherent genetic variation. *Tree Physiology* 31: 78-91.

Assmann SM, Snyder JA, Lee YRJ. 2000. ABA-deficient (*aba1*) and ABA insensitive (*abi1-1, abi2-1*) mutants of Arabidopsis have a wild-type stomatal response to humidity. *Plant, Cell & Environment* 23: 387-395.

Austin RB. 1989. Genetic variation in photosynthesis. *Journal of Agricultural Science* 112: 287-294.

Bacelar EA, Santos DL, Moutinho-Pereira JM, Gonçalves BC, Ferreira HF, Correia CM. 2006. Immediate responses and adaptive strategies of three olive cultivars under contrasting water

availability regimes: changes on structure and chemical composition of foliage and oxidative damage. *Plant Science* 170: 596-605.

Baltzer J, Gregoire DM, Bunyavejchewin S, Noor NSM, Davies SJ. 2009. Coordination of foliar and wood anatomical traits contributes to tropical tree distributions and productivity along the Malay-Thai Peninsula. *American Journal of Botany* 96: 2214-2223.

Barathi P, Sundar D, Ramachandra Reddy A. 2001. Changes in mulberry leaf metabolism in response to water stress. *Biologia Plantarum* 44: 83-87.

Barnard H, Ryan MG. 2003. A test of the hydraulic limitation hypothesis in fast-growing *Eucalyptus saligna*. *Plant, Cell & Environment* 26: 235-1245.

Bates LM, Hall AE. 1981. Stomatal closure with soil depletion not associated with changes in bulk leaf water status. *Oecologia* 50: 62-65.

Bates LS, Walderen RP, Teare ID. 1973. Rapid determination of free proline for water stress studies. *Plant and Soil* 39: 205-207.

Becana M, Aparicio-Tejo P, Irigoyen JJ, Sanchez-diaz M. 1986. Some enzymes of hydrogen peroxide metabolism in leaves and root nodules of *Medicago sativa*. *Plant Physiology* 82: 1169-1171.

Bedon F, Villar E, Vincent D, Dupuy J-W, Lomenech A-M, Mabialangoma A, Chaumeil P, Barré A, Plomion C, Gion J-M. 2010. Proteomic plasticity of two *Eucalyptus* genotypes under contrasted water regimes in the field. *Plant, Cell & Environment* 35: 790-805.

Ben Haj Salah H, Tardieu F. 1997. Control of leaf expansion rate of droughted maize plants under fluctuating evaporative demand. A superposition of hydraulic and chemical messages? *Plant Physiology* 114: 893-900.

Bernacchi CJ, Portis AR, Nakano H, von Caemmerer S, Long SP. 2002. Temperature response of mesophyll conductance. Implications for the determination of Rubisco enzyme kinetics and for limitations to photosynthesis *in vivo*. *Plant Physiology* 130: 1992-1998.

Bhaskar R, Ackerly DD. 2006. Ecological relevance of minimum seasonal water potentials. *Physiologia Plantarum* 127: 353-359.

Bhaskar R, Valiente-Banuet A, Ackerly DD. 2007. Evolution of hydraulic traits in closely related species pairs from Mediterranean and non-Mediterranean environments of North America. *New Phytologist* 176: 718-726.

Bhattacharya S, Ghosh JS, Sahoo DK, Dey N, Pal A. 2010. Screening of superior fiber-quality-traits among wild accessions of *Bambusa balcooa*: efficient and non-invasive evaluation of fiber developmental stages. *Annals of Forest Science* 67: 611

Biasiolo M, Canal MTDa, Tornadore N. 2004. Micromorphological characterization of ten mulberry cultivars (*Morus* spp.). *Economic Botany* 58: 639-646.

Blödner C, Majcherczyk A, Kües U, Polle A. 2007. Early drought-induced changes to the needle proteome of Norway spruce. *Tree Physiology* 27: 1423-1431.

Bloom AJ, Zwieniecki MA, Passioura JB, Randall LB, Hoolbrook NM, St Clair DA. 2004. Water relations under root chilling in a sensitive and tolerant tomato species. *Plant, Cell & Environment* 27: 971-979.

Borel C, Simonneau T, This D, Tardieu F. 1997. Stomatal conductance and ABA concentration in the xylem sap of barley lines of contrasting genetic origins. *Australian Journal of Plant Physiology* 24: 607-15.

Boursiac Y, Chen S, Luu DT, Sorieul M, van den Dries N, Maurel C. 2005. Early effects of salinity on water transport in Arabidopsis roots. Molecular and cellular features of aquaporin expression. *Plant Physiology* 139: 790-805.

Bramley H, Turner DW, Tyerman SD, Turner NC. 2007. Water flow in the roots of crop species: the influence of root structure, aquaporin activity, and water logging. *Advances in Agronomy* 96: 133-196.

Braun HJ. 1970. Funktionelle Histologie der sekunda¨ren Sprossachse. In: Zimmermann W, Ozenda P, and Wulff HD [eds.], *Encyclopedia of plant anatomy*, 2nd ed., 1-190. Gebrüder Borntraeger, Berlin, Germany.

Bréda N, Huc R, Granier A, Dreyer E. 2006. Temperate forest trees and stands under severe drought: a review of ecophysiological responses, adaptation processes and long-term consequences. *Annals of Forest Science* 63: 625-644.

Breshears DD, Cobb NS, Rich PM, Price KP, Allen CD, Balice RG, Romme WH, Kastens JH, Floyd ML, Belnap J *et al*. 2005. Regional vegetation die-off in response to global-change type drought. *Proceedings of the National Academy of Sciences,* USA 102: 15144-15148.

Breshears DD, McDowell NG, Goddard KL, Dayem KE, Martens SN, Meyer CW, Brown KM. 2008. Foliar absorption of intercepted rainfall improves plant water status and enables drought recovery. *Ecology* 89: 41-47.

Breshears DD, Myers OB, Meyer CW, Barnes FJ, Zou CB, Allen CD, McDowell NG, Pockman WT. 2009. Tree die-off in response to global change-type drought: mortality insights from a decade of plant water potential measurements. *Frontiers in Ecology and the Environment* 7: 185-189.

Brodribb TJ Holbrook NM. 2003. Changes in leaf hydraulic conductance during leaf shedding in seasonally dry tropical forest. *New Phytologist* 158: 295-303.

Brodribb TJ, Cochard H. 2009. Hydraulic failure defines the recovery and point of death in water-stressed conifers. *Plant Physiology* 149: 575-584.

Brodribb TJ, Feild T, Jordan G. 2007. Leaf maximum photosynthetic rate and venation are linked by hydraulics. *Plant Physiology* 144: 1890-1898.

Brodribb TJ, Feild TS. 2000. Stem hydraulic supply is linked to leaf photosynthetic capacity: evidence from New Caledonian and Tasmanian rainforests. *Plant, Cell & Environment* 23: 1381-1388.

Brodribb TJ, Holbrook NM, Zwieniecki MA, Palma B. 2005. Leaf hydraulic capacity in ferns conifers and angiosperms: impacts on photosynthetic maxima. *New Phytologist* 165: 839-846.

Brodribb TJ. 2009. Xylem hydraulic physiology: The functional backbone of terrestrial plant productivity. *Plant Science* 177: 245-251.

Bucci SJ, Goldstein G, Meinzer FC, Scholz FG, Franco AC *et al*. 2004a. Functional convergence in hydraulic architecture and water relations of tropical savanna trees: from leaf to whole plant. *Tree Physiology* 24: 891-899.

Bucci SJ, Scholz FG, Goldstein G, Meinzer FC, Hinojosa JA, Hoffmann WA, Franco AC. 2004b. Processes preventing nocturnal equilibration between leaf and soil water potential in tropical savanna woody species. *Tree Physiology* 24: 1119-1127.

Buckley TN, Mott KA, Farquhar GD. 2003. A hydromechanical and biochemical model of stomatal conductance. *Plant, Cell & Environment* 26: 1767-1785.

Buckley TN. 2005. The control of stomata by water balance. *New Phytologist* 168: 275-291.

Bukhov NG, Carpentier R. 2004. Effects of water stress on the photosynthetic efficiency of plants. In: Papageorgiou GC, Govindjee (eds) *Chlorophyll a fluorescence – A signature of photosynthesis*. Netherlands: Springer. pp 623-635.

Bunce JA. 2006. How do leaf hydraulics limit stomatal conductance at high water vapour pressure deficits? *Plant, Cell & Environment* 29:1644-1650.

Bunn SM, Rae AM, Herbert CS, Taylor G. 2004. Leaf-level productivity traits in *Populus* grown in short rotation coppice for biomass energy. *Forestry* 77: 307-323.

Burdett AN. 1979. A nondestructive method for measuring the volume of intact plant parts. *Canadian Journal of Forest Research* 9: 120-122.

Burgess SSO, Adams MA, Turner NC, Beverly CR, Ong CK, Khan AAH, Bleby TM. 2001. An improved heat pulse method to measure low and reverse rates of sap flow in woody plants. *Tree Physiology* 21: 589-598.

Burggraaf PD. 1972. Some observations on the course of the vessels in the wood of *Fraxinus excelsior* L. *Acta Botanica Neerlandica* 21: 32-47.

Campanello PI, Gatti MG, Goldstein G. 2008. Coordination between water-transport efficiency and photosynthetic capacity in canopy tree species at different growth irradiances. *Tree Physiology* 28: 85-94.

Campbell WJ, Ogren WL. 1995. Rubisco activase activity in spinach leaf extracts. *Plant & Cell Physiology* 36: 215-220.

Castillo FJ. 1996. Antioxidative protection in the inducible CAM plant *Sedum album* L. following the imposition of severe water stress and recovery. *Oecologia* 107: 469-477.

Chaitanya KV, Jutur PP, Sundar D, Reddy AR. 2003. Water stress effects on photosynthesis in different mulberry cultivars. *Plant Growth Regulation* 40: 75-80.

Chaitanya KV, Rasineni GK, Ramachandra Reddy A. 2009. Biochemical responses to drought stress in mulberry (*Morus alba* L.): evaluation of proline, glycine betaine, and abscisic acid accumulation in five cultivars. *Acta Physiologia Plantarum* 31: 437-443.

Chaitanya KV, Sundar D, Ramachandra Reddy A. 2001. Mulberry leaf metabolism under high temperature stress. *Biologia Plantarum* 44: 379-384.

Charilaos Y, Yiannis M, George KP. 2006. Leaf and green stem anatomy of the drought deciduous Mediterranean shrub *Calicotome villosa* (Poiret) Link. (Leguminosae). *Flora* 201: 102-107.

Chaturvedi HK, Sarkar A. 2000. Optimum size and shape of the plot for mulberry experiments. *Indian Journal of Sericulture* 39: 66-69.

Chaumont F, Barrieu F, Wojcik E, Chrispeels MJ, Jung R. 2001. Aquaporins constitute a large and highly divergent protein family in maize. *Plant Physiology* 125: 1206-1215.

Chave J, Coomes D, Jansen S, Lewis SL, Swenson NG, Zanne AE. 2009. Towards a worldwide wood economics spectrum. *Ecology Letters* 12: 351-366.

Chaves MM, Flexas J, Pinheiro C. 2009. Photosynthesis under drought and salt stress: regulation mechanisms from whole plant to cell. *Annals of Botany* 103: 551-560.

Chaves MM, Marcoco JP, Pereia JS. 2003. Understanding plant responses to drought – from genes to the whole plant. *Functional Plant Biology* 30: 239-264.

Chaves MM, Zarrouk O, Francisco R, Costa JM, Santos T, Regalado AP, Rodrigues ML, Lopes CM. 2010. Grapevine under deficit irrigation: hints from physiological and molecular data. *Annals of Botany* 105: 661-676.

Chiu ST, Ewers FW. 1993. The effect of segment length on conductance measurements in *Lonicera fragrantissima*. *Journal of Experimental Botany* 44: 175-181.

Choat B, Ball M, Luly J, Holtum J. 2003. Pit membrane porosity and water stress-induced cavitation in four co-existing dry rainforest tree species. *Plant Physiology* 131: 41-48.

Choat B, Ball MC, Luly JG, Holtum JAM. 2005. Hydraulic architecture of deciduous and evergreen dry rainforest tree species from north-eastern Australia. *Trees-Structure and Function* 19: 305-311.

Choat B, Cobb AR, Jansen S. 2008. Structure and function of bordered pits: new discoveries and impacts on whole-plant hydraulic function. *New Phytologist* 177: 608-626.

Christersson L. 2010. Wood production potential in poplar plantations in Sweden. *Biomass and Bioenergy* 34:1289-1299.

Cinnirella S, Magnani F, Saracino A, Borghetti M. 2002. Response of a mature Pinus laricio plantation to a three-year restriction of water supply: structural and functional acclimation to drought. *Tree Physiology* 22: 21-30.

Cochard H, Coll L, Roux XL, Ameglio T. 2002. Unraveling the effects of plant hydraulics on stomatal closure during water stress in walnut. *Plant Physiology* 128: 282-290.

Cochard H. 2006. Cavitation in trees. *Comptes Rendus Académie des Sciences Physique* 7: 1018-1026.

Cocozza C, Cherubini P, Regier N, Saurer M, Frey B, Tognetti R. 2010. Early effects of water deficit on two parental clones of *Populus nigra* grown under different environmental conditions. *Functional Plant Biology* 37: 244-254.

Collins A. 2001. Carotenoids and genomic stability. *Mutation Research* 475: 1-28.

Comparot S, Morilon R, Badot PM. 2000. Water permeability and revolving movement in *Phaseolus vulgaris* L. *Plant & Cell Physiology* 41: 114-118.

Comstock JP, Sperry JS. 2000. Theoretical considerations of optimal conduit length for water transport in vascular plants. Tansley Review No. 119. *New Phytologist* 148: 195-218.

Comstock JP. 2002. Hydraulic and chemical signalling in the control of stomatal conductance and transpiration. *Journal of Experimental Botany* 53:195-200.

Connor DJ. 2005. Adaptation of olive (*Olea europaea* L.) to water-limited environments. *Australian Journal of Agricultural Research* 56: 1181-1189.

Corcuera L, Camarero JJ, Gil-Pelegrin E. 2004. Effects of a severe drought on *Quercus ilex* radial growth and xylem anatomy. *Trees-Structure and Function* 18: 83-92.

Cornic G. 2000. Drought stress inhibits photosynthesis by decreasing stomatal aperture – not by affecting ATP synthesis. *Trends in Plant Science* 5: 187-188.

Correia MJ, Pereira JS, Chaves MM, Rodrigues M, Pacheco CA. 1995. ABA xylem concentrations determine maximum daily leaf conductance of field-grown *Vitis vinifera* L. plants. *Plant, Cell & Environment* 18: 511-521.

Cowan IR. 1972. An electrical analogue of evaporation from, and flow of water in plants. *Planta* 106: 221-226.

Cruiziat P, Cochard H, Améglio T. 2002. Hydraulic architecture of trees: main concepts and results. *Annals of Forest Science* 59: 723-752.

Curtin F, Schulz P. 1998. Multiple correlations and Bonferroni's correction. *Biological Psychiatry* 44: 775-777.

Cuso LL, Fernández RJ. 2012. Phenotypic plasticity as an index of drought tolerance in three Patagonian steppe grasses. *Annals of Botany* 110: 849-857.

Dai A, Trenberth KE, Qian TT. 2004. A global dataset of Palmer Drought Severity Index for 1870–2002: relationship with soil moisture and effects of surface warming. *Journal of Hydrometeorology* 5: 1117-1130.

Dandin SB, Jayaswal J, Giridhar K. 2003. Mulberry cultivation. In: Dandin SB, Jayaswal J, Giridhar K (eds) *Handbook of Sericulture Technologies*. Central Silk Board, Bangalore, pp 35-55.

Das M, Tetoriya M, Haq QMR, Khurana P. 2011. Screening and expression analysis of HAL3a, dehydrin, ABC transporter and NHX1 in ten genotypes of mulberry for abiotic stress tolerance. *Sericologia* (in press).

Davies WJ, Zhang J. 1991. Root signals and the regulation of growth and development of plants in drying soil. *Annual Review of Plant Physiology* 42: 55-76.

De Ronde JA, Cress WA, Krüger GHJ, Strasser RJ, Staden J. Van. 2004. Photosynthetic responses of transgenic soybean plants, containing an *Arabidopsis P5CR* gene, during heat and drought stress. *Journal of Plant Physiology* 161: 1211-1224.

Demetriou G, Neonaki C, Navakoudis E, Kotzabasis K. 2007. Salt stress impact on the molecular structure and function of the photosynthetic apparatus-The protective role of polyamines. *Biochimica et Biophysics Acta* 1767: 272-280.

Demirevska K, Stoilova LS, Vassileva V, Feller U. 2008. Rubisco and some chaperone protein responses to water stress and rewatering at early seedling growth of drought sensitive and tolerant wheat varieties. *Plant Growth Regulation* 56: 97-106.

Dias PC, Araujo WL, Moraes GABK, Barros RS, DaMatta FM. 2007. Morphological and physiological responses of two coffee progenies to soil water availability. *Journal of Plant Physiology* 164: 1639-1647.

Diaz-Espejo A, Nicolas E, Fernandez JE. 2007. Seasonal evolution of diffusional limitations and photosynthetic capacity in olive under drought. *Plant, Cell & Environment* 30: 922-933.

Dickison WC. 2000. Integrative Plant Anatomy. Academic Press, New York.

Dietz KJ, Jacob S, Oelze ML, Laxa M, Tognetti V, Marina S, Miranda ND, Baier M, Finkemeier I. 2006. The function of peroxiredoxins in plant organelle redox metabolism. *Journal of Experimental Botany* 57: 1697-1709.

Dillen SY, Rood SB, Ceulemans R. 2010. Growth and Physiology. In: Jansson S *et al*. (eds) *Genetics and genomics of Populus*. Plant Genetics and Genomics: Crops and Models 8. Springer Science, pp 39-63.

Ditmarová L, Kurjak D, Palmroth S, Kmeť J, Střelcová K. 2010. Physiological responses of Norway spruce (*Picea abies*) seedlings to drought stress. *Tree Physiology* 30: 205-213.

Domec JC *et al*. 2008. Maximum height in a conifer is associated with conflicting requirements for xylem design, *Proceedings of the National Academy of Sciences of the Unites States of America* 105: 12069-12074.

Donaldson LA, Singh AP, Yoshinaga A, Takabe K. 1999. Lignin distribution in mild compression wood of *Pinus radiata*. *Canadian Journal of Botany* 77: 41-50.

Donovan LA, West JB, McLeod KW. 2000. *Quercus* species differ in water and nutrient characteristics in a resource-limited fallline sandhill habitat. *Tree Physiology* 20: 929-936.

Durand TC, Sergeant K, Renaut J, Planchon S, Hoffmann L, Carpin S, Label P, Morabito D, Hausman JF. 2011. Poplar under drought: comparison of leaf and cambial proteomic responses. *Journal of Proteomics* 74: 1396-1410.

Eberhard S, Finazzi G, Wollman F-A. 2008. The dynamics of photosynthesis. *Annual Review of Genetics* 42: 463-515.

Edreva A. 2005. Generation and scavenging of reactive oxygen species in chloroplasts: a submolecular approach. *Agriculture, Ecosystem & Environment* 106: 119-133.

Efeoğlu B, Ekmekçi Y, Çiçek N. 2009. Physiological responses of three maize cultivars to drought stress and recovery. *South African Journal of Botany* 75: 34-42.

Ehleringer JR. 1994. Variation in gas exchange characteristics among desert plants. *Ecological Studies* 100: 361-392.

Ellerby DJ, Ennos AR. 1998. Resistances to fluid flow of model xylem vessels with simple and scalariform perforation plates. *Journal of Experimental Botany* 49: 979-985.

Elsheery N, Cao KF. 2008. Gas exchange, chlorophyll fluorescence, and osmotic adjustment in two mango cultivars under drought stress. *Acta Physiologia Plantarum* 30: 769-777.

Engelbrecht BMJ, Tyree MT, Kursar TA. 2007. Visual assessment of wilting as a measure of leaf water potential and seedling drought survival. *Journal of Tropical Ecology* 23: 497-500.

Ewers BE, Oren R, Sperry JS. 2000. Influence of nutrient versus water supply on hydraulic architecture and water balance in *Pinus taeda*. *Plant, Cell & Environment* 23: 1055-1066.

Faria T, Silvério D, Breia E, Cabral R, Abadia A, Abadia J, Pereira JS, Chaves MM. 1998. Differences in the response of carbon assimilation to summer stress (water deficits, high light and temperature) in four Mediterranean tree species. *Physiologia Plantarum* 102: 419-428.

Feng Y-L, Fu G-L, Zheng Y-L. 2008. Specific leaf area relates to the differences in leaf construction cost, photosynthesis, nitrogen allocation, and use efficiencies between invasive and noninvasive alien congeners. *Planta* 228: 383-390.

Finazzi G, Forti G. 2004. Metabolic flexibility of the green alga *Chlamydomonas reinhardtii* as revealed by the link between state transitions and cyclic electron flow. *Photosynthesis Research* 82: 327-338.

Flexas J, Bota J, Escalona JM, Sampol B, Medrano H. 2002. Effects of drought on photosynthesis in grapevines under field conditions: an evaluation of stomatal and mesophyll limitations. *Functional Plant Biology* 29: 461-471.

Flexas J, Bota J, Galmés J, Medrano H, Ribs-Carbó M. 2006. Keeping a positive carbon balance under adverse conditions: responses of photosynthesis and respiration to water stress. *Physiologia Plantarum* 127: 343-352.

Flexas J, Escalona JM, Medrano H. 1998. Down-regulation of photosynthesis by drought under field conditions in grapevines leaves. *Australian Journal of Plant Physiology* 25: 893-900.

Flexas J, Medrano H. 2002. Drought-inhibition of photosynthesis in C_3 plants: stomatal and non-stomatal limitations revisited. *Annals of Botany* 89: 183-189.

Flood PJ, Harbinson J, Aarts MGM. 2011. Natural genetic variation in plant photosynthesis. *Trends in Plant Science* 16: 327-335.

Foot K, Morgan RPC. 2005. The role of leaf inclination, leaf orientation and plant canopy architecture in soil particle detachment by raindrops. *Earth Surface Processes and Landforms* 30, pp. 1509-1520.

Forti G, Caldiroli G. 2005. State transitions in *Chlamydomonas reinhardtii*. The role of the Mehler reaction in state 2-to-state 1 transition. *Plant Physiology* 137: 492-499.

Foyer CH, Noctor G. 2005. Oxidant and antioxidant signalling in plants: a re-evaluation of the concept of oxidative stress in a physiological context. *Plant, Cell & Environment* 28: 1056-1071.

Franks PJ, Drake PL, Froend RH. 2007. Anisohydric but isohydrodynamic: seasonally constant plant water potential gradient explained by a stomatal control mechanism incorporating variable plant hydraulic conductance. *Plant, Cell & Environment* 30: 19-30.

Franks PJ, Farquhar GD. 1999. A relationship between humidity response, growth form and photosynthetic operating point in C_3 plants. *Plant, Cell & Environment* 22: 1337-1349.

Franks PJ. 2004. Stomatal control and hydraulic conductance, with special reference to tall trees. *Tree Physiology* 24: 865-878.

Franks PJ. 2006. Higher rates of leaf gas exchange are associated with higher leaf hydrodynamic pressure gradients. *Plant, Cell & Environment* 29: 584-592.

Fu J, Huang B. 2001. Involvement of antioxidants and lipid peroxidation in the adaptation of two cool-season grasses to localized drought stress. *Environmental and Experimental Botany* 45: 105-114.

Fu YL, Yu GR, Sun XM, Li YN, Wen XF, Zhang LM, Li ZQ, Zhao L, Hao YB. 2006. Depression of net ecosystem CO_2 exchange in semi-arid *Leymus chinensis* steppe and alpine shrub. *Agricultural and Forest Meteorology* 137: 234-244.

Fujii T, Lee SJ, Kuroda N, Suzuki Y. 2001. Conductive function of intervessel pits through a growth ring boundary of *Machilus thunbergii*. *IAWA Journal* 22: 1-14.

Funada R. 2002. Immunolocalisation and visualisation of the cytoskeleton in gymnosperms using confocal laser scanning microscopy. In: N. Chaffey [ed.], *Wood formation in trees - cell and molecular biology techniques*, 143-157. Taylor and Francis, New York, New York, USA.

Galmes J, Abadia A, Medrano H, Flexas J. 2007. Photosynthesis and photoprotection responses to water stress in the wild-extinct plant *Lysimachia minoricensis. Environmental and Experimental Botany* 60: 308-317.

Galvez DA, Landhäusser SM, Tyree MT. 2011. Root carbon reserve dynamics in aspen seedlings: does simulated drought induce reserve limitation? *Tree Physiology* 31: 250-257.

Genty B, Briantais JM, Baker N. 1989. The relationship between the quantum yield of photosynthetic electron transport and quenching of chlorophyll fluorescence. *Biochimica et Biophysica Acta* 900: 87-92.

Gill SS, Tuteja N. 2010. Reactive oxygen species and antioxidant machinery in abiotic stress tolerance in crop plants. *Plant Physiology and Biochemistry* 48: 909-930.

Giridara Kumar S, Madhusudhan KV, Sreenivasulu N, Sudhakar C. 2000. Stress responses in two genotypes of mulberry (*Morus alba* L.) under NaCl salinity. *Indian Journal of Experimental Biology* 38:192-195.

Givnish TJ. 1995. Plant stems: biomechanical adaptation for energy capture and influence on species distributions. In B. L. Gartner [ed.], *Plant stems: physiology and functional morphology*, 3-41. Academic Press, San Diego, CA.

Gomes FP, Oliva MA, Mielke MS, Almeida A-AFde, Leite HG, Aquino LA. 2007. Photosynthetic limitations in leaves of young Brazilian Green Dwarf coconut (*Cocos nucifera* L. '*nana*') palm under well-watered conditions or recovering from drought stress. *Environmental and Experimental Botany* 62: 195-204.

Gong JR, Zhang XS, Huang YM. 2011. Comparison of the performance of several hybrid poplar clones and their potential suitability for use in northern China. *Biomass & Bioenergy* 35: 2755-2764

Gonzalez E, Milera M. 2002. Mulberry in Livestock Feeding Systems in Cuba: Forage Quality and Goat growth. In: *Mulberry for animal production* (M. D. Sanchez). Animal Health and Production Paper No. 147. FAO, Rome, Italy.

González-Rodríguez AM, Martín-Olivera A, Morales D, Jiménez MS. 2005. Physiological responses of tagasaste to a progressive drought in its native environment on the Canary Islands. *Environmental and Experimental Botany* 53: 195-204.

Gould KS, Mckelvie J, Markham KR. 2002. Do anthocyanins function as antioxidants in leaves? Imaging of H_2O_2 in red and green leaves after mechanical injury. *Plant, Cell & Environment* 25: 1261-1269.

Grassi G, Magnani F. 2005. Stomatal, mesophyll conductance and biochemical limitations to photosynthesis as affected by drought and leaf ontogeny in ash and oak trees. *Plant, Cell & Environment* 28: 834-849.

Griffith OW, Meister A. 1979. Potent and specific inhibition of glutathione synthesis by buthionine sulfoximine (*s*-*n*-butylhomocysteine sulfoximine). *Journal of Biological Chemistry* 254: 7558-7560.

Guidi W, Tozzini C, Bonari E. 2009. Estimation of chemical traits in poplar short-rotation coppice at stand level. *Biomass & Bioenergy* 33: 1703-1709.

Guo P, Baum M, Grando S, Ceccarelli S, Bai G *et al*. 2009. Differentially expressed genes between drought-tolerant and drought-sensitive barley genotypes in response to drought stress during the reproductive stage. *Journal of Experimental Botany* 12: 3531-3544.

Hacke UG, Jacobsen AL, Pratt RB. 2009. Xylem function of arid-land shrubs from California USA: an ecological and evolutionary analysis. *Plant, Cell & Environment* 32: 1324-1333.

Hacke UG, Sperry JS, Ewers B, Schafer K, Oren R. 2000. Influence of soil porosity on water use in *Pinus taeda*. *Oecologia* 124: 495-505.

Hacke UG, Sperry JS, Pittermann J. 2000. Drought experience and cavitation resistance in six shrubs from Great Basin, Utah. *Basic and Applied Ecology* 1: 31-41.

Hacke UG, Sperry JS, Pockman WT, Davis SD, McCulloh KA. 2001. Trends in wood density and structure are linked to prevention of xylem implosion by negative pressure. *Oecologia* 126: 457-461.

Hacke UG, Sperry JS, Wheeler JK, Castro L. 2006. Scaling of angiosperm xylem structure with safety and efficiency. *Tree Physiology* 26: 689-701.

Hacke UG, Sperry JS. 2001. Functional and ecological xylem anatomy. *Perspectives in Plant Ecology Evolution and Systematics* 4: 97-115.

Haldiman P, Strasser RJ. 1999. Effects of anaerobiosis as probed by the polyphasic chlorophyll *a* fluorescence rise kinetic in pea (*Pisum sativum* L.). *Photosynthesis Research* 62: 67-83.

Hanba YT, Shibasaka M, Hayashi Y, Hayakawa T, Kasamo K, Terashima I *et al*. 2004. Overexpression of the barley aquaporin HvPIP2; 1 increases internal CO_2 assimilation in the leaves of transgenic rice plants. *Plant & Cell Physiology* 45: 521-52.

Hao GY, Hoffmann WA, Scholz FG, Bucci SJ, Meinzer FC, Franco AC, Cao KF, Goldstein G. 2008. Stem and leaf hydraulics of congeneric tree species from adjacent tropical savanna and forest ecosystems. *Oecologia* 155: 405-415.

Hare PD, Cress WA. 1997. Metabolic implications of stress-induced proline accumulation in plants. *Plant Growth Regulation* 21: 79-102.

Hargrave KR, Kolb KJ, Ewers FW, Davis SD. 1994. Conduit diameter and drought-induced embolism in *Salvia mellifera* Greene (Labiatae). *New Phytologist* 126: 695-705.

Hashiguchi A, Ahsan N, Komatsu S. 2010. Proteomics application of crops in the context of climatic changes. *Food Research International* 43: 1803-1813.

Hazen SP, Pathan MS, Sanchez A, Baxter I, Dunn M *et al*. 2005. Expression profiling of rice segregating for drought tolerance QTLs using a rice genome array. *Funtional & Integrative Genomics* 5: 104-116.

He C, Zhang J, Duan A, Zheng S, Sun H, Fu L. 2008. Proteins responding to drought and high-temperature stress in *Populus x euramericana* cv. '74/76', *Trees-Structure and Function* 22: 803-813.

Henson IE, Jensen CR, Turner NC. 1989. Leaf gas exchange and water relations of lupins and wheat. I. Shoot responses to soil water deficits. *Australian Journal of Plant Physiology* 16: 401-413.

Hermans C, Smeyers M, Rodriguez RM, Eyletters M, Strasser RJ, Delhaye JP. 2003. Quality assessment of urban trees: a comparative study of physiological characterisation, airborne imaging and on site fluorescence monitoring by the OJIP-test. *Journal of Plant Physiology* 160: 81-90.

Hernandez JA, Ferrer MA, Jiménez A, Barceló AR, Sevilla F. 2001. Antioxidant systems and O_2 /H_2O_2 production in the apoplast of pea leaves, its relation with salt-induced necrotic lesions in minor veins. *Plant Physiology* 127: 817- 831.

Himmelsbach W, Treviño-Garza E J., González-Rodríguez H, González-Tagle MA., Meza M V G, Calderón O A A, Castillón A E E , Mitlöhner R. 2012. Acclimatation of three co-occurring tree species to water stress and their role as site indicators in mixed pine-oak forests in the Sierra Madre Oriental, Mexico. *European Journal of Forest Research* 131: 355-367.

Hinchee M, Rottamann W, Mullinax L, Zhang C, Chang S, Cunningham M, Pearson L, Nehra N. 2009. Short-rotation woody crops for bioenergy and biofuel applications. *In Vitro Cellular and Developmental Biology-Plant* 45: 619-629.

Holbrook NM, Zwieniecki MA. 1999. Embolism repair and xylem tension: do we need a miracle? *Plant Physiology* 120: 7-10.

Hong-Bo S, Li-Ye C, Ming-An S, Jaleel CA, Hong-Mei M. 2008. Higher plant antioxidants and redox signalling under environmental stresses. *Comptes Rendus Biologies* 331: 433-441.

Hubbard RM, Ryan MG, Stiller V, Sperry JS. 2001. Stomatal conductance and photosynthesis vary linearly with plant hydraulic conductance in ponderosa pine. *Plant, Cell and Environment* 24: 113-121.

Hultine KR, Koepke DF, Pockman WT, Fravolini A, Sperry JS, Williams DG. 2006. Influence of soil texture on hydraulic properties and water relations of a dominant warm-desert Phreatophyte. *Tree Physiology* 26: 313-323.

Hunt R. 1982. Plant Growth Curves. In *The Functional Approach to Plant Growth Analysis*, 248 (Ed Edward Arnold, London.

Hurkman WJ, Tanaka CK. 1986. Solubilization of plant membrane proteins for analysis by two-dimensional gel electrophoresis. *Plant Physiology* 81: 802-806.

IAWA Committee (1989) IAWA list of microscopic features for hardwood identification. *IAWA Bulletin* 10: 219-332.

Iovi K, Kolovou C, Kyparissis A. 2009. An ecophysiological approach of hydraulic performance for nine Mediterranean species. *Tree Physiology* 29: 889-900.

Ivanov AG, Sane PV, Krol M, Gray GR, Balseris A, Savitch LV, Öquist G, Hüner NPA. 2006. Acclimation to temperature and irradiance modulates PSII charge recombination. *FEBS Letters* 580: 2797-2802.

Jacobsen AL, Ewers FW, Pratt RB, Paddock WA, Davis SD. 2005. Do xylem fibres affect vessel cavitation resistance? *Plant Physiology* 139: 546-556.

Jacobsen AL, Pratt RB, Ewers FW, Davis SD. 2007. Cavitation resistance among 26 chaparral species of southern California. *Ecological Monograph* 77: 99-115.

Jang JY, Kim DG, Kim YO, Kim JS, Kang HS. 2004. An expression analysis of a gene family encoding plasma membrane aquaporins in response to abiotic stresses in *Arabidopsis thaliana*. *Plant Molecular Biology* 54: 713-725.

Jarbeau JA, Ewers FW, Davis SD. 1995. The mechanism of water-stress induced embolism in 2 species of chaparral shrubs. *Plant, Cell & Environment* 18: 189-196.

Jeżowski S, Głowacka K, Kaczmarek Z, Szczukowski S. 2011. Yield traits of eight common osier clones in the first three years following planting in Poland. *Biomass and Bioenergy* 35: 1205-1210.

Jiménez MS, González-Rodríguez AM, Morales D. 1999. Effect of dehydration on the photosynthetic apparatus of sun and shade leaves of laurel forest trees. *Zeitschrift für Naturforschung* 55c: 704-710.

Johanson U, Karlsson M, Johansson I, Gustavsson S, Sjövall S *et al*. 2001. The complete set of genes encoding major intrinsic proteins in *Arabidopsis* provides a framework for a new nomenclature for major intrinsic proteins in plants. *Plant Physiology* 126: 1358-1369.

Johansson I, Karlsson M, Johanson U, Larsson C, Kjellbom P. 2000. The role of aquaporins in cellular and whole plant water balance. *Biochimca et Biophysica Acta* 1465: 324-342.

Johansson I, Karlsson M, Shukla VK, Chrispeels MJ, Larsson C, Kjellbom P. 1998. Water transport activity of the plasmamembrane aquaporin PM28A is regulated by phosphorylation. *The Plant Cell* 10: 451-459.

Johnson SM, Doherty SJ, Croy RRD. 2003. Biphasic superoxide generation in potato tubers: A self amplifying response to stress. *Plant Physiology* 13: 1440-1449.

Jones H G. 1992. Plants and microclimate: A Quantitative approach to environmental plant physiology. Cambridge University Press, Cambridge.

Jones H G. 1998. Stomatal control of photosynthesis and transpiration. *Journal of Experimental Botany* 49: 387-398.

Jones HG, Sutherland RA. 1991. Stomatal control of xylem embolism. *Plant, Cell & Environment* 6: 607-612.

Kalaji HM, Govindjee, Bosa K, Kościelniak J, Żuk-Gołaszewska K. 2011. Effects of salt stress on photosystem II efficiency and CO_2 assimilation of two Syrian barley landraces. *Environmental and Experimental Botany* 73: 64-72.

Kamal-Eldin A, Appelqvist LA. 1996. The chemistry and antioxidant properties of tocopherols and tocotrienols. *Lipids* 31: 671-701.

Kanai Y, Fujita M, Takabe K. 1996. Vessel network tracing by wire insertion and pigment injection. *Bulletin of Kyoto University Forests* 68: 127-136.

Kapoor A. 2009. Sustainable Agriculture: Issues and Action Points In: Mendoza., Walter (Ed), *Indian network in Ethics and Climate Change (INECC)*, Visakhapatnam, pp 46-47.

Karaba NN, Sheshshayee MS, Udaykumar M. 2008. *Biotech News: Options for improvement-mulberry*, Vol III, No 5.

Karatassiou M, Parissi ZM, Abraham EM, Kyriazopoulos AP. 2008. Growth of *Morus alba* L. under water deficit conditions. *Options Méditerranéennes* Series A. 70: 315-318.

Karp A, Shield I. 2008. Bioenergy from plants and the sustainable yield challenge. *New Phytologist* 179:15-32.

Katul G, Leuning R, Oren R. 2003. Relationship between plant hydraulic and biochemical properties derived from a steady-state coupled water and carbon transport model. *Plant, Cell & Environment* 26: 339-350.

Kenzo T, Ichie T, Yoneda R, Kitahashi Y, Watanabe Y, Ninomiya I, Koike T. 2004. Interspecific variation of photosynthesis and leaf characteristics in canopy trees of five species of Dipterocarpaceae in a tropical rain forest. *Tree Physiology* 24: 1187-1192.

Keyes WJ, G Lynn D, Erbil WK., Taylor JV, Apkarianb RP. 2002. H_2O_2 in interspecies signaling: a new role in host detection. *Microscopy and Microanalysis* 8: 962-963.

Kitin P, Funada R, Sano Y, Ohtani J. 2000. Analysis by confocal microscopy of the structure of cambium in the hardwood *Kalopanax pictus*. *Annals of Botany* 86: 1109-1117.

Kitin P, Sano Y, Funada R. 2003. Three-dimensional imaging and analysis of differentiating secondary xylem by confocal microscopy. *IAWA Journal* 24: 211-222.

Kitin PB, Fujii T, Abe H, Funada R. 2004 . Anatomy of the vessel network within and between tree rings of *Fraxinus lanuginose* (Oleaceae). *American Journal of Botany* 91: 779 - 788.

Kotresha D, Rao AP, Srinivas N, Vidyasagar GM. 2007. Antioxidative response to drought and high temperature stress in selected mulberry genotypes. *Physiology and Molecular Biology of Plants* 13: 57-63.

Kozlowski TT, Pallardy SG. 2002. Acclimation and adaptive responses of woody plants to environmental stresses. *Botanical Review* 68: 270-334.

Kramer PJ. 1980. Drought stress and the origin of adaptations. In: *Adaptation to Water and High Temperature Stress*. Eds. N.C. Turner and P.J. Kramer. John Wiley and Sons, New York, pp 7- 20.

Kulkarni M, Borse T, Chaphalkar S. 2007. Anatomical variability in grape (*Vitis venifera*) genotypes in relation to water use efficiency (WUE). *American Journal of Plant Physiology* 2: 36-43.

Kulkarni M, Borse T, Chaphalkar S. 2008. Mining anatomical traits: A novel modelling approach for increased water use efficiency under drought conditions in plants. *Czech Journal of Genetics and Plant Breeding* 44: 11-21.

Kulkarni M, Deshpande U. 2006. Comparitive studies in stem anatomy and morphology in relation to drought resistance in tomato (*Lycopersicon esculentum*). *American Journal of Plant Physiology* 1: 82-88.

Lal S, Bhatnagar S, Khurana P. 2006. Screening of Indian mulberry for abiotic stress tolerance and ameliorative effect of calcium on salinity stress. *Physiology and Molecular Biology of Plants* 12: 193-199.

Lal S, Ravi V, Khurana JP, Khurana P. 2009. Repertoire of leaf expressed sequence tags (ESTs) and partial characterization of stress-related and membrane transporter genes from mulberry (*Morus indica* L.). *Tree Genetics and Genomes* 5: 359-374.

Lambers H, Chapin FSIII, Pons TL. 2008. *Plant physiological ecology*. New York: Springer Science.

Lambers H, Poorter H. 2004. Inherent variation in growth rate between higher plants: a search for physiological causes and ecological consequences. *Advances in Ecological Research* 34: 283-362.

Lancashire JR, Ennos AR. 2002. Modelling the hydrodynamic resistance of bordered pits. *Journal of Experimental Botany* 53: 1485-1493.

Larcher W. 2003. Physiological plant ecology. *Ecophysiology and stress physiology of functional groups*. 4th Edn. Springer-Verlag, Berlin, p. 513.

Larchevêque M, Maurel M, Desrochers A, Larocque G. R. 2011. How does drought tolerance compare between two improved hybrids of balsam poplar and an unimproved native species? *Tree Physiology* 31: 240-249.

Lawlor DW, Cornic G. 2002. Photosynthetic carbon assimilation and associated metabolism in relation to water deficits in higher plants. *Plant, Cell & Environment* 25: 275-294.

Lawlor DW. 1995. The effects of water deficit on photosynthesis. In: Smirnoff N (ed) *Environment and Plant Metabolism: Flexibility and Acclimation*. Bios Scientific Publishers Ltd, pp 129-160.

Levitt J. 1980. Response of plants to environmental stresses. Vol. 2: *Water, radiation, salt and other stresses*. 2nd Edn. New York Academic Press, New York, p. 606.

Lichtenthaler HK. 1987. Chlorophylls and carotenoids: pigments of photosynthetic biomembranes. In: *Methods in Enzymology*.Vol.148, pp 350-382.

Liu JX, Jun Yao YB, Yu JQ, Shi ZQ, Wang XQ. 2002. The nutritional value of mulberry leaves and their use as supplement to growing sheep fed ammoniated rice straw. In: *Mulberry for animal production* (M. D. Sanchez). Animal Health and Production Paper No. 147. FAO, Rome, Italy.

Livak KJ, Schmittgen TD. 2001. Analysis of relative gene expression data using realtime quantitative PCR and the $2^{\Delta\Delta}$C(T) Method. *Methods* 25: 402-408.

Lloret F, Siscart D, Dalmases C. 2004. Canopy recovery after drought dieback in holm-oak Mediterranean forests of Catalonia (NE Spain). *Global Change Biology* 10: 2092-2099.

Lo Gullo MA, Salleo S. 1991. Three different methods for measuring xylem cavitation and embolism – a comparison. *Annals of Botany* 67: 417- 424.

Lo Gullo MA, Salleo S. 1993. Different vulnerabilities of *Quercus ilex* L. to freeze- and summer drought-induced xylem embolism: an ecological interpretation. *Plant, Cell & Environment* 16: 511-519.

Lo Gullo, MA, Salleo S, Piaceri EC, Rosso R. 1995 Relations between vulnerability to xylem embolism and xylem conduit dimensions in young trees of *Quercus cerris*. *Plant, Cell & Environment*, 18: 661-669.

Loepfe L, Martinez-Vilalta J, Pinol J, Mencuccini M. 2007. The relevance of xylem network structure for plant hydraulic efficiency and safety. *Journal of Theoretical Biology* 247: 788-803.

Long SP, Zhu XG, Naidu SL, Ort DR. 2006. Can improvement in photosynthesis increase crop yields? *Plant, Cell & Environment* 29: 315-330.

Lopez BC, Sabatae S, Gracia CA, Rodriguez R. 2005. Wood anatomy, description of annual rings, and responses to ENSO events of *Prosopis pallida* H.B.K., a wide-spread woody plant of arid and semi-arid lands of Latin America. *Journal of Arid Environments* 61: 541-554.

Lopez-Portillo J, Ewers FW, Angeles G. 2005. Sap salinity effects on xylem conductivity in two mangrove species. *Plant, Cell & Environment* 28: 1285-1292.

Loukehaich R, Wang T, Ouyang B, Zaif K, Li H *et al*. 2012. SpUSP, an annexin-interacting universal stress protein, enhances drought tolerance in tomato. *Journal of Experimental Botany* 63: 5593-5606.

Loveys BR, Dry PR, Stoll M, McCarthy MG. 2000. Using plant physiology to improve the water efficiency of horticultural crops. *Acta Horticulturae* 537: 187-197.

Lovisolo C, HartungW, Schubert A. 2002. Whole-plant hydraulic conductance and root-to-shoot flow of abscisic acid independently affected by water stress in grapevines. *Functional Plant Biology* 29: 1349-1356.

Lovisolo C, Perrone I, Carra A, Ferrandino A, Flexas J, Medrano H, Schubert A. 2010. Drought-induced changes in development and function of grapevine (*Vitis* spp.) organs and their hydraulic and non-hydraulic interactions at the whole-plant level: a physiological and molecular update. *Functional Plant Biology* 37: 98-116.

Lovisolo C, Schubert A. 1998. Effects of water stress on vessel size and xylem hydraulic conductivity in *Vitis vinifera* L. *Journal of Experimental Botany* 49: 693-700.

Lu C, Zhang J, Zhang Q, LI L, Kuang T. 2001. Modification of photosystem II photochemistry in nitrogen deficient maize and wheat plants. *Journal of Plant Physiology* 158: 1423-1430.

Lu C, Zhang J. 1998. Effects of water stress on photosynthesis, chlorophyll fluorescence and photoinhibition in wheat plants. *Australian Journal of Plant Physiology* 25: 883-892.

Lu C, Zhang J. 1999. Effects of water stress on photosystem II photochemistry and its thermostability in wheat plants. *Journal of Experimental Botany* 50: 1199-1206.

Lu L, Tang Y, Xie J, Yuan Y. 2009. The role of marginal agricultural land-based mulberry planting in biomass energy production. *Renewable Energy* 34: 1789-1794.

Luu DT, Maurel C. 2005. Aquaporins in a challenging environment: molecular gears for adjusting plant water status. *Plant, Cell & Environment* 28: 85-96.

Machado S, Bynum ED, Archer JTL, Lascano RJ, Wilson LT, Bordovsky J, Segarra E, Bronson K, Nesmith DM, Xu W. 2002. Spatial and Temporal Variability of Corn Growth and Grain Yield: Implications for Site-Specific Farming. *Crop Science* 42: 1564-1576.

Machii H, Koyama A, Yamanouchi H. 2000. Mulberry breeding, cultivation and utilization in Japan. In: *Mulberry for Animal Production*. *FAO Electronic Conference*, Feed Resources Group (AGAP), FAO, Rome, Italy.

Madan M, Sharma S. 1999. Biomass yield of hybrid varieties of mulberry in a non-moriculture area. *Biomass & Bioenergy* 17: 427-433.

Magnani F, Mencuccini M, Grace J. 2000. Age-related decline in stand productivity: the role of structural acclimation under hydraulic constraints. *Plant, Cell & Environment* 23: 251-263.

Mahajan S, Tuteja N. 2005. Cold, salinity and drought stresses: An overview. *Archives of Biochemistry and Biophysics* 444: 139-158.

Maherali H, DeLucia EH. 2001. Influence of climate-driven shifts in biomass allocation on water transport and storage in ponderosa pine. *Oecologia* 129: 481-491.

Maherali H, Pockman WT, Jackson RB. 2004. Adaptive variation in the vulnerability of woody plants to xylem cavitation. *Ecology* 85: 2184-2199.

Maherali H, Sherrard ME, Clifford MH, Latta RG. 2008. Leaf hydraulic conductivity and photosynthesis are genetically correlated in an annual grass. *New Phytologist* 180: 240-247.

Marino G, Aqil M, Shipley B. 2010. The leaf economics spectrum and the prediction of photosynthetic light–response curves. *Functional Ecology* 24: 263-272.

Marron N, Dillen SY, Ceulemans R. 2007. Evaluation of leaf traits for indirect selection of high yielding poplar hybrids. *Environmental and Experimental Botany* 61: 103-116.

Marron N, Maury S, Rinaldi C, Brignolas F. 2006. Impact of drought and leaf development stage on enzymatic antioxidant system of two *Populus deltoides* × *nigra* clones. *Annals of Forest Science* 63: 323-327.

Martínez-Cabrera HI, Jones CS, Espino S, Schenk HJ. 2009. Wood anatomy and wood density in shrubs: responses to varying aridity along transcontinental transects. *American Journal of Botany* 96: 1388-1398.

Martínez-Vilalta J, Cochard H, Mencuccini M, Sterck F, Herrero A, Korhonen JFJ, Llorens P, Nikinmaa E, Nole´ A, Poyatos R, Ripullone F, Sass-Klaassen U, Zweifel R. 2009. Hydraulic adjustment of scots pine across Europe. *New Phytologist* 184: 353-364.

Martinez-Vilalta J, Pinñol J, Beven K. 2002a. A hydraulic model to predict drought-induced mortality in woody plants: an application to climate change in the Mediterranean. *Ecological Modelling* 155: 127-147.

Martinez-Vilalta J, Prat E, Oliveras I, Pinñol J. 2002b. Xylem hydraulic properties of roots and stems of nine Mediterranean woody species. *Oecologia* 133: 19-29.

Maseda P, Fernandez R. 2006. Stay wet or else: three ways in which plants can adjust hydraulically to their environment. *Journal of Experimental Botany* 57: 3963-3977.

Matysik J, Alia A, Bhalu B, Mohanty P. 2002. Molecular mechanisms of quenching of reactive oxygen species by proline under stress in plants. *Current Science* 82: 525-532.

Mauseth JD, Plemonsrodriguez BJ. 1997. Presence of paratracheal water storage tissue does not alter vessel characters in cactus wood. *American Journal of Botany* 84: 815-822.

Maxwell K, Johnson GN. 2000. Chlorophyll fluorescence – a practical guide. *Journal of Experimental Botany* 51: 659-668.

McCulloh KA, Meinzer FC *et al*. 2011. Comparative hydraulic architecture of tropical tree species representing a range of successional stages and wood density. *Oecologia* 167: 27-37.

McDowell N, Pockman WT, Allen CD, Breshears DD, Cobb N, Kolb T, Plaut J, Sperry J, West A, Williams DG, Yepez EA. 2008. Mechanisms of plant survival and mortality during drought: why do some plants survive while others succumb to drought? *New Phytologist* 178: 719-739.

McDowell NG, Adams HA, Bailey JD, Hess M, Kolb TE. 2006. Homeostatic maintenance of ponderosa pine gas exchange in response to stand density changes. *Ecological Applications* 16: 1164-1182.

McDowell NG, Licata J, Bond BJ. 2005. Environmental sensitivity of gas exchange parameters in different-sized trees. *Oecologia* 145: 9-20.

McDowell NG, Phillips N, Lunch C, Bond BJ, Ryan MG. 2002. An investigation of hydraulic limitation and compensation in large, old Douglas-fir trees. *Tree Physiology* 22, 763-774.

McDowell NG. 2011. Mechanisms linking drought, hydraulics, carbon metabolism, and vegetation mortality. *Plant Physiology* 155: 1051-1059.

McElrone AJ, Bichler J, Pockman WT, Addington RN, Linder CR, Jackson RB. 2007. Aquaporin-mediated changes in hydraulic conductivity of deep tree roots accessed via caves. *Plant, Cell & Environment* 30: 1411-1421.

McElrone AJ, Pockman WT, Martinez-Vilalta J, Jackson RB. 2004. Variation in xylem structure and function in stems and roots of trees to 20 m depth. *New Phytologist* 163: 507–517.

Medrano H, Escalona JM, Bota J, Gulías J, Flexas J. 2002. Regulation of photosynthesis of C_3 plants in response to progressive drought: stomatal conductance as a reference parameter. *Annals of Botany* 89: 895-905.

Medrano H, Flexas J, Galmes J. 2009. Variability in water use efficiency at the leaf level among Mediterranean plants with different growth forms. *Plant and Soil* 317: 17-29.

Meinzer FC, Bond BJ, Karanian JA. 2008. Biophysical constraints on leaf expansion in a tall conifer. *Tree Physiology* 28: 197-206.

Meinzer FC, Goldstein G, Franco AC, Bustamante M, Igler E, Jackson P, Caldas L, Rundel PW. 1999. Atmospheric and hydraulic limitations on transpiration in Brazilian cerrado woody species. *Functional Ecology* 13: 273-282.

Meinzer FC, Goldstein G, Jackson PJ, Holbrook NM, Gutierrez MV. 1995. Environmental and physiological regulation of transpiration in tropical forest gap species: the influence of boundary layer and hydraulic properties. *Oecologia* 101: 514-522.

Meinzer FC, Grantz DA. 1990. Stomatal and hydraulic conductance in growing sugarcane: stomatal adjustment to water transport capacity. *Plant, Cell & Environment* 13: 383-388.

Meinzer FC. 2002. Co-ordination of vapour and liquid phase water transport properties in plants. *Plant, Cell and Environment* 25: 265-274.

Mencuccini M, Bonosi L. 2001. Leaf/sapwood area ratios in Scots pine show acclimation across Europe. *Canadian Journal of Forest Research* 31: 442-456.

Mencuccini M, Comstock J. 1997. Vulnerability to cavitation in populations of two desert species, *Hymenoclea salsola* and *Ambrosia dumosa*, from different climatic regions. *Journal of Experimental Botany* 48: 1323-1334.

Mencuccini M. 2003. The ecological significance of long-distance water transport: short-term regulation, long-term acclimation and the hydraulic costs of stature across plant life forms. *Plant, Cell & Environment* 26: 163-182.

Metcalfe DB, Meir P, Aragao L *et al*. 2010. Shifts in plant respiration and carbon use efficiency at a large-scale drought experiment in the eastern Amazon. *New Phytologist* 187: 608-621.

Meyer AJ. 2008. The integration of glutathione homeostasis and redox signalling. *Journal of Plant Physiology* 165: 1390-1403.

Mishra S, Dandin SB. 2010. Molecular characterization of mulberry genotypes in relation to photosynthetic efficiency. *Indian Journal of Sericulture* 49: 50-57.

Mittler R, Vanderauwera S, Gollery M, Van Breusegem F. 2004. Reactive oxygen gene network of plants. *Trends in Plant Science* 9: 490-498.

Mittler R. 2002. Oxidative stress, antioxidants and stress tolerance. *Trends in Plant Science* 7: 405-410.

Molinari HBC, Marur CJ, Daros E, de Campos MKF, de Carvalho FFRP, Filho JCB, Pereira LFP, Vieira L GE. 2007. Evaluation of the stress-inducible production of proline in transgenic sugarcane (*Saccharum* spp.): osmotic adjustment, chlorophyll fluorescence and oxidative stress. *Physiologia Plantarum* 130: 218-229.

Møller IM. 2001. Plant mitochondria and oxidative stress: electron transport, NADPH turnover, and metabolism of reactive oxygen species. *Annual Review of Plant Physiology and Plant Molecular Biology* 52: 561-591.

Monclus R, Dreyer E, Delmotte FM, Villar M, Delay D, Boudouresque E, Petit JM, Marron N, Bréchet C, Brignolas F. 2005. Productivity, leaf traits and carbon isotope discrimination in 29 *Populus deltoids* x *P. nigra* clones. *New Phytologist* 167: 53-62.

Mott KA, Buckley TN. 2000. Patchy stomatal conductance: emergent collective behaviour of stomata. *Trends in Plant Science* 5: 258-262.

Mullineaux PM. Rausch T. 2005. Glutathione, photosynthesis and the redox regulation of stress-responsive gene expression. *Photosynthesis Research* 86: 459-474.

Munday JC, Govindjee. 1969. Light-induced changes in the fluorescence yield of chlorophyll *a in vivo*. 3. The dip and the peak in the fluorescence transient of *Chlorella pyrenoidosa*, *Biophysical Journal* 9: 1-21.

Munne-Bosch S, Alegre L. 2000. Changes in carotenoids, tocopherols and diterpenes during drought and recovery, and the biological significance of chlorophyll loss in *Rosmarinus officinalis* plants. *Planta* 207: 925-931.

Munné-Bosch S, Alegre L. 2004. Die and live: leaf senescence contributes to plant survival under drought stress. *Functional Plant Biology* 31: 203-216.

Munné-Bosch S. 2005. The role of α-tocopherol in plant stress tolerance. *Journal of Plant Physiology* 162: 743-748.

Murchie EH, Pinto M, Horton P. 2008. Agriculture and the new challenges for photosynthesis research. *New Phytologist* 181: 532-552.

Murray FW. 1967. On the computation of saturation vapour pressure. *Journal of Applied Meteorology* 6: 203-204.

Nagakura J, Shigenaga H, Akama A, Takahashi M. 2004. Growth and transpiration of Japanese cedar (*Cryptomeria japonica*) and Hinoki cypress (*Chamaecyparis obtuse*) seedlings in response to soil water content. *Tree Physiology* 24: 1203-1208.

Naidoo G. 2006. Factors contributing to dwarfing in the mangrove *Avicennia marina*. *Annals of Botany* 97: 1095-1101.

Narasaiah ML. 2003. In: *Problems and Prospects of Sericulture*. Discovery Publishing House, pp 32-39.

Nardini A, Salleo S, Raimondo F. 2003. Changes in leaf hydraulic conductance correlate with leaf vein embolism in Cercis siliquastrum L. *Trees – Structure and Function* 17: 529-534.

Nardini A, Tyree MT, Salleo S. 2001. Xylem cavitation in the leaf of *Prunus laurocerasus* L. and its impact on leaf hydraulics. *Plant Physiology* 125: 1700-1709.

Nebelsick RA, Mosbrugger DUV, Kerp H. 2001. Evolution and function of leaf venation architecture: a review. *Annals of Botany* 87: 553-566.

Ni B, Pallardy SG. 1990. Responses of liquid flow resistance to soil drying in seedlings of four deciduous angiosperms. *Oecologia* 84: 260-264.

Nijsse J. 2001. Functional anatomy of the water transport system in cut chrysanthemum. *PhD thesis*. Wageningen University, The Netherlands.

Nikolopoulos D, Liakopoulos G, Drossopoulos I, Karabourniotis G. 2002. The relationship between anatomy and photosynthetic performance of heteroboric leaves. *Plant Physiology* 129: 235-243.

Niyogi KK, Shih C, Chow WS, Pogson BJ, Dellapenna D, Bjorkman O. 2001. Photoprotection in a zeaxanthin-and lutein-deficient double mutant of Arabidopsis. *Photosynthesis Research* 67: 139-145.

Noblin X, Mahadevan L, Coomaraswamy IA, Weitz DA, Holbrook NM, Zwieniecki MA. 2008. Optimal vein density in artificial and real leaves. *Proceedings of the National Academy of Sciences of the Unites States of America* 105: 9140-9144.

Nogueira A, Martinez CA, Ferreira LL, Prado CHBA. 2004. Photosynthesis and water use efficiency in twenty tropical tree species of differing succession status in a Brazilian reforestation. *Photosynthetica* 42: 351-356.

Nonami H, Boyer JS. 1993. Direct demonstration of a growth induced water potential gradient. *Plant Physiology* 100: 13-19.

Ogle K, Reynolds JF. 2002. Desert dogma revisited: coupling of stomatal conductance and photosynthesis in the desert shrub *Larrea tridentata*. *Plant, Cell & Environment* 25: 909-921.

Ohnishi N, Allakhverdiev SI, Takahashi S, Higashi S, Watanabe M, Nishiyama Y. 2005. Two-step mechanism of photo damage to photosystem II: step 1 occurs at the oxygen-evolving complex and step 2 occurs at the photochemical reaction centre. *Biochemistry* 44: 8494-8499.

Omaye ST, Turnbull JD, Sauberilich HE. 1979. Selected methods for the determination of ascorbic acid in animal cells, tissues and fluids. In: *Methods in Enzymology*, New York: Academic Press, pp 3-11.

Oosterhuis DM, Wullschleger SD. 1987. Water flow through cotton roots in relation to xylem anatomy. *Journal of Experimental Botany* 38: 1866-1874.

Oren R, Sperry JS, Katul G, Pataki DE, Ewers BE, Phillips N, Schafer KVR. 1999. Survey and synthesis of intra- and inter specific variation in stomatal sensitivity to vapour pressure deficit. *Plant, Cell & Environment* 22: 1515-1526.

Osório M, Rodrigues BE, Osório A, Roux JLe, Daudet X, Ferreira FA, Chaves MM. 2006. Limitations to carbon assimilation by mild drought in nectarine trees growing under field conditions. *Environmental and Experimental Botany* 55: 235-247.

Otieno DO, Schmidt MWT, Adiku S, Tenhunen J. 2005. Physiological and morphological responses to water stress in two *Acacia* species from contrasting habitats. *Tree Physiology* 25: 361-371.

Otto B, Kaldenhoff R. 2000. Cell-specific expression of the mercury insensitive plasma-membrane aquaporin NtAQP1 from *Nicotiana tabacum*. *Planta* 211: 167-172.

Oukarroum A, Madidi SE, Schansker G, Strasser RJ. 2007. Probing the responses of barley cultivars (*Hordeum vulgare* L.) by chlorophyll *a* fluorescence OLKJIP under drought stress and rewatering. *Environmental and Experimental Botany* 60: 438-446.

Oukarroum A, Schansker G, Strasser RJ. 2009. Drought stress effects on photosystem I content and photosystem II thermotolerance analyzed using Chl a fluorescence kinetics in barley varieties differing in their drought tolerance. *Physiologia Plantarum* 137: 188-199.

Pääkkönen E, Vahala J, Pohjolai M, Holopainen T, Kärenlampi L. 1998. Physiological, stomatatal and ultrastructural ozone responses in birch (*Betula pendula* Roth.) are modified by water stress. *Plant, Cell & Environment* 21: 671-684.

Pancović D, Sakač Z, Kevrešan S, Plesničar M. 1999. Acclimation to long-term water deficit in the leaves of two sunflower hybrids: photosynthesis, electron transport and carbon metabolism. *Journal of Experimental Botany* 50: 127-138.

Papanastasis VP, Yiakoulaki MD, Decandia M, Dini-Papanastasi O. 2008. Integrating woody species into livestock feeding in the Mediterranean areas of Europe. *Animal Feed Science and Technology* 140: 1-17.

Parry MAJ, Reynolds M, Salvucci ME, Raines C, Andralojc PJ, Zhu X-G, Price GD, Condon AG, Furbank R. 2011. Raising yield potential of wheat. II. Increasing photosynthetic capacity and efficiency. *Journal of Experimental Botany* 62: 453-467.

Pataki DE, Oren R, Phillips N. 1998. Responses of sap flux and stomatal conductance of *Pinus taeda* L. trees to stepwise reductions in leaf area. *Journal of Experimental Botany* 49: 871-876.

Pearson CH, Halvorson AD, Moench RD, Hammon RW. 2010. Production of hybrid poplar under short-term, intensive culture in Western Colorado. *Industrial Crops and Products* 31: 492-498.

Peek MS, Russek-Cohen E, Wait DA, Forseth IN. 2002. Physiological response curve analysis using nonlinear mixed models. *Oecologia* 132: 175-180.

Pelloux J, Jolivet Y, Fontaine V, Banvoy J, Dizengremel P. 2001. Changes in rubisco and rubisco activase gene expression and polypeptide content in *Pinus halpensis* M. subjected to ozone and drought, *Plant, Cell & Environment* 24: 123-131.

Perneger T V. 1998. What's Wrong with Bonferroni Adjustments. *British Medical Journal* 316: 1236-1238.

Peterhansel C, Niessen M, Kebeish RM. 2008. Metabolic engineering towards the enhancement of photosynthesis. *Photochemisty and Photobiology* 84: 1317-1323.

Phillips N, Ryan MG, Bond BJ, McDowell NG, Hinckley T, Cermak J. 2003. Reliance on stored water increases with tree size in three species in the Pacific Northwest. *Tree Physiology* 23: 237-245.

Pickard WF, Melcher PJ. 2005. Perspectives on the Biophysics of Xylem Transport. In: *Vascular Transport in Plants*. Eds: Holbrook NM and Zwieniecki MA. Elsevier/Academic Press, Oxford, 3-18.

Pieters AJ, Souki SEl. 2005. Effects of drought during grain filling on PS II activity in rice. *Journal of Plant Physiology* 162: 903-911.

Pietrini F, Iannelli MA, Massacci A. 2002. Anthocyanin accumulation in the illuminated surface of maize leaves enhances protection from photo-inhibitory risks at low temperature, without further limitation to photosynthesis. *Plant, Cell & Environment* 25: 1251-1259.

Pinheiro HA, Damatta FM, Chaves ARM, Fontes EPB, Loureiro ME. 2004. Drought tolerance in relation to protection against oxidative stress in clones of *Coffea canephora* subjected to long-term drought. *Plant Science* 167: 1307-1314.

Pittermann J, Sperry JS, Hacke UG, Wheeler JK, Sikkema EH. 2005. Torus-margo pits help conifers compete with angiosperms. *Science* 310: 1924-11924.

Pliura A, Zhang SY, MacKay J, Bousquet J. 2007. Genotypic variation in wood density and growth traits of poplar hybrids at four clonal trials. *Forest Ecology and Management* 238: 92-106.

Pockman WT, Sperry JS. 2000. Vulnerability to xylem cavitation and the distribution of Sonoran vegetation. *American Journal of Botany* 87: 1287-1299.

Pockman WT, Sperry JS. 2000. Vulnerability to xylem cavitation and the distribution of Sonoran Desert vegetation. *American Journal of Botany* 87: 1287-1299.

Pontailler JY, Ceulemans R, Guittet J. 1999. Biomass yield of poplar after five 2-year coppice rotations. *Forestry* 72: 157-163.

Poorter L, Bongers F, Sterck FJ, Wöll H. 2005. Beyond the regeneration phase: differentiation of height-light trajectories among tropical tree species. *Journal of Ecology* 93: 256-267.

Pou A, Medrano H, Tomas M, Martorell S, Ribas-Carbo M, Flexas J. 2012. Anisohydric behavior in grapevines results in better performance under moderate water stress and recovery than isohydric behavior. *Plant and Soil* 359: 335-349.

Praxedes SC, DaMatta FM, Loureiro ME, Ferrão MAG, Cordeiro AT. 2006: Effects of long-term soil drought on photosynthesis and carbohydrate metabolism in mature robusta coffee (*Coffea canephora* Pierre var. kouillou) leaves. *Environmental and Experimental Botany* 56: 263-273.

Preston KA, Cornwell WK, Denoyer JL. 2006. Wood density and vessel traits as distinct correlates of ecological strategy in 51 California coast range angiosperms. *New Phytologist* 170: 807-818.

Ramachandra Reddy A, Chaitanya KV, Jutur PP, Sumithra K. 2004. Differential antioxidative responses to water stress among five mulberry (*Morus alba* L.) cultivars. *Environmental and Experimental Botany* 52: 33-42.

Ramanjulu S, Sreenivasalu N, Giridara KS, Sudhakar C. 1998. Photosynthetic characteristics in mulberry during water stress and rewatering. *Photosynthetica* 35: 259-263.

Ramanjulu S, Sudhakar C. 1997. Drought tolerance is partly related to amino acid accumulation and ammonia assimilation: A comparative study in two mulberry genotypes differing in drought sensitivity. *Journal of Plant Physiology* 150: 345-350.

Rao DMR, Susheelamma BN, Rajashekar K, Sarkar A, Bajpai AK. 1997. In vitro screening of mulberry genotypes (*Morus* spp.) for drought tolerance. *Indian Journal of Sericulture* 36: 60-62.

Reddy AR, Chaitanya KV, Jutur PP, Gnanam A. 2005. Photosynthesis and oxidative stress responses to water deficit in five different mulberry (*Morus alba* L.) cultivars. *Physiology and Molecular Biology of Plants* 11: 291-298.

Reddy AR, Chaitanya KV, Jutur PP, Sumitra K. 2004a. Differential antioxidative responses to water stress among five mulberry (*Morus alba* L.) cultivars. *Environmental and Experimental Botany* 52: 33-42.

Reddy AR, Chaitanya KV, Vivekanandan M. 2004b. Drought-induced responses of photosynthesis and antioxidant metabolism in higher plants. *Journal of Plant Physiology* 161: 1189–1202.

Redillas MCFR, Strasser RJ, Jeong JS, Kim YS, Kim J-K. 2011. The use of JIP test to evaluate drought-tolerance of transgenic rice overexpressing *OsNAC10*. *Plant Biotechnology Report* 5: 169-175.

Ren YH. 2009. Protective enzyme activity and physiological properties of four mulberry varieties affected by drought stress in the Panxi Region of Sichuan Province, China. *Forestry Studies in China* 11: 190-195.

Riccardi F, Gazeau P, Jacquemont M, Vincent D, Zivy M. 2004. Deciphering genetic variations of proteome responses to water deficit in maize leaves. *Plant Physiology and Biochemistry* 42: 1003-1011.

Rice KJ, Matzner SL, Byer W, Brown JR. 2004. Patterns of tree dieback in Queensland, Australia; the importance of drought stress and the role of resistance to cavitation. *Oecologia* 139: 190-198.

Ritchie SW, Nguyen HT, Holaday AS. 1990. Leaf water content and gas exchange parameters of two wheat genotypes differing in drought resistance. *Crop Science* 30: 105-111.

Robert EMR, Koedam N, Beeckman H, Schmitz N. 2009. A Safe Hydraulic Architecture as Wood Anatomical Explanation for the Difference in Distribution of the Mangroves *Avicennia* and *Rhizophora*. *Functional Ecology* 23: 649-657.

Rodriguez-Gamir J, Intrigliolo DS, Primo-Millo E, Forner-Giner MA. 2010. Relationships between xylem anatomy, root hydraulic conductivity, leaf/root ratio and transpiration in citrus trees on different rootstocks. *Physiologia Plantarum* 139: 159-169.

Rogiers S, Greer DH, Hatfield JM, Hutton RJ, Clarke SJ, Hutchinson PA, Somers A. 2011. Stomatal response of an anisohydric grapevine cultivar to evaporative demand, available soil moisture and ABA. *Tree Physiology* 32: 249-261.

Rokka A, Zhang L, Aro EM. 2001. Rubisco ativase: an enzyme with a temperature-dependent dual function? *Plant Journal* 25: 463-471.

Ryan MG, Bond BJ, Law BE, Hubbard RM, Woodruff D, Cienciala E, Kucera J. 2000. Transpiration and whole-tree conductance in ponderosa pine trees of different heights. *Oecologia* 124: 553-560.

Sack L, Frole K. 2006. Leaf structural diversity is related to hydraulic capacity in tropical rainforest trees. *Ecology* 87: 483-491.

Sack L, Holbrook NM. 2006. Leaf hydraulics. *Annual Review of Plant Biology* 57: 361-381.

Sack L, Melcher PJ, Zwieniecki MA, Holbrook NM. 2002. The hydraulic conductance of the angiosperm leaf lamina: a comparison of three measurement methods, *Journal of Experimental Botany* 53: 2177–2184.

Sage RF, Kubien DS. 2007. The temperature response of C3 and C4 photosynthesis. *Plant, Cell & Environment* 30: 1086-1106.

Said E, Hugh JE. 2005. Physiological limitations to photosynthetic carbon assimilation in cotton under water stress. *Crop Science* 45: 2374-2382.

Sakurai J, Ishikawa F, Yamaguchi T, Uemura M, Maeshima M. 2005. Identification of 33 rice aquaporin genes and analysis of their expression and function. *Plant & Cell Physiology* 46: 1568-1577.

Sala A, Tenhnunen JD. 1994. Site-specific water relations and stomatal response of *Quercus ilex* L. in a Mediterranean watershed. *Tree Physiology* 14: 601-617.

Saliendra NZ, Meinzer FC. 1989. Relationship between root/soil hydraulic properties and stomatal behavior in sugarcane. *Australian Journal of Plant Physiology* 16: 241-250.

Salleo S, Hynkley TM, Kikuta SB, Lo Gullo MA, Weilgony P, Yoon TM, Richter H. 1992. A method for inducing xylem emboli in situ: experiments with a field-grown tree. *Plant, Cell & Environment* 15: 491-497.

Salleo S, Lo Gullo MA, De Paoli D, Zippo M. 1996. Xylem recovery from cavitation induced embolism in young plants of Laurus nobilis, a possible mechanism. *New Phytologist* 132: 47-56.

Salleo S, Lo Gullo MA, Trifilo P, Nardini A. 2004. New evidence for a role of vessel associated cells and phloem in the rapid xylem refilling of cavitated stems of *Laurus nobilis* L. *Plant, Cell & Environment* 27: 1065-1076.

Salleo S, Nardini A, Pitt F, Lo Gullo MA. 2000. Xylem cavitation and hydraulic control of stomatal conductance in Laurel (*Laurus nobilis* L.). *Plant, Cell & Environment* 23: 71-79.

Salvucci ME, Crafts-Brandner SJ. 2004. Inhibition of photosynthesis by heat stress: the activation state of Rubisco as a limiting factor in photosynthesis. *Physiologia Plantarum* 120: 179-186.

Sánchez MD. 2000. Mulberry: an exceptional forage available almost worldwide! World Animal Review. In: Sánchez MD (ed) *Mulberry for animal production*. Animal Health and Production Paper No. 147. FAO, Rome.

Sano Y, Jansen S. 2006. Perforated pit membranes in imperforate tracheary elements of some angiosperms *Annals of Botany* 97: 1045-1053.

Santiago LS, Goldstein G, Meinzer FC, Fisher JB, Machado K, Woodruff D, Jones T. 2004. Leaf photosynthetic traits scale with hydraulic conductivity and wood density in Panamanian forest canopy trees. *Oecologia* 140: 543-550.

Sarvanan RS, Rose JKC. 2004. A critical evaluation of sample extraction techniques for enhanced proteomic analysis of recalcitrant plant tissues. *Proteomics* 4: 2522-2532.

Savoure A, Jaoua S, Hua X-J, Ardiles W, Van Montagu M, Verbruggen N. 1995. Isolation, characterization, and chromosomal location of a gene encoding the D1-pyrroline-5 carboxylate synthetase in *Arabidopsis thaliana*. *FEBS Letters* 372: 13-19.

Sayar R, Khemira H, Kameli A, Mosbahi M. 2008. Physiological tests as predictive appreciation for drought tolerance in durum wheat (*Triticum durum* Desf.). *Agronomy Research* 6: 79-90.

Schmitz N, Jansen S, Verheyden A, Kairo JG, Beeckman H, Koedam N. 2007. Comparative anatomy of intervessel pits in two mangrove species growing along a natural salinity gradient in Gazi Bay, Kenya. *Annals of Botany* 100: 271-281.

Schmitz N, Koch G, Schmitt U, Beeckman H. Koedam N. 2008. Intervessel pit structure and histochemistry of two mangrove species as revealed by cellular UV microspectrophotometry and electron microscopy: intraspecific variation and functional significance. *Microscopy and Microanalysis* 14: 387-397.

Schmitz N, Verheyden A, Beeckman H, Kairo JG, Koedam N. 2006. Influence of a salinity gradient on the vessel characters of the mangrove species *Rhizophora mucronata*. *Annals of Botany* 98: 1321-1330.

Schulte PJ, Gibson AC, Nobel PS. 1987. Xylem anatomy and hydraulic conductance of *Psilotum nudum*. *American Journal of Botany* 74: 1438-1445.

Schulte PJ. 1999. Water flow through a 20-pore perforation plate in vessels of *Liquidambar styraciflua*. *Journal of Experimental Botany* 50: 1179-1187.

Schultz HR, Matthews MA. 1988. Resistance to Water Transport in Shoots of *Vitis vinifera* L. *Plant Physiology* 88: 718-724.

Schultz HR, Matthews MA. 1997. High vapour pressure deficit exacerbates xylem cavitation and photoinhibition in shadegrown *Piper auritum* H.B. & K. during prolonged sunflecks. I. Dynamics of plant water relations. *Oecologia* 110: 312-319.

Schultz HR. 1996. Water relations and photosynthetic responses of two grapevine cultivars of different geographical origin during water stress. *Acta Horticulturae* 427: 251-266.

Schultz HR. 2003. Differences in hydraulic architecture account for near-isohydric and anisohydric behaviour of two field-grown *Vitis vinifera* L. cultivars during drought. *Plant, Cell & Environment* 26: 1393-1405.

Schwanz P, Polle A. 1998. Antioxidative systems, pigment and protein contents in leaves of adult mediterranean oak species (*Quercus pubescens* and *Q. ilex*) with lifetime exposure to elevated CO_2. *New Phytologist* 140: 411-423.

Scoffoni C, McKown AD, Rawls M, Sack L. 2012. Dynamics of leaf hydraulic conductance with water status: quantification and analysis of species differences under steady state. *Journal of Experimental Botany* 63: 643-658.

Scoffoni C, Pou A, Aasamaa K, Sack L. 2008. The rapid light response of leaf hydraulic conductance: new evidence from two experimental methods. *Plant, Cell & Environment* 31: 1803-1812.

Secchi F, Lovisolo C, Uehlein N, Kaldenhoff R, Schubert A. 2007. Isolation and functional characterization of three aquaporins from olive (*Olea europaea* L.). *Planta* 225: 381-392.

Sellin A, Kupper P. 2007. Temperature, light and leaf hydraulic conductance of little-leaf linden (*Tilia cordata*) in a mixed forest canopy. *Tree Physiology* 27: 679-688.

Sellin A. 1998. The dependence of water potential in shoots of *Picea abies* on air and soil water status. *Annals of Geophysics* 16: 470-476.

Sengupta S, Majumder AL. 2009. Insight into the salt tolerance factors of wild halophytic rice, *Porteresia coarctata*: a physiological and proteomic approach. *Planta* 229: 911-929.

Sergeant K, Spieß N, Renaut J, Wilhelm E, Hausman JF. 2011. One dry summer: A leaf proteome study on the response of oak to drought exposure. *Journal of Proteomics* 74: 1385-1395.

Shao H-B, Chu L-Y, Lu Z-H, Kang C-M. 2008. Primary antioxidant free radical scavenging and redox signalling pathways in higher plant cells. *International Journal of Biological Sciences* 4: 8-14.

Sherwin HN, Pammenter NW, February E, Vander Willigen C, Farrant JM. 1998. Xylem hydraulic characteristics, water relations and wood anatomy of the resurrection plant *Myrothamnus flabellifolius* Welw. *Annals of Botany* 81: 567-575.

Sherwin HW, Farrant JM. 1998. Protection mechanisms against excess light in the resurrection plants *Craterostigma wilmsii* and *Xerophyta viscosa*. *Plant Growth Regulation* 24: 203-210.

Shevchenko A, Wilm A, Vorm O, Mann M. 1996. Mass spectrometric sequencing of protein from silver- stained polyacrylamide gels. *Analytical Chemistry* 68: 850-858.

Shimizu M, Ishida A, Hogetsu T. 2005. Root hydraulic conductivity and whole-plant water balance in tropical saplings following a shade-to-sun transfer. *Oecologia* 43: 189-197.

Shvaleva AL, Silva E, Costa F, Breia E, Jouve J, Hausman JF, Almeida MH, Maroco JP, Rodrigues ML, Pereira JS, Chaves MM. 2006. Metabolic responses to water deficit in two *Eucalyptus globulus* clones with contrasting drought sensitivity. *Tree Physiology* 26: 239-248.

Siefritz F, Tyree MT, Lovisolo C, Schubert A, Kaldenhoff R. 2002. PIP1 plasma membrane aquaporins in tobacco: from cellular effects to function in plants. *The Plant Cell* 14: 869-876.

Siemens JA, Zwiazek JJ. 2004. Changes in water flow properties of solution culture-grown trembling aspen (*Populus tremuloides*) seedlings under different intensities of water-deficit stress. *Physiologia Plantarum* 121: 44-49.

Šircelj H, Tausz M, Grill D, Batic F. 2007. Detecting different levels of drought stress in apple trees (*Malus domestica* Borkh.) with selected biochemical and physiological parameters. *Plant Science* 113: 362-369.

Slabbert RM, Krüger GHJ. 2011. Assessment of changes in photosystem II structure and function as affected by water deficit in *Amaranthus hypochondriacus* L. and *Amaranthus hybridus* L. *Plant Physiology and Biochemistry* 49: 978-984.

Slot M, Poorter L. 2007. Diversity of tropical tree seedling responses to drought. *Biotropica* 39: 683-690.

Soar C, Speirs J, Maffei S, Penrose A, McCarthy M, Loveys B. 2006. Grapevine varieties Shiraz and Grenache differ in their stomatal response to VPD: apparent links with ABA physiology and gene expression in leaf tissue. *Australian Journal of Grape Wine Research* 12: 2-12.

Socias X, Correia MJ, Chaves M, Medrano H. 1997. The role of abscisic acid and water relations in drought responses of subterranean clover. *Journal of Experimental Botany* 311: 1281-1288.

Sofo A, Manfreda S, Fiorentino M, Dichio B, Xiloyannis C. 2008. The olive tree: a paradigm for drought tolerance in Mediterranean climates. *Hydrology and Earth System Science* 12: 293-301.

Sophia R, George KP. 2003. Development and structure of drought-tolerant leaves of the mediterranean shrub *Capparis spinosa* L. *Annals of Botany* 92: 377-383.

Sperry JS, Alder NN, Eastlack SE. 1993. The effect of reduced hydraulic conductance on stomatal conductance and xylem cavitation. *Journal of Experimental Botany* 44: 1075-1082.

Sperry JS, Donnelly JR, Tyree MT. 1988. A method for measuring hydraulic conductivity and embolism in xylem, *Plant, Cell & Environment* 11: 35-40.

Sperry JS, Hacke UG, Oren R, Comstock JP. 2002. Water deficits and hydraulic limits to leaf water supply, *Plant, Cell & Environment* 25: 251-263.

Sperry JS, Hacke UG, Wheeler JK. 2005. Comparative analysis of end wall resistivity in xylem conduits. *Plant, Cell & Environment* 28: 456-465.

Sperry JS, Pockman WT. 1993. Limitation of transpiration by hydraulic conductance and xylem cavitation in Betula occidentalis. *Plant, Cell & Environment* 16: 279-287.

Sperry JS, Tyree MT. 1990. Water-stress-induced xylem embolism in three species of conifers. *Plant, Cell & Environment* 13: 427-436.

Sperry JS. 2000. Hydraulic constraints on plant gas exchange. *Agricultural and Forest Meteorology* 104:13-23.

Sperry JS. 2003. Evolution of water transport and xylem structure. *International Journal of Plant Sciences* 164: S115-S127.

Srivastava A, Guissé B, Greppin H, Strasser RJ. 1997. Regulation of antenna structure and electron transport in photosystem II of *Pisum sativum* under elevated temperature probe by fast polyphasic chlorophyll a fluorescence transient: OKJIP. *Biochimica et Biophysica Acta* 1320: 95-106.

Steinberg SL, McFarland MJ, Miller JC. 1989. Effect of water stress on stomatal conductance and leaf water relations of leaves along current-year branches of peach. *Australian Journal of Plant Physiology* 16: 549-560.

Steppe K, Cnudde V, Girard C, Lemeur R, Cnudde JP, Jacobs P. 2004. Use of X-ray computed microtomography for non-invasive determination of wood anatomical characteristics. *Journal of Structural Biology* 148: 11-21.

Sterck FJ, Zweifel R, Sass-Klaassen U, Chowdhury Q. 2008. Persistent soil drought reduces leaf specific conductivity in Scots pine (*Pinus sylvestris*) and pubescent oak (*Quercus pubescens*). *Tree Physiology* 28: 529-536.

Steudle E. 2000a. Water uptake by roots: effects of water deficit. *Journal of Experimental Botany* 51: 1531-1542.

Steudle E. 2000b. Water uptake by plant roots: an integration of views. *Plant and Soil* 226: 45-56.

Steudle E. Peterson CA. 1998. How does water get through roots? *Journal of Experimental Botany* 49: 775-788.

Stiller V, Lafitte HR, Sperry JS. 2003. Hydraulic properties of rice and the response of gas exchange to water stress. *Plant Physiology* 132: 1698-1706.

Stirbet A, Govindjee. 2011. On the relation between the Kautsky effect (chlorophyll a fluorescence induction) and Photosystem II: basics and applications of the OJIP fluorescence transient. *Journal of Photochemistry and Photobiology:Biology*104: 236-257.

Stoll M, Loveys BR, Dry PR. 2000. Hormonal changes induced by partial rootzone drying of irrigated grapevine. *Journal of Experimental Botany* 51:1627-1634.

Strasser A, Tsimilli-Michael M, Srivastava A. 2004. Analysis of the fluorescence transient. In: G.C. Papageorgiou, Govindjee (Ed.), *Chlorophyll fluorescence: A Signature of Photosynthesis*, Springer, Dordrecht, pp 321-362.

Strasser BJ. 1997. Donor side capacity of Photosystem II probed by chlorophyll a fluorescence transients. *Photosynthesis Research* 52: 147-155.

Strasser RJ, Srivastava A, Govindjee. 1995. Polyphasic chlorophyll-a fluorescence transients in plants and cyanobacteria. *Journal of Photochemistry and Photobiology. B: Biology* 61: 32-42.

Strasser RJ, Srivastava A, Tsimilli-Michael M. 2000. The fluorescence transient as a tool to characterise and screen photosynthetic samples. In: Yunus M, Pathre U, Mohanty P (eds) *Probing Photosynthesis: Mechanisms, Regulation & Adaptation*. Taylor & Francis, London, UK, pp 445-483.

Strasser RJ, Stirbet AD. 1998. Heterogeneity of photosystem II probed by the numerically simulated chlorophyll *a* fluorescence rise (O-J-I-P). *Mathematics and Computers in Simulation* 48: 3-9.

Strasser RJ, Tsimilli-Micheal M. 2001. Stress in plants, from daily rhythm to global changes, detected and quantified by the JIP-Test. *Chimie Nouvelle (SRC)* 75: 3321-3326.

Suarez ML, Ghermandi L, Kitzberger T. 2004. Factors predisposing episodic drought-induced tree mortality in *Nothofagus* – site, climatic sensitivity, and growth trends. *Journal of Ecology* 92: 954-966.

Suga S, Komatsu S, Maeshima M. 2002. Aquaporin isoforms responsive to salt and water stresses and phytohormones in radish seedlings. *Plant & Cell Physiology* 43: 1229-1237.

Sugihara K, Hanagata N, Dubinsky Z, Baba S, Karube I. 2000. Molecular characterization of cDNA encoding oxygen evolving enhancer protein 1 increased by salt treatment in the mangrove *Bruguiera gymnorrhiza*. *Plant & Cell Physiology* 41: 1279-1285.

Sun J, Yang L, Wang Y, Ort DR. 2009. FACE-ing the global change: opportunities for improvement in photosynthetic radiation use efficiency and crop yield. *Plant Science* 177: 511-522.

Susheelamma BN, Jolly MS, Giridhar K, Sengupta K. 1990. Evaluation of germplasm genotypes for the drought resistance in mulberry. *Sericologia* 30: 327-340.

Suzuki T, Kitano M, Kohno K. 1988. Lateral bud outgrowth on decapitated shoots of low-pruned mulberry (*Morus alba* L.). *Tree Physiology* 4: 53-60.

Swenson NG, Enquist BJ. 2007. Ecological and evolutionary determinants of a key plant functional trait: wood density and its community-wide variation across latitude and elevation. *American Journal of Botany* 94: 451-459.

Szira F, Bálint AF, Börner A, Galiba G. 2008. Evaluation of drought-related traits and screening methods at different developmental stages in spring barley. *Journal of Agronomy and Crop Science* 194: 334-342.

Tardieu F, Lafarge T, Simonneau Th. 1996. Stomatal control by fed or endogenous xylem ABA in sunflower: interpretation of observed correlations between leaf water potential and stomatal conductance in anisohydric species. *Plant, Cell & Environment* 19: 75-84.

Tardieu F, Simonneau T. 1998. Variability among species of stomatal control under fluctuating soil water status and evaporative demand: modelling isohydric and anisohydric behaviours. *Journal of Experimental Botany* 49: 419-432.

Tardieu F. 1993. Will progresses in understanding soil-root relations and root signalling substantially alter water flux models? Philosophical Transactions of the Royal Society London 341: 57-66.

Tardieu F. 2005. Plant tolerance to water deficit: physical limits and possibilities for progress. *Comptes Rendus Geoscience* 337: 57-67.

Tausz M, Hietz P, Briones O. 2001. The significance of carotenoids and tocopherols in photoprotection of seven epiphytic fern species of Mexican cloud forest. *Australian Journal of Plant Physiology* 28: 775-783.

Tausz M, Wonisch A, Grill D, Morales D, Jimenez MS. 2003. Measuring antioxidants in tree species in natural environment: from sampling to data evaluation. *Journal of Experimental Botany* 54: 1505-1510.

Terashima I, Wong SC, Osmond CB, Farquhar GD. 1988. Characterisation of non-uniform photosynthesis induced by abscisic acid in leaves having different mesophyll anatomies. *Plant and Cell Physiology* 29: 385-394.

Terman A, Brunk UT. 2006. Oxidative stress, accumulation of biological 'Garbage', and aging. *Antioxidants and Redox Signaling* 8: 197-204.

Teskey RO, Hinckley TM, Grier CC. 1983. Effect of interruption of flow path on stomatal conductance of *Abies amabilis*. *Journal of Experimental Botany* 34: 1251-1259.

Tewary PK, Sharma A, Raghunath MK, Sarkar A. 2000. In vitro response of promising mulberry (*Morus* sp.) genotypes for tolerance to salt and osmotic stresses. *Plant Growth Regulation* 30: 17-21.

Thimmanaik S, Giridara KS, Jyothshna KG, Suryanarayan N. 2002. Photosynthesis and the enzymes of photosynthetic carbon reduction cycle in mulberry during water stress and recovery. *Photosynthetica* 40: 233-236.

Thomas DS, Montagu KD, Conroy JP. 2006. Effects of leaf and branch removal on carbon assimilation and stem wood density of *Eucalyptus grandis* seedlings. *Trees-Structure and Function* 20: 725-733.

Tilman D, Cassman KG, Matson PA, Naylor R, Polasky S. 2002. Agricultural sustainability and intensive production practices. *Nature* 418: 671-677.

Tjoelker MG, Oleksyn J, Reich PB. 1999. Acclimation of respiration to temperature and CO_2 in seedlings of boreal tree species in relation to plant size and relative growth rate. *Global Change Biology* 5: 679-691.

Tognetti R, Cherubini P, Marchi S, Raschi A. 2007. Leaf traits and tree rings suggest different water-use and carbon assimilation strategies by two co-occuring *Quercus* species in a Mediterranean mixed-forest stands in Tuscany, Italy. *Tree Physiology* 27: 1741-1751.

Tomlinson PB, Fisher JB, Spangler RE, Richer RA. 2001. Stem vascular architecture in the rattan palm *Calamus* (Arecaceae-Calamoideae-Calaminae). *American Journal of Botany* 88: 797-809.

Trebst A, Depka B, Holländer-Czytko H. 2002. A specific role for tocopherol and of chemical singlet oxygen quenchers in the maintenance of photosystem II structure and function in *Chlamydomonas reinhardtii*. FEBS Letters 516: 156-160.

Trenberth KE, Jones PD, Ambenje P, Bojariu R, Easterling D, Tank AK, Parker D, Rahimzadeh F, Renwick JA, Rusticucci M, Soden B, Zhai P. 2007. Observations: surface and atmospheric climate change. In: Solomon S, Qin D, Manning M, Chen Z, Marquis M, Averyt KB, Tignor M, Miller HL (Eds.), *Climate Change 2007: The Physical Science Basis. Contribution of Working Group I to the Fourth Assessment Report of the Intergovernmental Panel on Climate Change*. Cambridge University Press, Cambridge, United Kingdom and New York, USA.

Tsimilli-Michael M, Strasser RJ. 2008. In vivo assessment of plants' vitality: applications in detecting and evaluating the impact of Mycorrhization on host plants. In: A. Varma (ed.), *Mycorrhiza: state of the art, genetics and molecular biology, ecofunction, biotechnology, eco-physiology, structure and systematics*, Springer, Dordrecht, pp. 679-703.

Turner NC. 1979. Drought resistance and adaptation to water deficit in crop plants. In: Mussel H, Staples RC (eds) *Stress Physiology in Crop Plants*. New York, Wiley, pp 343-372.

Tyerman SD, Niemietz CM, Bramley H. 2002. Plant aquaporins: multifunctional water and solute channels with expanding roles. *Plant, Cell & Environment* 125: 173-194.

Tyree M, Salleo S, Nardini A, Lo Gullo M, Mosca R. 1999. Refilling of embolized vessels in young stems of Laurel. Do we need a new paradigm? *Plant Physiology* 120: 11-21.

Tyree M, Zimmermann MH. 2002. Xylem structure and the ascent of sap. Springer-Verlag, New York.

Tyree MT, Davis SD, Cochard H. 1994. Biophysical perspectives of xylem evolution: is there a tradeoff of hydraulic efficiency for vulnerability to dysfunction? *IAWA Journal* 15: 335-360.

Tyree MT, Sperry JS. 1988. Do woody plants operate near the point of catastrophic xylem dysfunction caused by dynamic water stress? *Plant Physiology* 88: 574-580.

Tyree MT, Sperry JS. 1989. Vulnerability of xylem to cavitation and embolism. *Annual Review of Plant Physiology and Plant Molecular Biology* 40: 19-38.

Tyree MT, Zimmermann MH. 2002. *Xylem structure and the ascent of sap*. Berlin: Springer.

Tyree MT. 2003. Hydraulic limits on tree performance: Transpiration, carbon gain and growth of trees. *Trees-Structure and Function* 17: 95-100.

Tyree MT, Sperry JS. 1988. Do woody plants operate near the point of catastrophic xylem dysfunction caused by dynamic water stress? Plant Physiology 88: 574-580.

Uemura A, Ishida A, Tobias DJ, Koike N. Matsumoto Y. 2004. Linkage between gas exchange and hydraulic acclimation in the top canopy leaves of *Fagus* trees in a mesic forest in Japan. *Trees-Structure and Function* 18: 452-459.

van der Molen MK, Dolman A J, Ciais P, Eglin T, Gobron N, Law BE, Meir P, Peters W, Phillips OL, Reichstein M, Chen T, Dekker SC, Doubkova M, Friedl M A, Jung M, van den Hurk BJJM, de Jeu RAM, Kruijt B, Ohta T, Rebel KT, Plummer S, Seneviratne SI, Sitch S, Teuling AJ, van der Werf GR, Wang G. 2011. Drought and ecosystem carbon cycling. *Agricultural and Forest Meteorology* 151: 765-773.

van Heerden PDR, Swanepoel JW, Krüger GHJ. 2007. Modulation of photosynthesis by drought in two desert scrub species exhibiting C_3-mode CO_2 assimilation. *Environmental and Experimental Botany* 61: 124-136.

van Heerden PDR, Tsimilli-Michael M, Krüger GHJ, Strasser RJ. 2003. Dark chilling effects on soybean genotypes during vegetative development: Parallel studies of CO_2 assimilation, chlorophyll-a fluorescence kinetics O-J-I-P and nitrogen fixation. *Physiologia Plantarum* 117: 476-491.

Van Ieperen W, Nijsse J, Keijzer CJ, Van Meeteren U. 2001. Induction of air embolism in xylem conduits of pre-defined diameter. *Journal of Experimental Botany* 52: 981-991.

Vandeleur RK, Mayo G, Shelden MC, Gilliham M, Kaiser BN, Tyerman SD. 2009. The role of plasma membrane intrinsic protein aquaporins in water transport through roots: diurnal and drought stress responses reveal different strategies between isohydric and anisohydric cultivars of grapevine. *Plant Physiology* 149: 445-460.

Vijayan K, Chakraborti SP, Ercisli S, Ghosh PD. 2008. NaCl induced morpho-biochemical and anatomical changes in mulberry (*Morus* spp.). *Plant Growth Regulation* 56: 61-69.

Vijayan K, Chakraborti SP, Ghosh PD. 2003. In vitro screening of mulberry for salinity tolerance. Plant Cell Reports 22: 350-357.

Vijayan K, Doss SG, Chakraborti SP, Ghosh PD, Saratchandra B. 2010. Character association in mulberry under different magnitude of salinity stress. *Emirates Journal of Food and Agriculture* 22: 318-325.

Vilagrosa A, Bellot J, Vallejo VR, Gil-Pelegrin E. 2003. Cavitation, stomatal conductance, and leaf dieback in seedlings of two co-occurring Mediterranean shrubs during an intense drought. *Journal of Experimental Botany* 54: 2015-2024.

Villagra PE, Juñent FAR. 1997. Wood structure of *Prosopis alpataco* and *P. argentina* growing under different edaphic conditions. *IAWA Journal* 18: 37-51.

Villar-Salvador P, Castro-Diez P, Perez-Rontome C, Montserrat-Marti G. 1997. Stem xylem features in three *Quercus* (Fagaceae) species along a climatic gradient in NE Spain. *Trees-Structure and Function* 12: 90-96.

Violle C, Navas ML, Vile D, et al. 2007. Let the concept of trait be functional! *Oikos* 116: 882-892.

Wang P, Duan W, Takabayashi A, Endo T, Shikanai T, Ye JY, Mi H. 2006. Chloroplastic NAD(P)H dehydrogenase in tobacco leaves functions in alleviation of oxidative damage caused by temperature stress. *Plant Physiology* 141: 465-474.

Wang X, Li X, Li Y. 2007. A modified Commassie Brilliant Blue staining method at nanogram sensitivity compatible with proteomic analysis. *Biotechnology Letters* 29: 1599-1603.

Wartinger A, Heilmeier H, Hartung W, Schultze E-D. 1990. Daily and seasonal courses of leaf conductance and abscisic acid in the xylme sap of almond trees (*Prunus dulcis* M.) under desert conditions. *New Phytologist* 116: 581-587.

Weiner J. 2004. Allocation, plasticity and allometry in plants. *Perspectives in Plant Ecology, Evolution and Systematics* 6: 207-215.

West AG, Hultine KR, Burtch KG, Ehleringer JR. 2007b. Seasonal variations in moisture use in a piñon–juniper woodland. *Oecologia* 153: 787-798.

West AG, Hultine KR, Jackson TL, Ehleringer JR. 2007a. Contrasting hydraulic strategies explain differential summer moisture use of *Pinus edulis* and *Juniperus osteosperma*. *Tree Physiology* 27: 1711-1720.

Westoby M, Wright IJ. 2006. Land-plant ecology on the basis of functional traits. *Trends in Ecology & Evolution* 21: 261-268.

Wheeler JK, Sperry JS, Hacke UG, Hoang N. 2005. Inter-vessel pitting and cavitation in woody Rosaceae and other vesselled plants: a basis for a safety versus efficiency trade-off in xylem transport. *Plant, Cell & Environment* 28: 800-812.

Whitehead D, Livingston NJ, Kelliher FM, Hogan KP, Pepin S, McSeveny TM, Byers JN. 1996. Response of transpiration and photosynthasis to a transient change in illuminated foliage area for a *Pinus radiata* D. Don tree. *Plant, Cell & Environment* 19: 949-957.

Whitehead D. 1998. Regulation of stomatal conductance and transpiration in forest canopies. *Tree Physiology* 18: 633-644.

Wilhelm C, Selmar. 2011. Energy dissipation is an essential mechanism to sustain the viability of plants: The physiological limits of improved photosynthesis. *Journal of Plant Physiology* 168: 79-87.

Wilkinson S. Davies WJ. 2008. Manipulation of the apoplastic pH of intact plants mimics stomatal and growth responses to water availability and microclimatic variation. *Journal of Experimental Botany* 59: 619-631.

Woo NS, Badger MR, Pogson BJ. 2004. A rapid, non-invasive procedure for quantitative assessment of drought survival using chlorophyll fluorescence. *Plant Methods* 4: 27.

Woodruff DR, Bond BJ, Meinzer FC. 2004. Does turgor limit growth in tall trees? *Plant, Cell & Environment* 27: 229-236.

Wright IJ, Falster DS, Pickup M, Westoby M. 2006. Cross-species patterns in the coordination between leaf and stem traits, and their implications for plant hydraulics. *Physiologia Plantarum* 127: 445-456.

Wu G, Wei ZK, Shao HB. 2007. The mutual responses of higher plants to environment: physiological and microbiological aspects. *Biointerfaces* 59: 113-119.

Wu YY, Liu CQ, Li PP, Wang JZ, Xing D, Wang BL. 2009. Photosynthetic characteristics involved in adaptability to Karst soil and alien invasion of paper mulberry (*Broussonetia papyrifera* (L.) Vent.) in comparison with mulberry (*Morus alba* L.). *Photosynthetica* 47: 155-160.

Wullschleger SD, Meinzer FC, Vertessey RA. 1998. A review of whole-plant water use studies in trees. *Tree Physiology* 18: 499-512.

Xiang C, Werner BL, Christensen EM, Oliver DJ. 2001. The biological functions of glutathione revisited in Arabidopsis transgenic plants with altered glutathione levels. *Plant Physiology* 126: 564-574.

Xiloyannis C, Uriu K, Martin GC. 1980. Seasonal and diurnal variations in absicic acid, water potential, and diffusive resistance in leaves from irrigated and non-irrigated peach trees. *Journal of the American Society for Horticultural Science* 105: 412-415.

Xu Y-H, Liu R, Yan L, Liu Z-Q, Jiang S-C. et al. 2012. Light-harvesting chlorophyll a/b-binding proteins are required for stomatal response to abscisic acid in *Arabidposis*. *Journal of Experimental Botany* 63: 1095-1106.

Yadav MS, Singh M, Sharma SK, Tewari JC, Burman U. 1997. Silvi-pastoral systems arid and semi-arid ecosystems. CAZRI, Jodhpur, pp 1-472.

Yanbao L, Chunyang Y, Chunyang L. 2006. Differences in some morphological, physiological, and biochemical responses to drought stress in two contrasting populations of *Populus przewalskii*. *Physiologia Plantarum* 127: 182-191.

Yáñez-Espinosa L, Terrazas T, Lopez-Mata L. 2001. Effects of flooding on wood and bark anatomy of four species in a mangrove forest community. *Trees-Structure and Function* 15: 91-97.

Yen GC, Wu SC, Duh PD. 1996. Extraction and identification of antioxidant components from the leaves of mulberry (*Morus alba* L.). *Journal of Agricultural and Food Chemistry* 44: 1687-1690.

Yildiz-Aktas L, Dagnon S, Gurel A, Gesheva E, Edreva A. 2009. Drought tolerance in cotton: Involvement of non-enzymatic ROS-scavenging compounds. *Journal of Agronomy and Crop Science* 195: 247-253.

Yin C, Peng Y, Zang R, Zhu Y, Li C. 2005. Adaptive responses of *Populus kangdingensis* to drought stress. *Physiologia Plantarum* 123: 445-451.

Yordanov I, Velikova V, Tsonev T. 2000. Plant responses to drought, acclimation and stress tolerance, *Photosynthetica* 38: 171-186.

Zhang J, Kirkham MB. 1996. Antioxidant responses to drought in sunflower and sorghum seedlings. *New Phytologist* 132: 36-73.

Zhang JL, Cao KF. 2009. Stem hydraulics mediates leaf water status, carbon gain, nutrient use efficiencies and plant growth rates across dipterocarp species. *Functional Ecology* 23: 658-667.

Zhang T, Gong H, Wen X, Lu C. 2010. Salt stress induces a decrease in excitation energy transfer from phycobilisomes to photosystem II but an increase to photosystem I in the cyanobacterium *Spirulina platensis*. *Journal of Plant Physiology* 167: 951-958.

Zhang Y, Wang Z, Chai T, Wen Z, Zhang H. 2008. Indian mustard aquaporin improves drought and heavy-metal resistance in tobacco. *Molecular Biotechnology* 40: 280-292.

Zhu JK. 2002. Salt and drought stress signal transduction in plants. *Annual Review of Plant Biology* 53: 247-273.

Zhu XG, Long SP, Ort DR. 2010. Improving photosynthetic efficiency for greater yield. *Annual Review of Plant Biology* 61: 235-261.

Zimmerman MH. 1971. In: Zimmerman MH, Brown CL, eds. *Trees, structure and function*. New York: Springer-Verlag.

Zimmermann MH, Milburn JA. 1982. Transport and storage of water. In: Lange, O.L., Nobel, P.S., Osmond, C.B., Ziegler, H. (eds.), *Physiological plant ecology II: Water relations and carbon assimilation*. Encyclopedia of Plant Physiology, New Series, vol. 12B. Springer-Verlag, Berlin, pp. 135-151.

Zimmermann MH, Tomlinson PB. 1966. Analysis of complex vascular systems in plants: optical shuttle method. *Science* 152: 72-73.

Zimmermann MH. 1983. Xylem structure and the ascent of sap, In: Timell TE (Ed.), *Springer Series on Wood Science*, Springer-Verlag, Berlin, p. 143.

Zimmermann P, Zentgraf U. 2005. The correlation between oxidative stress and leaf senescence during plant development. *Cellular and Molecular Biology Letters* 10: 515-534.

Zlatev ZS, Yordanov IT. 2004. Effects of soil drought on photosynthesis and chlorophyll fluorescence in bean plants. *Bulgarian Journal of Plant Physiology* 30: 3-18.

Publications

Research papers published:

1. Rasineni K G, **Guha A** and Attipalli R Reddy, Elevated CO_2 atmosphere significantly increased photosynthesis and productivity in a fast growing tree species, *Gmelina arborea* Roxb, 2013, *Climate Change and Environmental Sustainability*, 1, 81-94.

2. **Guha A**. Sengupta D, Attipalli R Reddy, Polyphasic chlorophyll a fluorescence kinetics and leaf protein analyses to track dynamics of photosynthetic performance in mulberry during progressive drought, 2013, *Journal of Photochemistry and Photobiology*, 119, 71-83.

3. Kumar A, **Guha A**, Bimolata W, Attipalli R Reddy et al., Leaf gas exchange physiology in rice genotypes infected with bacterial blight: An attempt to link photosynthesis with disease severity and rice yield, 2013, *Australian Journal of Crop Science,* 7, 32-39.

4. **Guha A**, Attipalli R Reddy, Leaf functional traits and stem-wood characteristics influencing biomass productivity of mulberry (*Morus* spp. L.) genotypes grown in short rotation coppice system, 2012, *Bioenergy Research* (DOI 10.1007/s12155-012-9270-7).

5. Kumar S**,** Ghatty S**,** Satyanarayana J**, Guha A,** Chaitanya BSK and Attipalli R Reddy, Paclobutrazol treatment as a potential strategy for higher seed and oil yield in field-grown *Camelina sativa* L. Crantz, 2012, *BMC Research Notes*, 5, 137.

6. **Guha A**, Rasineni K G and Attipalli R Reddy, Non-enzymatic antioxidative defence in drought-stressed mulberry (*Morus indica* L.) genotypes, 2012, *Trees- Structure and Function*, 26, 903-918.

7. Rasineni G K, **Guha A** and Attipalli R Reddy, Responses of *Gmelina arborea*, a tropical tree species, to elevated atmospheric CO_2: Growth, biomass productivity and carbon sequestration efficacy. 2011, *Plant Science*, 181, 428-438.

8. Rasineni G K, **Guha A** and Attipalli R Reddy, Elevated atmospheric CO_2 mitigated photoinhibition in a tropical tree species, *Gmelina arborea*, 2011, *Journal of Photochemistry and Photobiology*, 103, 159-165.

9. **Guha A**, Sengupta D and Attipalli R Reddy, Physiological optimality, allocation trade-offs and antioxidant protection linked to better leaf yield performance in drought exposed mulberry, 2010, *Journal of the Sciences of Food and Agriculture*, 90, 2649-2659.

10. **Guha A**, Rasineni K G and Attipalli R Reddy, Drought tolerance in mulberry (*Morus* spp L.): A physiological approach with insights to growth dynamics and leaf yield production, 2010, *Experimental Agriculture* 46,471-488.

11. **Guha A**, Sengupta D, Rasineni K G and Attipalli R Reddy, An integrated diagnostic approach to understand drought tolerance in mulberry (*Morus indica* L.), 2010, *Flora* 205, 144-151.

Published in conferences, seminars and workshops:

1. **Guha A** and Attipalli R Reddy. Ecophysiological responses of anisohydric mulberry to summer drought at a hot semi-arid steppe experimental site of southern India. *Plant Ecophysiology Techniques Workshop*, Lisbon, Portugal, 10-15th September 2012, organised by Plant Environmental Physiology Group, University of Essex, UK (oral).

2. **Guha A** and Attipalli R Reddy. Genotypic diversity of photosynthesis in mulberry (*Morus* spp L.): Leaf/stem traits, their intrarelations, interrelations and correlations with photosynthetic performance. *Plant Science Colloquium-2012*, University of Hyderabad, India (oral).

3. **Guha A**, Sengupta D and Attipalli R Reddy. Drought-induced ecophysiological and molecular responses in *Morus indica* to predict anisohydric functionality of trees for future climate change. Conference '*Research Dialogue in the Life Sciences' organized by German Research Foundation (DFG)*, 2012, University of Hyderabad, India (poster).

4. **Guha A**, Rasineni G K and Attipalli R. Reddy. Photosynthetic Leaf gas exchange, radiation use efficiency and chlorophyll fluorescence indices associated with leaf yield in water-limited *Morus* cultivars. *National Symposium on Frontiers in Photobiology* (FIP-2009), BARC, India (poster).

5. **Guha A**. Rasineni G K and Attipalli R Reddy. Diffusive resistance to CO_2 as a limitation to net photosynthesis in water-stressed mulberry leaves. International conference "*Photosynthesis in the global perspective*" held in honour of Govindjee, November 27-29, 2008, Devi Ahilya University, Indore, India (poster).

6. **Guha A**, Sengupta D and Attipalli R Reddy. Drought-induced oxidative stress in mulberry (*Morus* spp. L), *Bioquest-2008*, School of Life Sciences, University of Hyderabad, Hyderabad (March 15-16th, 2008) (poster).